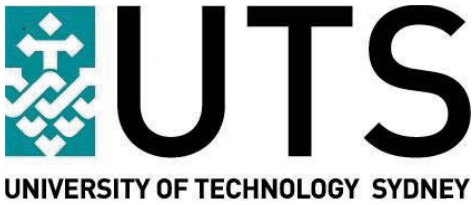


# Better Utilization of Fly Ash and other SCMs in Lean Concrete and Durable Concrete Pavements and Structural Concrete Applications

A thesis by

**Farzad Moghaddam**

Supervisors: Prof Vute Sirivivatnanon and Dr Kirk Vessalas

A thesis submitted in fulfilment of the requirements for the degree of

**Doctor of Philosophy**

Faculty of Engineering and Information Technology

School of Civil and Environmental Engineering

University of Technology Sydney

May 2018

## CERTIFICATE OF ORIGINAL AUTHORSHIP

I certify that the work in this thesis has not previously been submitted for a degree nor has it been submitted as part of requirements for a degree except fully acknowledged within the text.

I also certify that the thesis has been written by me. Any help that I have received in my research work and the preparation of the thesis itself has been acknowledged. In addition, I certify that all information sources and literature used are indicated in the thesis.

Farzad Moghaddam

Production Note:
Signature removed prior to publication.

Date: 08/05/2018

*Sincerely dedicated to*

*my lovely wife and son*

## ***ACKNOWLEDGEMENTS***

This thesis would not have been completed without the guidance, advice and support of a number of individuals whose contribution I would gratefully like to acknowledge. I would specially like to express my gratitude to my supervisors, *Professor Vute Sirivivatnanon* and *Dr Kirk Vessalas*. I would like to express my deepest gratitude to *Professor Vute Sirivivatnanon*, who has been my principal supervisor for this research, not only because of his invaluable guidance and expert advice throughout the research but also on account of his strong support, being a kind father during the last three and half years. The author would also very much like to record his appreciation to Dr Vessalas for his valuable advice and constant support from the commencement of this project to the end. I also greatly appreciate my retired co-supervisor, Dr. Rasiah Sri Ravindrarajah, for his mentorship and unfailing assistance and support throughout the course of this research. It should be mentioned that this research is supported by the Australian Government Research Training Program.

I would also like to convey my thanks to University of Technology Sydney (UTS) Civil Engineering Laboratories staff, specially the laboratories manager *Mr Rami Haddad*, who kindly helped me in project experimental stages.

Furthermore, I am obliged to many of my colleagues and friends who assisted me during my studies. Special thanks must go to my dear friends, Dr Amin Noushini, Mr Hammed Mahdavi, *Ms Marie Joshua Tapas and Mr Daniel John Pospischil* for their unfailing assistance and support in this research work.

My deepest gratitude is to my wife Ghazal for her unwavering understanding during all the years of this work, her selfless love and support throughout, and her encouragement and companionship during the preparation of this thesis. Her understanding of the demands required to complete this work has been inspirational. And finally to my son, Kian whose birth during the thesis preparation encouraged me to get it done as soon as I could.

Lastly, I would like to extend my love and gratitude to my dearest parents for their support and encouragement. I want to sincerely thank them from the bottom of my heart and acknowledge that without them none of this could have happened and I would not have been able to achieve most of the things I have in my life.

## ***LIST OF PUBLICATIONS BASED ON THIS RESEARCH***

- Moghaddam, F., Sri Ravindrarajah, R. & Sirivivatnanon, V. 2015, 'Properties of metakaolin concrete-a review', Paper presented to the International Conference on Sustainable Structural Concrete 2015, La Plata, Argentina.
- Moghaddam, F., Sri Ravindrarajah, R. 2016, 'Properties of fly ash concrete – a review ', Concrete Institute of Australia Journal. 42(4): p. 50-53
- Moghaddam, F., Sirivivatnanon, V., Vessalas, K. 2017, ' Effect of run-of-station fly ash and other SCMs on various properties of concrete ', Concrete Institute of Australia's Biennial National Conference, Adelaide, Australia.
- Moghaddam, F., Vessalas, K., Sirivivatnanon, V. 2017, ' Use of run-of-station fly ash and other SCMs in concrete pavement construction', Australian Society for Concrete Pavements 4th Concrete Pavements Conference, Kingscliff, Australia.
- Moghaddam, F., Sirivivatnanon, V., Vessalas, K. 2018, ' The effect of fly ash fineness on heat of hydration, microstructure, flow and compressive strength of blended cement pastes', Construction and Building Materials – under review
- Moghaddam, F., Vessalas, K., Sirivivatnanon, V. 2018, ' Investigation on the influence of supplementary cementitious materials on heat of hydration of blended cement pastes', ready for submission

## *TABLE OF CONTENTS*

## ***LIST OF FIGURES***

## ***LIST OF TABLES***

## ***ABBREVIATIONS***

| | |
|---|---|
| AMBT | Accelerated Mortar Bar Test |
| AEA | Air Entraining Agent |
| ASR | Alkali-Silica Reactivity |
| ACI | American Concrete Institute |
| AVPV | Apparent Volume of Permeable Void |
| AS | Australian Standard |
| CH | Calcium Hydroxide |
| C-S-H | Calcium Silicate Hydrate |
| CCAA | Cement Concrete & Aggregate Australia organisation |
| CFA | Classified Fly Ash |
| ESP | Electrostatic Precipitators |
| FF | Fabric Filter |
| FA | Fly Ash |
| GGBFS | Ground Granulated Blast Furnace Slag |
| GRFA | Grounded Run-of-Station Fly Ash |
| HPC | High-Performance Concrete |
| HWR | High-range Water Reducer |
| LOI | Loss-Of-Ignition |
| MIP | Mercury Intrusion Porosimetry |
| MK | Metakaolin |
| MAU | Microstructural Analysis Unit |
| OFA | Original Fly Ash |
| PSA | Particle Size Analysis |
| PC | Portland Cement |
| RCPT | Rapid Chloride Permeability Test |
| RH | Relative Humidity |
| RMS | Road and Maritime Services |
| RFA | Run-of-the-Station Fly Ash |
| SSD | Saturated-Surface-Dry |
| SEM | Scanning Electron Microscopy |
| SL | Slag |
| SAI | Strength Activity Index Test |
| SCMs | Supplementary Cementitious Materials |
| $C_3A$ | Tricalcium Aluminate |

| | |
|---|---|
| UNSW | University of New South Wales |
| UTS | University of Technology Sydney |
| WR | Water Reducer |
| XRD | X-ray Diffraction |
| XRF | X-ray Fluorescence |

## ***ABSTRACT***

The utilization of supplementary cementitious materials (SCMs) for the partial replacement of cement in concrete introduces several environmental and economical benefits. Some of the major benefits include the conservation of natural resources, the reduction of greenhouse gas emissions and a reduction in cement use. The use of SCMs in concrete also have technical merit and are multifaceted in their approach by enhancing the workability, strength and durability of concrete. In recent years, Australian road authorities have been increasingly concerned with the shortage of classified fly ash (CFA) predicted to occur in the near future with renewable energies finding their way into the market. Finding alternative SCMs is a critical issue due to a shortage of national resources available. Run-of-station fly ash (RFA) can be a possible alternative to CFA. However, the lack of enough information available in the literature hinders the use of RFA, and additional work needs to be carried out to investigate its efficiency in different concrete mixes.

In this investigation, an experimental study has been carried out to evaluate the effect of fineness of three fly ashes (ground run-of-station fly ash (GRFA), RFA and CFA) on the heat of hydration behaviour, flow and compressive strength properties of blended cement pastes. The study has been extended to also assess the influence of fineness, types and levels of SCMs (fly ash, slag or metakaolin) on the fresh and hardened properties of mortars. Finally, the effect of RFA and other SCMs on the fresh, hardened and durability properties of concretes for different applications such as lean, pavement and bridge work have also been studied.

Among all the SCMs investigated, metakaolin (MK) was found to have the highest fineness followed by slag (SL), GRFA, CFA and RFA. In addition, increasing the fineness of fly ash showed a reduction in the crystallinity of silica particles, which resulted in more reactivity suggesting possibly more amorphous silica particles present for pozzolanic reactivity. The presence of smaller quantities of crystalline silica particles in SL and MK also suggests a higher degree of pozzolanic reactivity may prevail. Results of the study on the blended pastes showed that the cumulative heat of hydration decreased by the incorporation of fly ash with different fineness (302, 368 and 495 $m^2$/kg), SL, or MK. This reduction was noted to increase with increasing SCM content. The finer grade fly ash (GRFA) generated higher heat of hydration compared to coarser grade fly ash (RFA). Furthermore, the consumption of portlandite increased with increasing fineness of fly ash at 28 days reflecting higher pozzolanic reactivity resulting in higher compressive strength than the blended pastes containing coarser grade fly ash.

Partially replacing cement with 20%, 30% and 40% fly ash of different fineness (CFA, RFA and GRFA ), and 35%, 50% and 65% SL in mortars (using a fixed w/b ratio) improved the flow compared to control mortar (devoid of SCM addition). The inclusion of 5%, 10% and 15% MK in the same mortar decreased the flow compared to control mortar. Increasing the fineness of fly ash from 302 to 495 $m^2$/kg improved the 28-day compressive strength of the mortar even to a similar level to the control mortar. However, the 28-day compressive strength of mortars containing SL and MK were even higher than control mortar at all replacement levels evaluated. The 56-day drying shrinkage of mortars was also

found to decrease considerably when partially replacing cement with SCMs. Compared to the control mortar, a reduction in drying shrinkage was noted with an increase in SCM replacement level.

Results from the study on lean concretes with 60% fly ash content revealed RFA is almost as effective as CFA in satisfying the strength and drying shrinkage requirements according to the RMS R82 specification despite having lower compressive strength development at all ages (up to 56 days) compared to the same concrete containing CFA. Replacing cement with 20% and 25% RFA in pavement and bridge concretes decreased 28-day compressive strength by about 11% and 11% respectively, compared to the same concretes containing CFA. In addition, there was a slight increase in drying shrinkage at all ages (up to 56 days) by replacing cement with RFA instead of CFA in all concretes investigated. It can be concluded that the concretes with RFA can achieve similar hardened properties to CFA concrete in pavement concrete and bridge applications by only adjusting the mix design such as lowering w/b ratio. This statement is based on the results of fineness level, crystaline phase indetification and oxide composition of CFA and RFA particles and also strength development from the pastes and mortars. Moreover, partially replacing cement with SL or MK could be another alternative to CFA in pavement concrete and bridge applications due to the high fineness confirmed by mortar and concrete results. However, only the relative performance of concrete used for bridge applications was assessed for durability properties.

According to the qualitative tests carried out on the bridge concretes containing SCMs, it was noted that the level of penetrability of chloride and sulfate ions into the concrete was reduced by replacing cement with 25% CFA or

RFA compared to the control concrete at 28 days. This reduction in penetrability level was significant for the concretes containing 50% SL or 15% MK. In addition, the results from the accelerated mortar bar test revealed that partially replacing cement with SCMs decreased the expansion of mortar bars due to alkali-silica reaction (ASR); the reduction in expansion increased with an increase in SCM content. For the reactive aggregate investigated in this study, incorporation of 25% CFA or 25% RFA or 50% SL or 15% MK is needed to control the expansion of mortar bars due to ASR.

This experimental investigation has demonstrated the value and benefits of using RFA as an alternative SCM in concrete. RFA has proven abilities to achieve the same level of performance as CFA when used in various concrete applications such as lean, pavement and bridge concrete mix designs. SL and MK could also be used as other alternatives to CFA in concrete.

# Chapter 1

## Introduction

# 1 INTRODUCTION

## 1.1 Background to the project

The achievement of sustainable development has been a major challenge facing the concrete industry for years [1]. Improvement in the concrete production process and optimization of the mix proportion by adopting technological developments such as using supplementary cementitious materials (SCMs) is an inevitable part influencing various properties of concrete [2]. The first application of fly ash in Australia was in producing mass concrete in dam construction in the 1950s. The main reason was to reduce the heat of hydration in mass concrete structures. Additionally, in 1970, fly ash was used in building works in order to produce pumpable concrete for high-rise buildings. Fly ash concrete represents more than 90% of the concrete produced in Sydney and Brisbane. High volume fly ash structural concrete was developed in Australia in the 1990s for specific aggressive environments. Slag cement was first developed for marine applications in Australia in the late 1980s. It is also used to produce light colour cement for render and off-form concrete construction [3]. In recent years, metakaolin has been introduced as a highly active and effective pozzolan to partially replace cement in concrete. The calcination of high-purity kaolinite at temperatures (700 to 850°C) produces metakaolin which consists of silica and alumina in an active form which reacts with calcium hydroxide (CH) at room temperature [4, 5].

The readily availability of fly ash in some States was (and is) due to the reliance on coal-fired electricity generation in Australia — the majority of this involving the firing of pulverised–fuel black coal. Classified fly ash which complies with the requirements of Australian Standard AS 3582.1 [6] has been

available throughout much of Australia for about 40 years. Victoria is excluded from this equation because of its reliance on brown coal for electricity generation. Victoria has been supplied with fly ash from other states, as the fly ashes produced from Victorian brown coal are not (generally) suitable for use in concrete.

However, in recent years there have been changes, both technical and policy driven, that have the potential to affect the availability of classified fly ash. These are not issues for Australia alone. An increased focus on particulate and gaseous emissions from coal-fired power stations has resulted in two major changes [7]. Particulate emissions are now controlled using fabric filter (FF) technology rather than Electrostatic Precipitators (ESP) for fly ash collection. FF has much higher particulate collection efficiencies than ESPs, but do not as effectively separate the fly ash into a number of separate particle size fractions as do ESPs. Fly ash collected in an FF plant generally requires processing (classification) to create a 'concrete grade' product. A larger potential effect on 'concrete grade' fly ash quality and availability is from changes in combustion technology — particularly the advent (usually retrofitting) of low-NOx burner technology [8]. The new burners and some power station operating philosophies have impacted (in some regions) the quantity of 'concrete grade' fly ash available due to increased Loss-of-Ignition (LOI) levels in fly ash as well as increased LOI variability [7]. Also, switching to the renewable materials instead of burning coal to generate electricity is widely increasing. For instance, in Australia, since 2004, coal-fired electricity generation has fallen from about 75% to 60%; renewable energy has increased from 8% to 15% and will grow to about 23% by 2020 [9].

Therefore, in recent years, there is a concern about the possible shortage of classified fly ash which complies with the requirements of Australian Standard AS 3582.1 [6]. The possible use of run-of-station fly ash and other SCMs such as slag and metakaolin in concrete is essential and can provide economic, technical and environmental benefits, which should be exploited by the specifiers and the supplier to produce concrete with performance requirements for specific applications.

The lack of suitable information available in the literature hinders the use of run-of-station fly ash, and additional work needs to be carried out in this area to investigate its efficiency in different concrete mixes.

## 1.2 Research objective

The research objective of this thesis is to evaluate the important characteristics of run-of-the-station fly ash (RFA) and supplementary cementitious materials (SCMs) like ground granulated blast furnace slag (SL) and metakaolin (MK) as alternatives to classified fly ash (CFA) in influencing the properties of concretes.

## 1.3 Specific objectives

The specific objectives of this research project are:

- To assess the effect of fineness of SCMs on microstructure morphology, heat of hydration and consumption of calcium hydroxide of the blended cement paste;
- To determine the important characteristics of cement and SCMs on a range of mortar and concrete performances;

- To examine the possible use of RFA in replacing CFA in lean concrete (e.g. RMS R82 specifications);
- To evaluate the possible use of RFA, SL and MK in replacing CFA in pavement & high- performance concrete for infrastructure applications (e.g. RMS R83 & B80 specifications respectively);
- To determine the minimum level of RFA, CFA, SL and MK in mitigating Alkali-Silica Reactivity (ASR).

## 1.4 Organisation of dissertation

The structure of the thesis is outlined in this section to provide an overview of what this document entails. This thesis consists of eight chapters as explained below:

- Chapter 1 provides the general introduction to the problem to be solved which is the aim of this research. The research objectives and the arrangement of the thesis chapters are also covered.
- Chapter 2 of the report provides a comprehensive review of available literature regarding the influence of three different supplementary cementitious materials: fly ash, ground granulated blast furnace slag and metakaolin on fresh, hardened and durability properties of mortar and concrete to identify gaps in the knowledge.
- Chapter 3 outlines the research methodology used in the current study to achieve the objectives of this research. In addition, an explanation of the adopted methods was provided for all the experimental works including

raw material characterisation, and the procedure of designing, mixing, casting, curing and testing the paste, mortar and concrete specimens.

- Chapter 4 presents and discusses the results of some important characteristics of cementitious and pozzolanic materials (General Purpose Portland cement, classified fly ash, run-of-station fly ash, ground run-of-station fly ash, slag and metakaolin) as well as fine and coarse aggregates used in this research.
- Chapter 5 is dedicated to the results of experimentation with a discussion of the influence of fly ash fineness on the heat of hydration, calcium hydroxide intensity and microstructure in addition to the flow and compressive strength of blended cement pastes. Also, those results were assessed and evaluated against the control paste (cement only).
- In Chapter 6, the effects of different types and levels of supplementary cementitious materials, as well as the influence of fineness and levels of fly ash on the selected fresh and hardened properties of mortars was discussed.
- In Chapter 7, the possible use of run-of-station fly ash and other supplementary cementitious materials in concrete applications was assessed and evaluated. The results and discussion of the influence of run-of-station fly ash, slag and metakaolin on critical properties of lean concrete and high-performance concrete (pavement and bridge mixes) was presented and compared to classified fly ash concrete according to Road and Maritime Services (RMS) specifications.

- Finally, summary and conclusions are presented in Chapter 8, followed by Appendix A, Appendix B and a bibliography.

# Chapter 2

## Literature Review

# 2 LITERATURE REVIEW – INFLUENCE OF CHARACTERISTICS AND LEVELS OF SCMS ON PROPERTIES OF MORTAR & CONCRETE

## 2.1 Preface

This chapter provides an overview of the available scientific literature regarding the use of supplementary cementitious materials in mortar and concrete.

## 2.2 Physical characteristics and chemical composition of SCMs

Fly ash (FA) is a by-product generated during the combustion of pulverised coal in coal-fired power stations at 1200–1700°C. It consists of fine, powdery particles predominantly spherical in shape, being either solid or hollow and mostly glassy (amorphous) in nature [10]. Roy et al. [11] indicated that the diameter of FA particles usually ranges from 1–100μm, specific gravity ranges from 2.1–3.0, while its specific surface area may vary from 170–1000 $m^2$/kg [11]. The colour of FA can vary from tan to grey to black depending on the amount of unburned carbon in the fly ash. The morphology of FA particles mainly depends on the combustion temperature and subsequent cooling rate.

Kutchko and Kim [12] reported that FA particles mainly consist of solid spheres, hollow spheres (cenospheres) and irregular unburned carbon, which was revealed by Scanning electron microscopy (SEM) analysis. Silica, alumina, ferrous oxide, and calcium oxide with varying amounts of carbon as measured by a Loss of Ignition (LOI) test are the main components of FA [13]. Type of coal burned to produce FA is responsible for FA chemistry. As Manz [14] reported, higher CaO, MgO, and $SO_3$ and lower $SiO_2$, and $Al_2O_3$ usually are found in FAs

from sub-bituminous and lignite coals, while FAs from bituminous coal contain less than 10% CaO in total, often consisting mainly of aluminosilicate glass and usually not containing any crystalline compounds of calcium. Ahmaruzzaman [13] reported a general overview of the chemical composition of fly ash as a function of coal type reported, as shown in Table 2-1. In addition, Mehta [15] reported the nature of two kinds of fly ashes and the results are shown in Table 2-2.

**Table 2-1: Chemical composition of fly ash by coal type [13]**

| Component (wt. %) | Bituminous | Sub-bituminous | Lignite |
|---|---|---|---|
| $SiO_2$ | 20-60 | 40-60 | 15-45 |
| $Al_2O_3$ | 5-35 | 20-30 | 10-25 |
| $Fe_2O_3$ | 10-40 | 4-10 | 4-15 |
| CaO | 1-12 | 5-30 | 15-40 |
| MgO | 0-5 | 1-6 | 3-10 |
| $Na_2O$ | 0-4 | 0-2 | 0-6 |
| $K_2O$ | 0-3 | 0-4 | 0-4 |
| $SO_3$ | 0-4 | 0-2 | 0-10 |
| LOI | 0-15 | 0-3 | 0-5 |

**Table 2-2: Physical properties of fly ash [15]**

| Property | Low-CaO fly ash | High-CaO fly ash |
|---|---|---|
| Shape | Spherical | Spherical |
| Median size (μm) | 5-20 | 2-20 |
| Surface area ($m^2$/kg) | 300-500 | 300-500 |
| Colour | Grey | Grey to buff white |
| Nature of reaction | Pozzolanic | Pozzolanic and hydraulic |
| Specific gravity | 1.9-2.8 | 1.9-2.8 |

The major reasons which influence the variability of fly ash production in coal-fired power stations are the type and mineralogical composition of the coal, the degree of coal pulverisation, type of furnace, oxidation conditions and the methods of collecting, handling and storing of fly ash before usage [16].

Ground granulated blast furnace slag (GGBFS) is a by-product from the blast furnaces used to make iron at a temperature of about 1500°C. Molten iron and molten slag are produced by melting the iron ore, coke and limestone in the blast furnace. The main components of the molten slag are mostly silicates and alumina from the original iron ore combined with some oxides from the limestone. Next, the molten slag is rapidly quenched by high-pressure water jets and forms granular particles not bigger than 5 mm. The resulting granular material is comprised of around 95% non-crystalline calcium-aluminosilicates and fewer large crystals due to the rapid cooling process. Slag mostly consists of the glassy

structure due to the rapid cooling the molten slag as the glass is responsible for hydraulic or cementitious properties. The granulated slag is further processed by being dried and then ground in a rotating ball mill to a very fine powder, which is GGBFS. In addition, the reactivity of GGBFS increases by increasing the fineness. The grinding of the slag to fineness in the range of 400 to 650 $m^2/kg$ produces angular-shaped particles with a similar particle size distribution as Portland cement (PC). The colour of GGBFS varies from beige to dark to off-white, depending on the moisture content, chemistry, and efficiency of granulation [10, 16]. The cementitious properties of GGBFS derive from its glassy content (about 85 to 90%). GGBFS is comprised mainly of CaO, $SiO_2$, $Al_2O_3$, and MgO. The main chemical constituents of GGBFS are similar to PC, although GGBFS is much lower in calcium and higher in silica than PC [17]. Tasong et al. [17] reported physical and chemical properties of slag as shown in Tables 2-3 and 2-4 respectively.

**Table 2-3: Typical chemical composition of slag [17]**

| Chemical composition | % by mass |
|---|---|
| $SiO_2$ | 35.34 |
| $Al_2O_3$ | 11.59 |
| $Fe_2O_3$ | 0.35 |
| CaO | 41.99 |
| MgO | 8.04 |
| MnO | 0.45 |
| $SO_3$ | 0.23 |
| $S_2$ | 1.18 |

**Table 2-4: Physical properties of slag [17]**

| Property | Value |
|---|---|
| Specific gravity | 2.9 |
| Bulk density (kg/m$^3$) | 1200 |
| Specific surface (m$^2$/kg) | 425-470 |

Metakaolin (MK) is produced by calcination of high-purity kaolinite at temperatures 700 to 850°C. It mainly consists of silica and alumina in an active form, which reacts with calcium hydroxide (CH) at room temperature. Thermal activation of kaolinite at 700 to 850°C by dehydroxylation causes partial or complete breakdown of the crystal lattice structure, forming a transition phase amorphous structure with high pozzolanic reactivity [4, 18]. A carefully controlled production process refines its colour by removing the impurities and tailoring the particle size. The high purity whitish powder of MK produced has the following (typical) physical properties: specific surface area of 16.8 m$^2$/g; median particle size of 1.3μm which is smaller than that of cement (approximately 10μm) and larger than that of silica fume (approximately 0.1μm) and the specific gravity of 2.60 compared to 3.15 for cement. Typical physical and chemical compositions of MK are shown in Tables 2-5 and 2-6 respectively. The combined amount of reactive silica and alumina in MK is over 90%, and the major chemical compound is $Al_2O_3.2SiO_2$ ($AS_2$).

**Table2-5: Physical properties of metakaolin [4]**

| Property | Value |
|---|---|
| Specific gravity | 2.6 |
| Bulk density(kg/m$^3$) | 300 to 400 |
| Physical form | Powder |
| Colour | Off-white |
| Fineness (m$^2$/kg) | 12000-30000 |

**Table 2-6: Typical chemical composition of metakaolin [4]**

| Oxides | $SiO_2$ | $Al_2O_3$ | $Fe_2O_3$ | CaO | MgO | $Na_2O$ | $K_2O$ | $TiO_2$ | L.O.I |
|---|---|---|---|---|---|---|---|---|---|
| % by mass | 51.50 | 40.20 | 1.23 | 2.00 | 0.12 | 0.08 | 0.53 | 2.27 | 2.01 |

## 2.3 Hydration and pozzolanic reaction

When fly ash is incorporated in concrete, the calcium hydroxide (CH) liberated during hydration of PC reacts slowly with the amorphous alumino-silicates, the pozzolanic compounds, present in the FA. The products of these reactions, termed as pozzolanic reaction products, are time-dependent but are mainly of the same type and characteristics of the products of the cement hydration. Thus additional cementitious products become available which impart additional strength to concrete [10]. Marsh and Day [19] reported the amount of CH per gram of cement remains approximately constant for all replacement level of FA with cement in early ages, but FA shows significant reaction by depletion

in the CH content after 14 days, which is due to the pozzolanic reaction. CH depletion increases with time and a higher FA replacement. The pozzolanic reaction is the primary effect of FA, which produces a more hydrated gel due to the reaction of $Al_2O_3$ and $SiO_2$ in FA with $Ca(OH)_2$, a product of cement hydration. Since the gel produced from the pozzolanic reaction can fill in the capillary in concrete, it effectively contributes to concrete strength [20]. Fly ash reacts with lime, which is generated by the Portland clinker hydration and water to form calcium silicate hydrates. The activation of fly ash at 20°C needs a pH of more than 13 because the alkalinity of Portland cement at 20°C only develops to a level higher than 13 with time [21].

Ground granulated blast furnace slag is not a pozzolan but is considered to be a latent hydraulic material. Mixing slag with water hydrates it; however, the hydration products form a thin Si-rich layer on the surface of the slag grains, which essentially stifles any further hydration. Therefore, in order to prevent the formation of the impermeable layer around the slag particles, an alkaline activator has to be used to raise the pH >12 in the vicinity of the slag and thus allowing the continued dissolution of the glass. The hydration of Portland cement produces both CH and alkali hydroxides, and Portland cement is an excellent choice to work as an alkali activator for the hydration of slag [10].

C-S-H, CH, AFm ($C_3A.CaSO_4.12H_2O$), and AFt ($C_3A.3CaSO_4.32H_2O$) are the main products forming from the hydration of a mix of PC and slag which are similar to those that form in a pure PC mix. However, parts of CH are consumed by the hydration of slag, and thus the quantity of the remaining CH is lower than the produced amount of hydration of only PC.

Figure 2-1 shows the amount of slag hydrated as a function of time. It demonstrates that the rate of slag hydration is significantly slower than that of Portland cement, although it is faster than fly ash in the early ages. Approximately 50% slag remains unreacted after one year. The amount of glass in the slag, chemical composition, the proportion and fineness of slag, composition of the cement (particularly the alkali content) and temperature are the main factors affecting the rate of reaction of slag when blended with Portland cement [16].

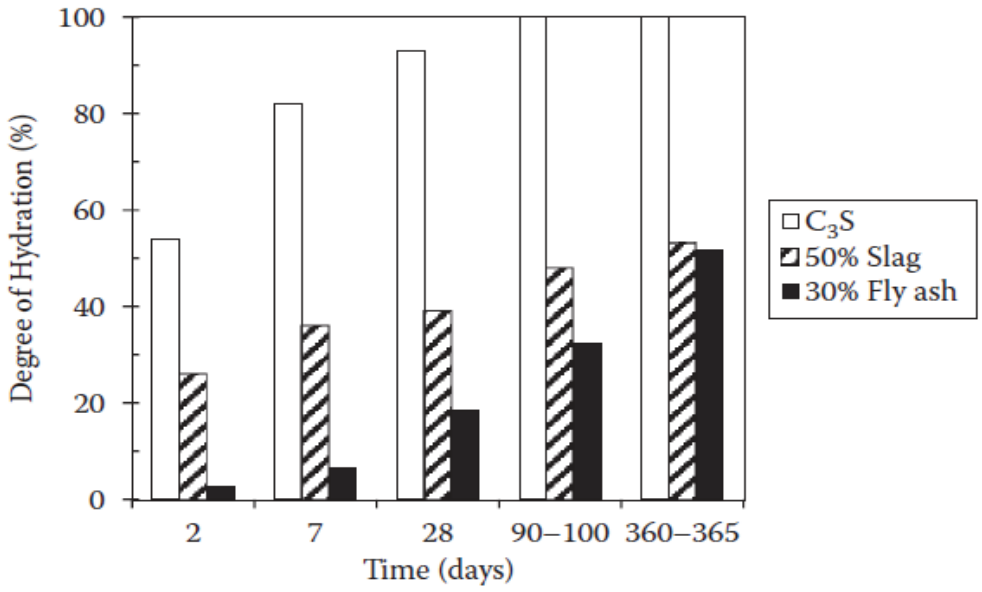


**Figure 2-1: Degree of hydration of $C_3S$ in cement clinker, slag, and fly ash in blended cement [16]**

The pozzolanic reaction of $AS_2$ with CH liberated from cement hydration produces: (i) C-S-H gel; (ii) crystalline calcium aluminate hydrates($C_4AH_{13}$ and $C_3AH_6$); and (iii) crystalline calcium alumino-silicate ($C_2ASH_8$). The crystalline products depend principally on the $AS_2$/CH ratio and calcining temperature [22, 23]. Murat [18] suggested the following equations for the pozzolanic reaction of MK:

$\boldsymbol{AS_2}$ + 6CH + 9H = $C_4AH_{13}$ + 2C-S-H Equation 2-1

$\boldsymbol{AS_2}$ + 5CH + 3H = $C_3AH_6$ + 2C-S-H Equation 2-2

$\boldsymbol{AS_2}$ + 3CH + 6H = $C_2ASH_8$ + C-S-H Equation 2-3

Ambroise et al. [4] observed the following changes during the hydration of cement-metakaolin blended paste: (i) calcium hydroxide was quickly consumed; (ii) microstructure became rich with C-S-H gel and crystalline $CASH_8$; and (iii) pore sizes were reduced with pore structure refinement. MK acted as an accelerating admixture when cement was replaced with MK up to 30% by weight. X-ray Diffraction (XRD) studies by Kim et al. [24] showed that pozzolanic reactivity of MK reduced the CH content depending on the MK content, while the weak peaks of calcium aluminate hydrates (C–A–H) was slightly increased. Metakaolin is superior to silica fume in relation to strength enhancement of concrete at early ages due to increased cement hydration in the presence of metakaolin [25].

## 2.4 Influence of type, fineness, and level of SCMs on consistency and heat of hydration of mortar & concrete

### 2.4.1 Consistency

Sumer [26] reported that the enhanced mortar flow and concrete workability associated with the incorporation of FA into a relevant mix lies in morphological effects associated with fly ash. According to Sumer [26], "the morphologic effect states that there are many microbeads in FA, working as 'lubricating balls' when incorporated in fresh concrete". Helmuth [27] has reported that if the water reduction was due to the spherical shape of the fly ash particles or the lack of chemical reactivity, the water reduction would progressively increase with an increase in fly ash content. However, it is not the case for high volume fly ash content mixes. Mora et al. [28] reported that the flowability of the mix was improved by increasing the fineness of fly ash because of the increased amount of particles per unit mass, which increases the lubricant effect compared to coarser ones.

Several researchers have tried to demonstrate the effect of GGBFS usage and replacement level on the workability and rheology of concrete or mortar. Shi and Qian [29] reported the effect of partially replacing cement with GGBFS up to 60% on the workability of concrete. The test results revealed that substituting part of cement with GGBFS in concretes enhanced workability compared to the concrete without GGBFS. Moreover, the workability increased significantly by increasing the GGBFS level due to better cementitious particle dispersion and surface characteristics of the GGBFS particles, which are smooth, dense, and thus absorb little water during mixing. Meusel and Rose [30] investigated the effect of

substituting cement with highly active slag at 30–50% in concrete. They observed that partially replacing cement with slag improved the workability of concrete mixes, and the improvement increased with higher slag content. However, higher fineness of slag did not have a significant effect on the workability.

Bai et al. [31] reported that the slump of concrete with given water content was significantly reduced with the increase of MK content. Figure 2-2 shows that the high slump concrete experienced a relatively rapid loss of its consistency with the increase of MK content compared to low slump concrete. The reduction in consistency may be attributed to the increase in the surface area of the binder materials, considering the high fineness and low density of MK compared to those of cement. Although MK concretes exhibited reduced slump, Bai et al. [31] experienced that full compaction of MK concretes was achieved due to the ability of MK to impart some degree of thixotropy to concrete.

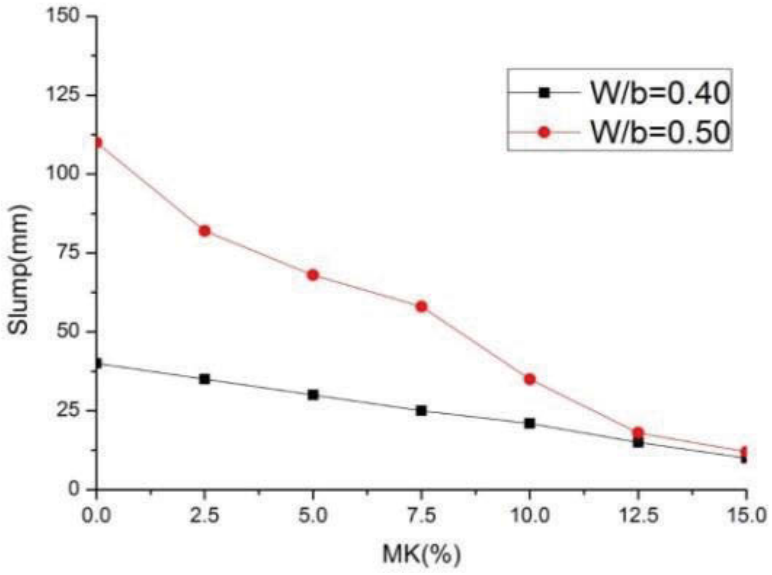


**Figure 2-2: Effect of MK content on the consistency of concretes [31]**

### 2.4.2 **Heat of hydration**

The hydration reaction of cement minerals alite ($C_3S$), belite ($C_2S$), tricalcium aluminate ($C_3A$) and tetracalcium aluminoferrite ($C_4AF$) is an exothermal chemical process. The primary hydration products are calcium silicate hydrate (C-S-H), calcium hydroxide (CH), Ettringite and monosulfate. The hydration process of plain Portland cement can be distinguished by five stages in heat generation in early ages, as reported by several researchers [32-35] shown in Figure 2-3.

In the initial stage, within minutes of mixing cement with water, the aluminate reacts with water and sulfate, forming a gel-like material (ettringite), which can also be roughly annotated as (C-A-S-H) around the cement grains. This reaction releases a huge amount of heat and initiates the first peak of hydration. However, it is hard to detect the first hydration peak as wetting of cement usually happens outside the calorimeter.

Secondly, the dormancy stage: there is a dormant stage for about two to four hours after mixing in which aluminate reaction is controlled by ettringite gel around the cement grain due to limiting access of water to the cement grains, controlling the rate of aluminate reaction and thus little heat is released. However, the alite and belite, main components of cement, slowly dissolve and accumulate calcium and hydroxyl ions in the solution.

Thirdly, the acceleration stage after super-saturation of the solution with calcium ions mainly from dissolving alite and belite, fibre-like C-S-H gel and crystalline CH start to form with significant heat evolution which indicates the second peak of hydration. During this acceleration process, needle-like ettringite (C-A-S-H) also forms as a result of continuing reactions of aluminate and sulfate.

Fourthly, the deceleration stage- the interaction of C-S-H gel and crystalline CH with contact between remaining water and undissolved cement grains slows the alite reaction and thus reduces the heat of hydration. In the meanwhile, the amount of sulfate starts to be depleted, and thus the remaining aluminate reacts with ettringite to form monosulfate, generating a small amount of heat generation which may be associated with the third hydration peak.

Finally, the slow continued reaction stage- belite dissolves and releases calcium ions very slowly and starts to produce C-S-H and CH after several days. However, as long as alite and belite remain and there is water in the system, the silicates will continue to hydrate [34, 35].

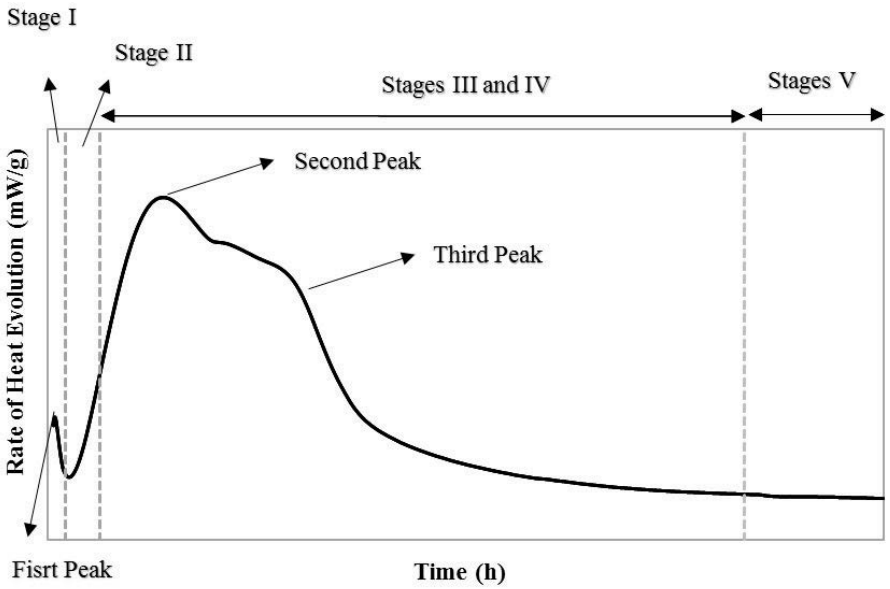


**Figure 2-3: Common cement heat evolution curve [34]**

Snelson et al. [36] investigated the effect of fly ash replacement levels of up to 40% on the rate of heat evolution during hydration, and the heat of hydration in the paste. For binary PC–FA blends, there is a systematic reduction in heat output and the cumulative heat of hydration (up to 120 h) with an increase in the FA replacement level as shown in Figures 2-4 and 2-5. They concluded that this reduction could be due to the relatively lower specific surface area of FA and also the low solubility of alumino-silicate glass in the alkaline environment created by PC hydration compared to PC only.

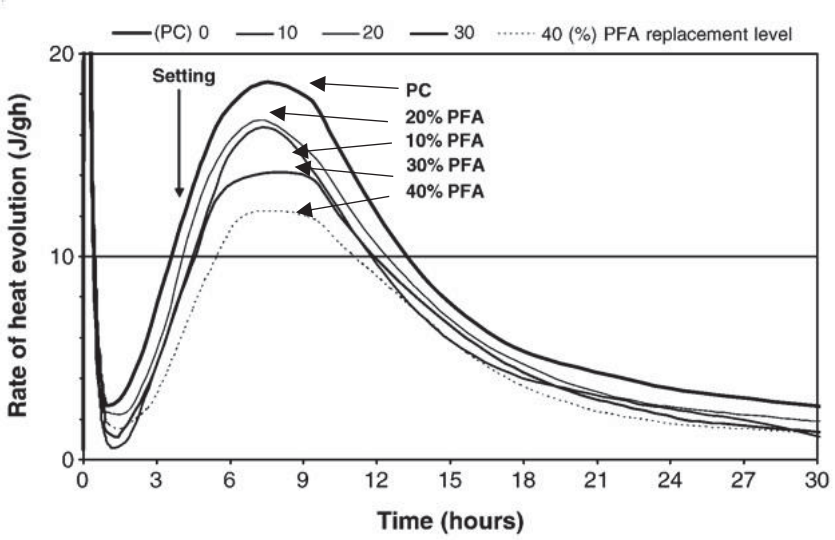


**Figure 2-4: Maximum heat evolution rate versus PC replacement level for binary PC–FA blends [36]**

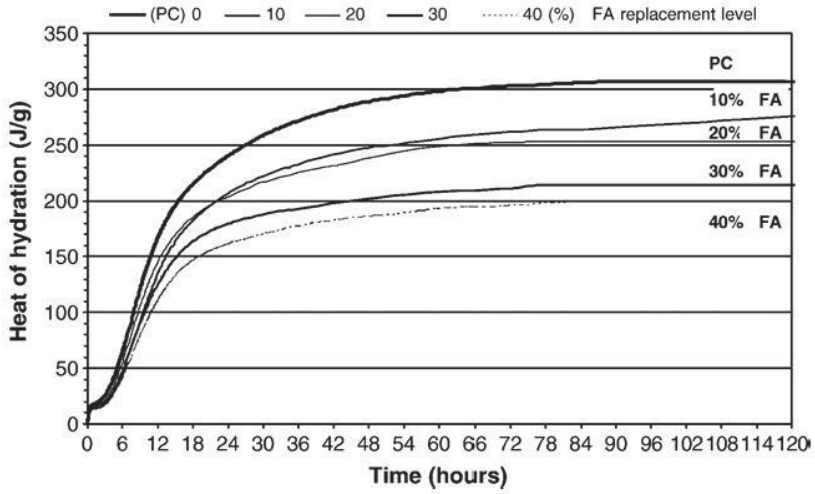


**Figure 2-5: Cumulative heat of hydration of PC–FA blends at 120 h relative to PC [36]**

Pacewska et al. [37] investigated physicochemical properties of three different fly ashes (PF, PP, PM) on cement hydration with specific surface areas of 8.3, 5.9 and 4.6 $m^2/g$ respectively. Cement was replaced by 10, 20 and 30% of mentioned fly ashes and constant water to binder ratio (w/b) of 0.5 was used for all mixes. Heat evolution curves and heat released values are shown in Figures 2-6 and 2-7. They noted that the kind of coal and fineness of fly ash influence the heat evolution. In addition, flatter and extended in time heat evolution curves can be seen by partially replacing cement with fly ash (especially 30% replacement) compared to control cement paste. The induction period is also elongated possibly due to slow formation of the hydration products. Łaskawiec et al. [38] reported that heat evolution rate decreases with the increased amount of fly ash and it is accompanied with delayed and extended time, forming of silicate phases. Ballim et al. [39] also reported that the rate to reach peak rates of heat evolution in FA blended binders decreases with increasing FA content.

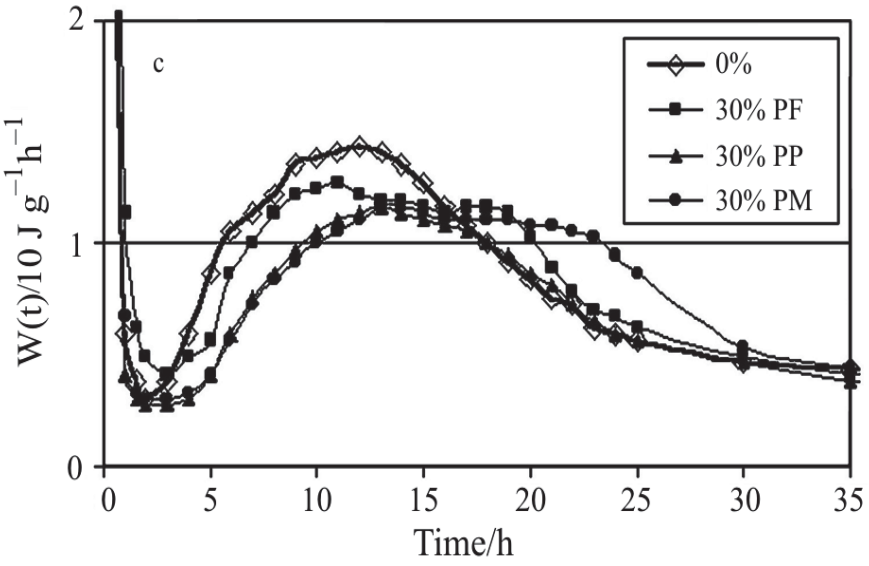


**Figure 2-6: Heat evolution curves for cement pastes with 30% fly ash replacement [37]**

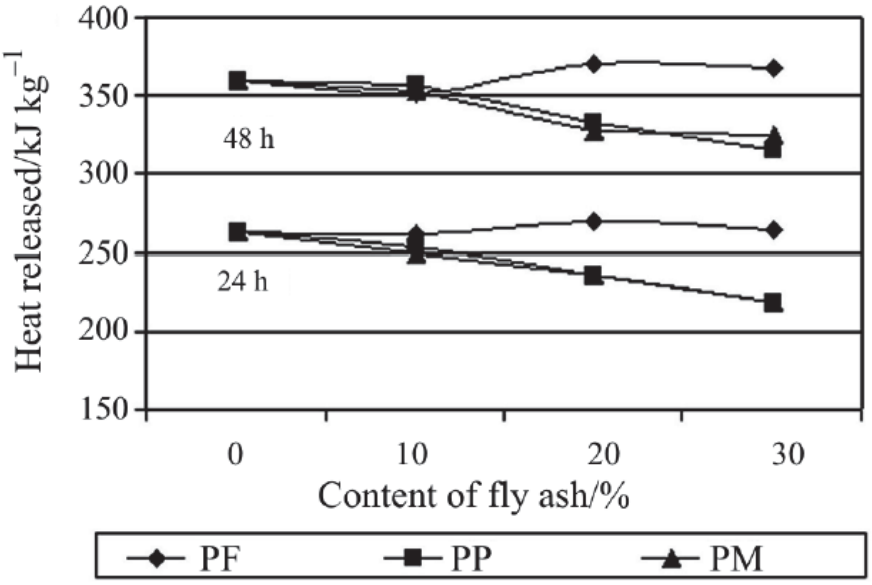


**Figure 2-7: Heat evolved within 24 and 72 hours of hydration [37]**

The effect of various levels of GGBFS was investigated in the rate of heat evolution during the early stages of hydration in concrete by Ballim and Graham [39]. They replaced cement with 20%, 40%, 60% and 80% GGBFS with fixed water to binder ratio of 0.67. The concrete specimens were subjected to the heat of the hydration test under adiabatic conditions. Figure 2-8, demonstrates the reduction in the peak hydration heat rate by increasing the GGBFS content. The reason for this reduction is due to the dilution effect as the reactive Portland cement is replaced by slag which is less reactive.

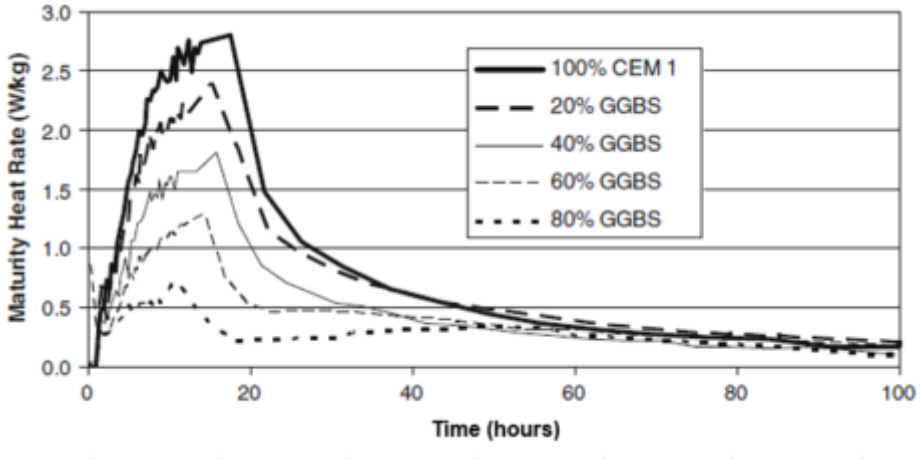


**Figure 2-8: Heat rate profiles for the concrete containing cement and GGBFS [38]**

Gruyaert et al. [40] studied the effect of various levels of GGBFS on the heat of hydration in pastes. Besides the control mixes containing the only PC as a binder, some mixes with 15–85% level of cement replacement with GGBFS were made. Isothermal calorimetric measurements were carried out at 10°C, 20°C, and 35°C. The fixed water-to-binder ratio (w/b) of 0.5 was used for all mixes. All the mix components were kept in a test place for 48 hours before the mix to avoid significant temperature difference between the paste and the isothermal

environment. Subsequently, mixing was carried out manually. The first hydration peak could not be registered entirely as mixing happened outside the calorimeter.

Figure 2-9 shows the change of the heat production rate (mW/g binder) in time at 10°C, 20°C and 35°C by increasing GGBFS content. As can be seen, the hydration of binders accelerates by increasing the curing temperatures and thus causing larger hydration peaks which appearing earlier. Besides the first (rapid reaction, not shown) and second hydration peak (hydration of $C_3S$), a third hydration peak can be seen by partially replacing cement with GGBFS. They reported that releasing a sufficient amount of CH by cement hydration and reaching the correct alkalinity in pore solution activate the slag reaction and thus the third peak in heat evolution curves appears. Secondly, earlier appearance of the second hydration peak with increasing GGBFS content is due to the effect of GGBFS, which accelerates the PC hydration.

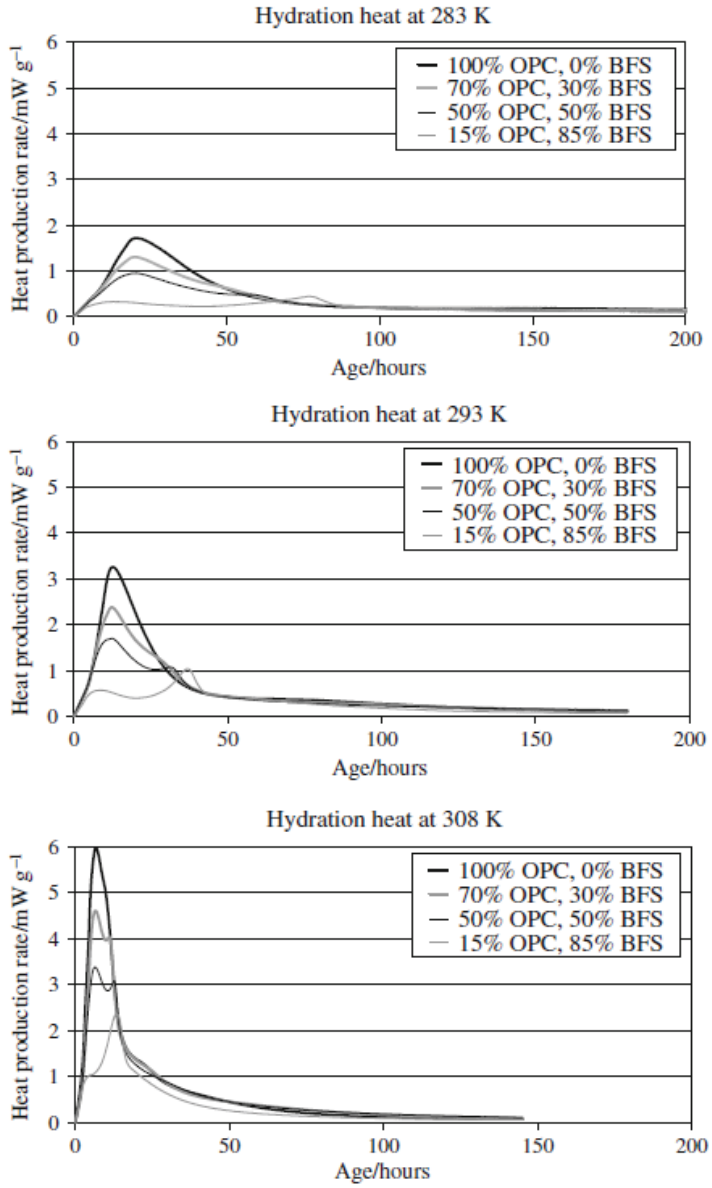


**Figure 2-9: Heat production rate mW g-1 in function of age under isothermal conditions (10 °C, 20 °C and 35 °C) for pastes with slag-to binder ratios of 0, 30, 50 or 85% [40]**

Snelson et al. [36] investigated the effect of replacing cement with MK up to 20% on the rate of heat evolution during hydration, and the heat of hydration in the paste for up to 120 hours. For the binary PC–MK blends, the pozzolanic reaction of MK had a significant contribution to the cumulative heat of hydration

as shown in Figures 2-10 and 2-11. However, the reaction of MK is governed not only by the available water but also by the supply of $Ca^{2+}$ ions due to PC hydration; as the MK to PC ratio increases the supply of $Ca^{2+}$ ions will decrease and thus the MK reaction will diminish.

As Kadri et al. [41] reported, acting as nucleation sites for hydration precipitation, followed by the dissolution of amorphous silica and alumina at early hours because of great fineness of the MK particles, accelerates the cement hydration process. The observation is in agreement with that found by Frıas et al. [42], who reported that calcium silica hydrate gel was first formed at about six hours, followed by hydrated calcium aluminate at between 13 to 20 hours which could be due to the reaction of the amorphous alumina in MK. In addition, ettringite formation and its subsequent transformation to monosulfate as a result of high $Al_2O_3$ content of MK is likely another reason for acceleration of the rate of heat evolution in the MK mixes, especially the third peak [43, 44].

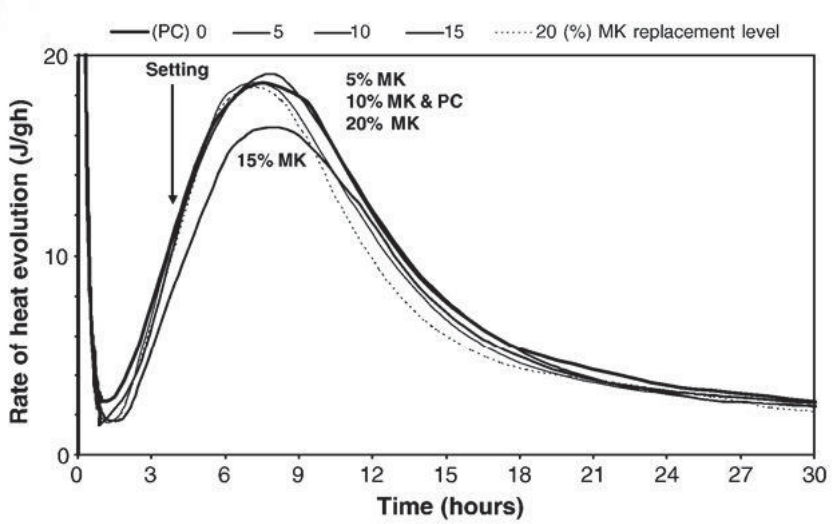


**Figure 2-10: Maximum heat evolution rate versus PC replacement level for binary PC–MK blends [36]**

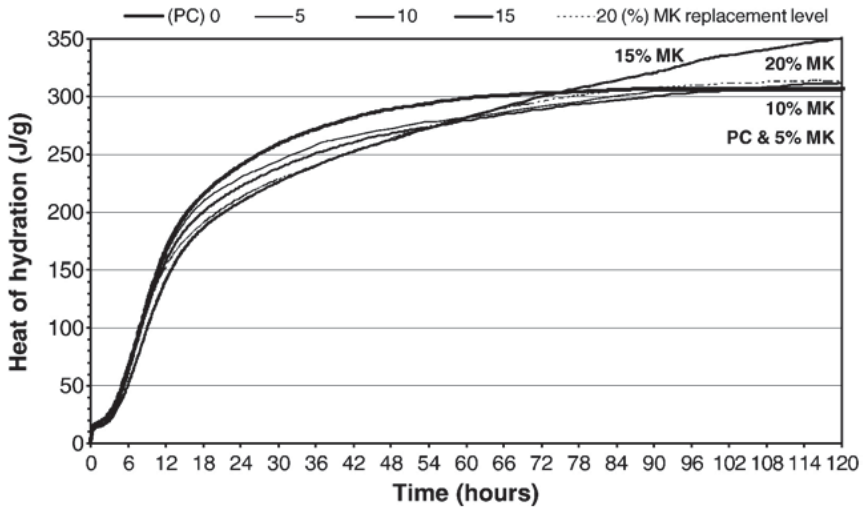


**Figure 2-11: Cumulative heat of hydration of PC–FA blends at 120 h relative to PC [36]**

## 2.5 Effect of type, fineness, and level of SCMs on hardened properties of mortar & concrete

### 2.5.1 Porosity and pore size distribution

Chindaprasirt et al. [45] indicated that the pore sizes of hardened blended cement paste with a water to binder ratio of 0.35 were significantly affected by the rate of replacement and the fineness of fly ash. The substitution of cement at 0%, 20%, and 40% (by weight) by original fly ash (OFA) with a median particle size of 19.1μm decreased the average pore sizes of blended cement paste. There was a further decrease in the average pore sizes of blended cement paste with the incorporation of classified fly ash (CFA) with a median particle size of 6.4 μm as shown in Figure 2-12. It is possibly due to the gradual filling of large pores formed by hydration reaction, the nucleation effect, the packing effect, and the pozzolanic reaction of fly ash particles. From Figure 2-13, incorporation of both fly ashes, especially in higher replacement level, increased the percentage of gel

porosity of the blended cement paste compared to that of PC paste. However, finer fly ash was more effective in increasing the gel porosity compared to the coarser fly ash due to better dispersion in the cement paste.

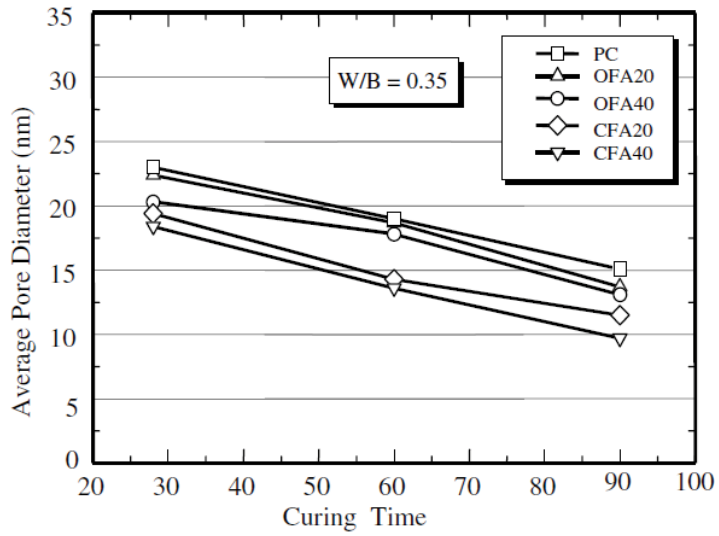


**Figure 2-12: Average pore diameters of pastes at 28, 60 nd 90 days [45]**

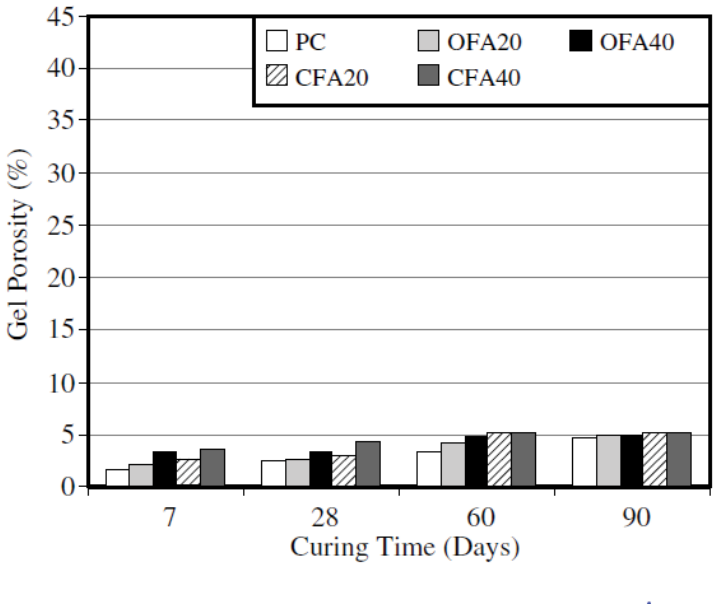


**Figure 2-13: Gel pores of pastes at 7, 28, 60 and 90 days [45]**

Chindaprasirt et al. [46] also reported the X-ray diffraction (XRD) results at 90 days with 20% cement replacement with both fly ashes are shown in Figure 2-14. This indicated that the blended cement paste with classified fly ash was more effective at reducing the intensity of $Ca(OH)_2$ than that of the original fly ash. It is well known that the degree of pozzolanic reaction in a blended cement paste is directly related to $Ca(OH)_2$ consumption. The main factors which influence the pozzolanic reactivity are fineness and the glassy phase content of fly ash as confirmed by other researchers [47, 48]. This showed that fly ash with smaller particle size provides more silica and alumina compounds which increase the pozzolanic reactivity as a result of higher specific surface area compared to the coarser fly ash. Therefore, the consumption of $Ca(OH)_2$ increases and thus less $Ca(OH)_2$ remains in the system.

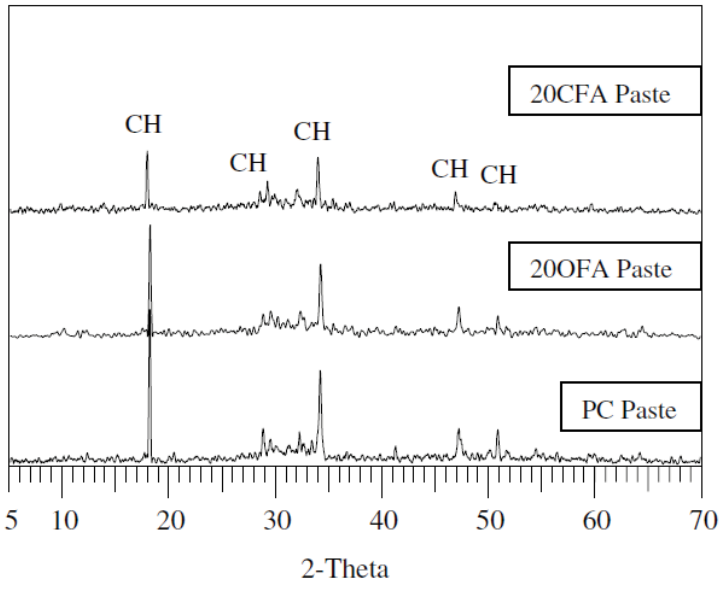


**Figure 2-14: XRD patterns of PC, 40OFA and 40CFA pastes at 90 days [46]**

Johari et al. [49] reported that the effect of partially replacing cement with FA, GGBFS and MK in reducing the porosity of mortar with a fixed water to binder ratio of 0.28 at the age of 28 days, measured using the Mercury Intrusion Porosimetry (MIP) apparatus. The effect of SCMs on the value of porosity, median pore diameter and volume of pores are shown in Tables 2-7 and 2-8. The pores are subdivided into mesopores (<15 nm, 15–30 nm and 30–50 nm) and macropores (>50 nm). It can be noted that the influence of the SCMs is to shift the distribution of pore size towards a finer distribution in addition to the reduction in the porosity and the median pore size of the high strength mortars.

The pozzolanic reaction and possibly the filler effect due to partially replacing cement with SCMs are the major reasons for the substantial reduction in the volume of macropores and the significant increase in the volume of mesopores in high strength mortar mixes [50, 51]. As a result of the pozzolanic reaction, the calcium hydroxide ($Ca(OH)_2$) is transformed into secondary C–S–H gel and thus leads to refining the pore structure by transforming of coarser pores into finer ones. It is well known that the higher $Ca(OH)_2$ content in the hydrated binder matrix is responsible for increasing the volume of continuous pores. However, the pozzolanic reaction refines the pore structure by producing the secondary C–S–H gel due to the consumption of the calcium hydroxide ($Ca(OH)_2$) in the system, thus transforming the coarser pores into finer ones.

**Table 2-7: Summary of the test results for pore structure of mortar [49]**

| Mortar Mix | Porosity (%) | Relative Reduction (%) | Median Pore Diameter (nm) | Relative Reduction (%) | Average Pore Diameter (%) | Relative reduction |
|---|---|---|---|---|---|---|
| OPC | 13.0 | - | 37.1 | - | 35.6 | - |
| GGBFS20 | 11.4 | 14.5 | 25.2 | 32.1 | 19.6 | 44.9 |
| GGBFS40 | 9.0 | 30.7 | 25.6 | 31.0 | 19.6 | 44.9 |
| GGBFS60 | 9.2 | 29.3 | 20.1 | 45.8 | 10.6 | 70.2 |
| FA10 | 11.5 | 12.0 | 30.9 | 16.7 | 21.7 | 39.0 |
| FA20 | 11.5 | 11.5 | 24.2 | 34.8 | 14.4 | 59.6 |
| FA30 | 11.8 | 9.7 | 21.8 | 41.2 | 14.3 | 59.8 |
| MK5 | 10.0 | 23.6 | 18.4 | 50.4 | 13.1 | 63.2 |
| MK10 | 9.7 | 25.8 | 11.8 | 68.2 | 9.0 | 74.7 |
| MK15 | 9.4 | 27.6 | 7.8 | 79.0 | 6.8 | 80.9 |

**Table 2-8: The influence of SCMs on the percentage of the volume of pores in the size range of mesopores and macropores [49]**

| Mortar mix | Volume of pores in different size range (%) | | | | | | | |
|---|---|---|---|---|---|---|---|---|
| | <15nm | Relative increase (%) | 15-30nm | Relative increase (%) | 30-50nm | Relative reduction (%) | >50nm | Relative reduction (%) |
| OPC | 6.2 | | 7.4 | | 43.3 | | 43.3 | |
| GGBFS20 | 11.8 | 92.0 | 44.9 | 510.6 | 24.8 | 42.7 | 18.5 | 57.2 |
| GGBFS40 | 11.6 | 88.3 | 46.1 | 526.7 | 29.6 | 31.7 | 12.8 | 70.4 |
| GGBFS60 | 36.3 | 490.6 | 27.1 | 269.0 | 9.7 | 77.6 | 26.9 | 37.8 |
| FA10 | 9.1 | 47.8 | 29.8 | 305.3 | 43.3 | -0.2 | 17.8 | 58.9 |
| FA20 | 25.4 | 312.4 | 26.7 | 262.7 | 34.9 | 19.3 | 13.1 | 69.7 |
| FA30 | 27.1 | 341.3 | 36.4 | 395.6 | 20.2 | 53.2 | 16.2 | 62.5 |
| MK5 | 29.2 | 375.4 | 48.2 | 555.9 | 14.5 | 66.5 | 8.0 | 81.4 |
| MK10 | 57.3 | 831.1 | 32.6 | 343.9 | 4.2 | 90.3 | 5.9 | 86.4 |
| MK15 | 70.5 | 1045.9 | 16.7 | 127.8 | 3.3 | 92.5 | 9.5 | 78.0 |

Khatib and Wild [52] studied the porosity and pore size distribution of cement paste containing 5, 10 and 15% MK at a water to binder ratio of 0.55 in periods from 3 to 365 days, determined using MIP apparatus. Figure 2-15 shows that the incorporation of MK in cement paste caused pore size refinement in hardened cement paste. In addition, the proportion of pores with radii smaller than 20 μm was increased while it decreased with radii bigger than 20 μm as the cement replacement level with MK was increased. The inclusion of MK refined the pore structure of the binder paste and reduced the permeability. The secondary CSH due to the reaction of MK with calcium hydroxide, filled the voids in the interfacial transition zone surrounding aggregate particles [53].

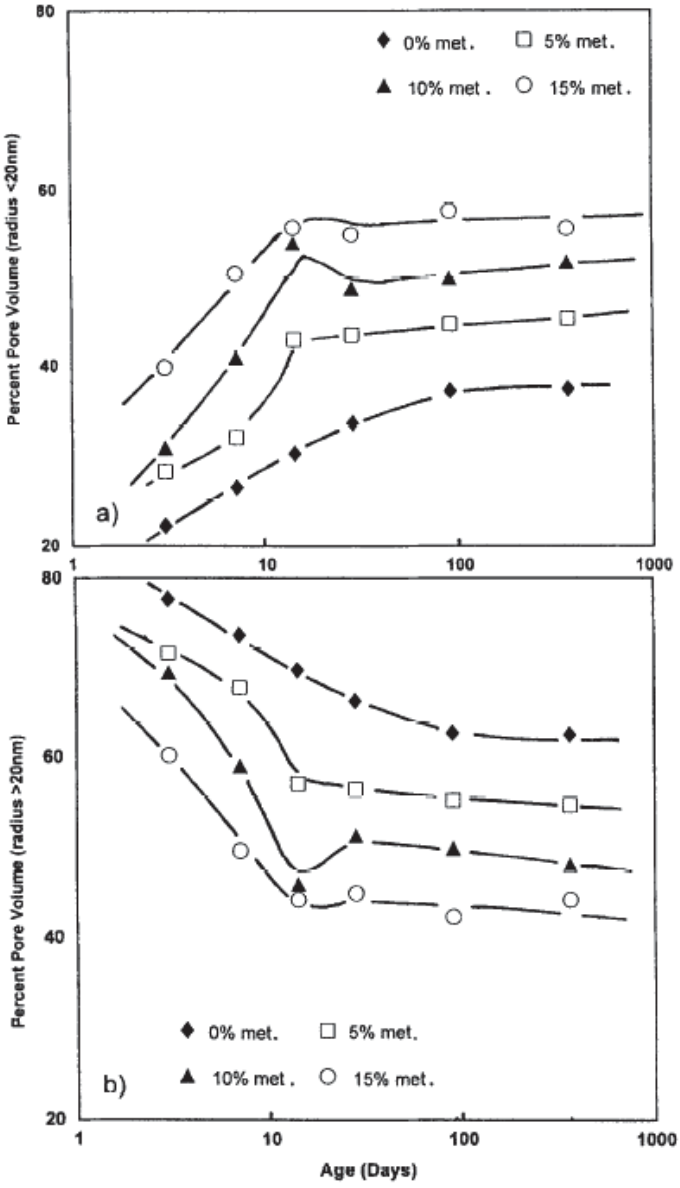


**Figure 2-15: Pore size distribution versus curing time for a) radii<20µm and b) radii>of µm pastes [52]**

Poon et al. [25] investigated the average pore diameter of high-performance cement paste blended with MK having w/b ratio of 0.3. They observed a significant drop in the average pore diameter with the increase in MK as the cement replacement material; the results are shown in Figure 2-16. For 90-day old blended paste with 20% MK, the average pore diameter was 0.0114 µm compared

to 0.0348 μm for cement paste of the same age. At the same time, the total porosity was 9.21% for blended paste compared to 14.0% for cement paste.

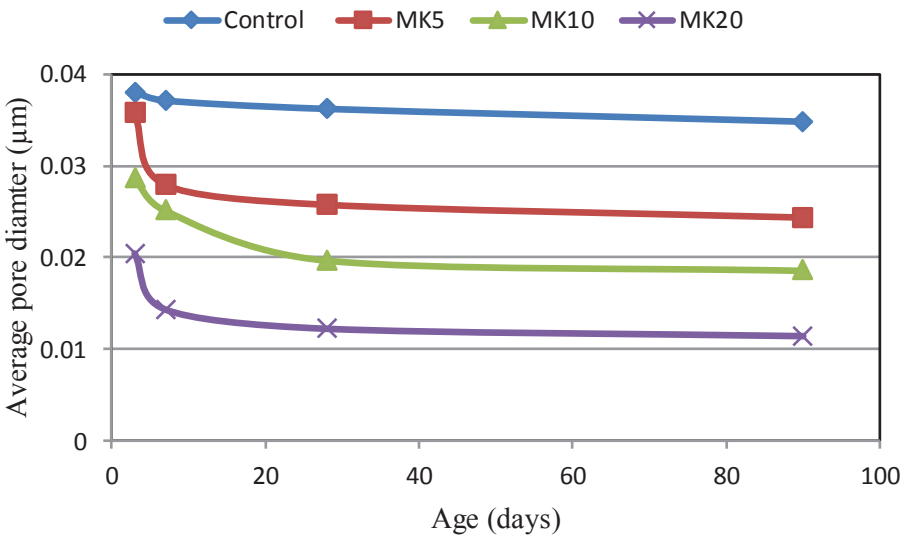


**Figure 2-16: Average pore diameter of blended cement pastes [25]**

Poon et al. [54] reported the variation in total porosity with age for high performance concretes shown in Figure 2-17, having the water to binder ratio of 0.30 and 10% cement replacement with either metakaolin or silica fume. The total porosity of concrete has dropped with increasing age due to the combined effects of cement hydration and pozzolanic reaction. MK is found to be superior to silica fume in reducing the total porosity.

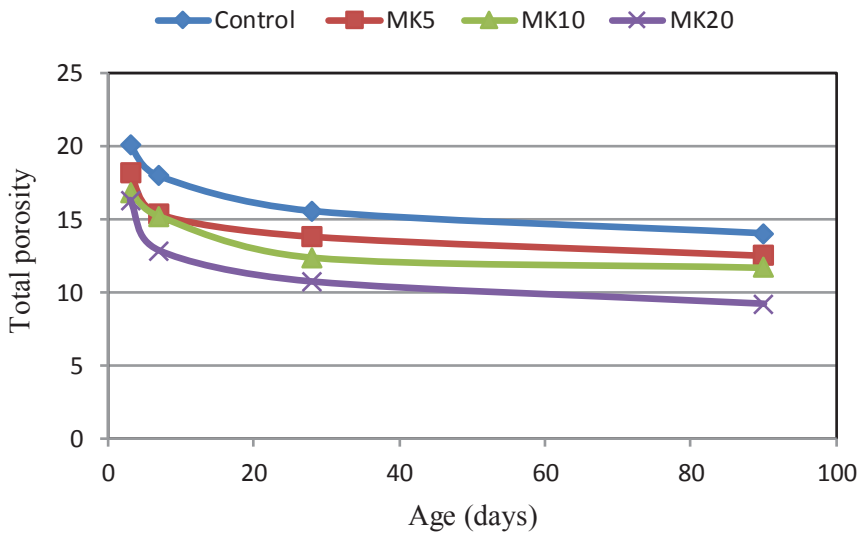


**Figure 2-17: Total porosity of high-performance concrete [54]**

### 2.5.2 Strength properties

Johari et al. [49] reported the significant reduction in 1-day compressive strength of the high strength concrete containing 10%, 20% and 30% FA compared to PC concrete at a fixed w/b ratio. The reduction in compressive strength at the age of 1 day increased at higher replacement levels. The slow rate of pozzolanic reaction between FA and calcium hydroxide generated from cement hydration could be the main reason for this effect. However, the 28-day relative strength of the high strength concrete containing fly ash was enhanced compared to the PC concrete.

Joshi and Lohita [55] also noted that the reduction of compressive strength in early ages (up to 28 days) could be due to dilution of total quantity of cement which is able to hydrate and provide early-age strength with partial cement replacement with FA which has the potential to inhibit the strength development of the mortar mixes. The effect is more evident at higher replacement level due to

the slow pozzolanic reaction between the fly ash and calcium hydroxide (CH) generated from cement hydration.

The effect of partially replacing fine aggregate (sand) with varying percentages of fly ash (10%, 20%, 30%, 40% and 50%) on the flexural strength up to 365 days was investigated by Siddique [56]. The results showed an increase in flexural strength with age at all fly ash percentages compared to control mix, due to the slow reaction of fly ash with calcium hydroxide, a product of cement hydration as presented in Figure 2-18. The ACI committee [57] reported that the siliceous glass is the primary contributor from the fly ash to the pozzolanic reaction in concrete since it is the amorphous silica that combines with free lime and water to form calcium silicate hydrate (C-S-H), the binder in concrete.

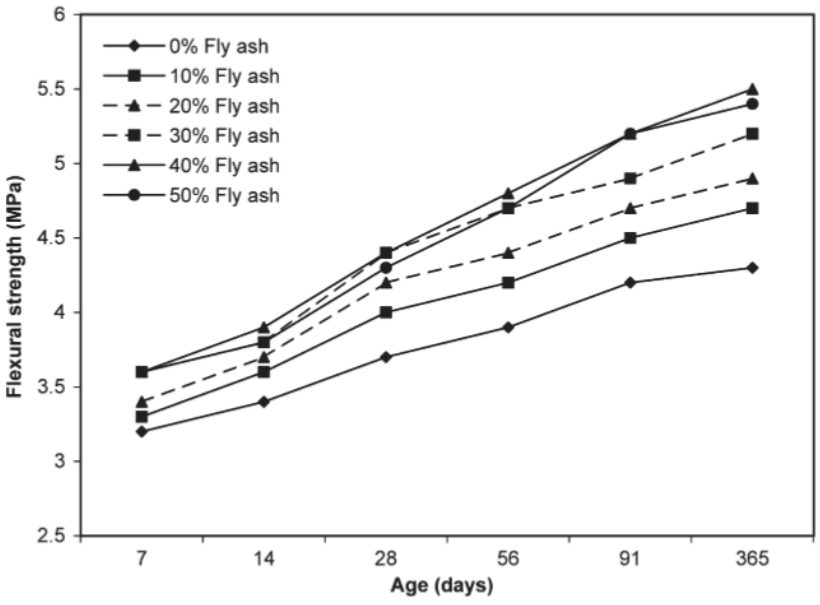


**Figure 2-18: Flexural strength development versus age [56]**

Cheng et al. [58] investigated the effect of replacing cement with 40% and 60% GGBFS on the compressive strength of concrete with a fixed binder content and a fixed water to binder ratio of 0.55 and then comparing the results with the

control mix without any GGBFS content. The results after 91 days revealed that the compressive strength of mixes containing 40% and 60% GGBFS was higher than that of control mix as shown in Figure 2-19. This possibly could be due to the slow reaction of the glassy compounds in GGBFS with water, and it takes time to obtain hydroxyl ions from the hydration product of Portland cement to break down the glassy slag particles at an early age.

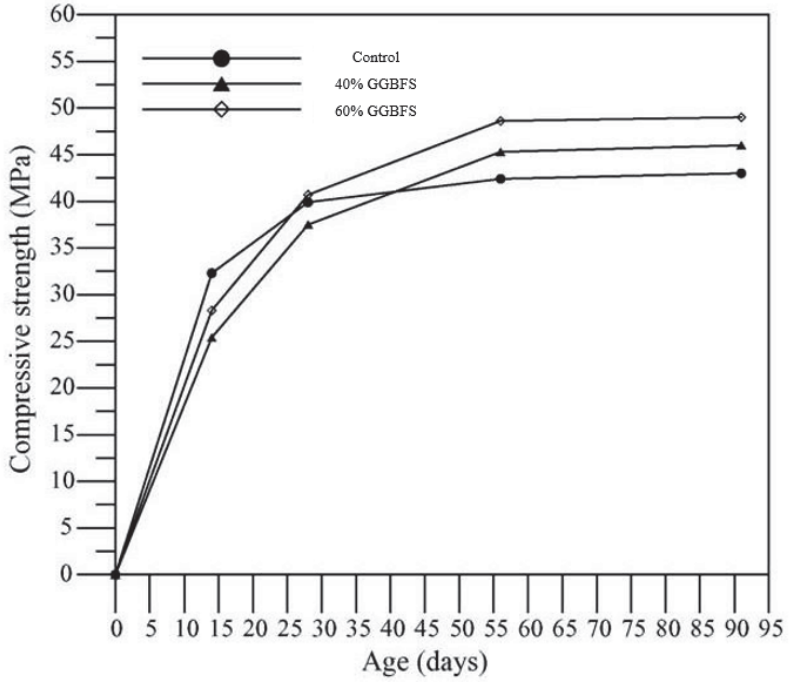


**Figure 2-19: Compressive strength development curves versus age [58]**

Khatib and Hibbert [59] investigated the influence of GGBFS on the compressive and flexural strengths of concrete for up to 90 days by partially replacing PC with 40, 60 and 80% GGBFS (by mass) with fixed binder content and fixed water to binder ratio of 0.50 as shown in Figures 2-20 and 2-21, respectively. There was a systematic decrease in compressive strength with an increase in GGBFS content during the early stages of hydration. Beyond 28 days

and up to at least 90 days, the presence of GGBFS was highly beneficial at 40 and 60% replacement, with a strength exceeding that of the control. A noticeable strength reduction at all ages is observed at 80% GGBFS. It is likely due to the slow-developing reactivity of GGBFS in early age as well as the dilution effect, as part of cement was substituted by slow reactive material [60, 61].

The flexural strength of concrete containing 60% GGBFS was noticeably higher than that of the control, whereas a slight decrease at 40% and marked decrease at 80% replacement were observed. In general, The pozzolanic material in concrete contributes to the strength improvement in concrete mainly in three main ways: (i) filler effect (immediate); (ii) accelerating effect (within 24h), and (iii) pozzolanic effect (time-dependent) [59].

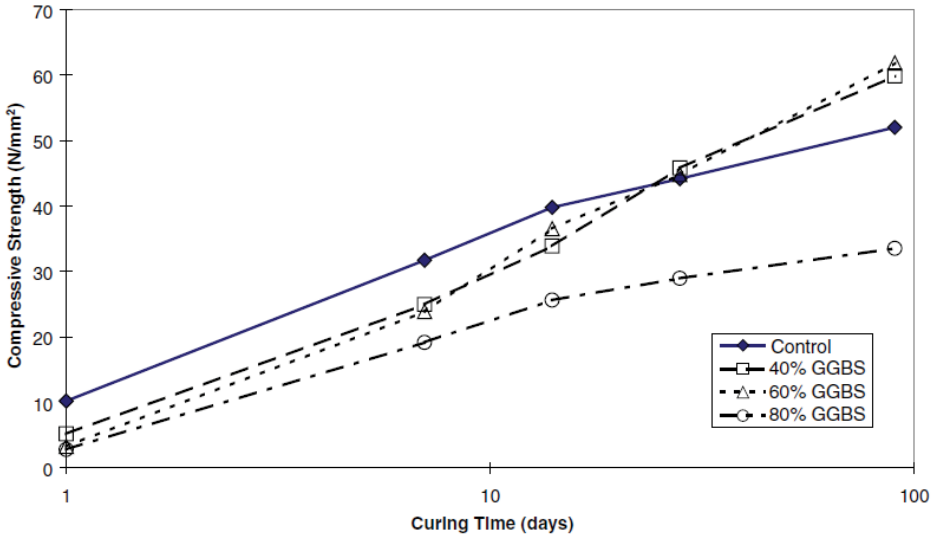


**Figure 2-20: Effect of GGBFS on compressive strength development [59]**

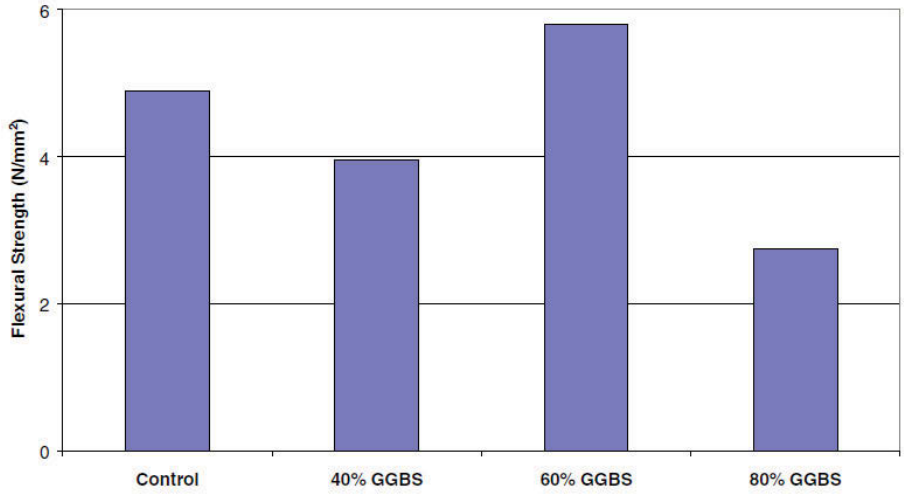


**Figure 2-21: Effect of GGBS on flexural strength at 90 days [59]**

Quin and Li [62] studied the mechanical properties of concrete with increasing MK content at a w/b ratio of 0.38. Table 2-9 summarises the results, and Figure 2-22 compares the hardened concrete properties of MK concrete at 28 days. The compressive and flexural strengths of concrete are found to increase with the increase in the MK content at all ages. The results show that compressive strength is the most enhanced property of concrete. With 15% MK, the compressive strength was increased by 84% and 34% at 28 and 90 days, respectively. Therefore, the effectiveness of MK in improving the compressive strength is reduced with the increase of age of concrete. The early age strength increases could be due to the finer particle size (3.5μm) and higher specific surface area of MK, which accelerates the hydration reaction and packs into cement particles gaps. On the other hand, the long-term strength of concrete is increased through the pozzolanic reaction of MK particles with calcium hydroxide, a by-product of cement hydration.

**Table 2-9: Effect of metakaolin content on the compressive and flexural strength of concrete [62]**

| Age (days) | Property | Control (MPa) | Cement replacement with MK | | |
|---|---|---|---|---|---|
| | | | 5% | 10% | 15% |
| | | | Increase percentage (%) | | |
| 3 | Compressive strength | 27.9 | 1.29 | 1.40 | 1.51 |
| 28 | | 37.8 | 1.21 | 1.68 | 1.84 |
| 60 | | 58.0 | 1.08 | 1.15 | 1.34 |
| 28 | Flexural strength | 4.7 | 1.02 | 1.32 | 1.38 |
| 80 | | 5.7 | 1.02 | 1.13 | 1.24 |

Qian and Li [62] observed that MK is less effective in improving the flexural strength compared to compressive strength shown in Figure 2-22. Five percent MK had 2% improvement in the flexural strength of concrete at 28 days shown in Table 2-9. At 10% MK, the flexural strength was increased by 32% and further improvements of 38% were recorded at 15% MK. The results also showed that with the increase in age from 28 to 80 days, the flexural strength improvement of the mix containing 10% MK had dropped from 32% to 13%. In general, the effectiveness of MK in increasing the compressive strength even in early age is due to finer particle size and higher specific surface area of MK, which accelerate the pozzolanic reaction and packs into cement particles gaps. The loose structure of MK after heated activation at high temperatures is another reason for its high reactivity [63].

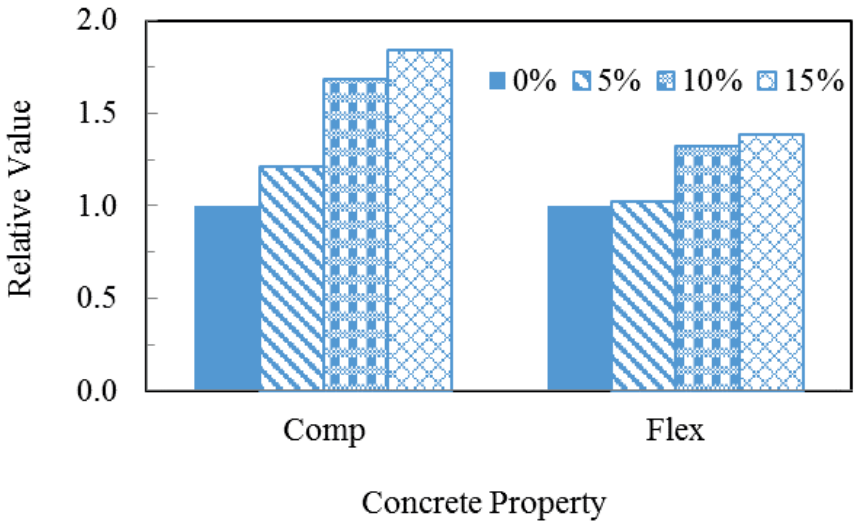


**Figure 2-22: Effectiveness of MK on 28-day properties of concrete [62]**

Poon et al. [54] studied the effectiveness of MK content up to 15% on the compressive strength of concrete over 90 days at the w/b ratios of 0.30 and 0.50. The results shown in Figure 2-23 indicate that the effectiveness of MK was optimum at 10% MK content and increased with the increase in the w/b ratio.

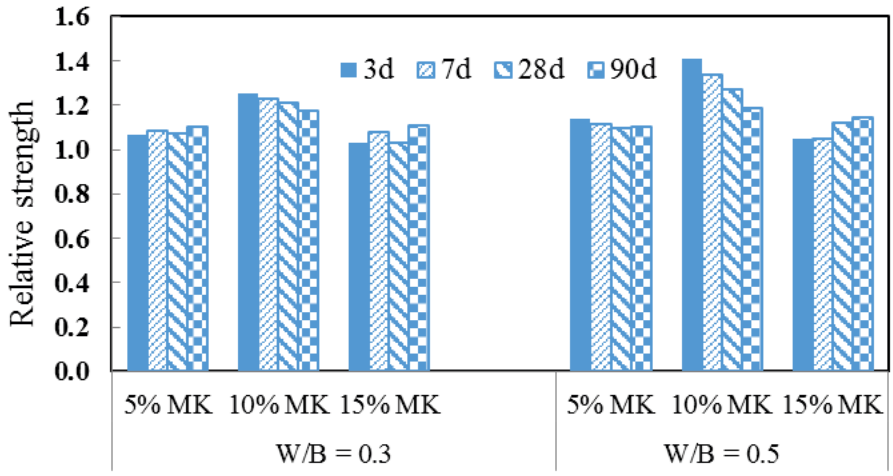


**Figure 2-23: Effectiveness of MK in concrete - function of age and w/b ratio [54]**

### 2.5.3 **Drying shrinkage**

The effect of different replacement levels of FA on drying shrinkage of mortar at fixed w/b ratio of 0.5 was investigated by Atis et al. [64]. They reported that the shrinkage of fly ash mortar decreased with increasing cement replacement level with FA. Shrinkage of mortar, containing 10, 20 and 30% fly ash was 25, 37 and 43%, respectively, lower than that for Portland cement mortar at the end of 5 months. This could be attributed to the reduction in the amount of cement paste in a unit volume of the mortar mix with cement replacement with fly ash.

Li and Yao [65] studied the drying shrinkage of three high-performance concrete mixes as shown in Table 2-10, with the same water content and water to binder ratio, up to 180 days. The results showed partially replacing cement with ultrafine GGBFS (concrete B), and ultrafine GGBFS and silica fume (SF) (concrete C) had a considerable effect in decreasing the drying shrinkage of concrete compared to the control mix (concrete A) as shown in Figure 2-24. In their research, the binder was the only factor, which changed among many factors, such as type and amount of aggregate, the curing system, and water content influencing the drying shrinkage value. The reduction in drying shrinkage by partially replacing cement with ultrafine GGBFS and SF is possibly due to increasing the amount of C-S-H gel hydrates and the density of hardened cement paste, which makes concrete stronger and restricts the water evaporation.

**Table 2-10: Mix proportioning (kg/$m^3$) [65]**

| Concrete | Cement (kg) | GGBS (kg) | SF (kg) | SP (%) | Coarse aggregate (kg) | Fine aggregate (kg) | Water (kg) |
|---|---|---|---|---|---|---|---|
| A | 600 | - | - | 1.6 | 1134 | 610 | 156 |
| B | 420 | 180 | - | 1.6 | 1134 | 610 | 156 |
| C | 360 | 180 | 60 | 1.6 | 1134 | 610 | 156 |

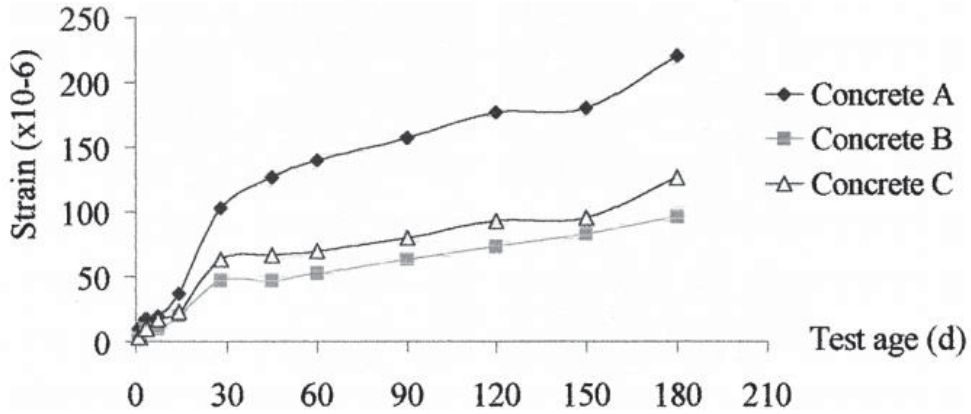


**Figure 2-24: Test results of drying shrinkage of concrete [65]**

Brooks and Johari [66] investigated the effectiveness of MK (5%, 10% and 15% ) on the drying shrinkage of high-strength concrete with the same water content and fixed water to binder ratio of 0.28 as shown in Figure 2-25. It can be seen that 200-day drying shrinkage of concrete had dropped from 416 microstrain (for control concrete) to 228, 199 and 189 microstrains for concretes with to 5%, 10%, and 15% MK content, respectively. This could be due to the reduced moisture loss from MK concrete as fine particles of MK accelerate the pozzolanic reaction with calcium hydroxide and consumes part of the water in the system and thus leaving less water available for drying.

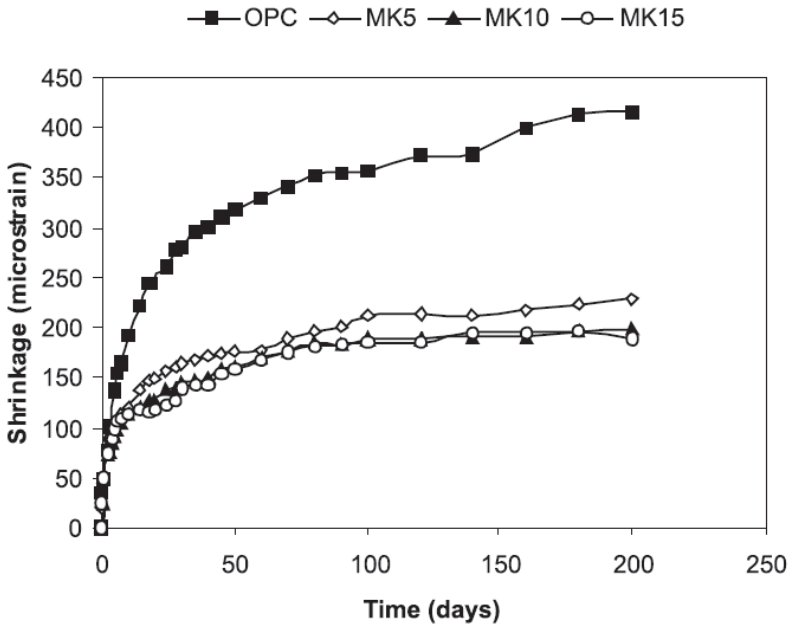


**Figure 2-25: Effect of metakaolin on drying shrinkage [66]**

## 2.6 Influence of type, fineness, and level of SCMs on durability properties of mortar & concrete

### 2.6.1 Chloride resistance

The main result of a chloride attack in the concrete is to cause corrosion of the steel reinforcement, thus damaging the surrounding concrete. It is widely accepted that most deterioration mechanisms affecting concrete are either influenced or promoted by the availability and transportation of water through the permeable voids (interconnected voids) of the pore structure of concrete. Water provides the medium by which many aggressive agents (i.e. chlorides, sulfates etc.) are transported into concrete. Restricting the movement of moisture into the concrete has a major effect in controlling the deterioration processes such as corrosion of the steel reinforcement, chloride ingress, alkali-aggregate reactions, and sulfate and chemical attacks in the concrete. For many structures, the primary

transport mechanism is considered to be the absorption of surface water due to capillary suction, particularly in their early lives, while the ionic diffusion is more significant when the concrete is saturated [67].

There are different methods of increasing the chloride binding capacity as well as impermeability of concrete to chloride attack. As Justnes [68] reported, the rate of chloride binding depends on many factors among which some are related to the binder type. Firstly, the $C_3A$ and $C_4AF$ content in the cement is a major factor since the formation of calcium chloroaluminate, sometimes referred to as Friedel's salt, between chloride and monosulfoaluminate (AFm phases), removes considerable amounts of chloride from the pore solution, which is known as chemical binding [69]. Chloride ions can also be removed from pore solution due to adsorption by hydration products, which it is known as physical binding.

As Luping and Nilsson [70] reported, chloride binding capacity mainly depends on the amount of C-S-H gel in the concrete, regardless of w/c ratio and the aggregate content. Improving the chloride resistance of concrete by partially replacing cement with fly ash was reported by Arya et al. [71]. They concluded that this might be possibly due to improving the chloride binding capacity of the fly ash by both chemical binding due to higher proportions of active alumina and physical adsorption of chloride because of more C-S-H gel produced in the hydration process.

In addition, Dinakar et al. [72] reported that forming stable chloro complexes due to the reaction between $C_3A$ in SCMs (slag and fly ash), and aggressive chloride ion may be a reason for increasing chloride resistance of concrete. Moreover, the pozzolanic reaction of SCMs seems to be able to decrease

penetration of chloride ions by developing a discontinuous pore system since chloride ions usually penetrate in concrete by diffusion along the water paths or open pores.

The AVPV test method in accordance to AS1012.21 [73] gives a measure of the interconnected void space within the concrete (i.e. capillary pores, gel pores, air voids and microcracks) that can absorb water following normal immersion and subsequent boiling as a result of capillary suction. This is related to the ease with which water and water-borne ions enter the concrete and initiate corrosion. As the amount of water that can be absorbed into concrete is a function of the permeable pores of the concrete, it is cleared that concrete with fewer permeable pores or voids should better withstand an aggressive environment than concrete with more permeable pores or voids [74].

The Rapid Chloride Permeability test (RCPT) in accordance with ASTM C1202 [75] measures the electrical charge passing through the concrete specimens by maintaining the voltage gradient to force the chloride ions to migrate more rapidly through the porous materials under test. However, this approach is frequently regarded as an indirect way of measuring chloride ion permeability. The permeability of concrete is not measured by this method. The rapid chloride penetration test involves the determination of the electrical conductance of concrete to provide a rapid indication of its resistance to the penetration of chloride ions. The concrete conductivity is the factor, which is measured by this test. It has been shown that there is a fair correlation between concrete conductivity and concrete permeability.

As Sherman et al. [76] reported, the RCPT charge passed is a good indicator of chloride resistance of concrete as it correlates well with effective chloride diffusion coefficients. However, Shi et al. [77] reported that the electrical conductivity of concrete is related to both the pore structure characteristics and the electrical conductivity of pore solution, while transport of ions in the concrete only depends on the pore structure of the concrete. Therefore, partially replacing cement with SCMs can decrease the electrical conductivity of concrete, more due to the change in the chemical composition of the pore solution, which has little to do with the transport of chloride ions in concrete.

Papadakis [78] studied chloride ion penetration resistance of concrete by using Rapid chloride permeability test (RCPT) as well as measuring the total chloride concentration at different layers of the specimens immersed for 100 days in a chloride solution using Nordtest method NT Build 443. He observed that concrete containing low and high calcium fly ash exhibits a lower degree of chloride penetration in comparison to PC concrete (without fly ash). RCPT results confirmed that partially replacing cement with both fly ashes up to 30% showed a significant reduction in electrical charge passed through the concrete compared to the control mix. This is possibly due to the fact that both fly ashes are able to refine the capillary pore size and prevent the interconnectedness of capillary pores in concrete, minimising the movement of water and chloride ions through the concrete as they noticed in the scanning electron microscopy test.

Uysal and Akyuncu [20] studied a total of 39 mixes with different mix designs to assess chloride ion permeability using the RCPT test. He concluded the chloride ion permeability of the concrete containing fly ashes decreased when the

fly ash content was increased. It is possibly due to the reaction of fly ash with free lime during the hydration, producing additional tobermorite gels to the silicate gels of cement and thus decreasing the capillary pores as confirmed by sorptivity test results. The formation of a less porous, denser microstructure and a discontinuous pore system becomes critical for reduced chloride ion permeability. This is in agreement with the finding of other researchers [71, 79].

Partially replacing cement with GGBFS in concrete is beneficial in mitigating chloride ion penetration, and decreasing the permeability and sorptivity of concrete. Hadj-sadok [80] also examined the concentration of chloride ions diffusing into mortar specimens by partially replacing cement with 30% and 50% of GGBFS with fixed w/b ratio of 0.5 for up to 270 days. The trend in Figure 2-26 shows that the chloride ion concentration of the concrete decreases by increasing the GGBFS replacement levels. The reason for this reduction is that the consumption of calcium hydroxide during the hydration of GGBFS leads to the reduction in the volume of interconnected pores, thus making a denser microstructure. MIP and SEM observation results also confirmed these findings. The abbreviations, M0, M30 and M50 represent mortar samples where Portland cement was substituted by GGBFS, in the order of 0%, 30% and 50% respectively. Critically, the chloride ion diffusion of samples containing GGBFS was less than the control.

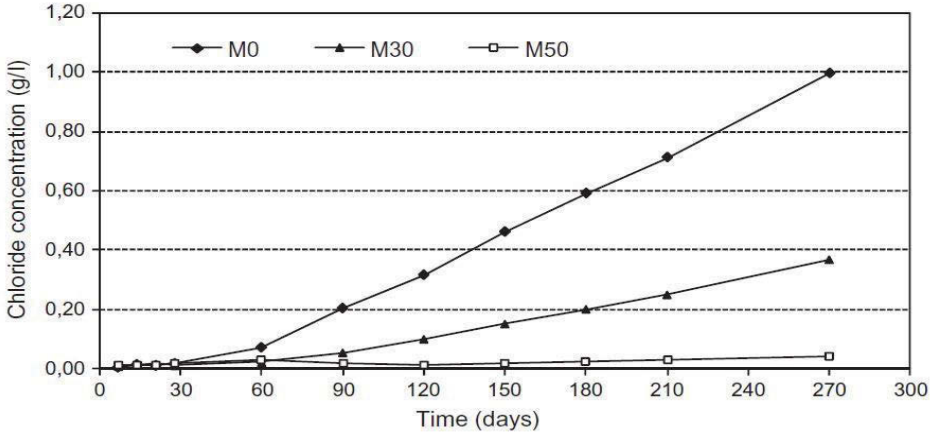


**Figure 2-26: Effect of increasing GGBFS levels on chloride concentration of concrete [80]**

Kim et al. [24] studied the chloride diffusion in high-strength MK concretes for up to 91 days, using rapid chloride permeability test. Figure 2-27 indicate that the chloride permeability in concrete decreased in relation to the increase of age and MK content. The decrease in the porosity and refinement in pore size, due to cement hydration and pozzolanic reaction, and thus consumption of more calcium hydroxide based on the XRD results, contribute to the reduction in the permeability of concrete.

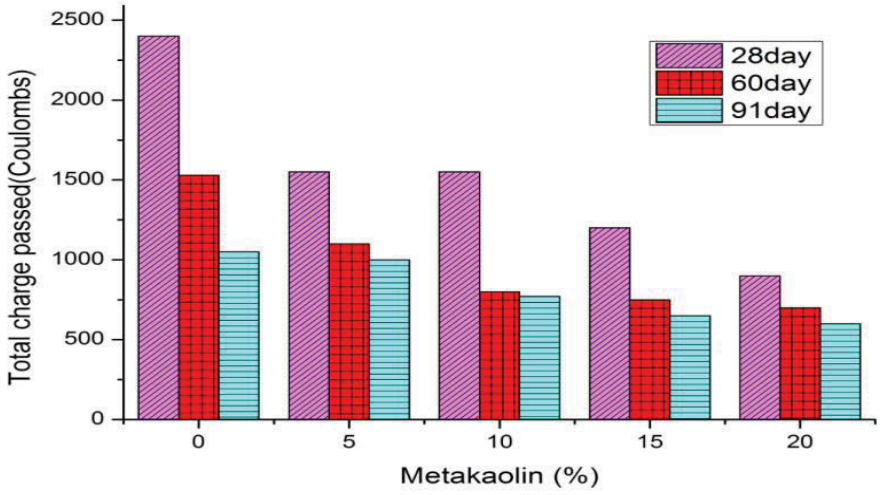


**Figure 2-27: Chloride permeability of MK concretes [24]**

Poon et al. [54] reported similar results as shown in Figure 2-28 for control concrete and 10% MK concrete at the w/b ratios of 0.30 and 0.50. The best performance for MK concrete was noted with 10% and 20% MK content at the w/b ratios of 0.30 and 0.50, respectively. This indicates that the increased MK content decreases the permeability of MK concrete, having a high initial porosity (or w/b ratio). It was confirmed by the total porosity results of concrete with w/b ratio of 0.3 using Mercury Intrusion Porosimetry (MIP) as shown in Table 2-11.

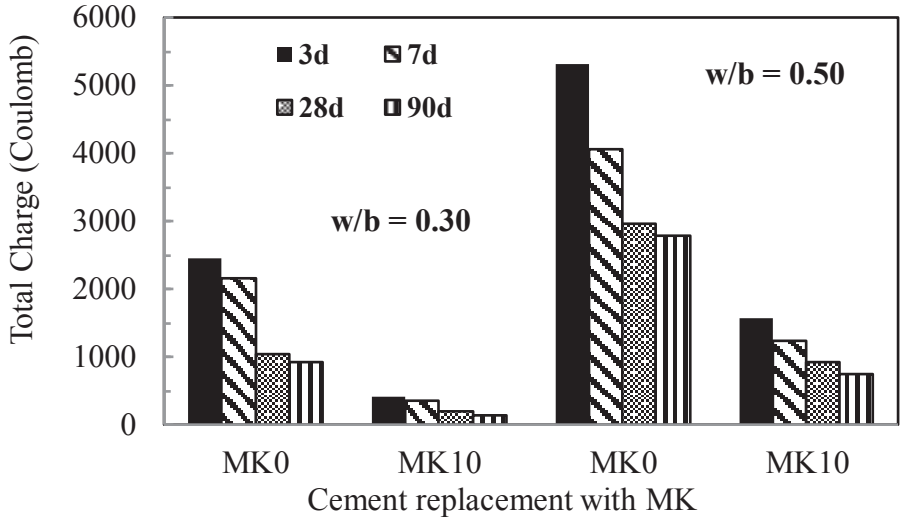


**Figure 2-28: Chloride permeability of control and MK concretes [54]**

**Table 2-11: MIP measured the total porosity of concrete with w/b=0.3 [54]**

| Mix | MIP measured total porosity (% v/v) | | |
|---|---|---|---|
| | 3 days | 7 days | 28 days |
| Control | 8.69 ± 0.11 | 8.44 ± 0.13 | 7.92 ± 0.12 |
| 5% MK | 7.22 ± 0.13 | 7.01 ± 0.15 | 6.40 ± 0.10 |
| 10% MK | 6.87 ± 0.14 | 7.01 ± 0.15 | 4.75 ± 0.09 |
| 20% MK | 6.59 ± 0.08 | 5.38 ± 0.12 | 4.66 ± 0.12 |

### 2.6.2 **Sulfate resistance**

Resistance of concrete to sulfate attack in aggressive environments is of vital importance to the performance of many substructures. The physical resistance of concrete to the penetration of the sulfate ions can be evaluated in relation to its resistance to water flow [81]. The results are expressed as coefficients of permeability [82].

The chemical resistance of most binders to sulfate attack can be gauged by using ASTM C1012 [83] test method which provides a means of assessing the sulfate resistance of mortars made using Portland cement, blends of Portland cement with pozzolans or slags, and blended hydraulic cement. In this test, the mortar bars, having a small cross-sectional area are placed in the sulfate solution once the mean compressive strength reaches 20 MPa by testing the cube specimens from the same mortar mix. In this state, the mortar bars are considered to have similar physical resistance to sulfate penetration. Hence, their susceptibility to expansion represents the relative chemical resistance of the binders used. Sulfate attack can result in extensive expansion and/or loss of elastic properties such as strength [84]. These are manifested from the formation of ettringite and gypsum, and the decalcification of C-S-H.

The physical resistance of concrete to sulfate ion penetration was traditionally derived by specifying mix design factors like maximum w/c ratio and minimum cement content while chemical resistance was achieved by using sulfate resistant cement. This is to ensure both physical resistance to penetration and capillary-induced migration of sulfate ions in concrete and the chemical resistance to the deleterious reactions.

Permeability is considered the key to the durability of concretes in various aggressive environments. In a critical review of sulfate attacks on concrete, Mehta concluded that for the prevention of sulfate attack "control of the permeability of concrete is more important than control of the chemistry of cement" [85]. Some other studies have also concluded that permeability is the key factor in providing resistance to chloride and sulfate environments [86, 87]. Barger et al. [88] reported that fly ash could enhance the resistance of concrete to sulfate attack by a formation of secondary CSH gel due to the pozzolanic reaction, which minimises the size and number of capillary pores and voids present within the concrete. In doing so, the concrete develops a denser microstructure, which decreases the penetration of sulfate ions into the concrete.

Sirivivatnanon and Khatri [89] proposed a performance specification based on water permeability of the concrete. Subsequently, a further attempt was made to develop a performance-based specification for sulfate resisting concrete based on cement chemical resistance (sulfate expansion) and the physical resistance of the concrete (e.g. water permeability, rapid sulfate permeability) as an area of research in Cement Concrete & Aggregate Australia organisation (CCAA). The rapid sulfate permeability determination test method was developed by Sirivivatnanon and Lucas [90] as shown in Figure 2-29. They proposed that using sulfate resistant cement and rapid sulfate permeability $\leq 2000$ coulombs would make the concrete perform well in both neutral and acidic sulfate conditions.

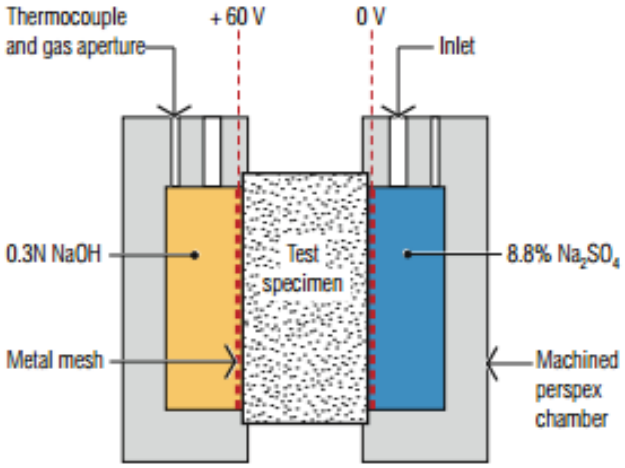


**Figure 2-29: An accelerated test set-up for rapid sulfate permeability determination [90]**

It is proved by many researchers [91, 92] that the sulfate resistance of concrete substantially increases by a partial replacement of cement with GGBFS due to the reduction in $C_3A$ content, soluble $Ca(OH)_2$ and permeability of concrete. They suggest that gypsum formation during sulfate attack is expansive, but ettringite might form afterwards, contributing to expansion.

Wee et al. [93] studied sulfate attack deterioration mechanism of GGBFS concretes under tropical climatic conditions. The water to binder ratio (0.40 and 0.50), moist curing time (3, 7, and 28 days), and fineness of GGBFS (4500, 6000, and 8000 $cm^2/g$) were experimental variables. Concrete prisms were monitored for linear expansion after submersion in a 5% $Na_2SO_4$ solution for 32 weeks. The experimental results were compared with those of ordinary PC and sulfate-resisting Portland cement concrete specimens. The results demonstrated that concrete mixes containing higher levels of GGBFS (for example, 75% and 85%) showed greater resistance to sulfate attack, irrespective of w/b (0.40 and 0.50) and moist curing time (3, 7, and 28 days).

Higgins [94] investigated the effect of GGBFS replacement ratio on the sulfate resistance of concrete (see Table 2-12). The results indicated that control concrete (without GGBFS) deteriorated entirely in $Na_2SO_4$ in 6 years, while only insignificant strength loss and specimen corner deterioration were observed in the GGBFS concretes. As expected, the resistance to sulfate attack increased by increasing the GGBFS replacement levels.

**Table 2-12: Variation of compressive strength due to the sulfate attack [94]**

| Mixes | Compressive Strength in water (MPa) | | | | | | Residual Strength in $Na_2SO_4$ (MPa) | | |
|---|---|---|---|---|---|---|---|---|---|
| | 3-d | 7-d | 28-d | 1-y | 2-y | 6-y | 1-y | 2-y | 6-y |
| PC | 34 | 41 | 53 | 66 | 68 | 69 | 97 | 87 | 0 |
| 60% GGBFS | 17 | 31 | 48 | 63 | 69 | 73 | 106 | 97 | 62 |
| 70% GGBFS | 13 | 28 | 49 | 63 | 66 | 71 | 105 | 89 | 90 |

Al-Akhras [95] investigated the behaviour of MK concretes (w/b of 0.50), with increasing MK content of up to 15%, exposed to sodium sulfate solution over 18 months. The sulfate attack was assessed in a number of ways: (i) expansion measurements in concrete prisms; (ii) compressive cube strength; and (iii) visual inspection of concrete prisms. Figures 2-30 and 2-31 shows the sulfate expansion and percentage of compressive strength reduction in concrete prisms as a function of age and MK content.

The sulfate resistance of concrete was improved with higher levels of cement being replaced with MK. Control concrete experienced the maximum expansion of 0.4% in 18 months while MK concretes with 10% and 15% MK showed the

expansion of 0.10% and 0.07% after the same exposure period. In addition, the reduction in compressive strength decreased by increasing the MK content. The improved sulfate resistance of MK concrete could be due to the following reasons: (i) cement replacement reduces the total amount of tricalcium aluminate hydrate in the hardened paste; (ii) pozzolanic reactivity of MK partially consumes the calcium hydroxide released by cement hydration which controls the formation of expansive gypsum; and (iii) permeability of concrete is reduced through pore structure refinement in MK concrete as confirmed by Mercury Porosimetry test results.

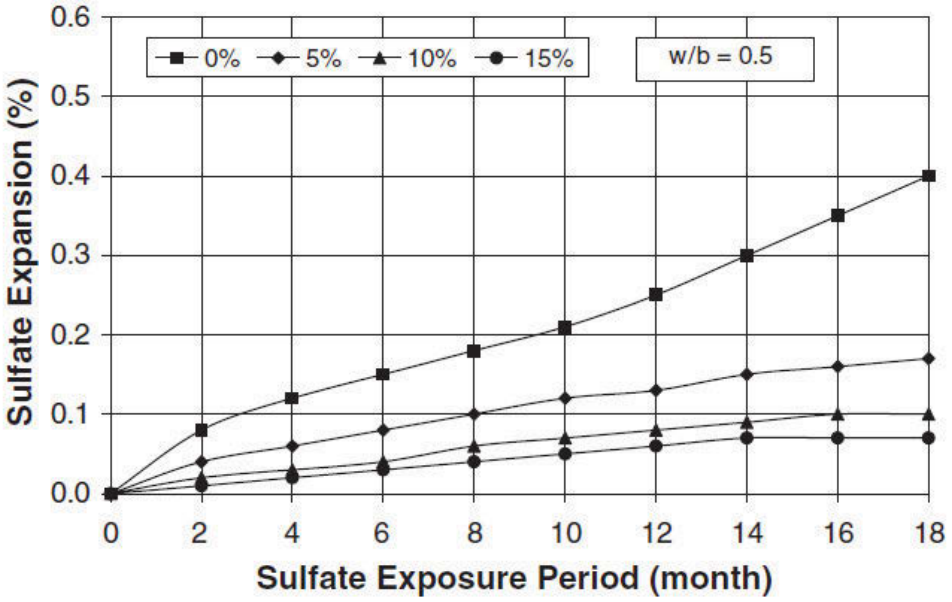


**Figure 2-30: Sulfate expansion of MK concretes [95]**

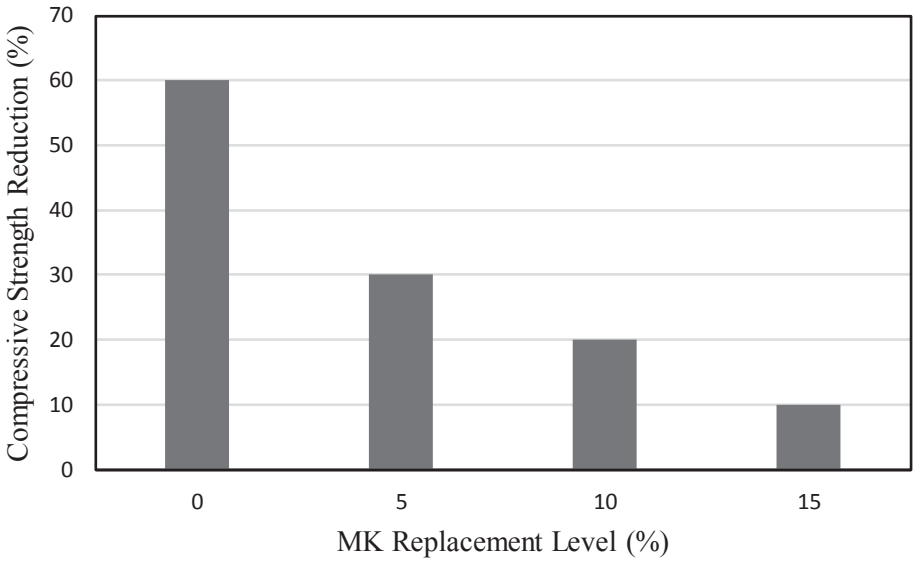


**Figure 2-31: Compressive strength reduction of MK concretes after 18 months in sodium sulfate solution [95]**

### 2.6.3 Alkali-silica mitigation

The reaction between the hydroxyl ions ($OH^-$) in the pore solution and reactive silica in the aggregate is the first step of alkali-silica reaction (ASR). Portland cement is the primary source of alkalis in the concrete, while SCMs, aggregates, admixtures may also contribute alkalis to the concrete [96]. There are a number of factors which affect the concentration of alkali metal hydroxides in the pore solution of concrete such as the alkali content of cement, the w/c ratio and degree of hydration [97]. Then, imbibing water from the surrounding pore solution by the alkali-silica gel results in swelling and thus causing the volumetric expansion of the concrete which ultimately leads to cracking [98].

There are some factors which affect the amount of expansion due to the alkali-silica reaction in the concrete including the availability of alkalis in the pore solution, the nature and amount of reactive silica in the aggregate and exposure conditions, particularly temperature and moisture availability. Partially replacing

cement by SCMs in the concrete mix only influences the availability of alkalis, although SCMs also contain some level of alkali or even sometimes more than cement. The alkalis released by the hydration can be found in one of the three ways: dissolved in the pore solution, bound by the hydration products or incorporated in the alkali-silica gel. However, the main reason that SCMs reduce expansion due to ASR is a reduction in the amount of available alkali in the pore solution [99].

The reduction in the concentration of alkali-hydroxides in the pore solution of pastes, mortar and concretes by partially replacing cement with most of SCMs is reported by Thomas [100]. He also mentioned that the reduction increases in higher levels of substituting cement with SCMs. The influence of SCMs in the reduction of alkalinity of the pore solution is also related to their composition and the alkali-binding capacity of the hydrates (especially C-S-H) [99].

Duchesne and Bérubé [101] reported that the competitive reaction exists between the aggregates and SCMs, and due to their finer size, SCMs react faster. Hence, the SCMs will consume the available alkalis in the concrete before a deleterious reaction with the aggregate can occur. Moreover, the composition of C-S-H phases formed has a decreased Ca/Si ratio, which causes more alkali ions to be entrapped in the hydrates. They concluded after a 9-year study on SCM efficacy that there is an excellent correlation between the drop of alkali ions in a pore solution and the expansion reduction in concrete.

Shehata et al. [102] studied the expansion of concrete prisms for two years using Canadian Standards Association Concrete Prism Test, CSA A23.2 Test 14A (equivalent to ASTM C 1293) [103]. They found the expansion of concrete prisms

increased due to the ASR for a given fly ash replacement level by increasing the calcium or alkali content of the fly ash or decreasing fly ash silica content as shown in Figure 2-32. The graph illustrates the variations in the efficiency of different fly ashes in controlling the expansion, i.e., the level of ash required to mitigate expansion to less than 0.04% varies considerably between fly ashes. However, it can be expected that even the less effective fly ashes have a beneficial impact on the expansion of the concrete beyond the role of merely diluting the cement alkalis. Similar results were observed by other researchers [99, 102].

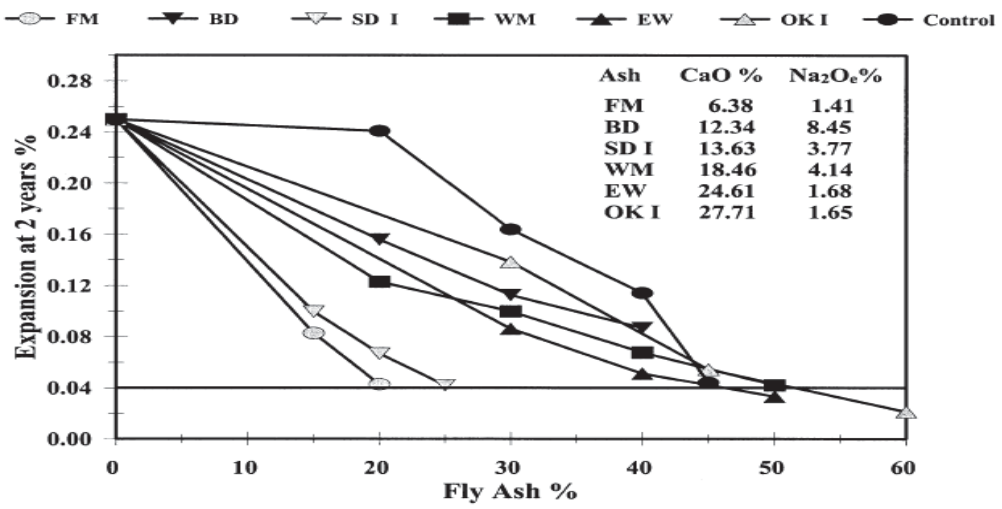


**Figure 2-32: Effect of ash composition and replacement level on expansion due to ASR [102]**

Hester et al. [104] carried out a modified version of British Standard concrete prism, BS 812 Part 123 [105] by adding 6 kg $Na_2O_{eq}/m^3$ on top of the alkali content from the cementitious materials. Portland cement was replaced with 50% GGBFS (alkali level of about 1%) and three reactive aggregates were used. They argued that, despite the increase in the alkalinity of concrete, which is associated with the incorporation of GGBFS within the concrete, the GGBFS possibly

inhibits the mobility of hydroxyl ions within the concrete. Consequently, ASR is minimised, because alkaline hydroxyl ions are not able to physically migrate to sources of silica (found on the surface of coarse aggregates) within the concrete.

With GGBFS having a typical calcium-to-silica ratio of approximately 1 (compared to a typical calcium-to-silica ratio of 3 for traditional Portland cement), the C-S-H gel formed by GGBFS contains a lower calcium-to-silica ratio than that formed by Portland cement. The low calcium-to-silica ratio characteristic of C-S-H gel containing GGBFS (relative to that of concrete containing only Portland cement) induces a negative surface charge onto C-S-H compounds formed by GGBFS. Consequently, the C-S-H attracts sodium and potassium hydroxyl (alkali) cations, present in the pore solution of the concrete, thus reducing the amount of available alkalis within the concrete pore solution able to facilitate ASR expansion [106].

Kwon [107] carried out an investigation on the effect of replacement level (up to 60%) and various fineness (4000, 6000 and 8000 $cm^2/g$) of GGBFS using the constant binder content of 450 $kg/m^3$ on the alkali-silica reaction of high-strength concrete. Results showed that the expansion of concrete mix containing 60% GGBFS was the lowest and followed by 45%, 30%, and 0%, as shown in Figure 2-33 a. and b. It is noted that increasing the fineness of GGBFS has a significant influence on the reduction of expansion due to the ASR possibly due to the more reactivity of finer particles. For instance, GGBFS with a fineness of 8000 $cm^2/g$ has the highest AAR inhibiting effect, decreasing the fineness to 6000 and 4000 $cm^2/g$ leading to a gradual decrease.

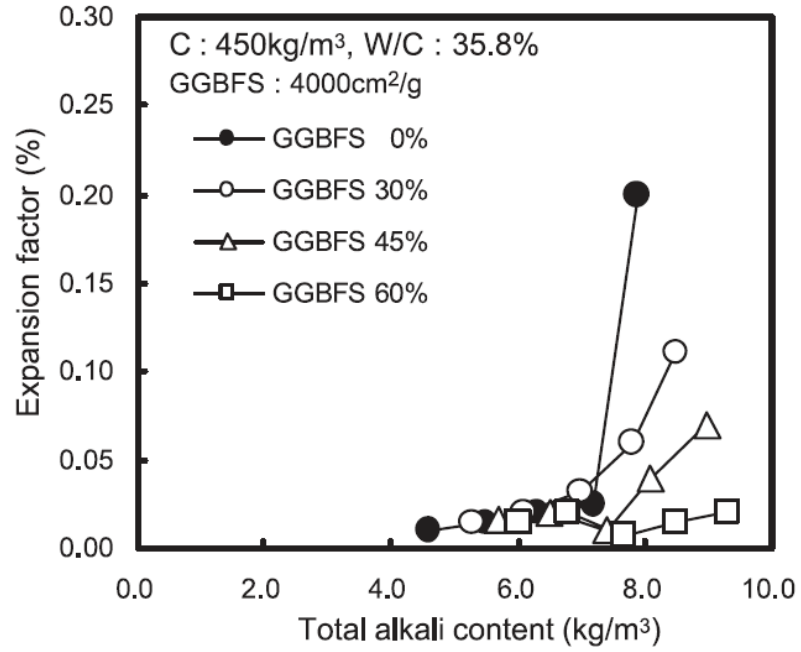


(a)

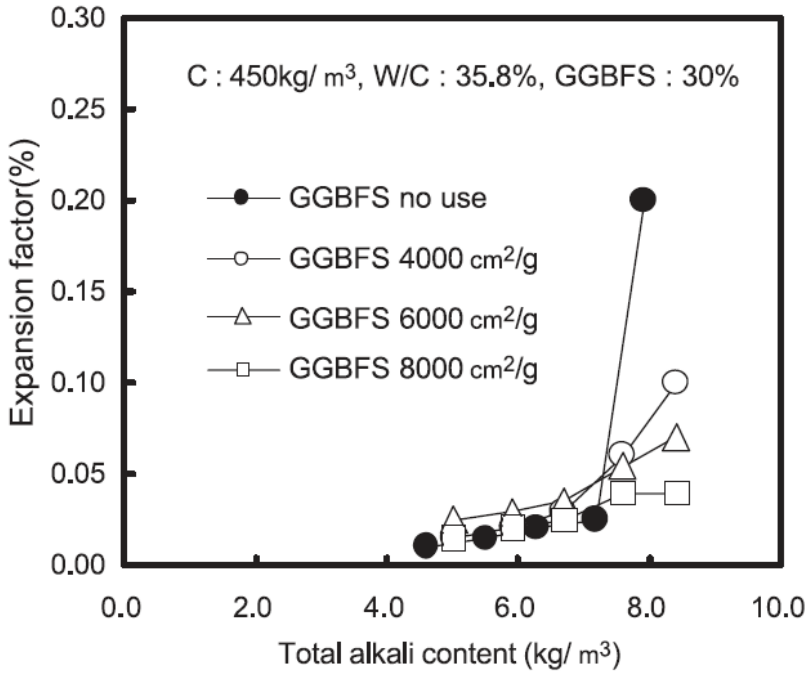


(b)

**Figure 2-33: ASR expansion (a) effect of GGBFS (b) effect of fineness [107]**

Ramlochan et al. [108] studied the efficacy of MK in controlling expansion due to alkali-silica reaction with a reactive aggregate by using the concrete prism method, and the results are shown in Figure 2-34. The results demonstrated that partially replacing cement with MK (15% and 20%) can control deleterious expansion below 0.04 after two years, depending on aggregate type. The results were confirmed by the pore solution analysis of the cement pastes over a 2-year period. From Figure 2-35, it is noted that replacing cement with 20% MK was significantly effective in reducing the alkalinity of pore solution, and thus making less alkali available for ASR.

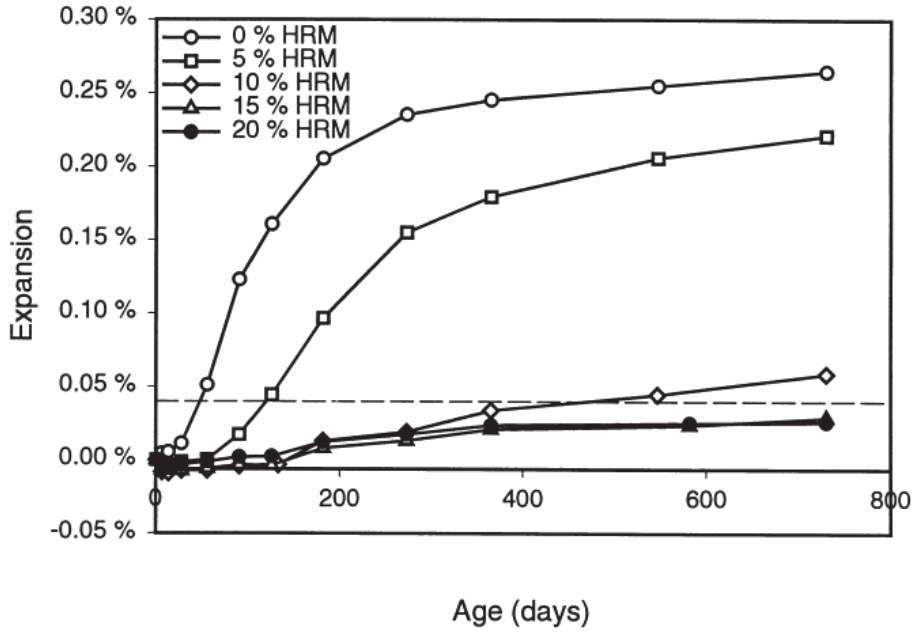


**Figure 2-34: Alkali-silica expansion in MK concrete prisms [108]**

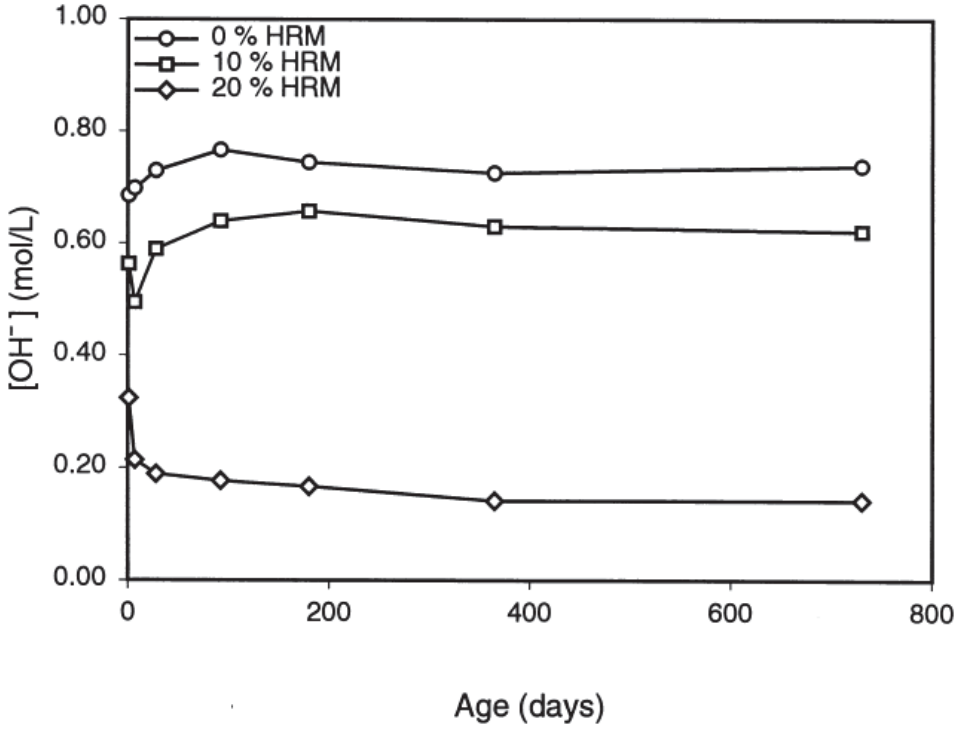


**Figure 2-35: Hydroxyl ion concentration of pore solutions expressed from pastes containing MK [108]**

## 2.7 Summary

The following summary based on the literature reviewed in this chapter are made from the review of the properties and performance of concrete containing fly ash, slag, and metakaolin as partial replacement of cement.

1. Workability of concrete was increased with the increase in fly ash content due to the morphological effects of fly ash particles. Having spherical shapes, fly ash particles act as lubricating balls when incorporated in fresh concrete.
2. Partially replacing cement with fly ash in blended cement paste decreased the intensity peak of $Ca(OH)_2$ and the reduction increased with an increase in fly ash content and fineness. In addition, the total porosity and capillary pores of blended cement paste containing finer fly ash decreased significantly compared to the blended paste containing coarser fly ash.
3. Partially replacing cement with fly ash, of different fineness, decreased the cumulative heat evolution; the reduction in heat evolved increased with an increase in fly ash content. However, the finer grade fly ash generated more heat in hydration compared to coarser grade fly ash.
4. Pozzolanic effects of fly ash did not greatly contribute to the early-age strength development of concrete. However, the secondary C-S-H formed by pozzolanic reactions filled capillary pores, increasing the compressive strength of the concrete in a later age by enhancing the concrete microstructural density (in particular, the interfacial transition zone of concrete) and reducing the porosity of the concrete.

5. Drying shrinkage of concrete was reduced by partially replacing cement with fly ash, and the reduction increased at higher fly ash content.
6. Pozzolanic effects of fly ash have greatly contributed to reducing chloride permeability, resistance to alkali-silica reactivity and sulfate attack.
7. Workability of concrete was improved with the increase in slag content due to better cementitious particle dispersion and surface characteristics of the slag particles.
8. Partially replacing cement with slag in concrete decreased significantly the volume of macropores and increased the volume of mesopores. It is possibly due to the pozzolanic and hydraulic reaction of slag particles, which refine the pore structure by transforming the coarser pores to the finer ones.
9. There was a systematic decrease in compressive strength of concrete with the increase in slag content during the early ages of hydration. However, the secondary C-S-H formed by pozzolanic reactions fills capillary pores, increasing the compressive strength of the concrete in a later age by enhancing the microstructural density of concrete (in particular, the interfacial transition zone of concrete) and reducing the porosity of the concrete.
10. Chloride permeability, resistance to alkali-silica reactivity and sulfate attack were reduced by partially replacing cement with slag.
11. The consistency of concrete was decreased with the increase in metakaolin content due to high fineness without affecting the compaction of concrete.

12. Relatively finer and highly pozzolanic metakaolin as a partial replacement of cement produced pore structure modification, reducing porosity and pore size refinement in hardening pastes and concrete.
13. Partial cement replacement with metakaolin significantly increased the compressive strength of concrete, and the degree of strength enhancement increased with an increase of metakaolin content and w/b ratio.
14. Drying shrinkage of concrete was reduced significantly with an increase in metakaolin content. It could be due to the reduced moisture loss from metakaolin concrete.
15. Partially replacing cement with metakaolin reduced the chloride permeability, resistance to alkali-silica reactivity and sulfate attack of concrete. 10% to 15% cement replacement with metakaolin was sufficient to control ASR-related expansion and sulfate attack.
16. In recent years, Australian road authorities have been increasingly concerned with the shortage of classified fly ash (CFA), predicted to occur in the near future due to the possible shutting down of coal-fired power stations. Finding alternative SCMs is a critical issue due to a shortage of national resources available. Run-of-station fly ash can be a possible alternative SCM to classified fly ash. However, the main requirements for any fly ash to be used in concrete applications according to AS 3582.1 is to comply with fineness and strength index requirements. The major reason prevents the use of run-of-station fly ash in practice is attributed to failure to comply with these prescriptive requirements in AS 3582.1. In addition, the fly ash standard AS 3582.1 is not a performance-based

specification and that is why there is an urgent need to look at the effect of fly ash with different fineness even with similar chemical composition on various plastic, mechanical and durability properties of concrete mixes. Therefore, in order to address mentioned gaps in practice and knowledge, additional work needs to be carried out to investigate and address this issue.

# Chapter 3

## Research Methodology

# 3 RESEARCH METHODOLOGY

## 3.1 Preface

In Chapter 2, a comprehensive literature review was done to fully understand the influence of characteristics and level of SCMs on plastic, hardened and durability properties of mortar and concrete. The prescriptive requirements in AS 3582.1 play a vital role in preventing the use of run-of-station in practice. The current fly ash standard AS 3582.1 is more prescriptive based by only looking at some properties such as fineness and strength index instead of being performance based. Therefore, it is necessary to investigate the effect of RFA on a range of performances including heat of hydration and microstructure of the blended pastes as well as its influence on various plastic, mechanical and durability properties of different concrete mixes. Research methodology has hence been chosen to address these knowledge gaps.

In Chapter 3, in order to achieve the objectives of this research, several investigations were performed. So, a brief overview of the experimental methodologies used is outlined below.

### 3.1.1 Characterisation of cement, SCMs and aggregates

This focuses specifically on the determination of the chemical compositions, fineness, particle size distribution, surface topography and amorphous content of the cement and SCMs including run-of-station fly ash. In addition, grading, water absorption and specific gravity of coarse and fine aggregate were determined.

### 3.1.2 Determination of the effect of fineness and levels of SCMs on the heat of hydration

This part of the program will be evaluating the effect of different types, fineness and levels of supplementary cementitious materials (SCMs), as well as different water to binder ratio on the heat of hydration and amount of heat evolution of blended cement, pastes by means of isothermal calorimetry during the first 48 hours of the hydration process. Fly ashes with different fineness: classified fly ash (CFA), run-of-station fly ash (RFA) and ground run-of-station fly ash (GRFA) from the same power station source in Australia are used to partially replace Portland cement at 20%, 30% and 40% by weight of Portland cement. In addition, in some mixes, Portland cement is substituted with 35%, 50% and 65% of ground granulated blast furnace slag (SL) and 5%, 10% and 15% of metakaolin (MK) by weight of Portland cement as shown in Table 3-1. The water to binder ratios of 0.40 and 0.55 are used for all the blended cement pastes.

**Table 3-1: Plan for determining the effectiveness of fineness and levels of SCMs on the heat of hydration**

| Pastes | SCMs | SCM replacement level (%) | W/b |
|---|---|---|---|
| Series 1 | GRFA | 20, 30, 40 | 0.40 |
| | CFA | 20, 30, 40 | |
| | RFA | 20, 30, 40 | |
| | SL | 35, 50, 65 | |
| | MK | 5, 10, 15 | |
| Series 2 | GRFA | 20, 30, 40 | 0.55 |
| | CFA | 20, 30, 40 | |
| | RFA | 20, 30, 40 | |
| | SL | 35, 50, 65 | |
| | MK | 5, 10, 15 | |

### 3.1.3 Effect of fly ash fineness on important properties of the blended cement paste

This focuses especially on the influence of fly ash fineness on microstructure morphology, consumption of calcium hydroxide by pozzolanic and hydraulic reactivity, flow and compressive strength of blended cement pastes and then assesses and evaluates the results against the control cement paste. Fly ashes with different fineness: classified fly ash (CFA), run-of-station fly ash (RFA) and ground run-of-station fly ash (GRFA) from the same power station source in Australia are used to partially replace Portland cement (PC) at 20% and 40% by weight using a fixed water-to-binder ratio of 0.40.

### 3.1.4 Determination of optimum binary binder systems in mortars

It is aimed to optimise various binary binder systems with respect to strength, drying shrinkage and flow. Mortar mixes with two levels of compressive strength with two different ranges of sand/binder and water/binder ratios were designed with a fixed dosage of Water-Reducing admixture (WR) which is 300 ml in 100 kg cement as shown in Table 3-2. The use of High-range Water Reducer (HWR) and Air Entraining Agent (AEA) will only be studied in concrete mixes.

**Table 3-2: Plan for determining optimum binary binder systems for mortars**

| Mixes | SCMs | SCM replacement level (%) | W/b | S/b | Chemical admixture |
|---|---|---|---|---|---|
| Series 1 | CFA | 20, 30, 40 | 0.4 | 2.5 | Fixed dosage WR |
| | RFA | 20, 30, 40 | | | |
| | SL | 35, 50, 65 | | | |
| | MK | 5, 10, 15 | | | |
| Series 2 | CFA | 50, 60, 70 | 0.55 | 5.0 | Fixed dosage WR |
| | RFA | 50, 60, 70 | | | |

### 3.1.5 **Effective level of SCMs in mitigating alkali-silica reactivity**

This part of the program will examine the effectiveness and level of the four SCMs as shown in Table 3-3 in mitigating ASR based on Accelerated Mortar Bar Test (AMBT) in accordance AS1141.60.1 [109] (extended to 35 days).

**Table 3-3: Plan for determining effectiveness level for mitigation ASR**

| Mixes | SCMs | Cement replacement level (%) | Aggregate |
|---|---|---|---|
| | CFA | 20, 30, 40 | Reactive |
| | RFA | 20, 30, 40 | |
| | SL | 35, 50, 65 | |
| | MK | 5, 10, 15 | |

### 3.1.6 Effectiveness of run-of-station fly ash in lean concrete

This focuses exclusively on 12 MPa subbase paving concrete mix to the properties specified in Roads and Maritime Services (RMS) R82 specification [110] for lean-mix concrete subbase. This part of the program will examine the effectiveness of partially replacing cement with run-of-station fly ash on the different properties of the lean concrete mix by comparing the results with the identical concrete mix containing classified fly ash.

### 3.1.7 Effect of run-of-station fly ash and other SCMs on properties of high-performance concrete

This focuses exclusively on the effectiveness of partially replacing cement with run-of-station fly ash on the various properties of High-Performance Concrete (HPC) mixes. HPC refers to 40 MPa base pavement mix in accordance RMS R83 specification [111] for concrete pavement base, and 50 MPa bridge mix in accordance with RMS B80 specification [112] for concrete work for bridges. For chloride and sulfate resistance, it may only be possible to determine relative performance rather than properties specified in B80 due to time constraints.

## 3.2 **Raw materials**

The raw materials used in this research are as follows.

- General purpose Portland cement conforming to AS 3972
- Fly ash (Eraring) conforming to AS 3582.1
- Ground granulated blast furnace slag conforming to AS 3582.2
- Metakaolin
- Coarse aggregate conforming to AS 2758.1
- Nepean coarse sand conforming to AS 2758.1
- Sydney fine sand conforming to AS 2758.1
- Water reducer (WR) - Daratard® GP conforming to AS 1478.1-2000
- High range water reducer (HWR)- ADVA® 650 conforming to AS 1478.1-2000
- Air entrained agent (AEA) - Darex® AEA EH conforming to ASTM C260
- Technical grade reagents (NaOH, NaCl, $Na_2SO_4$)
- Potable water

## 3.3 Experimental procedures

### 3.3.1 Testing methods for characterisation of raw materials

Characterisation of raw materials such as cement, SCMs and aggregates was carried out by using the following test methods**:**

**Particle Size Analysis of cementitious materials**

The particle size of the cementitious materials is a significant factor in determining the strength properties of the mortar and concrete specimens. Laser diffraction is a reliable and rapid method for measuring the particle size distribution of the cementitious materials, which was used in this research by using a Malvern Mastersize 2000 laser analyser at the University of Technology Sydney (UTS). Firstly, a small amount of cementitious materials were dispersed in 10 ml of ethanol and then agitated for five minutes in an ultrasonic bath to disperse the material properly. Then, the measurements were performed by illuminating particles in a collimated laser beam and measuring the scattered light over a range of angles. The angle to which particles scatter light depends on their size.

**Particle Morphology of cementitious materials**

Scanning electron microscopy (SEM) was carried out on the cementitious materials at the University of Technology Sydney (UTS) in the Microstructural Analysis Unit (MAU). All specimens were gold coated and placed under vacuum prior to imaging. The scanning electron microscope (SEM) is a type of electron microscope that images the sample surface by scanning it with a high-energy

beam of electrons across the sample surface. Samples with dimensions of less than 5 mm were selected from inside the paste.

## Identification/Quantification of crystalline Phase of cementitious materials

X-ray diffraction (XRD) analysis as a qualitative tool to identify the crystalline phases was carried out on cementitious materials at the University of Technology Sydney (UTS) in the Microstructural Analysis Unit (MAU). This test is a scattering technique carried out by bombarding the powder with X-rays whilst gradually rotating to represent every possible crystalline orientation. For this study, XRD testing was performed by using Bruker D8 Discover diffractometer.

## Chemical Composition of cementitious materials

Major elements of the cementitious materials were analysed using the X-ray fluorescence technique at the University of New South Wales (UNSW) laboratory by bombarding the sample with high-energy X-rays or gamma rays. The principle of this technique is to excite the individual atoms by an external energy source and then count the number of X-ray photons of each energy range emitted from the sample to identify of the source atoms.

## Specific gravity, Specific Surface Area, available alkali and 45µm Fineness of cementitious materials

The percentage of passing sieve No. 45, specific surface area (Blaine fineness), available alkali and specific gravity of cementitious materials were

determined according to AS 2350.9, AS 2350.8, AS 3583.12 and AS 3583.5 respectively [113-116].

**Specific gravity and water absorption of coarse and fine aggregate**

The relative density and water absorption of coarse and fine aggregate were measured using AS 1141.6.1 and AS 1141.5 respectively [117, 118].

**Particle size distribution of coarse and fine aggregate**

Sieve analysis was carried out to determine particle size distributions of fine aggregate and coarse aggregates according to the method presented in AS 1141.11 [119].

### 3.3.2 Paste mix design and mixing procedure

In both cement and blended cement pastes, the water to binder ratio was maintained at 0.40, by weight. In blended cement pastes, three types of fly ashes (CFA, RFA and GRFA) were used to replace type GP cement at the same replacement levels of either 20% or 40% by weight. The mixing was performed according to the ASTM C305-13 [120].

However, in the isothermal calorimetry test, pastes were prepared at water to binder ratios (w/b) of 0.40 and 0.55 with replacing cement with SCMs by mass levels of 20%, 30% and 40% for all fly ashes (CFA, RFA and GRFA); 35%, 50% and 65% for SL, and 5%, 10% and 15% for the MK throughout the investigation. Since the weight of the sample was relatively small, mixing of the paste was carried out manually stirring the cement, SCM, and water together with a steel rod in a plastic calorimetric cup.

In the present work,

Figure 3-1 denotes the abbreviations used to identify all paste mixes.

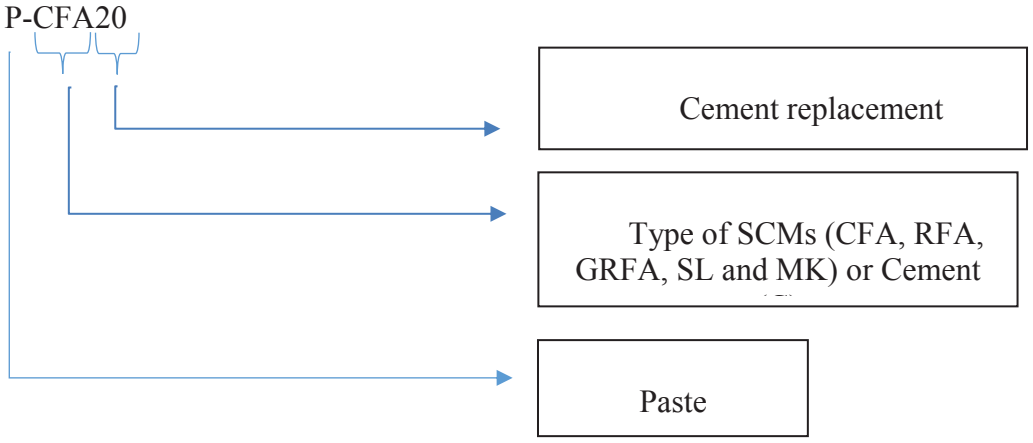


**Figure 3-1: Abbreviations used to denote paste mixes**

### 3.3.3 Casting and curing paste specimens

Immediately after the completion of mixing, a number of 50 mm cement paste cubes was cast in steel moulds and stored in a moist room at 21°C. After 24 hours, the test cubes were demoulded and cured in saturated lime water.

### 3.3.4 Paste testing details

The heat of hydration, and microstructure, as well as flow and the compressive strength of blended cement pastes, were assessed using following test methods:

#### Heat of Hydration

The heat of hydration of blended pastes was determined using an I-Cal 4000 isothermal calorimeter in accordance to ASTM C1679 [121] under isothermal conditions (25 ± 0.1°C) similar to the room temperature. Since the weight of the test sample was relatively small, mixing of the paste was carried out manually

stirring the cement, SCMs, and water together with a steel rod in a plastic calorimetric cup. Right after putting the cup inside the calorimeter unit, the heat of hydration generated from the cement system flowed quickly to its surroundings, causing the temperature difference across the sensor to create a voltage signal proportional to heat flow. The amount of heat evolution is then measured by converting the voltage signals every 60 seconds. The first peak caused by the reaction at the surface of the cement particles due to hydration of the $C_3A$ phase was not fully captured as mixing happened outside the calorimeter. However, a few percentages of the cumulative hydration is due to this reaction [122].

### Measuring the consumption of $Ca(OH)_2$

X-ray diffraction (XRD) analysis was carried out on ground paste samples at the University of Technology Sydney (UTS) in the Microstructural Analysis Unit (MAU). The blended cement paste fragments from cube specimens were ground using a ball mill at the specified ages of 1, 7 and 28 days. One gram of the powdered sample was used to measure the amount of calcium hydroxide (C-H) by XRD analysis using a Bruker D8 Discover diffractometer.

### Microstructure morphology of fracture surface

Scanning electron microscopy (SEM) was carried out on the paste specimens at the University of Technology Sydney (UTS) in the Microstructural Analysis Unit (MAU). Cube specimens were fractured from the centre into small pieces at 1, 7 and 28 days. Then, the fracture surfaces were gold coated and placed under vacuum prior to imaging using a Zeiss Supra 55VP SEM.

## Flow and compressive strength

Immediately after the completion of mixing, the fresh paste was assessed for its workability using mortar flow test, according to ASTM C1437 [123]. The compressive cube strength of hardened pastes was determined, in accordance with ASTM C109 [124] at the ages of 1, 7 and 28 days.

## Mortar mix design

In the present work, Figure 3-2 denotes the abbreviations used to identify all mortar mixes.

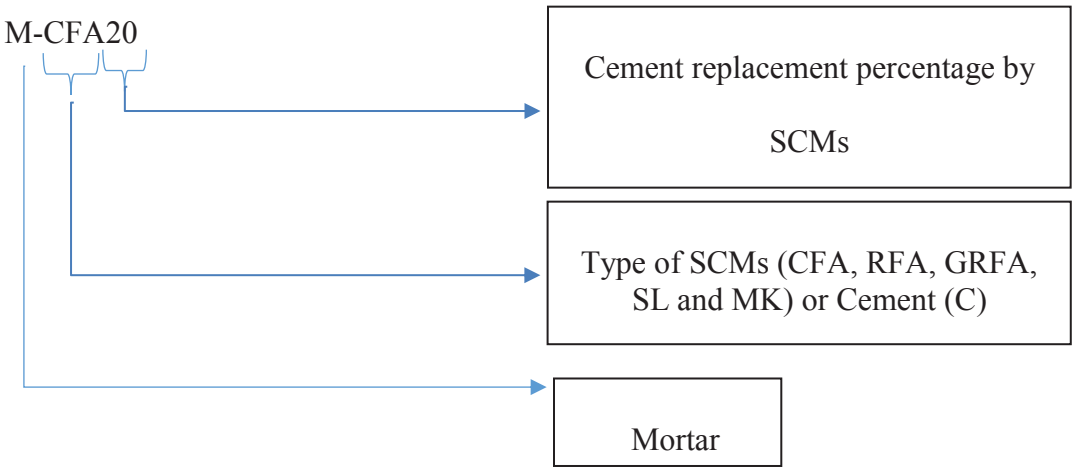


**Figure 3-2: Abbreviations used to denote mortar mixes**

The mortar mix design procedure of the current research included two different scenarios:

1- Mixes with a fixed water to binder ratio of 0.40 and sand to binder of 2.5 with a fixed dosage of water reducer (WR) as shown in Table 3-4.

2- Mixes with fixed water to binder ratio of 0.55 and sand to binder of 5.0 with a fixed dosage of water reducer (WR) as shown in Table 3-5.

**Table 3-4: Mix design composition for high strength mortar**

| Mix | Cement (g) | SCM (g) | Sand (g) | Water (mL) | WR (ml) | Flow (%) |
|---|---|---|---|---|---|---|
| M-C0 | 1300 | 0 | 3250 | 520 | 4 | 70 |
| M-CFA20 | 1040 | 260 | 3250 | 520 | 4 | 75 |
| M-RFA20 | 1040 | 260 | 3250 | 520 | 4 | 70 |
| M-GRFA20 | 1040 | 260 | 3250 | 520 | 4 | 80 |
| M-CFA30 | 910 | 390 | 3250 | 520 | 4 | 75 |
| M-RFA30 | 910 | 390 | 3250 | 520 | 4 | 70 |
| M-GRFA30 | 910 | 390 | 3250 | 520 | 4 | 85 |
| M-CFA40 | 780 | 520 | 3250 | 520 | 4 | 80 |
| M-RFA40 | 780 | 520 | 3250 | 520 | 4 | 75 |
| M-GRFA40 | 780 | 520 | 3250 | 520 | 4 | 90 |
| M-MK5 | 1235 | 65 | 3250 | 520 | 4 | 60 |
| M-MK10 | 1170 | 130 | 3250 | 520 | 4 | 55 |
| M-MK15 | 1105 | 195 | 3250 | 520 | 4 | 50 |
| M-SL35 | 845 | 455 | 3250 | 520 | 4 | 75 |
| M-SL50 | 650 | 650 | 3250 | 520 | 4 | 85 |
| M-SL65 | 455 | 845 | 3250 | 520 | 4 | 90 |

**Table 3-5: Mix design composition for low strength mortar**

| Mix | Cement (g) | SCM (g) | Sand (g) | Water (mL) | WR (mL) | Flow (%) |
|---|---|---|---|---|---|---|
| M-C0 | 700 | 0 | 3500 | 385 | 2 | 70 |
| M-CFA50 | 350 | 350 | 3500 | 385 | 2 | 75 |
| M-RFA50 | 350 | 350 | 3500 | 385 | 2 | 75 |
| M-CFA60 | 280 | 420 | 3500 | 385 | 2 | 75 |
| M-RFA60 | 280 | 420 | 3500 | 385 | 2 | 75 |
| M-CFA70 | 210 | 490 | 3500 | 385 | 2 | 75 |
| M-RFA70 | 210 | 490 | 3500 | 385 | 2 | 75 |

### 3.3.5 **Mortar mixing procedure**

In this research, the methodology for the mixing of mortar according to ASTM C305-13 [120] was modified. Because using water reducer admixture (WR) made a significant reduction in the amount of mixing water and thus some un-hydrated cement remained in the mix. Therefore, the modified mixing process was used in this research to avoid leaving un-hydrated cement in the mix as shown in Table 3-6. It should be mentioned that with the exception of the Accelerated Mortar Bar Test (AMBT), the methodology for the mixing of mortar as mentioned in ASTM C305-13 [120] was used.

**Table 3-6: Mixing procedures used for mortar mixes**

| ASTM C305 Mixing Process | Modified Testing Process Used with Water Reducer |
|---|---|
| Add cement to water | Add ¾ of total water to sand |
| Mix at low speed[1] for 30 seconds | Mix at low speed[1] for 30 seconds |
| Add sand over 30 second period at low speed[1] | Stop mixer |
| Stop mixer | Add cement at low speed[1] for 1 minute |
| Mix at high speed[2] for 30 seconds | Stop mixer |
| Stop mixer | Add remaining water incorporated water reducer |
| Let mix stand for 90 seconds and scrape slides of mixing bowl | Mix at high speed[2] for 1 minute |
| Mix at high speed[2] for 1 minute | Stop mixer |
| | Rest for 1 minute and scrape slides of mixing bowl |
| | Mix at high speed[2] for 1 minute |
| [1] low speed: Revolving the paddle at a rate of 140 ± 5 r/min, with a planetary motion of 62 r/min | |
| [2] High speed: Revolving the paddle at a rate of 285 ± 10 r/min, with a planetary motion of 125 r/min | |

### 3.3.6 Casting and curing and testing of mortar specimens

The flow and wet density of mortars were evaluated immediately after mixing in accordance with the ASTM C1437 and ASTM C188 respectively [123, 125]. The 50 mm cubes were cast for compressive strength and strength activity index tests. The compressive strength test was performed on specimens stored in saturated lime water at the age of 1, 7 and 28 days for mixes with w/b=0.40 while it was performed at 7, 28 and 56 days for the mixes with w/b=0.55 in accordance with ASTM C109 [124]. Strength activity Index test (SAI) of the mortars with 20% cement replacement with fly ash and 50% cement replacement with slag was performed on specimens cured in lime-saturated water at 7 and 28 days in according to ASTM C311 and ASTM C989 respectively [126, 127]. For metakaolin, there is no specific standard for SAI determination; therefore, 10% cement replacement was considered from preliminary work, and the SAI test was carried out at the age of 7 and 28 days. The drying shrinkage specimens were prepared using prismatic moulds 40 x 40 x 150 mm and covered with a moist towel for preventing possible evaporation and stored in a moist atmosphere for the first 24 hours. The next day after demoulding, the initial reading was carried out, and then the specimens were kept under drying conditions of 50±5% RH and 23±2 °C. The length of specimens was measured at 7, 14, 21, 28 and 56 days from demoulding in accordance with AS 2350.13 [128]. Mortar bars were cast according to the AMBT test method, AS1141.60.1 using 25×25×285 mm prisms and cured for 24 hours at 23±2 °C and relative humidity, not less than 95% [109]. Then, they were stripped, immersed in water and maintained at 80°C for another 24 hours. After that, samples were taken out, their initial lengths were measured,

and they were immersed in 1 M NaOH solution at 80°C throughout the testing period. Length changes were measured at 3, 7, 10, 14, 21, 28 and 35 days.

### 3.3.7 Concrete mix design process

In the present work, the abbreviations used to identify all concrete mixes is denoted in Figure 3-3.

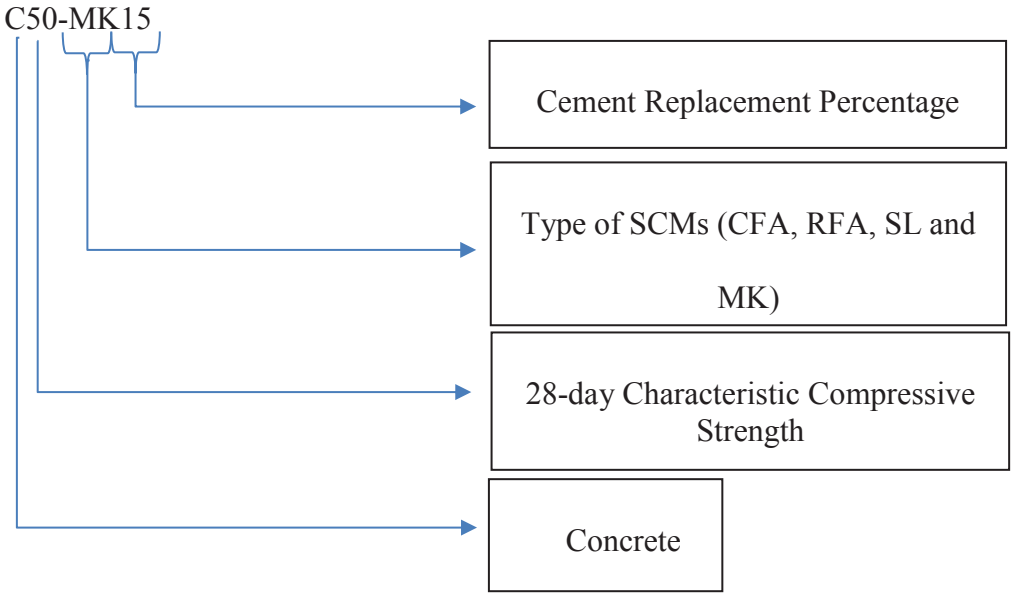


**Figure 3-3: Abbreviations used to denote concrete mixes**

In this research, all concrete mixes were designed according to the combined British method of concrete mix design popularly referred as the DOE method "Designing of normal concrete mixes" with unit water method [129].

Because the performance of concrete is highly dependent on the properties of the individual material, the proportioning procedure is meant to produce mix proportions based on the performance of laboratory trial batches. Usually, for concrete mixes with higher strength, chemical admixtures are used to limit the w/b ratio. Thus, many trial mixes are often required to generate the data necessary to identify optimum mix proportions. The mix design was done in several steps as

described below. It involves designing a control mix containing only cement as a binder and incorporating SCMs in required percentages later to produce final batches by adjustment of material quantities per unit volume.

Step 1: Determination of free water to cementitious ratio in relation to compressive strength

The first step is to calculate the target mean strength based on the characteristic strength and standard deviation as shown in Equation 3-1.

$$f_m = fc + ks \qquad \textbf{Equation 3-1}$$

where

$f_m$ = Target mean strength

fc = Specified characteristic strength

k = a constant

s = Standard deviation

K constant is derived from the mathematics of the normal distribution showing the appropriate percentage of defectives permitted below the specified characteristic strength and increases as the proportion of defectives is reduced as shown in Table 3-7.

**Table 3-7: K constant value based on defective percentage [129]**

| Defective | Constant K |
|---|---|
| 1% | 2.33 |
| 2.5% | 1.96 |
| 5% | 1.64 |
| 10% | 1.28 |

The variation in concrete strengths generally follows the normal distribution similar to the one shown in Figure 3-4. The total number of test results are shown by the area under the curve, and the area beneath the curve to the left-hand side of the vertical line drawn through the specified value represents that part of the results which are less than the specified value. In addition, increasing the specified characteristic strength up to the certain level increases standard deviation and above that level will be independent of the specified strength as shown in Figure 3-5.

It should be mentioned that if the air entrained agent is used in designing the mix, the strength of concrete will be decreased. The reduction of 5.5% in compressive strength will result for each 1% by volume of air entrained in the mix. Therefore, the modified target mean strength for an air-entrained mix is calculated by Equation 3-2.

$$\mathbf{f_m = \frac{fc + ks}{1 - 0.055a}} \qquad \textbf{Equation 3-2}$$

where

$f_m$ = Target mean strength

fc = Specified characteristic strength

k = a constant

s = Standard deviation

a = percentage by volume of air entrained

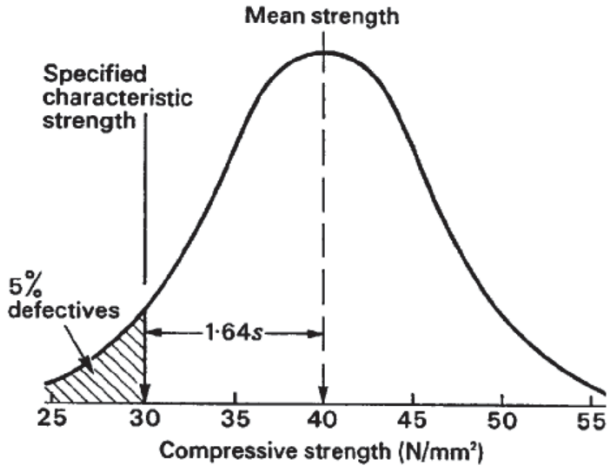


**Figure 3-4: Normal distribution of concrete strengths [129]**

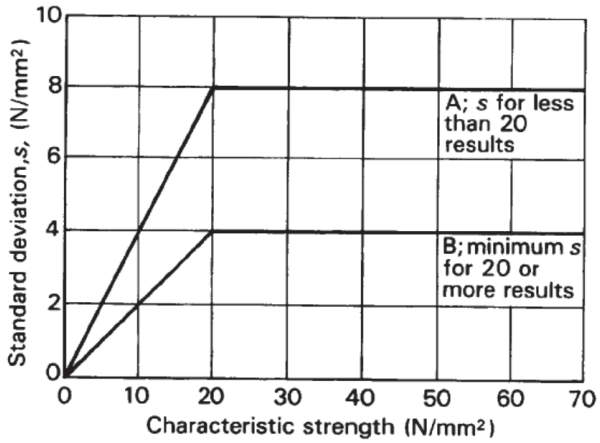


**Figure 3-5: Relationship between standard deviation and characteristic strength [129]**

After finding the target mean strength, a value is obtained for the strength based on the specified age, strength class of cement and the used aggregate for a mix made with a W/C ratio of 0.50 from Table 3-8.

Then, a curve is drawn on Figure 3-6, using this value parallel to the printed curves until it intercepts a horizontal line representing the target mean strength. The corresponding value for the free W/C ratio can be read from the horizontal

axis. This should be compared with any specified maximum free W/C ratio and the lower of these values used. It should be noted that if any kind of SCMs are used as a cement replacement in designing the mix, the appropriate cement efficiency factor (k) should be considered according to the type of SCMs. In this research, these factors were calculated from mortar mix results, which are 0.30, 1.00 and 1.25 for fly ash (CFA and RFA), slag (SL) and metakaolin (MK) respectively. Smith [130] proposed the use of the cement efficiency factor where kF is the mass of Portland cement class 42.5 equivalent to a mass of F (fly ash). Therefore, a concrete containing cement and fly ash will have the same strength as only Portland cement concrete with the similar workability if they follow the Equation 3-3.

$$\frac{W}{C+kF} = \frac{W1}{C1}$$ **Equation 3-3**

Where

W = free-water of cement and fly ash concrete

C = cement content of cement and fly ash concrete

F = fly ash content of cement and fly ash concrete

W1 = free-water of cement concrete

C1 = cement content of cement concrete

Furthermore, a value is obtained for the strength of the fly ash mix based on the only 28 days age, strength class of cement and the used aggregate for a mix made with a $\frac{W}{C+kF}$ ratio of 0.50 from Table 3-8.

**Table 3-8: Approximate compressive strength of concrete mixes made with free W/C ratio of 0.50 [129]**

| Cement strength class | Type of coarse aggregate | Compressive Strength ($N/mm^2$) | | | |
|---|---|---|---|---|---|
| | | Age (days) | | | |
| | | 3 | 7 | 28 | 91 |
| 42.5 | Uncrushed | 22 | 30 | 42 | 49 |
| | Crushed | 27 | 36 | 49 | 56 |
| 52.5 | Uncrushed | 29 | 37 | 48 | 54 |
| | Crushed | 34 | 43 | 55 | 61 |

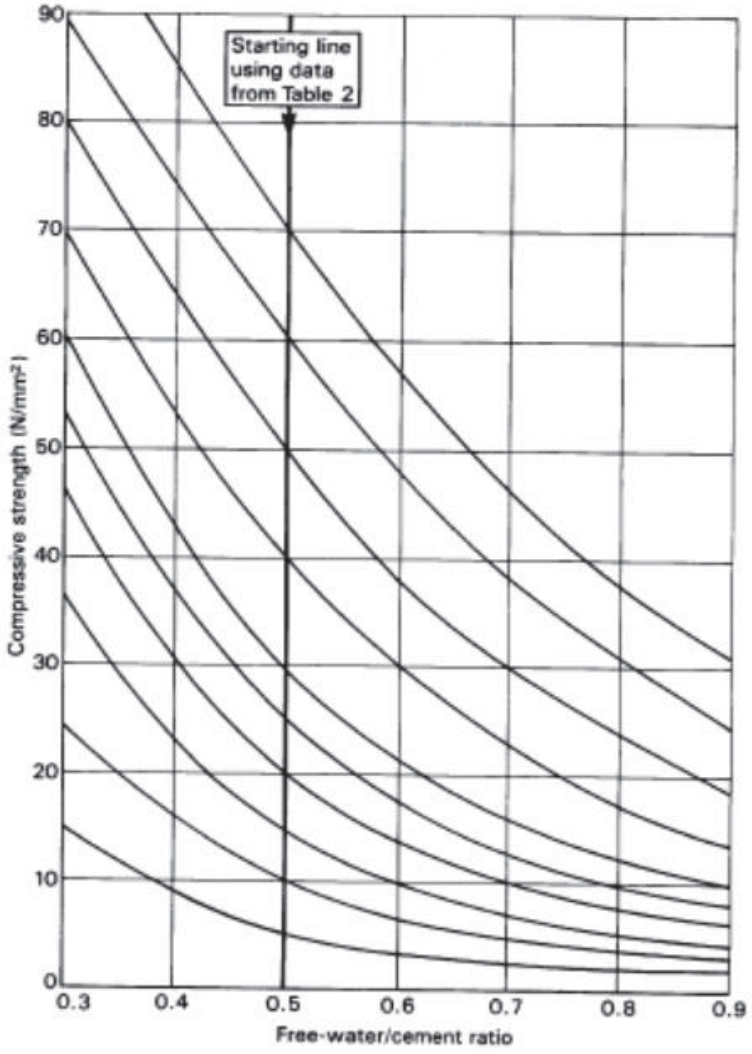


**Figure 3-6: Relationship between compressive strength and free W/C ratio [129]**

Step 2: Choosing the free water content

In this step, the free-water content is determined according to the type and maximum size of aggregate in order to give a concrete of the specified slump or Vebe time. However, when coarse and fine aggregates of different types are used, the free-water content is calculated by the Equation 3-4.

$$\text{Free-water content} = 2/3 \times W_f + 1/3 \times W_c \qquad \textbf{Equation 3-4}$$

Where

$W_f$ = free water content appropriate to type of fine aggregate

$W_c$ = free water content appropriate to type of coarse aggregate

It should be mentioned if the mix is designed using air-entrained agent, the smaller slump range should be selected from Table 3-9 for water content determination as introduction of entrained air into the mix increases the workability of the concrete. In addition, in the mixes containing fly ash as a supplementary cementitious material, water content can normally be reduced by 3% for each 10% cement replacement with fly ash. Therefore, the values presented in Table 3-9 are decreased according to the fly ash content. When slag (SL) is used to partially replace Portland cement, usually the water content given in Table 3-9 should be reduced by about 5 kg/m$^3$ as slag works as water-reducing agent.

**Table 3-9: Approximate free water contents required to give various levels of workability [129]**

| Slump (mm)<br>Vebe time (s) | | 0-10<br>>12 | 10-30<br>6-12 | 30-60<br>3-6 | 60-180<br>0-3 |
|---|---|---|---|---|---|
| Maximum size of aggregate (mm) | Type of aggregate | | | | |
| 10 | Uncrushed | 150 | 180 | 205 | 225 |
| | Crushed | 180 | 205 | 230 | 250 |
| 20 | Uncrushed | 135 | 160 | 180 | 195 |
| | Crushed | 170 | 190 | 210 | 225 |
| 40 | Uncrushed | 115 | 140 | 160 | 175 |
| | Crushed | 155 | 175 | 190 | 205 |

Step 3: Determination of cement content

Cement content is simply calculated from the Equation 3-5. The resulting value should be checked against any specified maximum or minimum value.

$$\textbf{Cement content} = \frac{free-water\ content}{free\ water\ to\ cement\ ratio} \qquad \textbf{Equation 3-5}$$

If calculated cement content > min cement ⟶ Proceed

If calculated cement content < min cement ⟶ Use min cement and calculate modified W/C ratio

However, cement and SCM content for a mix with cement replacement with SCMs can be calculated by Equations 3-6 and 3-7 respectively.

$$\textbf{Cement content} = \frac{(100-p)\times W}{(k\times p+(100-p))\times Y} \qquad \textbf{Equation 3-6}$$

$$\textbf{SCM content} = \frac{p\times C}{(100-p)} \qquad \textbf{Equation 3-7}$$

Where

W = water content

C = cement content

P = SCM replacement percentage

K = cement efficiency factor

Y = water to binder ratio of cement and SCM concrete

Step 4: Selection of fine and coarse aggregate content

In this step, the percentage of fine aggregate to total aggregate content is calculated from Figure 3-7 according to the maximum size of aggregate, the workability level, the grading of the fine aggregate (defined by its percentage passing a 600-μm sieve) and the free W/C ratio. After determination of coarse and fine aggregate content, the best combined grading for the 10 and 20 mm coarse aggregate as well as coarse and fine sand should be determined according to the recommended grading of Road Note No.4 as shown in Figure 3-8.

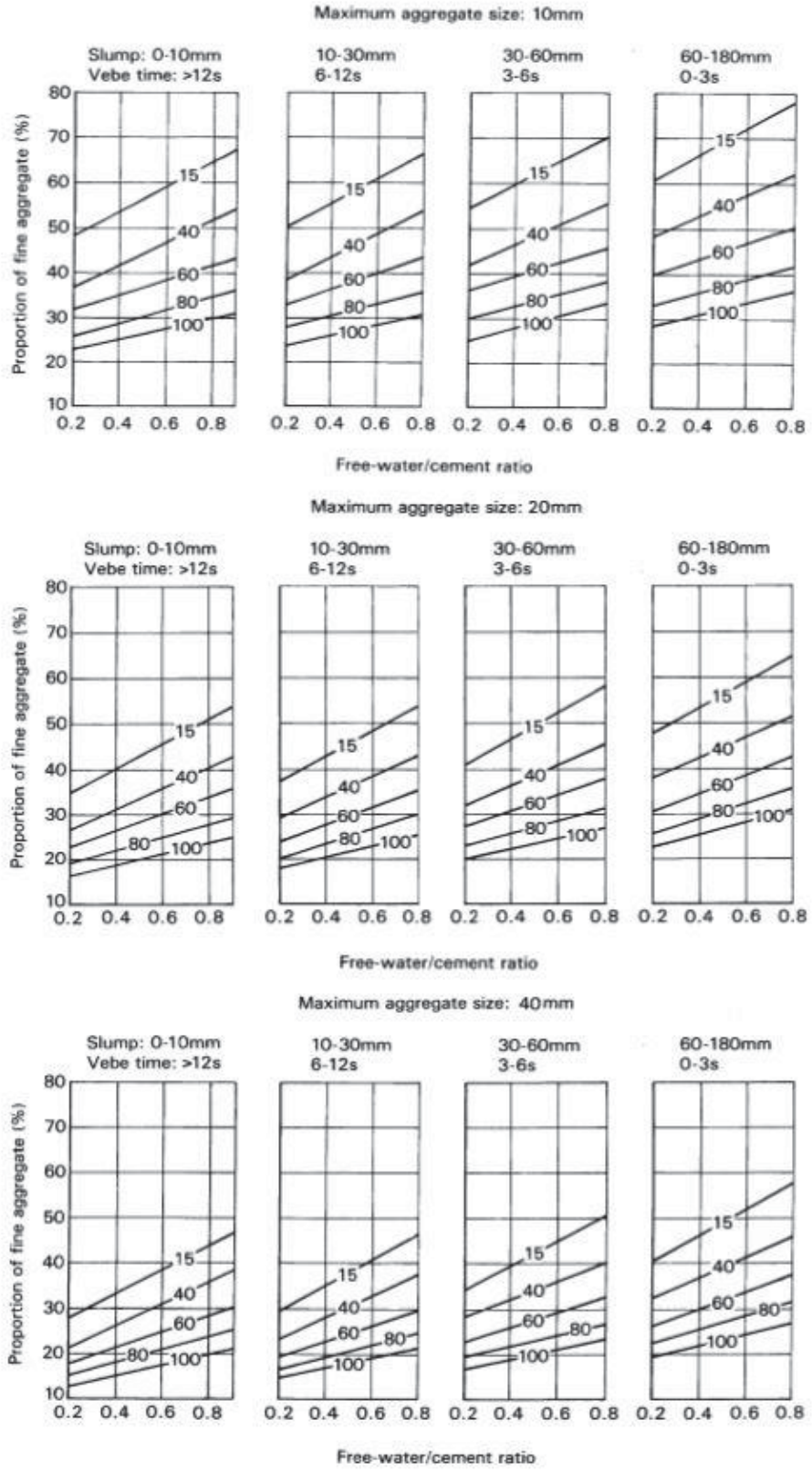


**Figure 3-7: Recommended proportions of fine aggregate according to percentage passing 600 µm sieve [129]**

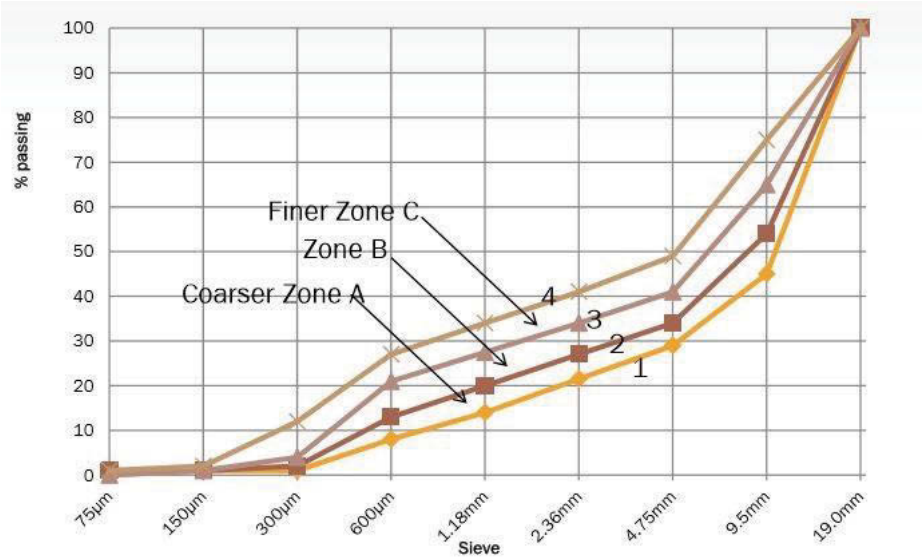


**Figure 3-8: Recommended combined aggregates according to Road Note No.4**

Step 5: Estimation of fine and coarse aggregate content

At the completion of stage 4, all the ingredients of the concrete have been estimated except the aggregate. However, the percentage of coarse and fine aggregate was determined. The total aggregate quantity can be determined by subtracting the volume of cementitious materials, water and air content from unit volume of concrete and then multiplying the result by the specific gravity of combined aggregate.

Finally, the coarse and fine aggregates themselves can be subdivided to required proportions according to the results from step 4. It should be noted that the quantities of aggregates in the mix design are determined based on Saturated-Surface-Dry (SSD) condition.

### 3.3.8 Concrete mixing procedure

All of the concrete mixes have been combined using a rotary pan concrete mixer, and then cured and compacted in accordance with AS1012.2 [131]. All the aggregates were soaked in water for one night and drained on the day of mixing. Prior to the proportioning and mixing of concrete, a representative sample of aggregates was taken to measure the moisture content to revise the mix accordingly.

### 3.3.9 Casting, curing and testing of concrete specimens

The workability using the slump test, the air content and mass per unit volume of the fresh concrete mixes were measured immediately after the mixing was completed, according to AS 1012.3.1 [132], AS 1012.4.2 [133] and AS 1012.5 [134] respectively. Concrete cylinders of 100 mm diameter and 200 mm height were cast for compressive strength, rapid chloride permeability and rapid sulfate permeability tests. The compressive strength test was performed on specimens stored in lime-saturated water for all concrete mixes at the age of 1, 7, 28 and 56 days in accordance with AS1012.9 [135]. The flexural strength test was carried out on specimens with dimensions of 100 × 100 × 350 mm for pavement concrete mixes after 7 and 28 days curing in lime-saturated water, according to AS 1012.11 [136]. Prisms of 75 × 75 × 280 mm in dimensions were cast for measurement of the drying shrinkage according to AS 1012.13 [137]. The specimens were removed from moulds 24 hours after casting and then cured under lime water until the 7th day when the initial length was recorded. The samples were left for drying in the laboratory at 23±2 °C, and 50% relative humidity and length change was recorded up to 56 days.

### 3.3.10 **Durability properties of concrete specimens**

Water absorption and apparent volume of permeable void (AVPV) tests were carried out on concrete cylinders of 100 mm diameter and 200 mm height in accordance with AS 1012.21 [73]. Chloride permeability was measured in accordance with the ASTM C1202 Standard at the age of 28 days [75]. The 50 mm thick specimens were cut from the middle of the cylinders. Then, the vacuum saturated specimens were subjected to 60 V DC electric potential for 6 hours. The chloride penetrability of the specimens was expressed as the total charge passed in coulombs during the test period. This is used as an indicative parameter of the chloride permeability of concrete. The rapid sulfate permeability test proposed by Sirivivatnanon and Khatri [89], was performed on the 50-mm thick slices obtained from 100 by 200 mm concrete cylinders at the age of 28 days. The slices are saturated in water in a vacuum suction. Then, a potential difference of 60 V DC was maintained across the ends of the specimen; one side is exposed to an 8.8% sodium sulfate solution, the other to a 0.3 N sodium hydroxide solution. Subsequently, the amount of electrical current passed, in coulombs, during a 6-h period was measured.

# Chapter 4

## CHARACTERISATION OF RAW MATERIALS

# 4 CHARACTERISATION OF RAW MATERIALS

## 4.1 Preface

Some important characteristics of cementitious and pozzolanic materials (PC, CFA, RFA, GRFA, SL and MK), as well as fine and coarse aggregates used in this research have been investigated. Fly ash used in this research was limited to one power station source, Eraring power plant, in Australia. However, samples were taken with an interval of one year to understand the variation in its characteristics with time. Therefore, the first batch of fly ashes is indicated by abbreviations of CFA1 and RFA1 and the second batch after one year is indicated by the abbreviations of CFA and RFA. However, Only CFA and RFA were used for all experimental studies in this research, as the physical and chemical characteristics of both batches of fly ash were similar. Additionally, RFA was ground to a finer particle size, which is indicated by the abbreviation GRFA in order to investigate the effect of fineness of fly ash on the properties of paste and mortar, which will be further discussed in Chapters 5 and 6.

### 4.1.1 Physical properties

Particle size analysis (PSA) of cement and SCMs was carried out by a Malvern Mastersize 2000 laser analyser using the laser diffraction technique. The PSA results are shown in Figures 4-1 and 4-2. The Blaine fineness, the percentage of passing sieve No.45, and specific gravity of cementitious materials were determined according to AS 2350.9, AS 2350.8 and AS 3583.5 respectively, as shown in Tables 4-1 to 4-3 [113-115]. From the results, it can be concluded that CFA has a finer particle size, higher specific surface area and higher specific

gravity compared to RFA. Moreover, the results of the surface area of SCMs are entirely consistent with the results of particle size distribution and the percentage of passing sieve No.45. A reduction in particle size has led to increased fineness with a higher specific surface area reported.

**Table 4-1: Specific surface area of cement and SCMs using Blaine's air permeability method**

| Material | Blaine Fineness ($m^2/kg$) |
|---|---|
| PC | 396 |
| CFA | 368 |
| RFA | 302 |
| CFA1 | 350 |
| RFA1 | 292 |
| GRFA | 495 |
| SL | 511 |
| MK | 624 |

**Table 4-2: Fineness of cement and SCMs passing 45-µm sieve**

| Material | Fineness % (passing 45µm sieve) |
|---|---|
| PC | 94 |
| CFA | 85 |
| RFA | 68 |
| CFA1 | 83 |
| RFA1 | 65 |
| GRFA | 100 |
| SL | 99 |
| MK | 86 |

**Table 4-3: Specific gravity of cement and SCMs**

| Material | Specific Gravity (SG) |
|---|---|
| PC | 3.09 |
| CFA | 2.08 |
| RFA | 2.06 |
| GRFA | 2.10 |
| SL | 2.90 |
| MK | 2.49 |

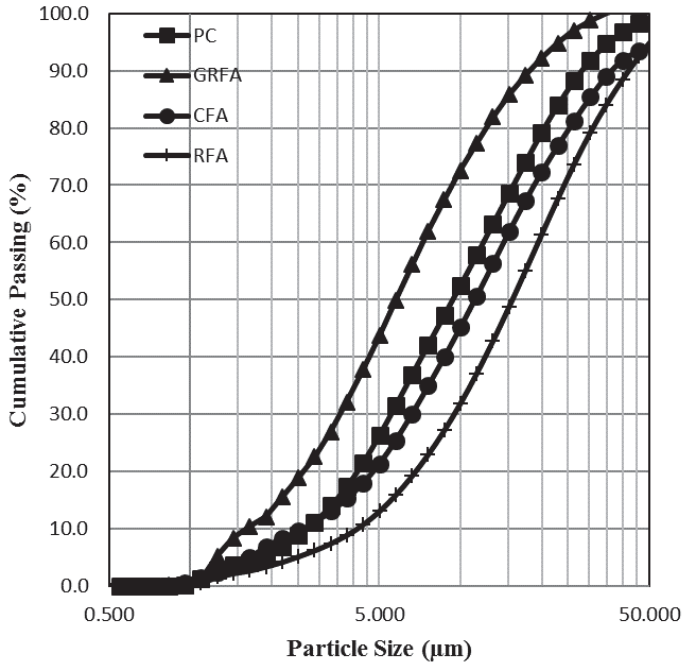


**Figure 4-1: Particle size distribution of cement and fly ashes using the laser diffraction technique**

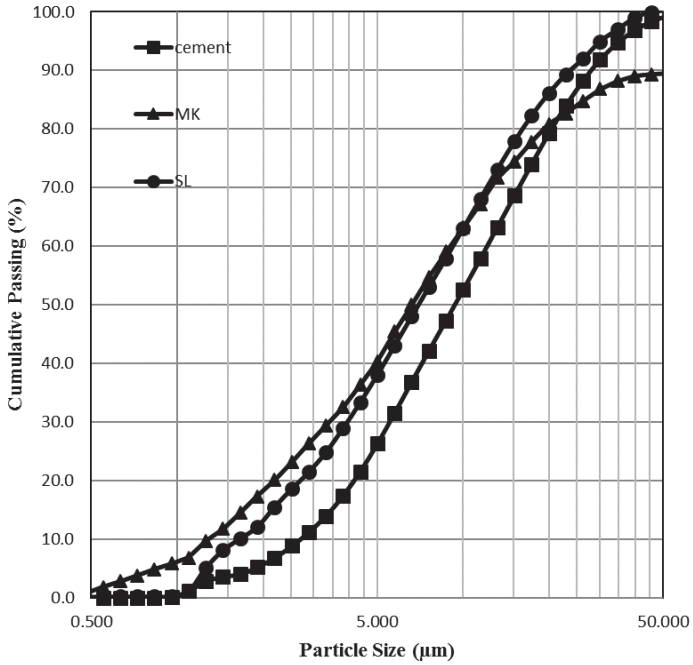


**Figure 4-2: Particle size distribution of cement, slag and metakaolin using the laser diffraction technique**

### 4.1.2 **Chemical composition**

X-ray fluorescence (XRF) analysis was carried out on cement and SCMs (CFA, RFA, SL and MK) by bombarding the sample with high-energy X-rays or gamma rays. The principle of this technique is to excite the individual atoms by an external energy source and then count the number of X-ray photons of each energy range emitted from the sample in order to identify the source atoms. The oxide compositions obtained by the XRF method is given in Table 4-4. The comparison between main oxide components of cement and SCMs are shown in Figure 4-3. The results indicate that run-of-station fly ash has a very similar chemical composition to classified fly ash as both are from the same source. As Taylor [138] reported, fly ash consists mainly of $SiO_2$, but can also contain significant quantities of $Al_2O_3$. The amount of CaO is limited but highly variable, depending on the origin of the fly ash. He also claimed that granulated blast-furnace slag (SL) contains more CaO but significantly less $Al_2O_3$ than fly ash. In addition, the calcination of high-purity kaolinite at high temperatures produces metakaolin (MK) which consist of silica and alumina in an active form [4, 18]. Lothenbach et al. [139] demonstrated the main chemical composition of mentioned SCMs in a $CaO–Al_2O_3–SiO_2$ ternary diagram as shown in Figure 4-4. It exhibits that the chemistry of SCMs is mostly characterized by lower calcium content than Portland cement, which causes the major differences in the formation of hydrates during the hydration process. Table 4-5 shows the available alkali, and alkali content percentage of SCMs measured according to the AS 3583.12 and XRF analyses respectively [116]. It is noted that the available alkali of fly ashes are three and four times higher than SL and MK respectively. It is mainly due to

higher alkali content in the chemical composition of the fly ashes making more alkali available in the mix.

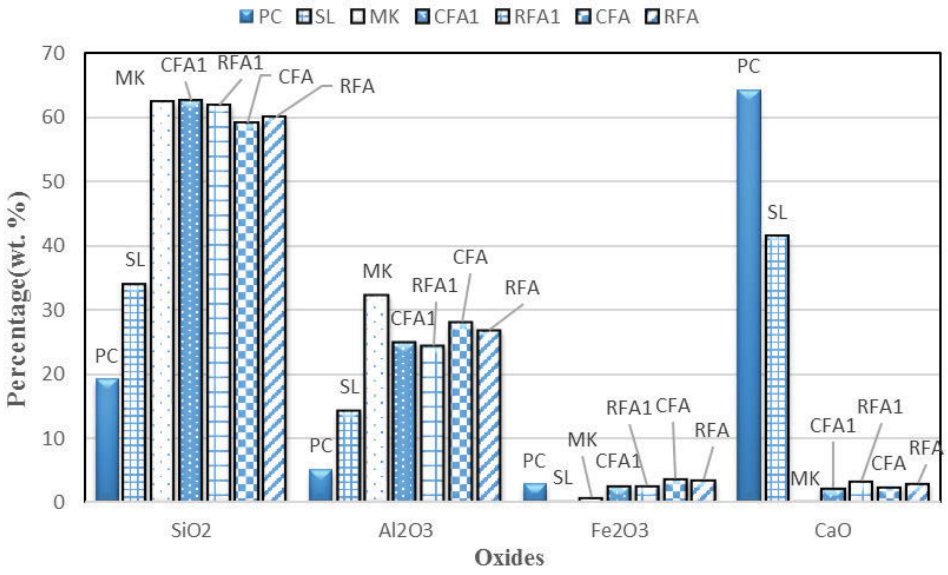


**Figure 4-3: Comparison of main oxide composition of cementitious materials using XRF analysis**

**Table 4-4: Oxide composition of cementitious materials using XRF analysis**

| Oxide wt.% | PC | SL | MK | CFA1 | RFA1 | CFA | RFA |
|---|---|---|---|---|---|---|---|
| $SiO_2$ | 19.23 | 34.12 | 62.50 | 62.71 | 62.07 | 59.21 | 60.06 |
| $Al_2O_3$ | 5.12 | 14.37 | 32.39 | 24.98 | 24.52 | 28.11 | 26.97 |
| $Fe_2O_3$ | 2.86 | 0.30 | 0.82 | 2.72 | 2.60 | 3.68 | 3.65 |
| CaO | 64.26 | 41.59 | 0.07 | 2.25 | 3.43 | 2.48 | 3.00 |
| $TiO_2$ | 0.31 | 0.87 | 1.02 | 1.00 | 0.97 | 1.11 | 1.05 |
| MgO | 1.28 | 5.31 | 0.67 | 0.49 | 0.46 | 0.53 | 0.59 |
| $Na_2O$ | 0.18 | 0.35 | 0.22 | 0.87 | 0.83 | 0.63 | 0.62 |
| $K_2O$ | 0.51 | 0.26 | 0.28 | 1.49 | 1.34 | 1.18 | 1.24 |
| $P_2O_5$ | 0.12 | 0.01 | 0.03 | 0.23 | 0.23 | 0.41 | 0.39 |
| $SO_3$ | 2.73 | 2.83 | 0.08 | 0.13 | 0.16 | 0.16 | 0.17 |
| L.O.I. | 4.06 | 0.35 | 1.75 | 2.00 | 2.52 | 1.05 | 1.20 |

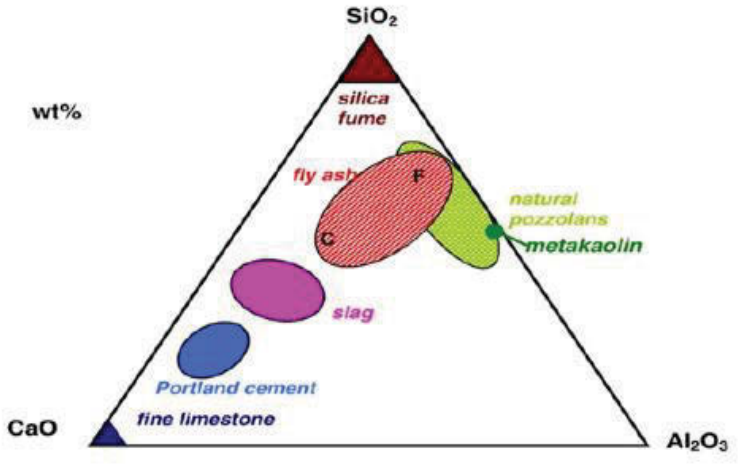


**Figure 4-4: $CaO–Al_2O_3–SiO_2$ ternary diagram of cementitious materials [139]**

**Table 4-5: Alkali and available alkali content of SCMs**

| Oxide (%) | SCMs | | | |
|---|---|---|---|---|
| | CFA | RFA | SL | MK |
| $Na_2O$ | 0.63 | 0.62 | 0.35 | 0.22 |
| $K_2O$ | 1.18 | 1.24 | 0.26 | 0.28 |
| $Na_2Oe$ | 1.41 | 1.44 | 0.52 | 0.40 |
| Available $Na_2O$ | 0.11 | 0.12 | 0.06 | 0.04 |
| Available $K_2O$ | 0.19 | 0.23 | 0.05 | 0.03 |
| Available $Na_2Oe$ | 0.24 | 0.27 | 0.09 | 0.06 |

The comparison between the physical properties and chemical composition of CFA and RFA with the specified requirement of Australian Standard AS3582.1 [6] is shown in Table 4-6. It indicated that CFA is categorised as a finer grade fly ash (grade 1) while RFA is classified as coarser grade fly ash (grade 2), which is in line with the results of particle size distribution and Blaine fineness reported. Considering the similar physical and chemical characteristics of both batches of

fly ash, it should be mentioned that only CFA and RFA were used for all experimental studies performed on paste, mortar and concrete in this research.

**Table 4-6: Comparison of fly ashes with the specified requirement of Australian Standard AS3582.1 [6]**

| Property | Grade 1 limits (AS3582.1) | Grade 2 limits (AS3582.1) | CFA | RFA | CFA1 | RFA1 |
|---|---|---|---|---|---|---|
| Fineness by mass passing 45 sieve, % minimum | 75 | 55 | 85 | 68 | 83 | 65 |
| Loss of ignition, % maximum | 4 | 6 | 1.05 | 1.02 | 2 | 2.52 |
| Sulfate (as $SO_3$) content, % maximum | 3 | 3 | 0.16 | 0.17 | 0.13 | 0.16 |
| Chemical composition in Australia ($Sio_2$+$Al_2O_3$+$Fe_2O_3$) | 70% minimum | | 91 | 91 | 90 | 90 |

### 4.1.3 Identification of crystalline phase

X-ray diffraction (XRD) analysis was carried out on SCMs (CFA, RFA, GRFA, SL and MK) using Bruker D8 Discover diffractometer. This test is a scattering technique achieved by bombarding the material with X-rays whilst gradually being rotated to represent every possible crystalline orientation. X-ray diffraction patterns of CFA, GRFA, RFA, SL and MK are shown in Figures 4-5 to 4-7. The height of the peaks representative of quartz was observed to decrease in intensity relative to the particle size of fly ash as shown in Figure 4-5. A reduction in peak intensity often indicates less crystallinity. Therefore, GRFA is more

reactive compared to CFA and RFA due to the smaller particle size and the higher specific surface area which makes more particles available for reaction as well as more glassy content as confirmed by Barry [140]. As explained by some researchers, the amorphous content of fly ash is the dominant factor that controls the extent of pozzolanic activity. The extent of pozzolanic activity is also influenced by particle size and increases with a reduction in particle size of the fly ash [141, 142]. Diamond [143] reported changes in crystallinity are apparent from the size and location of peaks in XRD diffractogram patterns of SCMs as amorphous phases do not produce a well-defined peaks.

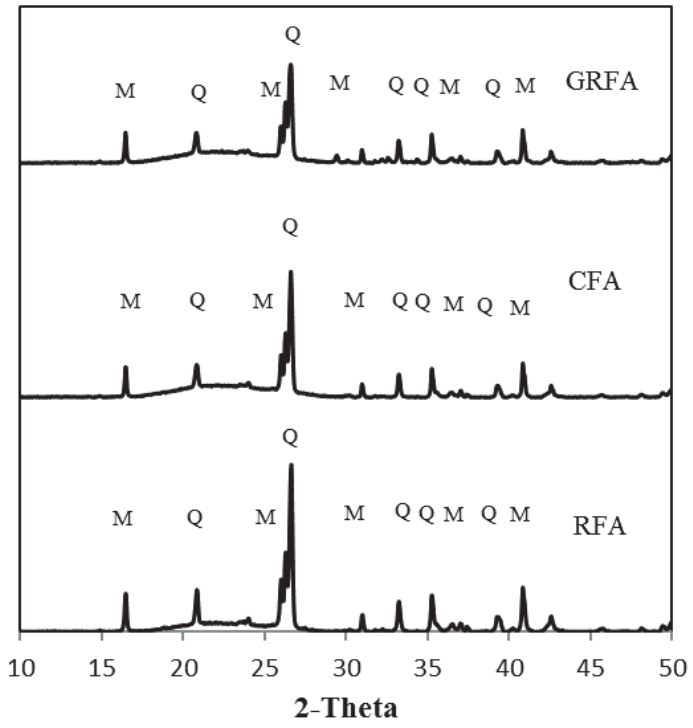


**Figure 4-5: X-ray diffraction patterns of CFA, RFA, GRFA (Q = quartz, M = mullite)**

As shown in Figure 4-6, a broad peak in the diffractogram, the presence of less peaks and reduced intensity in peak height, indicates a sufficient quantity of amorphicity present in the SL. Therefore, a high degree of reactivity will be expected from this SCM. This is in agreement with the findings of Hooton [144] that reported slag is entirely composed of an amorphous phase as it produces a broad peak rather than sharp peaks when analysed by XRD. The presence of amorphicity is considered to be a critical factor in determining the hydraulicity of slag as crystalline slag possesses little reactivity.

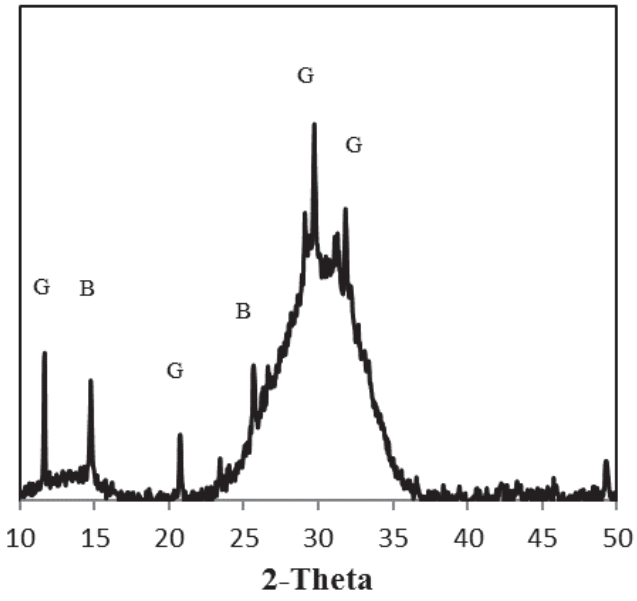


**Figure 4-6: X-ray diffraction of Slag (G = gypsum, B= Bassinite)**

The XRD pattern of MK, as shown in Figure 4-7, indicates that it mainly comprises an amorphous material with only a small quantity of crystallinity. This is due to the thermal activation of kaolinite which breaks down its structure and thus results in dehydroxylation and disordering of the structure leading to a highly reactive material [15].

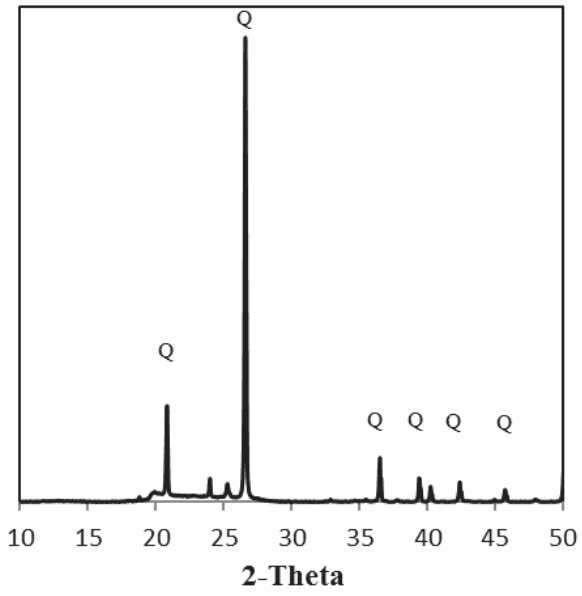


**Figure 4-7: X-ray diffraction of Metakaolin (Q = quartz)**

### 4.1.4 Surface Topography

Scanning electron microscopy (SEM) was carried out on the SCMs (CFA, RFA, GRFA, SL and MK) by scanning the sample surface with a high-energy beam of electrons. Specimens were prepared by using a gold coating and being placed under vacuum prior to imaging. SEM micrographs were taken at the same magnification level (x 300) and are shown in Figures 4-8 to 4-12. From the micrographs, it can be seen that both kinds of fly ashes have spherical and smooth shaped particles while slag and metakaolin have angular shaped particles due to attrition process (i.e., grinding) used to produce the material. These results are in agreement with the findings of Wilson & Kosmatka [145]. It can be seen that the effect of the grinding has resulted in a reduced median particle size of the RFA below that for CFA and PC. The grinding process has also altered the particle shape from being spherical to more angular in shape.

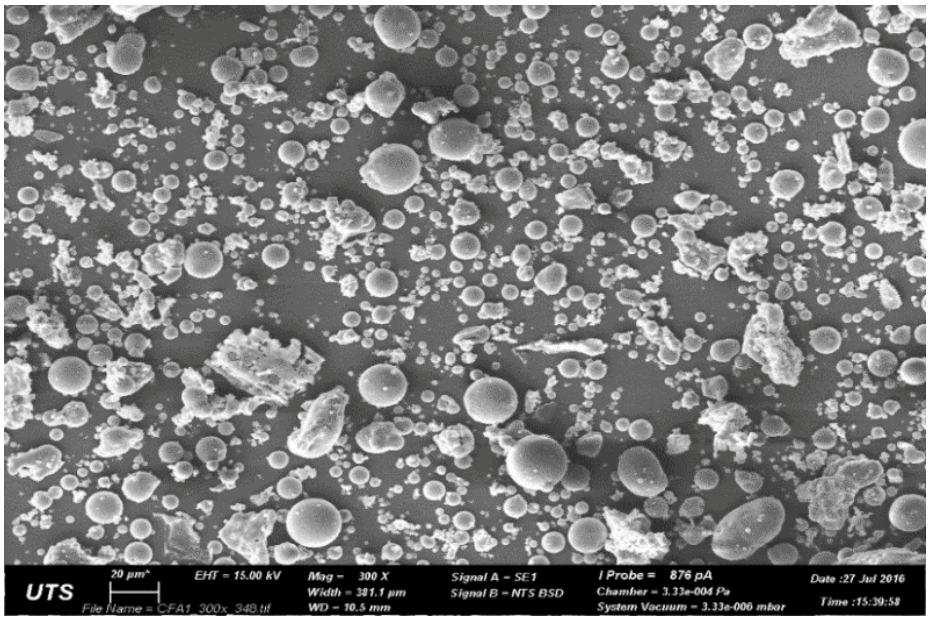


**Figure 4-8: SEM micrograph of classified fly ash (CFA) (x 300)**

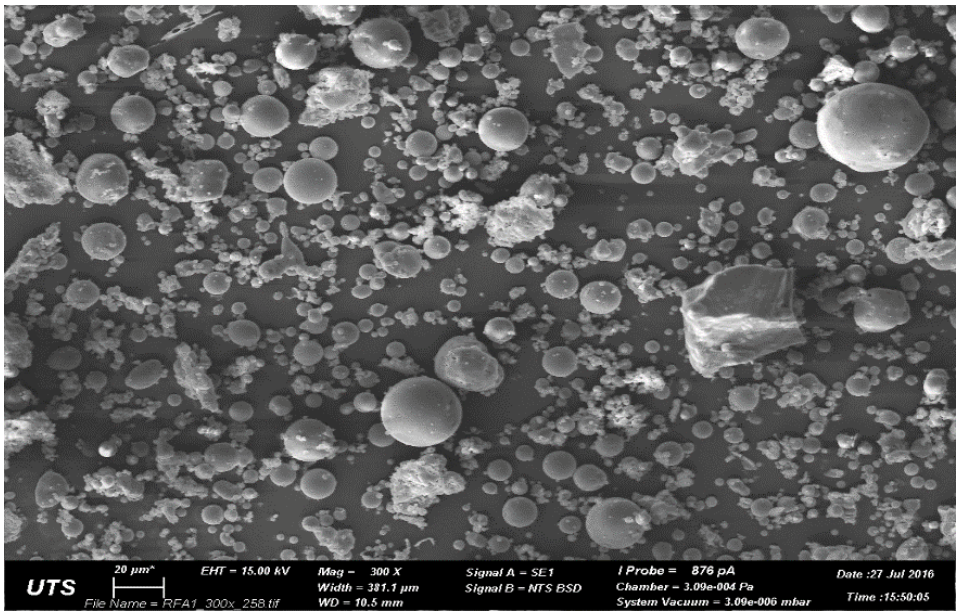


**Figure 4-9: SEM micrograph of run-of-station fly ash (RFA) (x 300)**

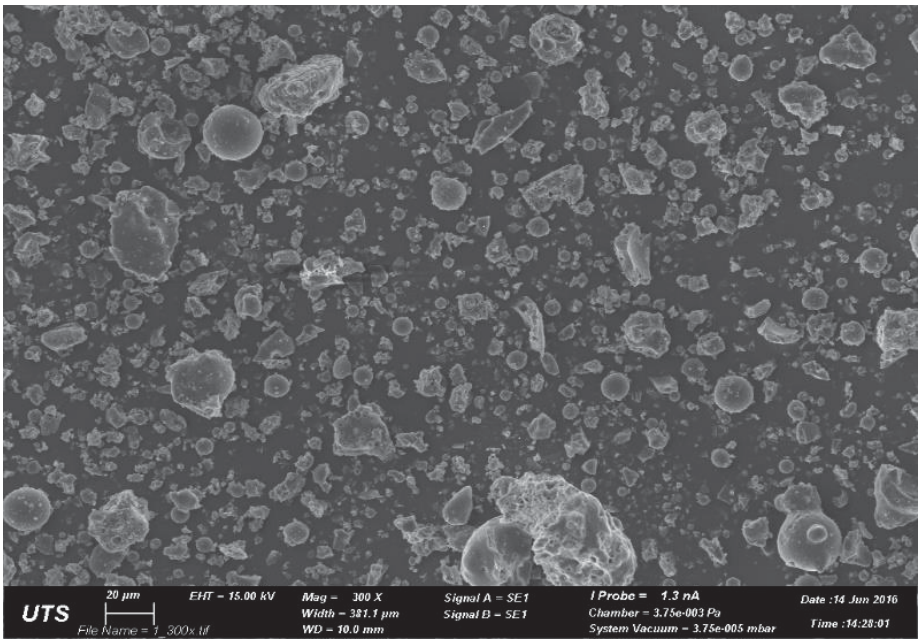


**Figure 4-10: SEM micrograph of ground run-of-station fly ash (GRFA) (x 300)**

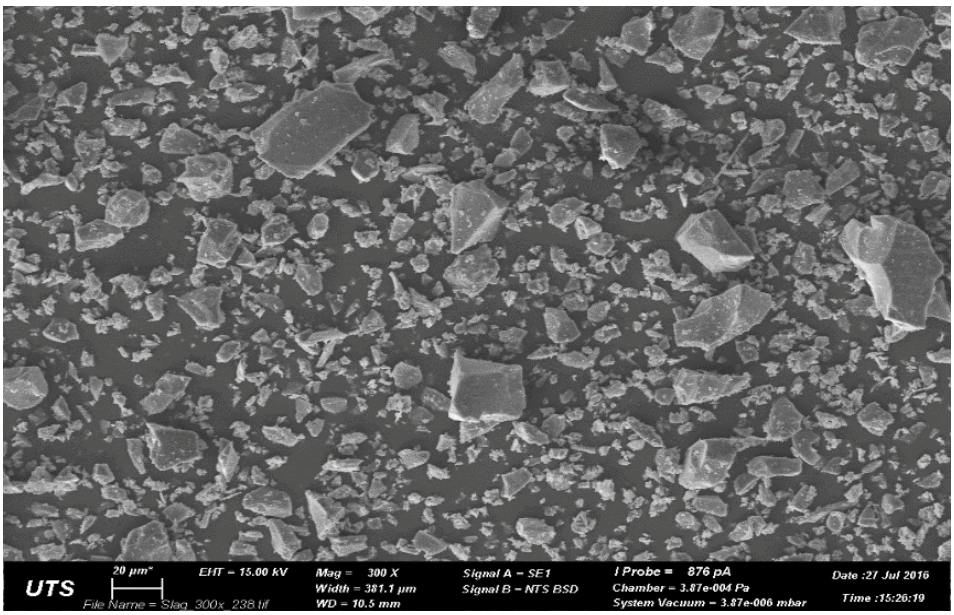


**Figure 4-11: SEM micrograph of slag (x 300)**

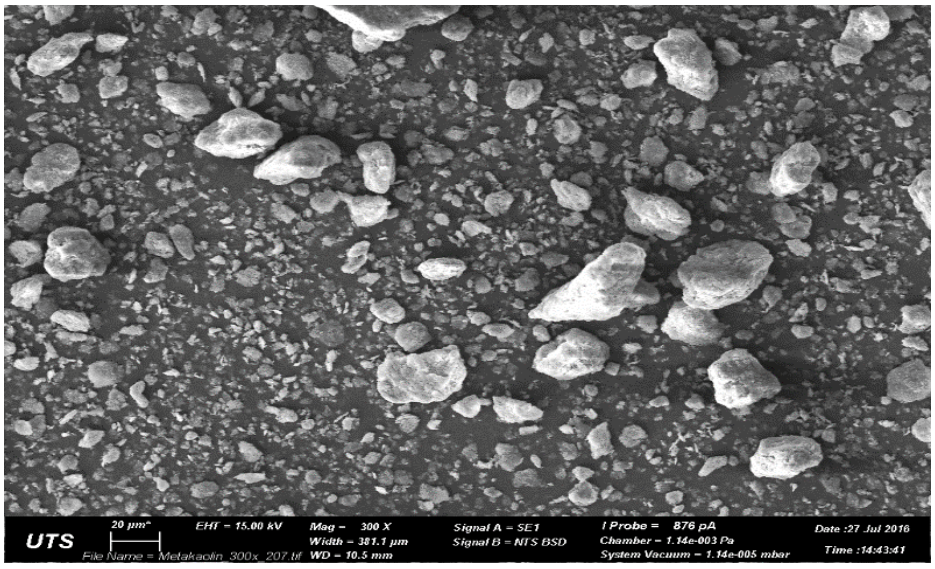


**Figure 4-12: SEM micrograph of metakaolin (x 300)**

## 4.2 Aggregate

### 4.2.1 Grading

Fine sand (Sydney sand) and coarse sand (Nepean river sand) complying with requirements of the specification range listed in AS 2758.1-2014 [146] were used as the source of aggregates in this study as shown in Table 4-7. The grading results achieved by using the sieving method for fine and coarse sands are given in Figures 4-13 and 4-14, respectively.

**Table 4-7: Sieve analysis for fine and coarse sands**

| Sieve Size (mm) | AS 2758.1 Limits (%) | Fine Sand Percent Passing (%) | Coarse Sand Percent Passing (%) |
|---|---|---|---|
| 4.75 | 90-100 | 100 | 98 |
| 2.36 | 60-100 | 100 | 85 |
| 1.18 | 30-100 | 100 | 68 |
| 0.600 | 15-100 | 100 | 40 |
| 0.300 | 5-50 | 45 | 13 |
| 0.150 | 0-20 | 1 | 5 |
| 0.075 | 0-5 | 0 | 0 |

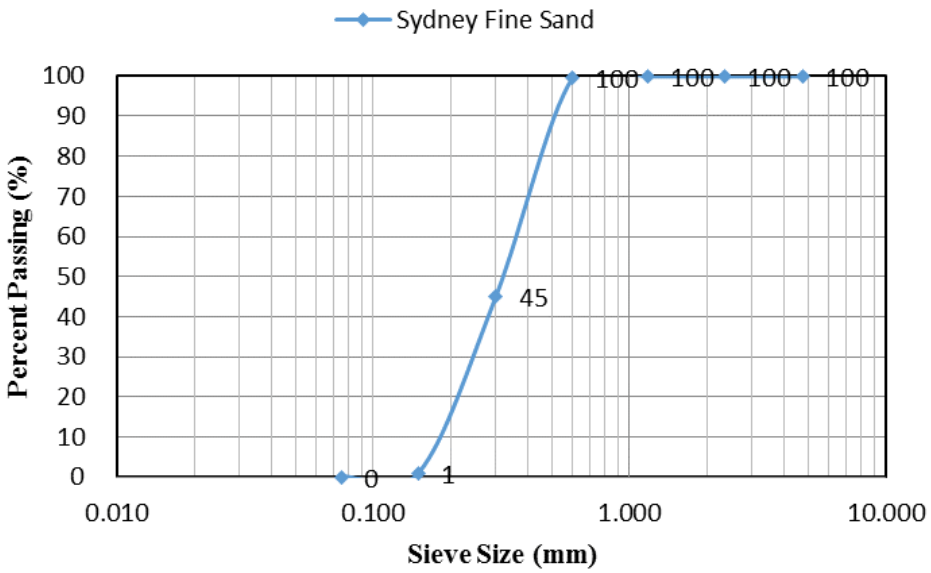


**Figure 4-13: Particle size grading of Sydney fine sand (sieving method)**

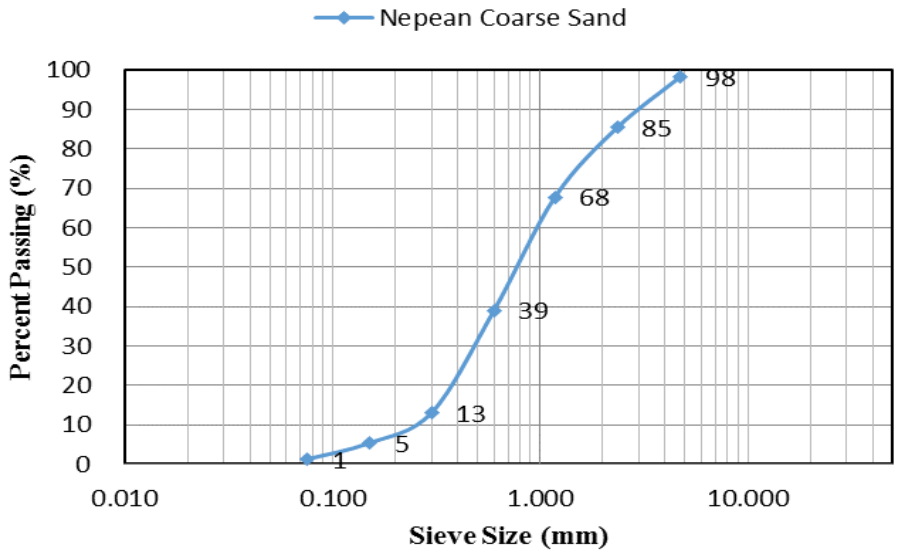


**Figure 4-14: Particle size grading of Nepean coarse sand (sieving method)**

Coarse aggregate (CA), being 10 mm and 20 mm gravel complying with the requirements of the specification range listed in AS 2758.1 [146], was also used in this study as shown in Table 4-8. The results for grading by the sieving method for both coarse aggregates are given in Figures 4-15 and 4-16, respectively.

**Table 4-8: Sieve analysis for 10 and 20 mm coarse aggregates**

| Sieve Size (mm) | AS 2758.1 Limits (%) | 10 mm aggregate Passing (%) | AS 2758.1 Limits (%) | 20 mm aggregate Passing (%) |
|---|---|---|---|---|
| 19.00 | 100 | 100 | 85-100 | 96 |
| 13.20 | 100 | 100 | 40-60 | 43 |
| 9.50 | 85-100 | 96 | 0-20 | 10 |
| 4.75 | 0-20 | 19 | 0-5 | 0 |
| 2.36 | 0-5 | 5 | - | 0 |
| 1.18 | - | 0 | - | 0 |

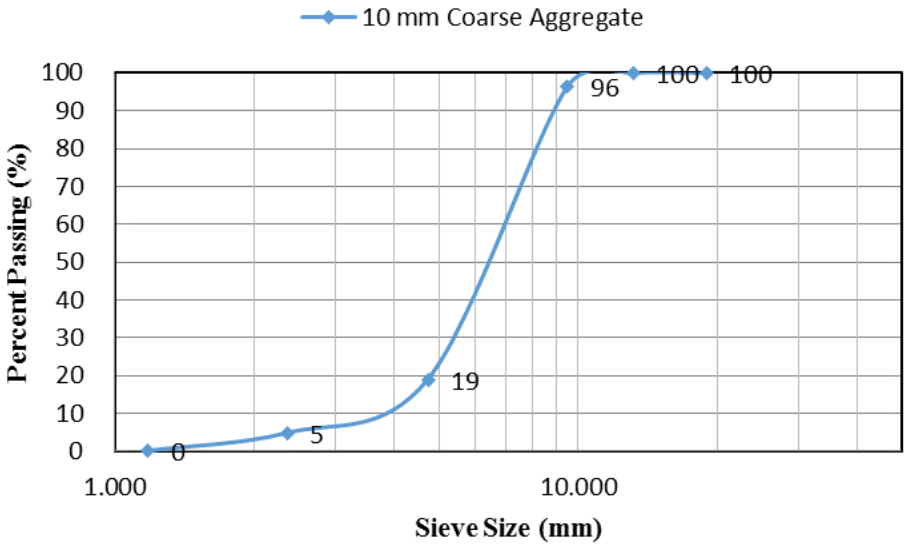


**Figure 4-15: Particle size grading of 10 mm aggregate (sieving method)**

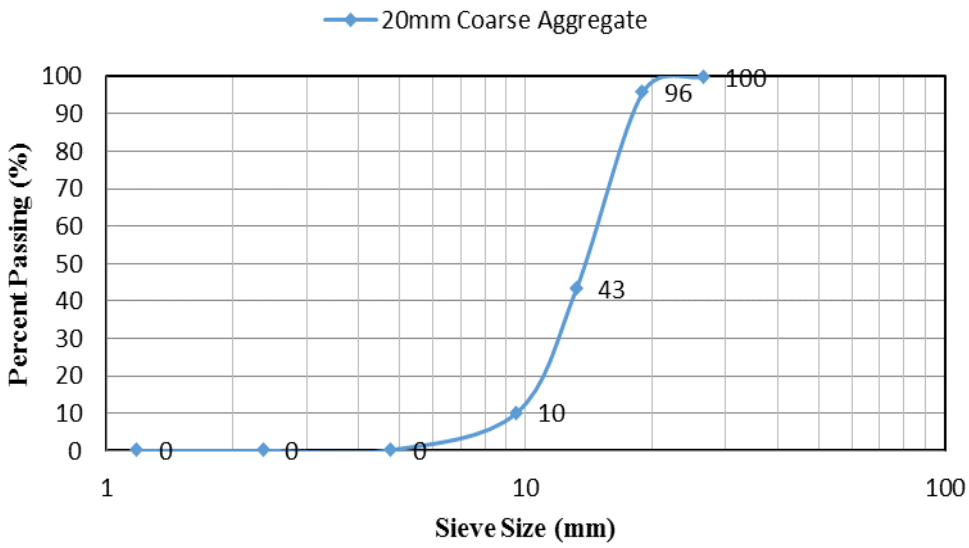


**Figure 4-16: Particle size grading of 20 mm aggregate (sieving method)**

### 4.2.2 Water absorption and specific gravity

Specific gravity and water absorption of fine and coarse aggregates were performed according to AS 1141.5 [118], and the results are shown in Table 4-9. The results show that water absorption by fine sand is the highest, followed by 10 mm coarse aggregate, 20 mm coarse aggregate and coarse sand while the specific gravity of all fine and coarse aggregates investigated are almost the same.

**Table 4-9: Fine and coarse aggregate properties**

| Material | Specific Gravity in SSD (SG) | Water Absorption (%) (WA) |
|---|---|---|
| Fine Sand | 2.60 | 2.00 |
| Coarse Sand | 2.48 | 1.11 |
| 10 mm coarse aggregate | 2.65 | 1.85 |
| 20 mm coarse aggregate | 2.65 | 1.68 |

# Chapter 5

## EFFECT OF FINENESS AND LEVEL OF DIFFERENT FLY ASHES AND SCMs ON IMPORTANT PROPERTIES OF THE CEMENT PASTE

# 5 EFFECT OF FINENESS AND LEVEL OF DIFFERENT FLY ASHES AND SCMs ON IMPORTANT PROPERTIES OF THE CEMENT PASTE

## 5.1 Preface

In this chapter, the effect of fly ash fineness on consumption of calcium hydroxide and microstructure, flow and compressive strength of blended cement pastes was assessed and evaluated against cement paste. Fly ashes with different fineness, CFA, RFA and GRFA, were used to partially replace Portland cement at 20% and 40% by weight of cement using a fixed water-to-binder ratio of 0.40. In addition, the effect of different types, fineness and levels of supplementary cementitious materials (SCMs): GRFA, CFA, RFA, SL and MK as well as different water to binder ratios were evaluated on the cumulative heat of hydration and the amount of heat evolution of blended cement pastes.

## 5.2 Heat of hydration

### 5.2.1 Stage of Hydration: Overview

The hydration reaction of cement minerals alite ($C_3S$), belite ($C_2S$), tricalcium aluminate ($C_3A$) and tetracalcium aluminoferrite ($C_4AF$) is an exothermic process. The primary hydration products are calcium silicate hydrate (C-S-H), calcium hydroxide (CH), ettringite and monosulfoaluminate. The hydration process of Portland cement can be distinguished by five stages in heat generation in the early ages as reported by several researchers [32] and as shown in Figure 5-1: (I) the initial stage: immediately within the first few minutes of mixing cement with water, the aluminate reacts with water and sulfate, forming a gel-like material

(ettringite) surrounding the cement grains. This reaction releases a significant amount of heat and is represented by the first peak of the hydration process. However, it is difficult to detect the first hydration peak as the wetting of cement particles usually happens outside the calorimeter; (II) the dormancy stage: there is a dormant stage of about two to four hours after mixing in which the aluminate reaction is controlled by the amount of ettringite gel surrounding the cement grains due to limited access of water to the cement grains, which controls the rate of the aluminate reaction, and thus little heat is released. However, alite and belite, the main components of cement, slowly dissolve and accumulate calcium and hydroxyl ions in the pore solution; (III) the acceleration stage: after super-saturation of the pore solution with calcium ions mainly from dissolving alite and belite, fibre-like C-S-H gel and crystalline C-H start to form with significant heat evolution. The acceleration stage is represented by the second peak of hydration. During this acceleration process, needle-like ettringite also forms as a result of the continuing reaction of aluminate and sulfate; (IV) the deceleration stage: interaction of C-S-H gel and crystalline C-H with remaining water and undissolved cement grains slows down the alite reaction thus reducing the heat of hydration. The amount of sulfate starts to deplete and thus the remaining aluminate reacts with ettringite to form monosulfate. The formation of monosulfate generates little heat, which may be associated to the third hydration peak; (V) the slow continued reaction stage: belite dissolves and releases calcium ions very slowly and starts to produce C-S-H and C-H after several days. However, as long as alite and belite remain in the cement system and there is

enough water available in the system, the silicates will continue to hydrate [34, 35].

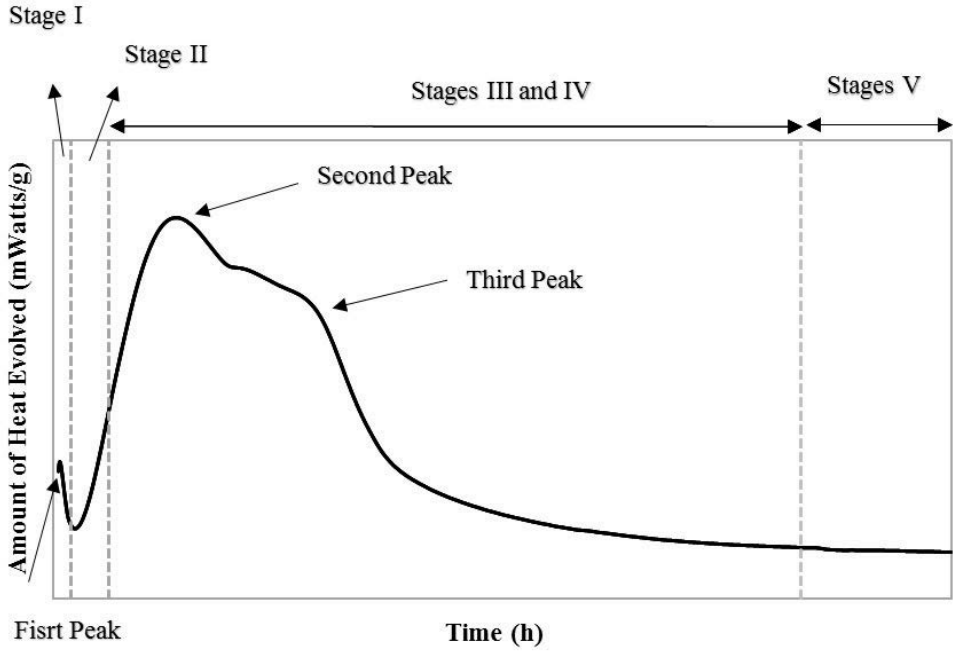


**Figure 5-1: Common cement heat evolution curve [34]**

### 5.2.2 Effect of different fly ashes

The effect of 20%, 30% and 40% substitution of cement with GRFA, CFA and RFA in the blended cement paste with a water to binder ratio of 0.40 and 0.55 on the amount of heat evolution is shown in Figures 5-2 and 5-3 respectively. The first peak which signifies the initial reaction at the surface of cement particles and represents the onset of hydration of the $C_3A$ phase was neglected as the mixing of the paste mixes was performed outside the calorimeter. All blended cement pastes showed less heat generated up to 10 hours especially in the second peak compared to the control cement paste devoid of fly ash addition. This reduction increased as the proportion of fly ash increased at both w/b ratios. For instance, the heat evolved for the P-RFA40 blend at w/b=0.40 was 2.51 mW/g whereas it was 4.27

mW/g for the PC-C0 control cement paste. A probable reason for this occurrence may be due to the dilution effect of cement with less $C_3S$ available for increasing fly ash addition. Moreover, the slow reaction that results between aluminosilicates in fly ash and C-H liberated from cement due to the lower solubility index of fly ash in pore solution might be another reason for the observed trend in data [36]. It can be seen that the third peak is more apparent for the blended pastes. The height of this peak was found to increase when the fly ash content was increased from 20% to 40% for both w/b ratios studied. For instance, at w/b=0.40, the amount of the heat evolved for the P-GRFA20 mix was 3.99 mW/g and increased to 4.41 mW/g for the P-GRFA40 blend. Compared to the blended pastes, the third peak was also found to be absent from the control cement paste. The increase in peak height observed for an increase in fly ash content might be due to the reaction of more tricalcium aluminate ($C_3A$) and the subsequent conversion of more ettringite to monosulfate as fly ash enhances the aforementioned reaction by providing a high number of nucleation sites for calcium aluminate hydrate to precipitate [35, 147]. The $C_3A$ is highly soluble and reacts rapidly with the gypsum present in the cement to form ettringite within several minutes of mixing. However, by gradually decreasing the concentration of sulfate ions available in the pore solution over a period of several hours the ettringite becomes unstable and converts to monosulfate. In addition, replacing cement with fly ash decreases the gypsum content and increases the reactivity of $C_3A$ in the mix allowing the $C_3A$ particles to undergo renewed and rapid hydration. This hydration reaction involves an exothermic process and contributes to the heat generated in the third peak [35, 148].

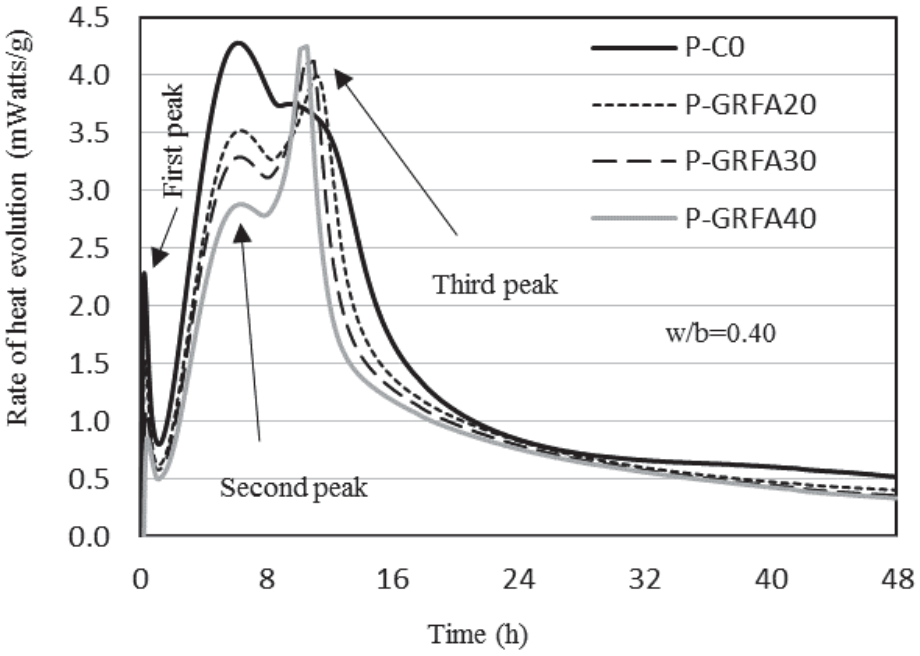
Rate of heat evolution (mWatts/g)
4.5
4.0
3.5
3.0
2.5
2.0
1.5
1.0
0.5
0.0
First peak
Second peak
Third peak
P-C0
P-GRFA20
P-GRFA30
P-GRFA40
w/b=0.40
0
8
16
24
32
40
48
Time (h)

(a)

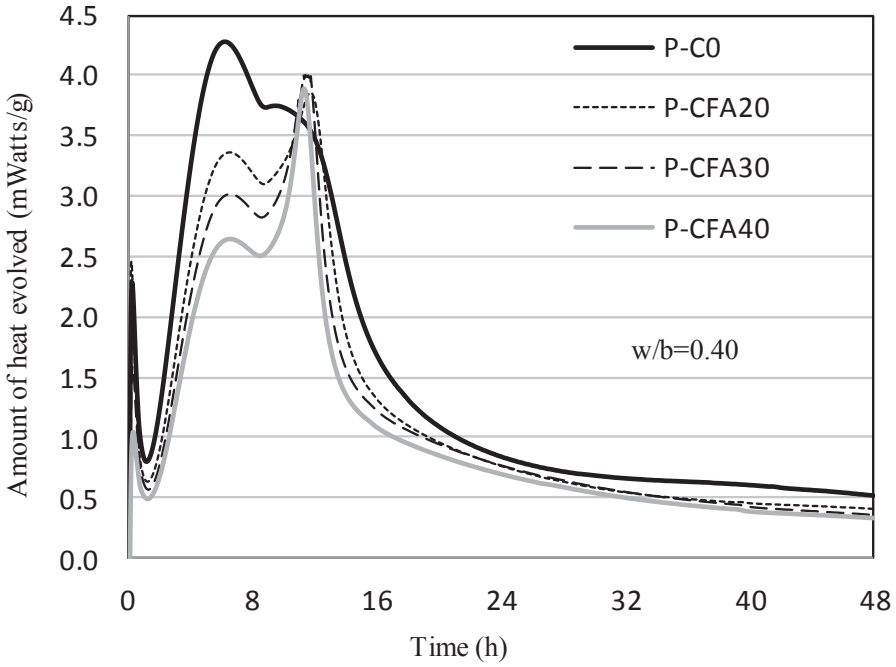
Amount of heat evolved (mWatts/g)
4.5
4.0
3.5
3.0
2.5
2.0
1.5
1.0
0.5
0.0
P-C0
P-CFA20
P-CFA30
P-CFA40
w/b=0.40
0
8
16
24
32
40
48
Time (h)

(b)

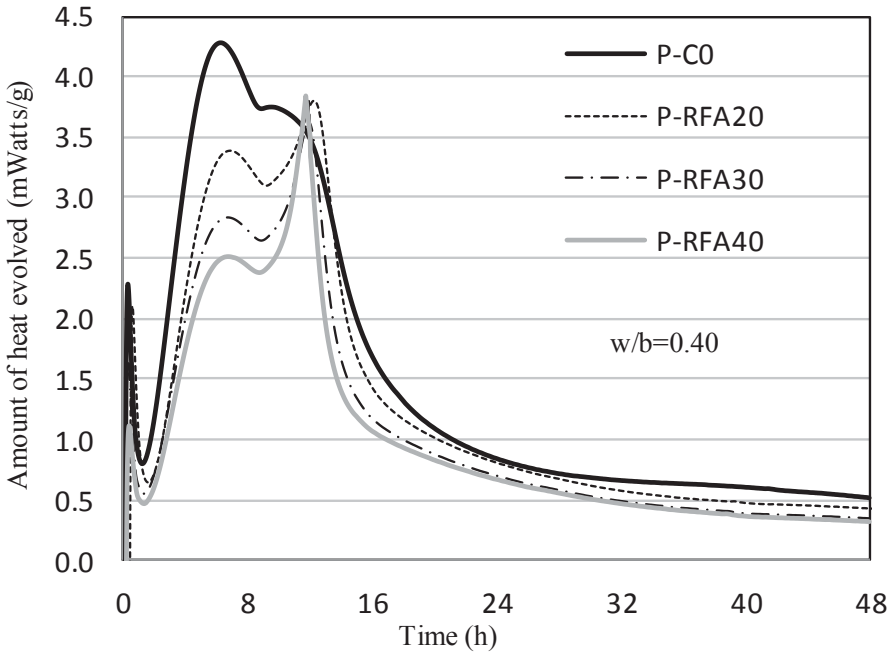


(c)

**Figure 5-2: Effects of levels of different fly ash on heat evolution at w/b=0.40 (a=GRFA, b=CFA and c=RFA)**

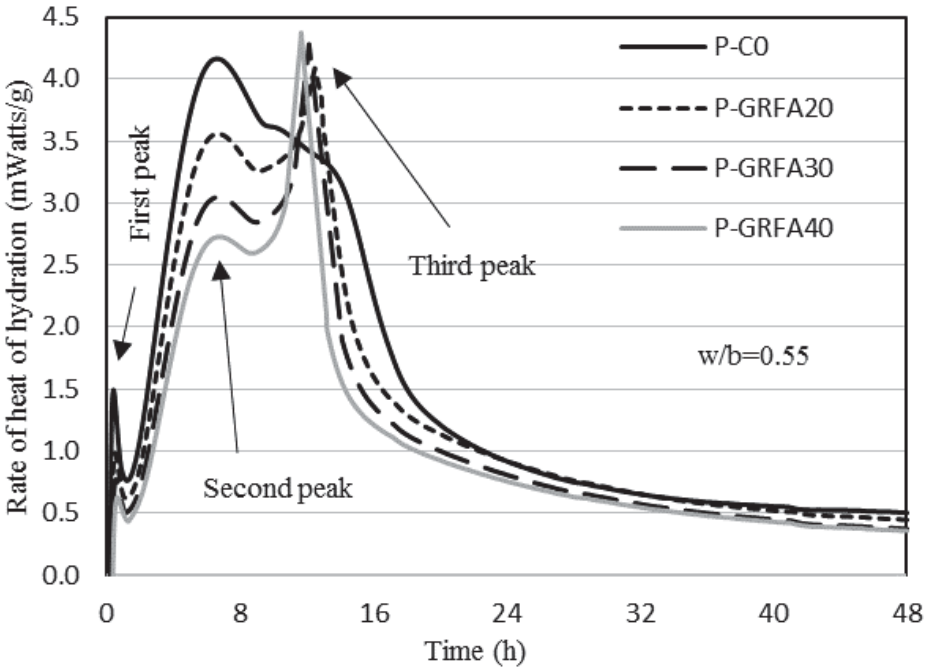


(a)

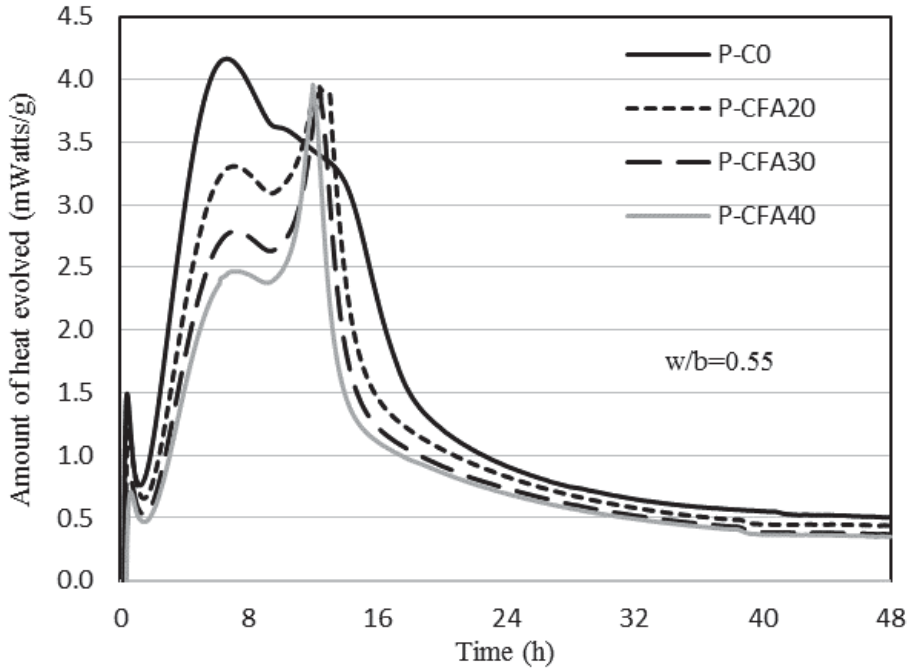


(b)

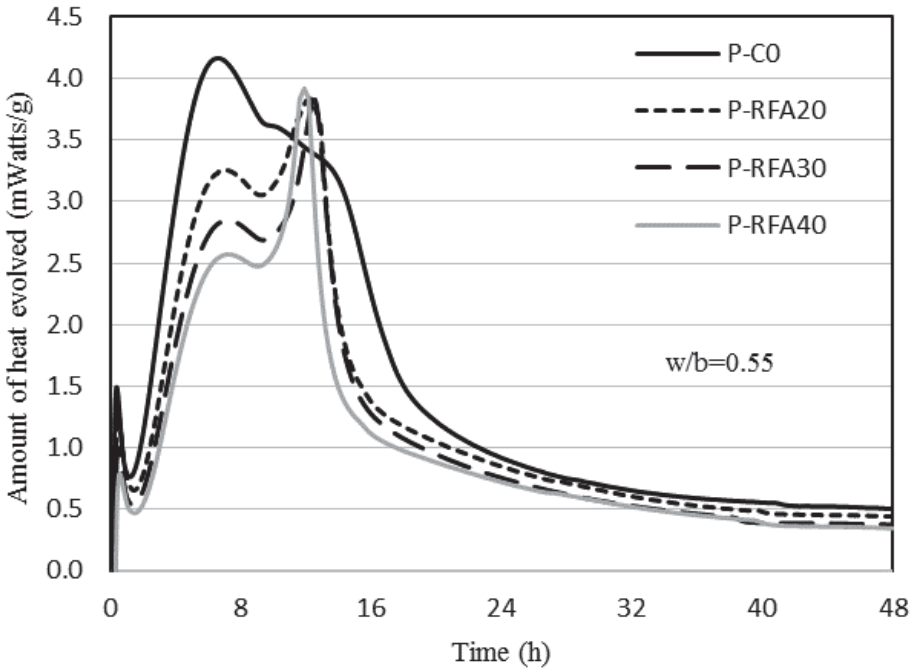


(c)

**Figure 5-3: Effects of levels of different fly ash on heat evolution at w/b=0.55 (a=GRFA, b=CFA and c=RFA)**

The effect of the fineness of fly ash on the amount of heat evolution of the blended cement paste containing 20%, 30% and 40% GRFA, CFA and RFA is shown in Figures 5-4 and 5-5. It can be seen that GRFA showed a higher amount of heat evolved in the second peak compared to CFA and RFA. The high fineness of GRFA also showed higher peak intensity for the second peak compared to the CFA and RFA. These observations are supported by the findings of Rahhal and Talero [149] who reported higher peak intensities with an increase of fineness of fly ash particles. It is noted that the height of the third peak increased by increasing the fineness of fly ash. For instance, at w/b=0.40, the heat evolved for the P-RFA40 blend was found to be 3.60 mW/g compared to 4.41 mW/g for the P-GRFA40 blend. This increase is possibly due to an increase in the number of nucleation sites available for the hydration reaction to proceed as a result of more specific surface area available for the finer grade fly ash (GRFA) to react compared to coarser grade fly ash (CFA and RFA) at both w/b ratios.

It can be noted that for blended pastes with a lower w/b ratio, the second peak was observed to be slightly higher than that of the blended pastes with a higher w/b ratio. This increase in peak height is possibly due to the acceleration of the hydration process in early hours due to faster saturation of lower water content with $Ca^{2+}$ ions. In contrast, the height of the third peak in blended pastes with lower w/b was slightly lower than the mixes with higher w/b for the same fly ash content. This is possibly due to more availability of water at higher w/b ratio at a later age, which makes better contact of cementitious particles with water and thus more hydration will result. This observation is in agreement with that of other researchers [150, 151]

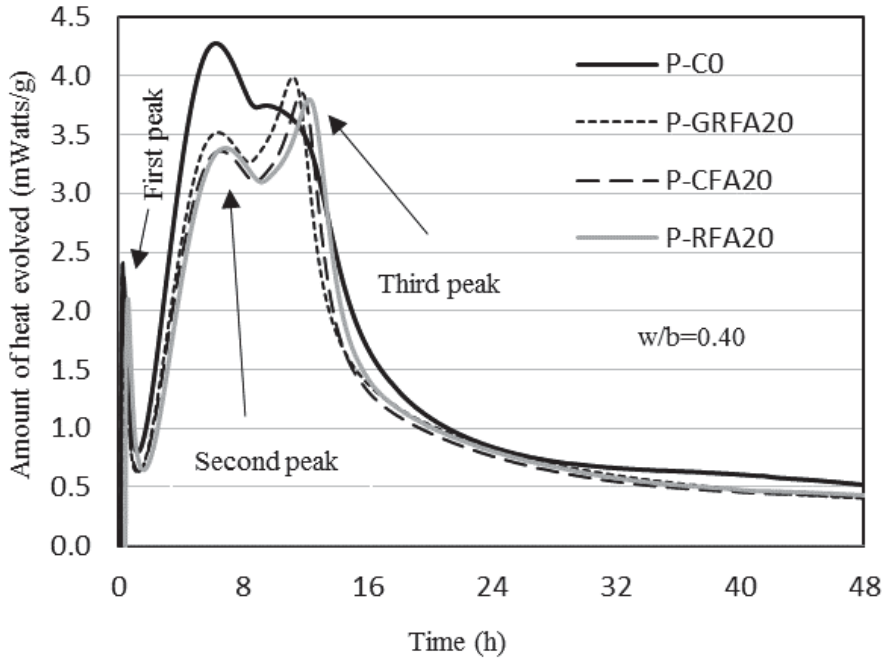
Amount of heat evolved (mWatts/g)
Time (h)
First peak
Second peak
Third peak
P-C0
P-GRFA20
P-CFA20
P-RFA20
w/b=0.40

(a)

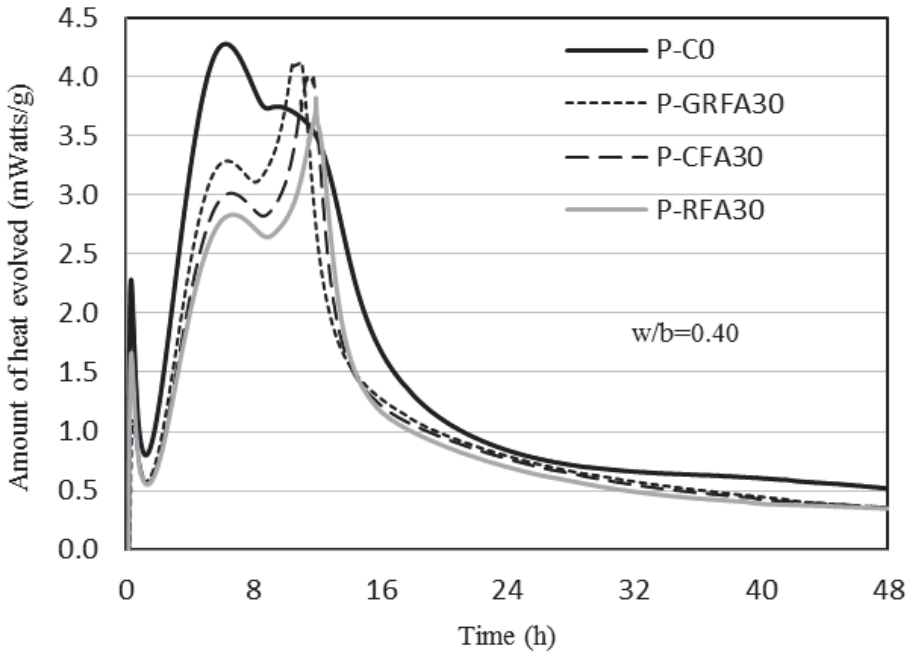
Amount of heat evolved (mWatts/g)
Time (h)
P-C0
P-GRFA30
P-CFA30
P-RFA30
w/b=0.40

(b)

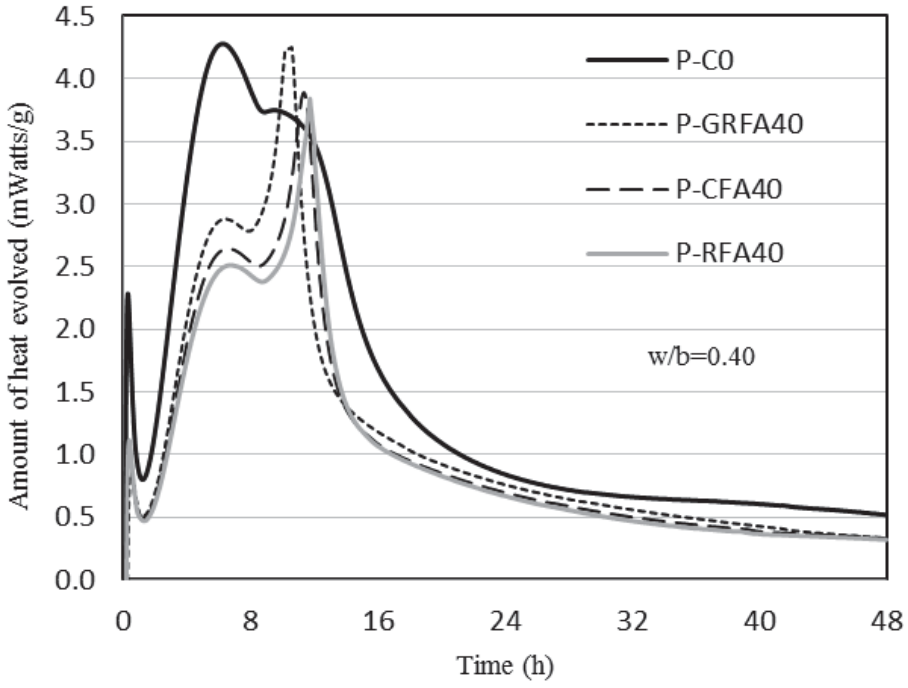


(c)

**Figure 5-4: Effect of fineness of fly ash on heat evolution at w/b=0.40 (a=20%, b=30% and c=40% fly ash content)**

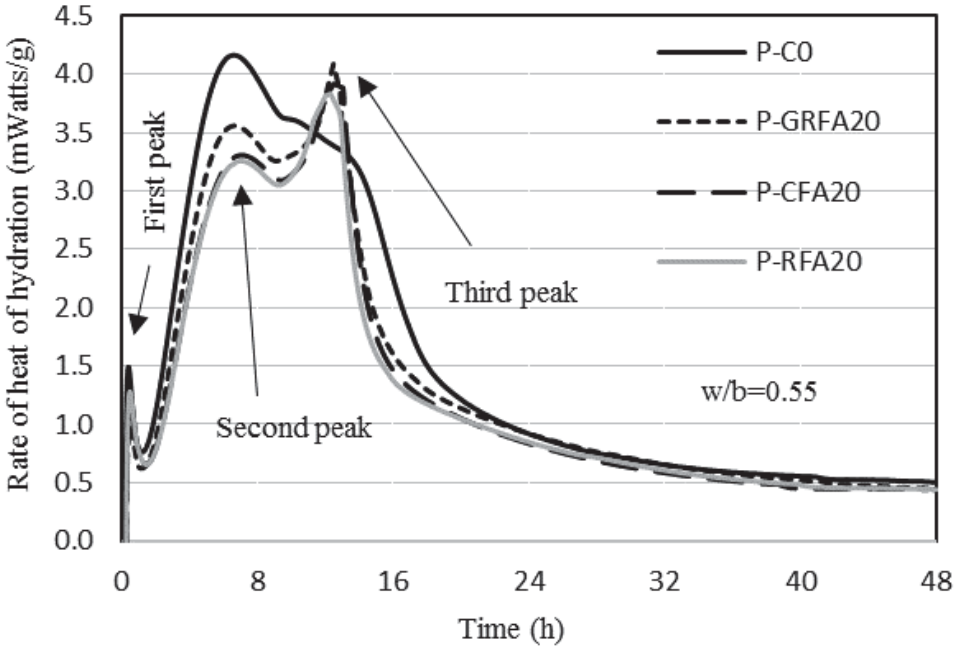


(a)

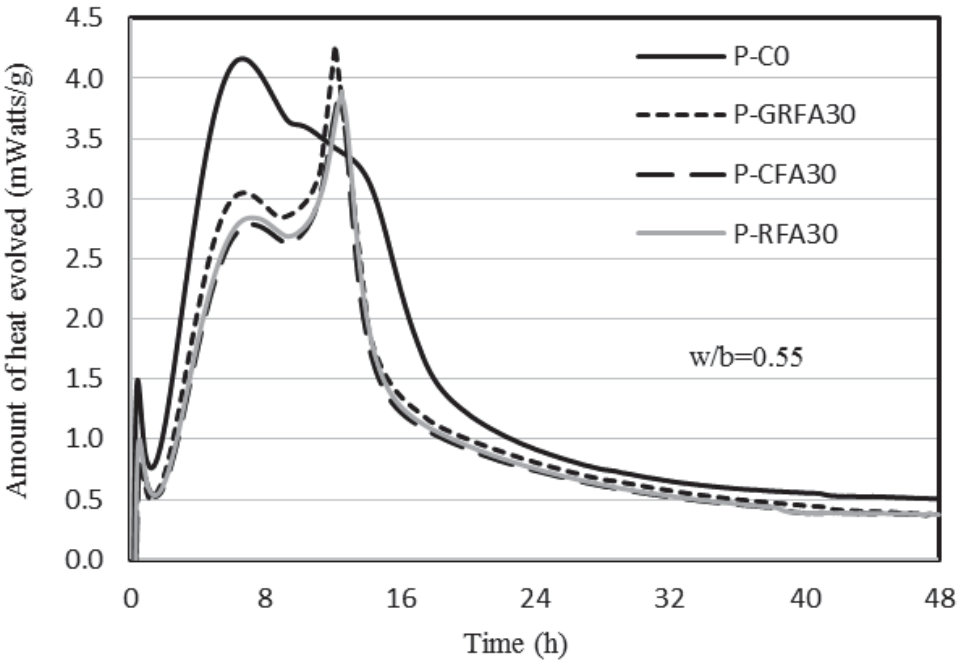


(b)

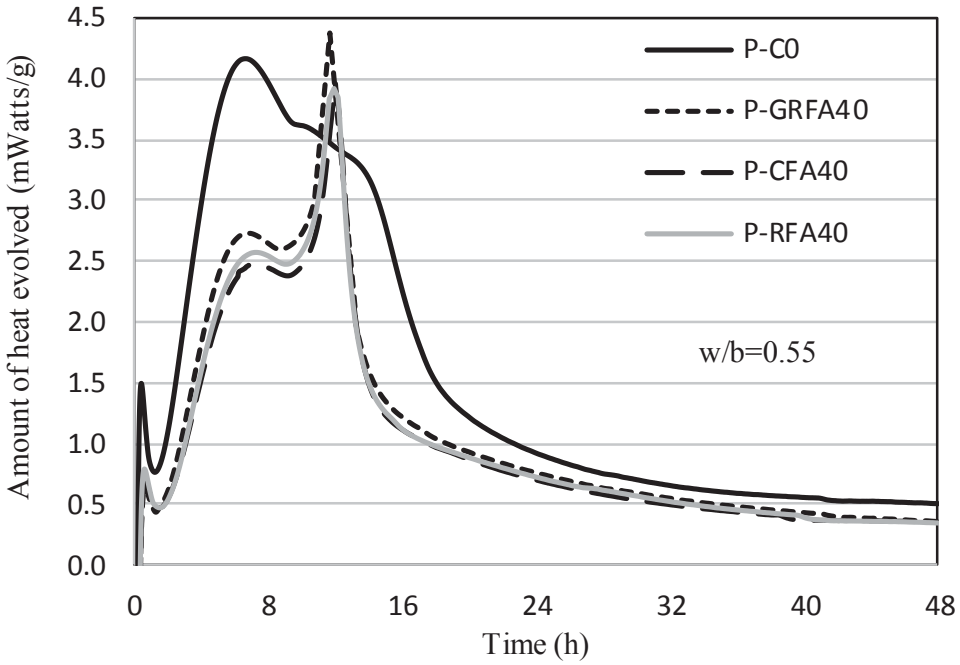


(c)

**Figure 5-5: Effect of fineness of fly ash on heat evolution at w/b=0.55 (a=20%, b=30% and c=40% fly ash content)**

The cumulative heat evolution of the blended pastes containing GRFA or CFA or RFA at w/b ratio of 0.40 and 0.55 over the testing period of 48 hours are shown in Figure 5-6. As expected, the cumulative heat of hydration generated for the blended pastes are lower than that for cement paste. Increasing the fly ash content in the blends also led to reducing the amount of heat evolved in both w/b ratios investigated. The combined effect of diluting the cement and increasing the amount of slow reactive fly ash available in the system has contributed to the observed trends.

Snelson et al. [36] reported that relatively low specific surface area and also the low solubility of the alumina-silicate present in the fly ash are the main contributing factors for a reduction in the cumulative heat of hydration. It can be seen, by increasing the fineness of fly ash, the cumulative heat evolution increased at both w/b ratios as a result of more reactivity of finer particles due to more silica content (assumed to be amorphous) as shown in the XRD results in Figure 4-5. This observation is in agreement with the findings of other researchers [39, 152]. However, the pastes with higher w/b ratio demonstrated more total heat of hydration after 48 hours than that of the pastes with lower w/b ratio. This might be due to more availability of water to coat the fly ash particles at higher w/b ratio which makes the hydration more complete, thus generating more heat compared to the lower w/b ratio [150, 152].

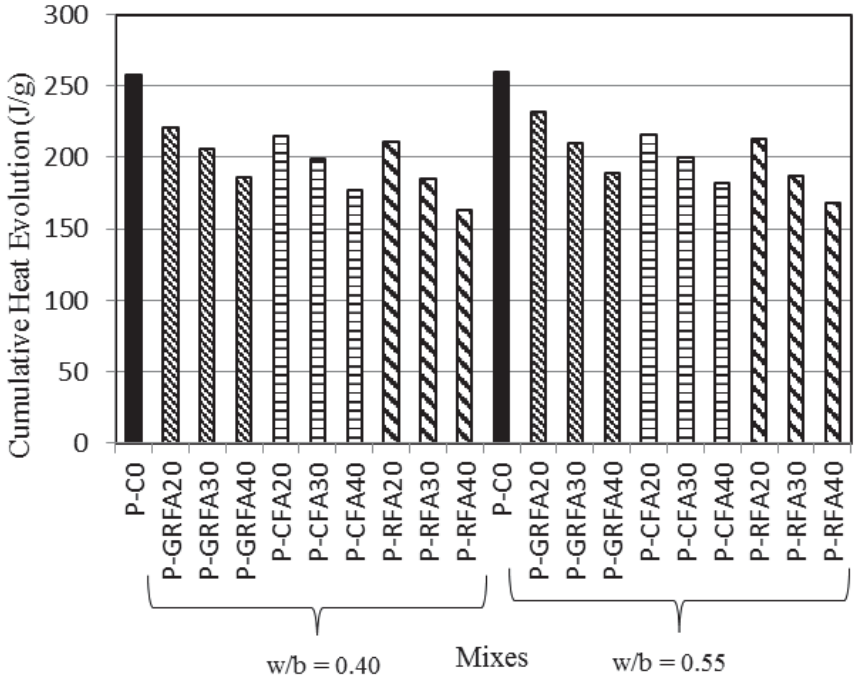


**Figure 5-6: Effect of fineness and level of fly ash on cumulative heat evolution**

### 5.2.3 Effect of slag

Figures 5-7 and 5-8 show the amount of heat evolution and cumulative heat evolution of the blended pastes containing 35%, 50% and 65% SL at the two different w/b ratios of 0.40 and 0.55, respectively. The first peak of the hydration process represents the initial reaction at the surface of cement particles due to the onset hydration of $C_3A$ phase. However, it was mostly neglected as the mixing of the paste mixes was carried out outside the calorimeter.

From Figure 5-7, it can be noted that the height of the second peak in blended cement pastes at low w/b ratio is slightly higher than that of the mix with higher w/b ratio. For instance, the heat evolution of the P-SL65 blend at w/b=0.40 was observed to be 1.84 mW/g whereas it was 1.69 mW/g for the P-SL65 blend at w/b=0.55. An increase in the amount of heat evolved at lower w/b in early hours

(up to 8 hours) might possibly be due to the better dispersion of cement particles in a given volume of water in a paste with a low w/b ratio and thus more hydration occurs compared to the paste with high w/b ratio [147]. Partially replacing cement with SL in blended paste made the third peak of hydration in heat evolution curve, which is not evident in cement paste without SL addition. This might be due to the late activation of SL by C-H as well as more availability of $C_3A$ to undergo renewed rapid hydration which is an exothermic reaction [153]. Hewlett [154] reported that activation of SL due to reaching to the correct alkalinity by releasing the sufficient amount of C-H by cement hydration, and thus this reaction appears as a third peak in heat evolution curves.

From Figure 5-8, the cumulative heat of hydration for cement and blended cement pastes over the period of 48 hours at lower w/b ratio exhibited less heat evolution than that of the pastes with higher w/b ratio. This might possibly be due to less availability of water as well as a shortage of space available for the growth of hydration products at a later age in a blend with a low w/b ratio. For instance, the cumulative hydration heat of the P-SL35 blend at w/b=0.55 was found to be 215.5 J/g whereas it was 206.9 J/g for the P-SL35 blend at w/b=0.40. However, the overall trend for heat evolution was similar for both w/b ratios investigated, which is in agreement with other researchers [152]. Additionally, the cumulative heat of hydration after 48 hours decreased as SL content in the blended paste increased as shown in Figure 5-8. This decreasing trend was seen at both water to binder ratios of 0.4 and 0.55. A possible reason for this reduction is due to the dilution effect as Portland cement is replaced by SL [150].

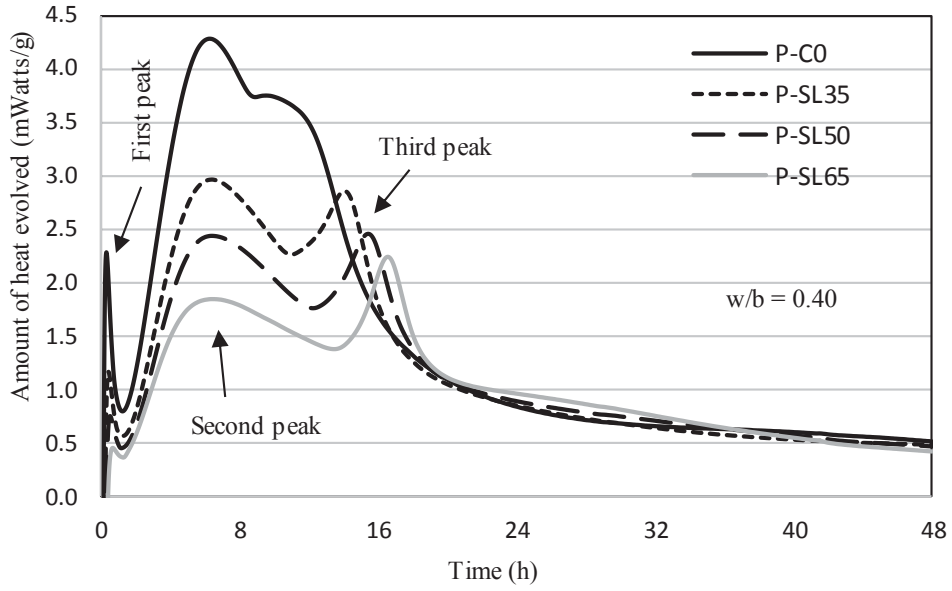


(a)

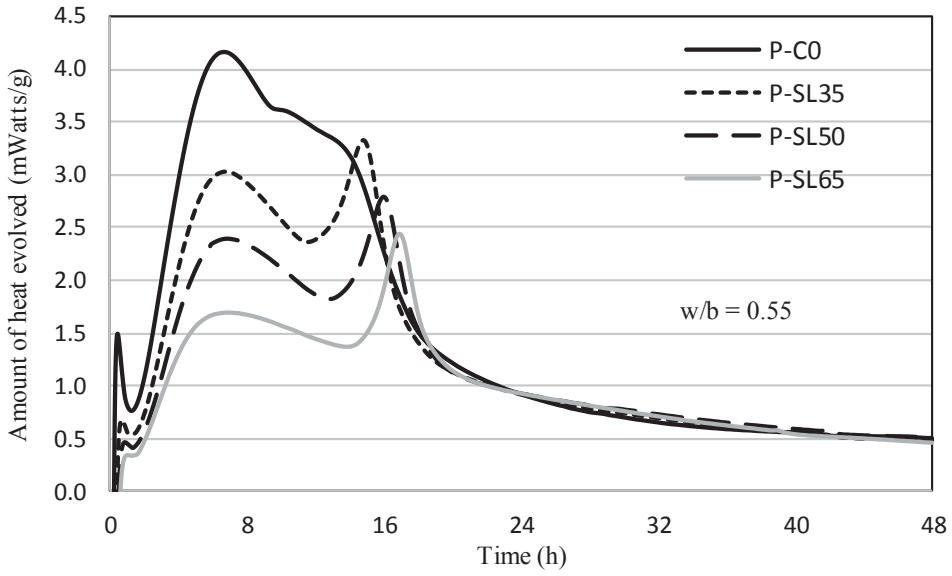


(b)

**Figure 5-7: Heat evolution of blended cement pastes containing slag**

**(a= w/b:0.40 and b= w/b:0.55)**

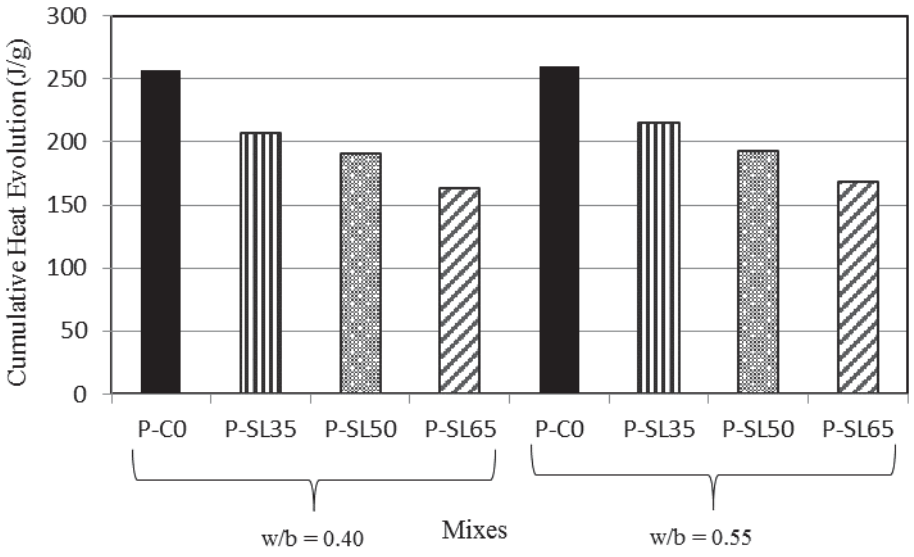


**Figure 5-8: Cumulative heat evolution of blended cement pastes containing slag**

### 5.2.4 Effect of metakaolin

The amount of heat evolution and cumulative heat evolution of the blended pastes containing 5%, 10% and 15% of MK at two different w/b ratios of 0.40 and 0.55 are shown in Figures 5-9 and 5-10, respectively. It can be seen that the height of the second peak decreased slightly by increasing the MK content at both w/b ratios. This might possibly be due to two reasons. Firstly, replacing cement with MK with the much higher specific surface, which adsorbs water more quickly than cement particles, diminishes the heat released in early hours (up to 8 hours) in blended cement paste [44]. Secondly, the dilution effect of cement with less $C_3S$ available due to partially replacing cement with MK is another reason for decreasing the amount of the heat of hydration at second peak. This reduction increased by increasing the MK content as a result of increasing the water demand.

Snelson et al. [36] reported that the reaction of MK is governed not only by the available water but also by the supply of $Ca^{2+}$ ions due to PC hydration. As the MK to PC ratio increases the supply of $Ca^{2+}$ ions will decrease, and thus the MK reaction will diminish. However, the rate of reduction is less at higher w/b ratios compared to lower w/b ratios. This might possibly be due to the availability of more water for cement hydration in w/b of 0.55 compared to 0.40, which enhances the hydration. At w/b=0.55, it can be seen that the height of the second peak in P- C0 cement paste is almost the same as for P-MK5 and P-MK10 blended pastes. After 8 hours, the amount of heat evolution starts to increase significantly in the blended pastes containing MK as it appears as the third peak of hydration in heat evolution curve while a reduction in heat release is observed for the control cement pastes shown in Figure 5-9. It can be seen the height of the peak increased by increasing the MK content.

This observation is in agreement with that of Frıas et al. [42], who reported calcium silica hydrate gel was first formed at about six hours followed by hydrated calcium aluminate at between 13 to 20 hours. In addition, ettringite formation and its subsequent transformation to monosulfate as a result of the high $Al_2O_3$ content of MK is likely to be another reason for the acceleration of the amount of heat evolution in the blended pastes especially in the third peak [43, 44].

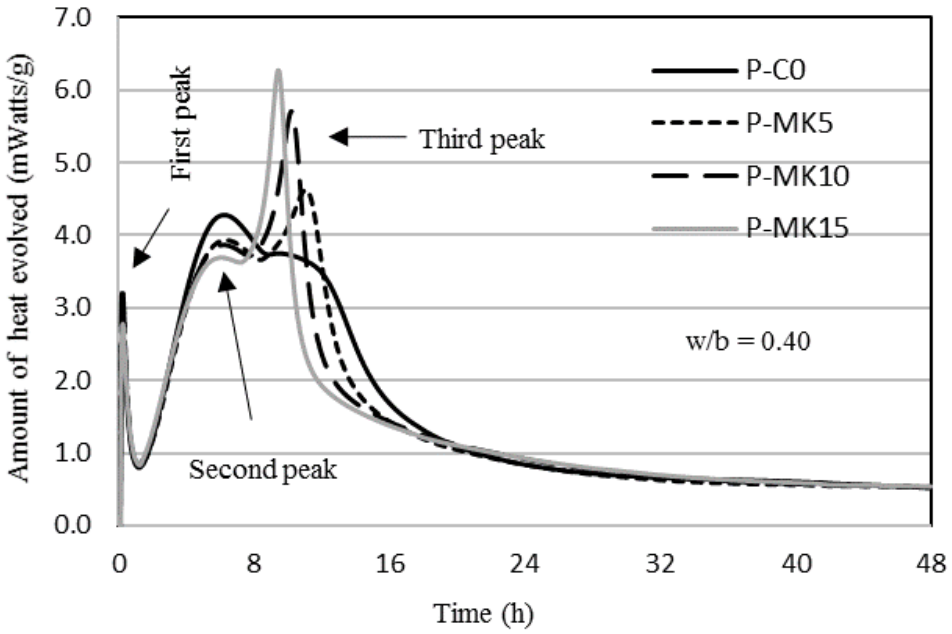


(a)

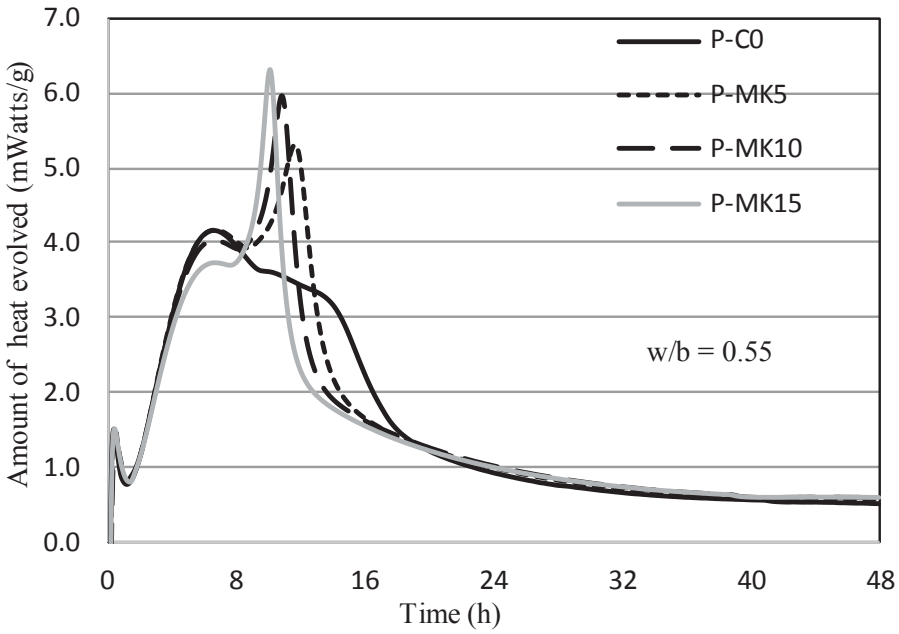


(b)

**Figure 5-9: Heat evolution of blended cement pastes containing metakaolin (a= w/b:0.40 and b= w/b:0.55)**

As summarised in Figure 5-10, the cumulative heat evolution of blended pastes at both w/b ratios is almost similar to the control cement paste. As Kadri et al. [41] reported that great fineness of the MK particles accelerates the cement hydration process by acting as nucleation sites for hydration precipitation, followed by the dissolution of amorphous silica and alumina at early hours.

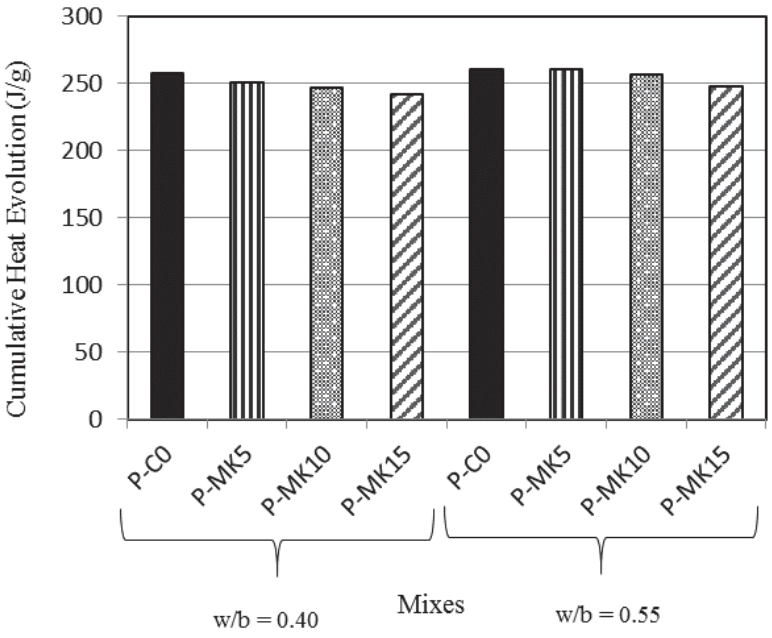


**Figure 5-10: Cumulative heat evolution of the blended cement pastes containing metakaolin**

## 5.3 Calcium hydroxide consumption

Figure 5-11 shows the XRD diffractogram patterns at the age of 7 days for cement and blended pastes with 20% of fly ash content of varying fineness. The XRD pattern of pure calcium hydroxide (C-H) has also been included for better understating the intensity of calcium hydroxide (portlandite) peaks detected in the XRD patterns of the blended cement pastes. Portlandite peaks representative of CH appeared at 2-Theta of 18.07, 28.75, 34.13, 47.12, and 50.85 degrees. At an

early age (up to 7 days), the fly ashes do not have enough influence to decrease the amount of C-H available in the system despite the fact they have differences in particle size distributions. It is seen that the intensity of the portlandite peaks are almost the same in all fly ash blends. This is possibly due to the slow pozzolanic reactivity of fly ash. There are no significant changes in the hydration process at this stage as cement hydration is in the dominant process. This is in agreement with the findings of other researchers reporting hydration reactions taking place at 7 days with the main reaction involving cement rather than fly ash [142, 155].

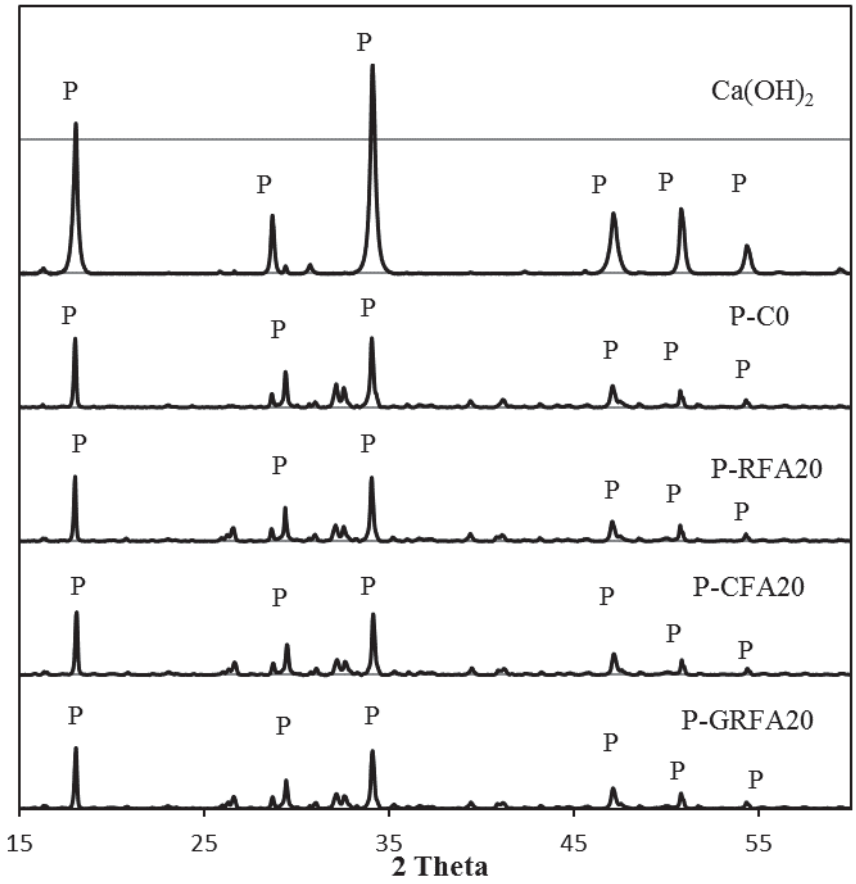


**Figure 5-11: XRD patterns of cement and 20% blended pastes at 7 days (P=portlandite)**

The XRD patterns for the blended pastes containing 20% of GRFA, CFA and RFA at 28 days are also shown in Figure 5-12. The results indicate that all blends have reduced portlandite available with increasing fineness of fly ash augmenting this difference. A probable reason for the noted decrease in portlandite peak intensity might be due to the increased reactivity of the finer grade fly ash having a higher surface area. Moreover, fly ash with high fineness provides increased nucleation sites for pozzolanic reactivity [15]. Sybertz and Wiens [47] also found that fly ash with smaller particle size has higher amorphous content, which increases pozzolanic reactivity and thus more C-H is consumed.

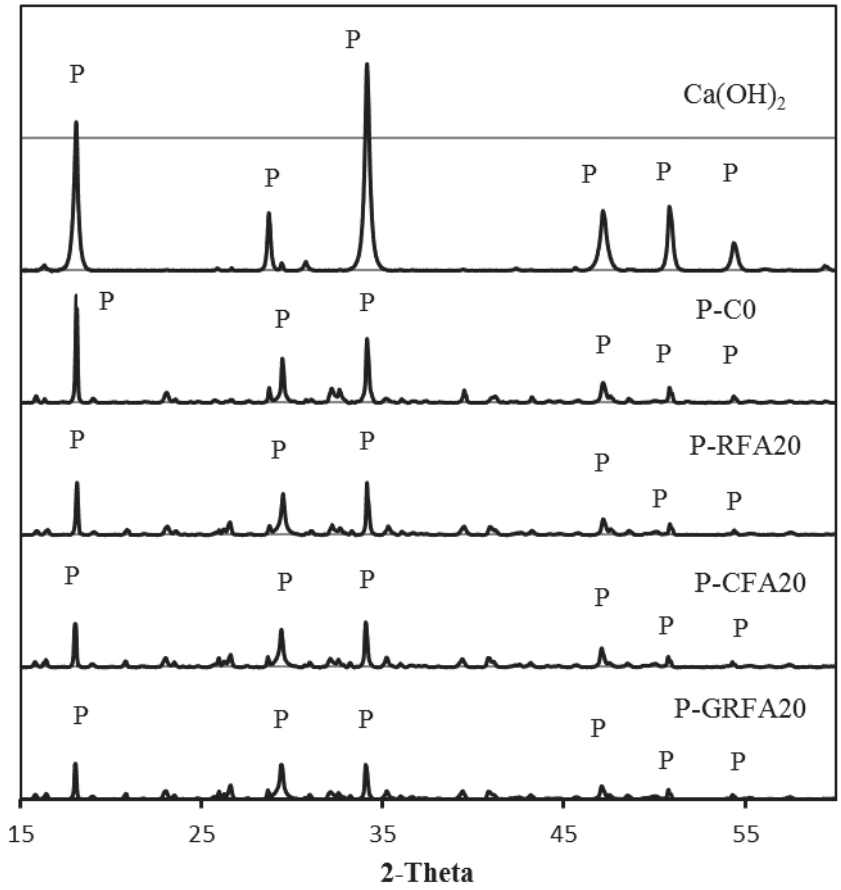


**Figure 5-12: XRD patterns of cement and blended pastes at 28 days (P=portlandite)**

## 5.4 Microstructure of hardened blended cement pastes

Figures 5-13 to 5-15 show the SEM micrographs of the blended cement pastes with 20% cement replacement level of GRFA, CFA and RFA at the ages of 1, 7 and 28 days. All micrographs have been taken at the same magnification level (3000 x). At one day, most of the fly ash particles appear to be unreacted with smooth surfaces still present. However, compared to CFA and RFA particles, the finer grade GRFA particles appear to be covered with fibrous C-S-H gel, which suggests a faster rate of reaction. This is possibly due to the increased fineness of GRFA thereby increasing the surface area available for the pozzolanic reaction. Furthermore, the presence of needle-like crystals representative of ettringite are also apparent in all blends. At this age, interstices between fly ash particles and empty pores are evident due to incomplete hydration. This is in agreement with the findings of Chindaprasirt et al. [46] and Xu and Sarkar [156] who reported the same phenomena.

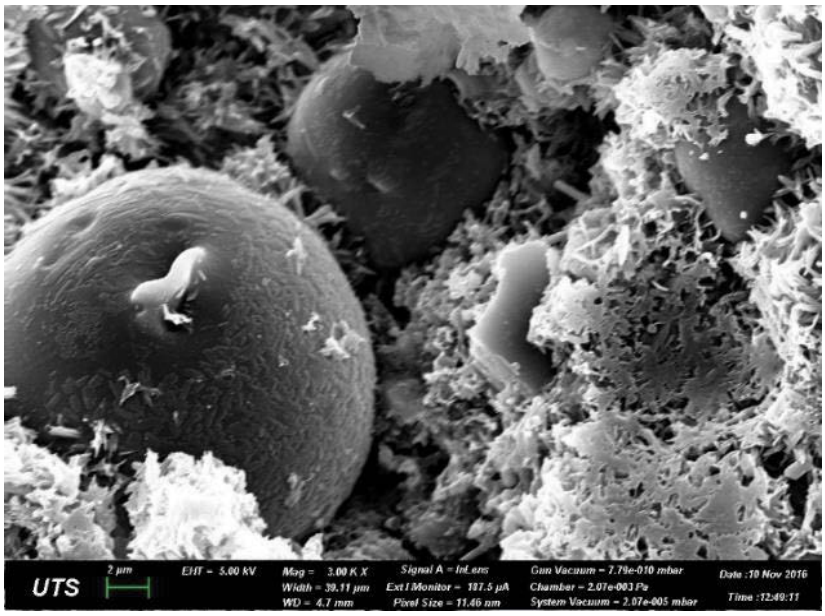


(a) P-RFA20

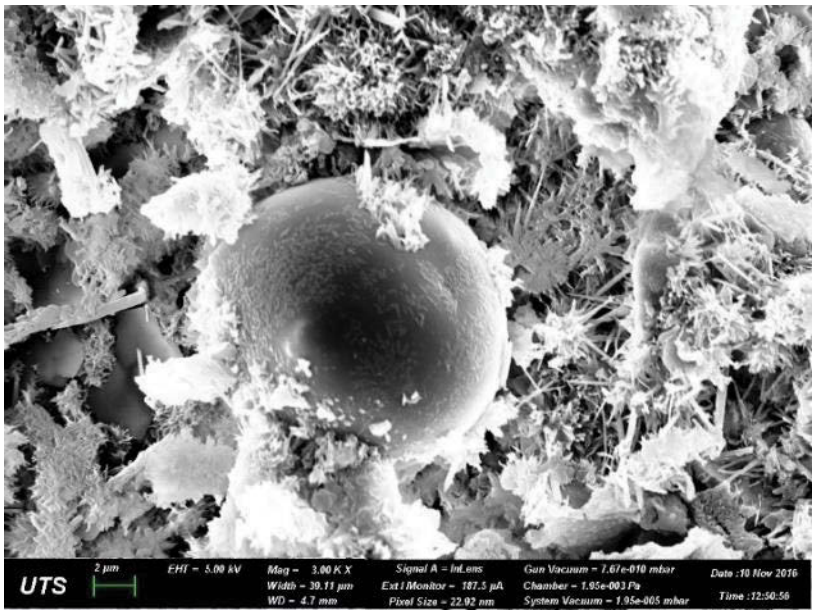


(b) P-CFA20

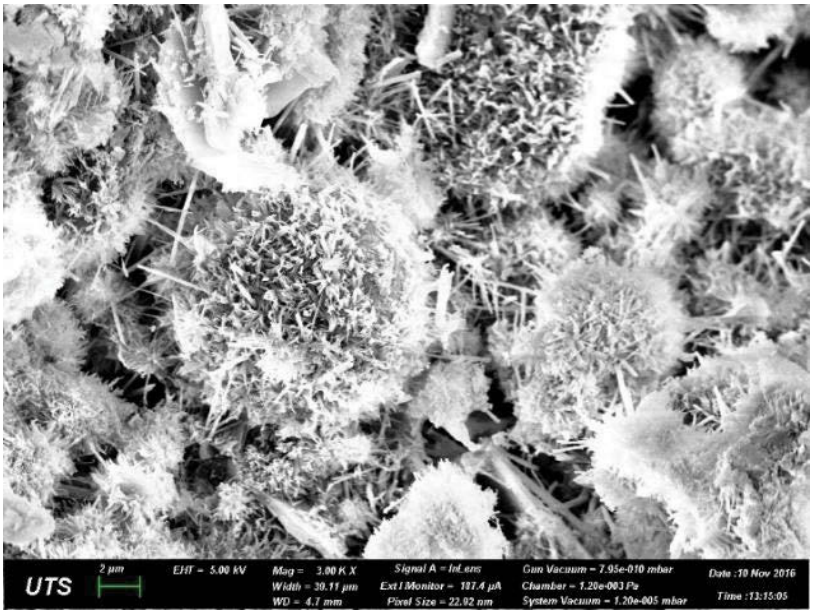


(c) P-GRFA20

**Figure 5-13: SEM micrographs of blended cement pastes with 20% fly ash at 1 day (x 3.00 K)**

At seven days (Figure 5-14), calcium silica gel (C-S-H) starts to fill the spaces between the fly ash particles. However, less C-S-H was found to be present in the RFA blends possibly due to less pozzolanic reactivity prevailing for the coarser grade of fly ash present [157]. These observations are in agreement with the XRD results reported in Section 5.3, which showed more C-H presence in RFA blends and thus less C-S-H formation. A much large number of GRFA particles were also observed to be coated on the surface with the presence of more hydration products (Figure 5-14c) compared to CFA particles which have been coated with a thinner layer of hydration products (Figure 5-14b). Most of the RFA particles were found to be uncoated and unreacted (Figure 5-14a).

At the age of 28 days, almost all the fly ash particles (GRFA, CFA, and RFA) were observed to be encased with hydration products. The voids between fly ash particles were found to be filled with hydration products contributing to a denser structure as shown in Figure 5-15. The high fineness of GRFA (Figure 5-15c) appeared to be more involved in the pozzolanic reaction compared to the lower fineness of CFA and RFA (Figures 5-15a and 5-15b). This is supported by XRD data in Figure 5-12, which showed lower amounts of calcium hydroxide present in the GFRA systems compared to CFA and RFA systems at 28 days. Moreover, a significant number of GRFA particles have also reacted and converted to C-S-H with more fibrous sheets evident. This is not the case for the coarser grade CFA and RFA particles with less C-S-H present. The finer particle size of GRFA has also reacted more rapidly than the coarser particle size of CFA and RFA despite having similar oxide compositions. The finer fly ash is more effective in making more nucleation sites available for pozzolanic reactions as well as reducing the

porosity than the coarser fly ash. However, some fly ash particles were observed to still remain smooth and unreacted in all systems, which suggests these particles have acted in part as a temporary inert material to improve particle packing density of the cementitious matrix [157, 158].

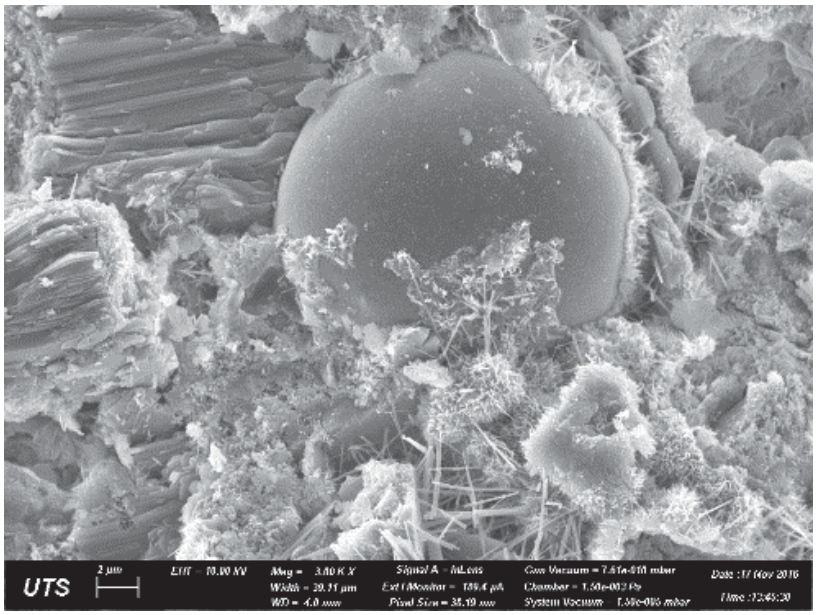


(a) P-RFA20

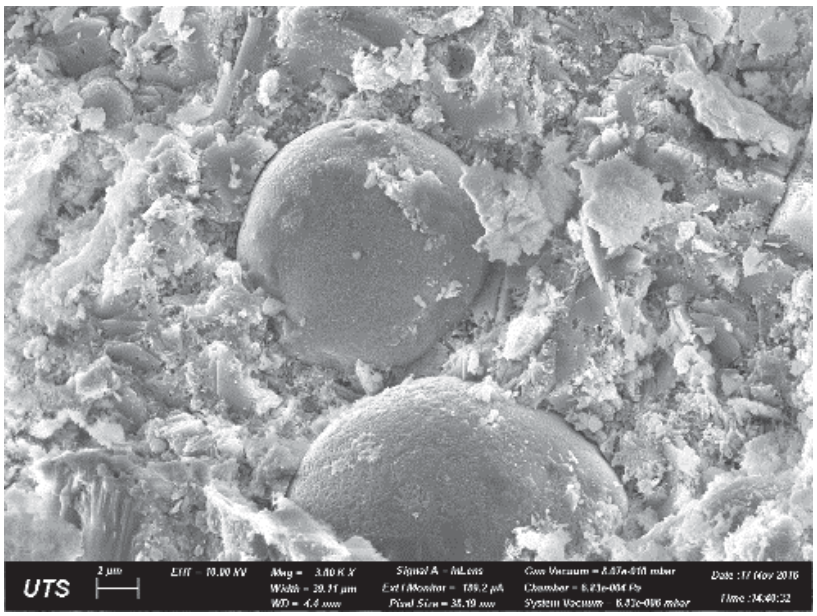


(b) P-CFA20

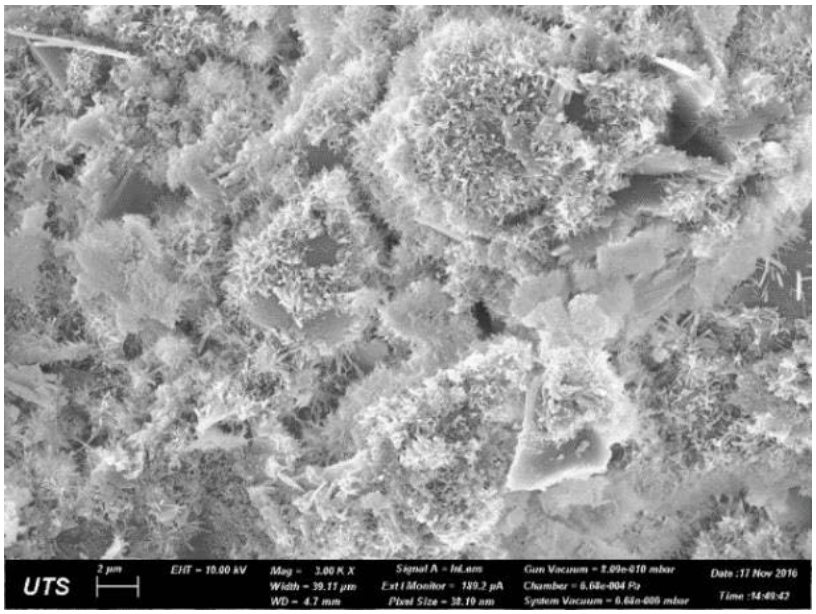


(c) P-GRFA20

**Figure 5-14: SEM micrographs of blended cement pastes with 20% fly ash at 7 days (x 3.00 K)**

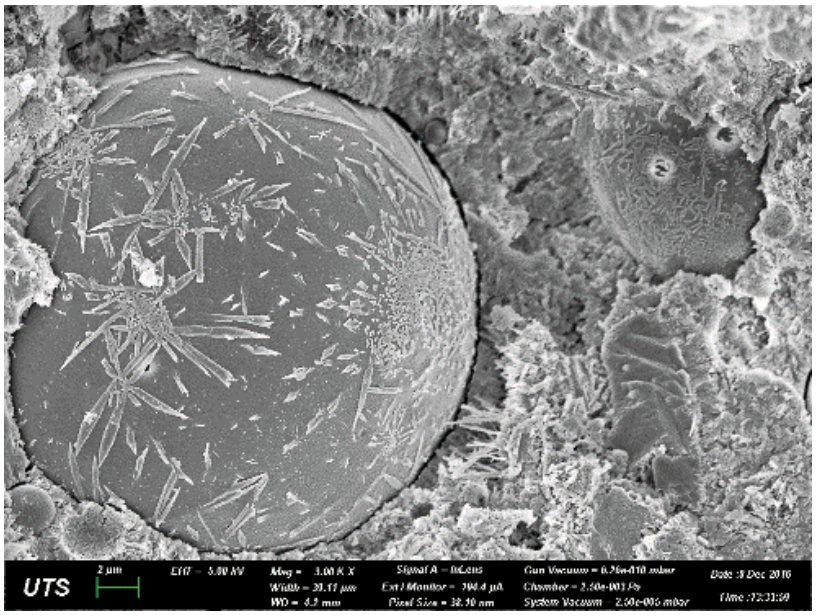


(a) P-RFA20

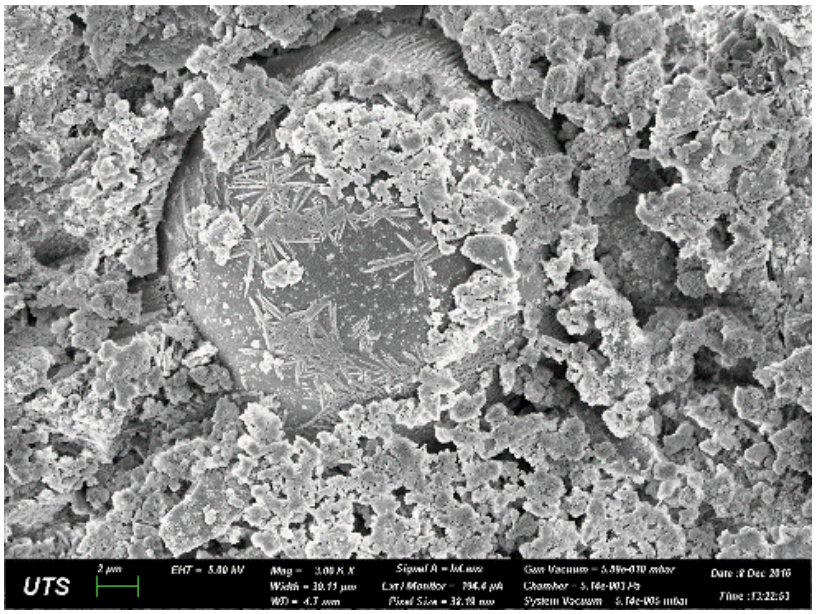


(b) P-CFA20

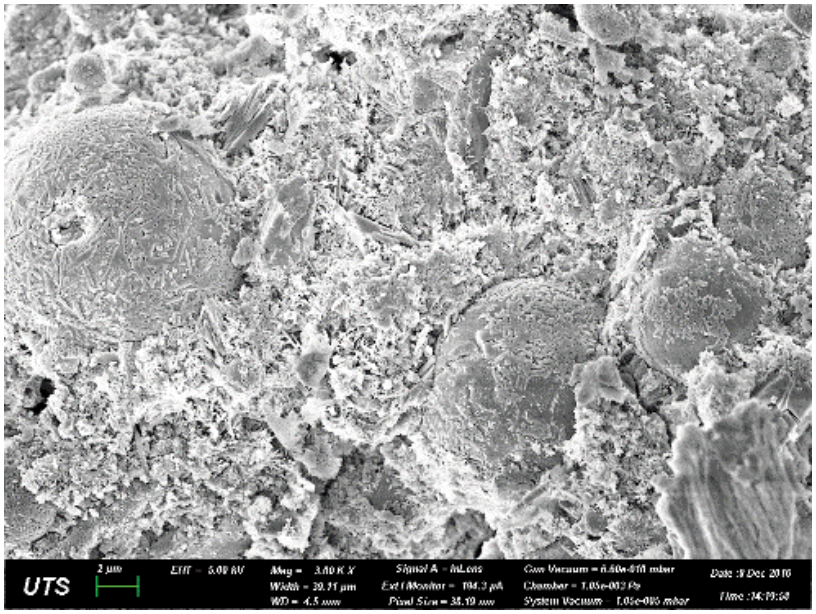


(c) P-GRFA20

**Figure 5-15: SEM micrographs of blended cement pastes with 20% fly ash at 28 days (x 3.00 K)**

## 5.5 Flow and strength properties

The effects of replacing cement with 20% and 40% GRFA, CFA and RFA on the flow of the blended pastes are shown in Figure 5-16. The flow varied between 105% and 140% for all the pastes evaluated in this study. It can be seen that GRFA and CFA marginally improved the flow of the blended pastes at both 20% and 40% fly ash contents. This might possibly be due to the ball bearing effect of fly ash particles improving flow due to their spherical shape with the effect being more apparent with increasing fly ash content. In addition, the reduction in the water adsorption capacity of fly ash particles due to the glassy and smooth surface texture compared to cement particles might be another reason for improving the flow.

Ferraris et al. [159] reported that lower particle density of fly ash compared to cement makes more paste content for a fixed binder content by volume and thus improves the flow, especially in the mix containing the finer grade fly ash. Mora et al. [28] stated a similar relationship with the flow of mortars improving for decreasing particle size of fly ash. These authors attributed the improvement in workability due to the increased amount of finer sized fly ash particles available per unit mass, which increased the lubricant effect in comparison to coarser sized particles.

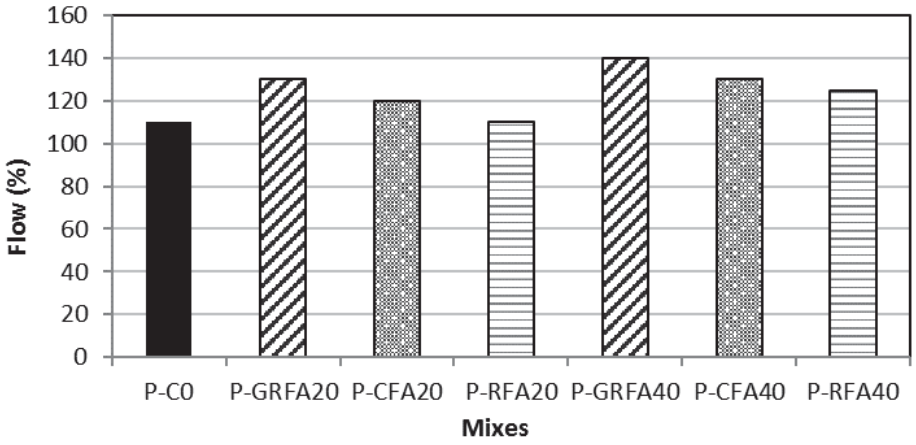


**Figure 5-16: Flow of the pastes containing fly ashes with different fineness and cement replacement levels**

Figures 5-17 and 5-18 show the development of compressive strength with age for blended pastes containing 20% and 40% CFA, RFA and GRFA. Figure 5-19 shows the relative strength of blended pastes at 7 and 28 days compared to cement paste devoid of fly ash addition. The results show that increasing the fly ash content from 20% to 40% contributes to decreasing the compressive strength at both 7 and 28 days. However, the relative strength of the blended pastes was found to increase with the use of fly ash of increased fineness. This noted increase in relative strength for increased fineness might possibly be due to the consumption of more C-H and the formation of more C-S-H gel in the system due to the pozzolanic reaction. These observed trends are in agreement with the XRD and SEM results reported in Sections 5.3 and 5.4, respectively, as well as the findings of other researchers [45, 160-162]. A similar relationship is observed for the CFA blends having gained more strength compared to the RFA blends at both 7 and 28 days.

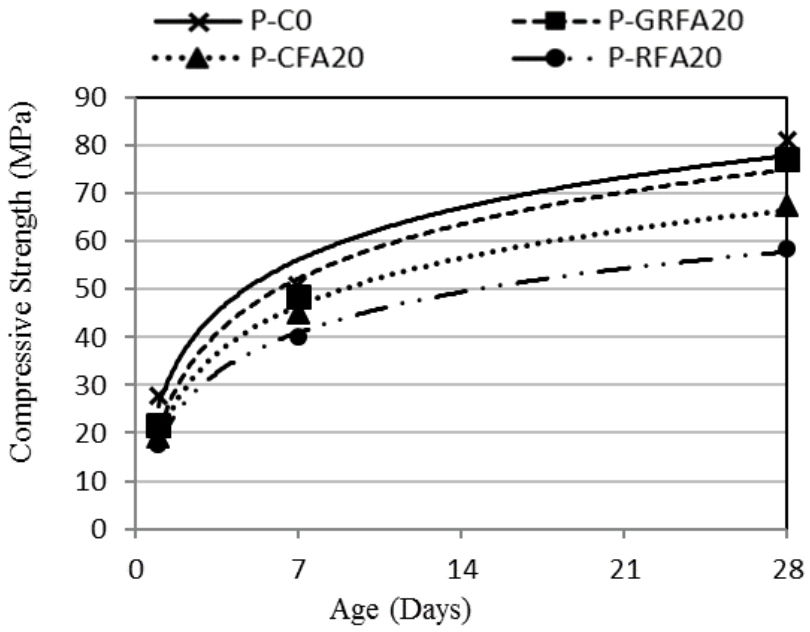


**Figure 5-17: Compressive strength development of the blended cement pastes containing 20% fly ash content of different fineness**

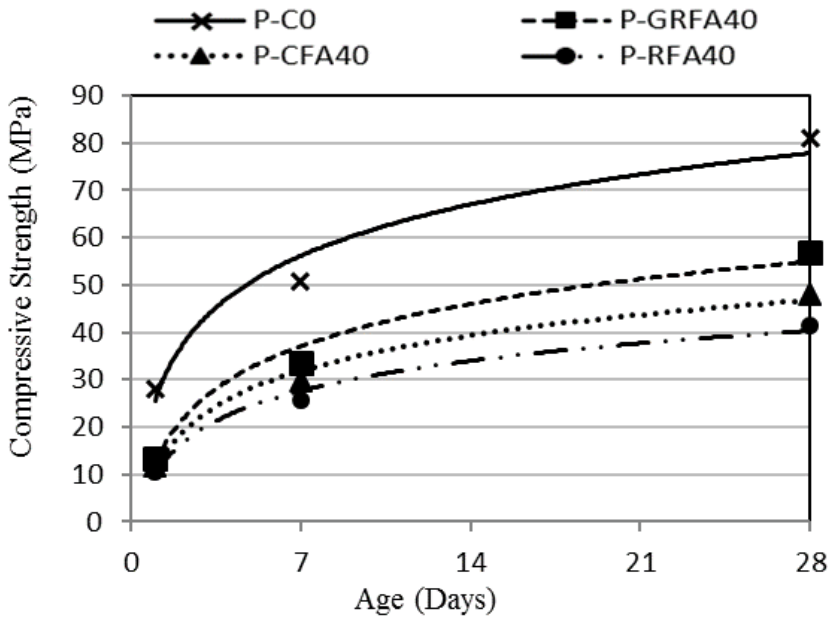


**Figure 5-18: Compressive strength development of the blended cement pastes containing 40% fly ash content of different fineness**

Figure 5-19 shows that at the ages of 7 and 28 days, the relative strength of the blended pastes incorporating 20% GRFA is comparable to the control cement paste devoid of fly ash addition. At the age of 28 days, the blended paste with 20% GRFA achieved about 96% of the strength of that of the control paste. However, the relative strength of the blended CFA and RFA pastes at the same cement replacement level was about 83% and 72%, respectively. At the same age of 28 days, an increase in fly ash content from 20% to 40% caused the relative strength of the GRFA, CFA and RFA pastes to decrease to 71%, 59% and 51%, respectively. Although the oxide compositions of all fly ashes investigated in this study were reported to be the same, it is quite possible that a more disordered structure exists in the GFRA compared to the CFA and RFA. Iyer and Scott [163] have reported that a higher level of reactivity of fly ash prevails for a more disordered structure of fly ash arising from such factors as changes in temperature and duration of combustion and quenching during the manufacturing process of the fly ash.

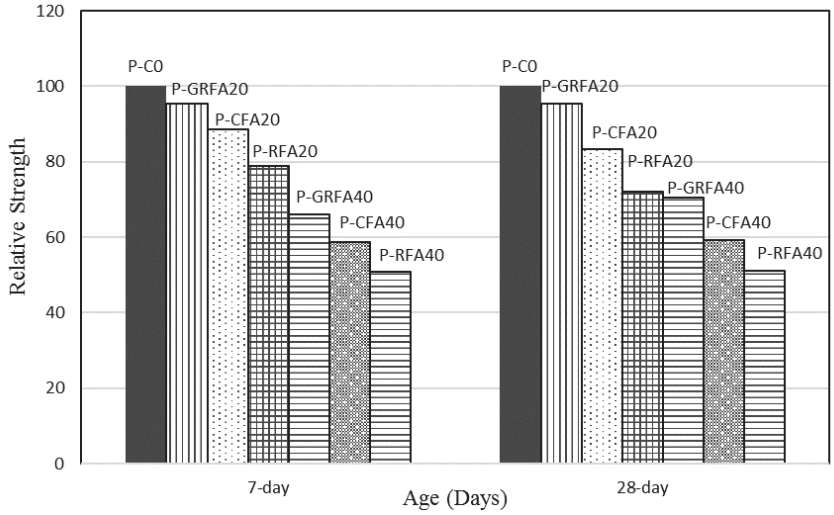


**Figure 5-19: Relative strength of the blended cement pastes containing varying fly ash content of different fineness**

## 5.6 **Summary**

From the isothermal calorimetry, XRD, SEM, flow and compressive strength tests performed on the blended cement pastes with two (2) cement replacement levels of fly ashes of different fineness, the following conclusions can be drawn.

1. Partially replacing cement with fly ashes with different fineness in cement paste decreased the cumulative heat evolution; the reduction in heat evolved increased with an increase in fly ash content. Finer grade fly ash generates more heat of hydration compared to coarser grade fly ash.
2. Blended pastes containing fly ash at higher w/b ratio showed higher cumulative heat evolution after 48 hours compared to the blended pastes with lower w/b ratio.
3. The cumulative heat of hydration of the blended pastes containing slag decreased compared to cement paste devoid of slag addition. The decrease was noted to increase at higher levels at both w/b ratios of 0.40 and 0.55. However, the blended pastes with lower w/b ratio generated less heat compared to the blended pastes with higher w/b ratio.
4. The blended pastes containing metakaolin decreased the height of the second peak in the heat evolution curve compared to the cement paste; the reduction increased at higher metakaolin content and less w/b ratio.
5. The cumulative heat of hydration of the blended pastes containing metakaolin was similar to the cement paste, especially at higher w/b ratio.

6. The blended paste with ground run-of-station fly ash exhibited increased hydration products on the fly ash particle surfaces especially at 28 days according to the SEM results.
7. The XRD results indicated that the fineness of fly ash did not have a significant influence on the consumption of the calcium hydroxide at the ages of 1 and 7 days; however, the consumption of calcium hydroxide increased at 28 days by increasing the fineness of the fly ash.
8. Increasing the fineness of fly ash marginally influenced the flow of the blended cement pastes.
9. The blended cement pastes containing finer grade fly ash demonstrated higher compressive strength than the coarser grade fly ash at both cement replacement levels (20% and 40%). The rapid pozzolanic reaction observed for finer grade fly ash by consuming more C-H and producing more secondary C-S-H gel in the system makes the microstructure denser compared to the mix containing coarser grade fly ash, and thus increases the compressive strength as supported by XRD and SEM results. In addition, the blended paste containing 20% ground run-of-station fly ash showed comparable results to the control cement paste devoid of fly ash addition at both 7 and 28 days.

# Chapter 6

## EFFECT OF FINENESS AND LEVEL OF FLY ASH AND OTHER SCM ADDITIONS ON FRESH AND HARDENED PROPERTIES OF CEMENT MORTAR

# 6 EFFECT OF FINENESS AND LEVEL OF FLY ASH AND OTHER SCM ADDITIONS ON FRESH AND HARDENED PROPERTIES OF CEMENT MORTAR

## 6.1 Preface

In this chapter, the effect of different types and levels of SCMs, as well as the influence of fineness and level of fly ash on the important fresh and hardened properties of mortars, were investigated. The properties of mortar are flow, compressive strength, strength activity index and the drying shrinkage. Portland cement was partially replaced by 20%, 30% and 40% of three kinds of fly ashes with different fineness (CFA, RFA, GRFA), 35%, 50% and 65% of ground granulated blast furnace slag (SL) and 5%, 10% and 15% of metakaolin (MK) by weight. A fixed water to binder ratio of 0.40 and sand to binder ratio of 2.5 with a fixed dosage of water reducer was maintained for these mixes. Moreover, some mixes containing 50%, 60% and 70% classified or run-of-station fly ash with a fixed water to binder ratio of 0.55 and sand to binder ratio of 5 were cast to evaluate the effect of fineness of fly ash in low strength mortar.

## 6.2 Effect of fineness and level of fly ash on important properties of mortar

### 6.2.1 Flow and wet density

The results of the effect of fineness and level of fly ash on flow of mortar mixes with various cement replacement percentages are shown in Figure 6-1. It is noted that GRFA and CFA improved the flow of the mix at all replacement levels compared to PC mix, while RFA was only effective in enhancing the flow in high replacement levels. However, GRFA was more effective in improving the flow

compared to CFA and RFA. This is possibly due to the smooth texture and spherical shape of the fly ash particles as well as the finer particle size improving the rheology of the mortars. In addition, the lower specific gravity of fly ash compared to cement makes more paste content for fixed binder content in the mix and thus increases the flow [159]. As reported by Mora et al. [28] the flow of the mix is increased by decreasing the particle size of fly ash. It is due to the fact that more particles of fly ash are available per unit mass which increases the lubricant effect in comparison to coarser sized fly ash particles.

From Figure 6-2, it is noted that there was a reduction in the wet density for the mortar mixes consisting of fly ash, especially at higher replacement levels compared to the control mix. The reduction in the wet density of mortar mixes increased by increasing the water to binder ratio. This is due to the specific gravity differences between the mentioned fly ashes and PC, which are 2.08, 2.06 and 2.10 for CFA, RFA and GRFA respectively, while specific gravity for PC is 3.09.

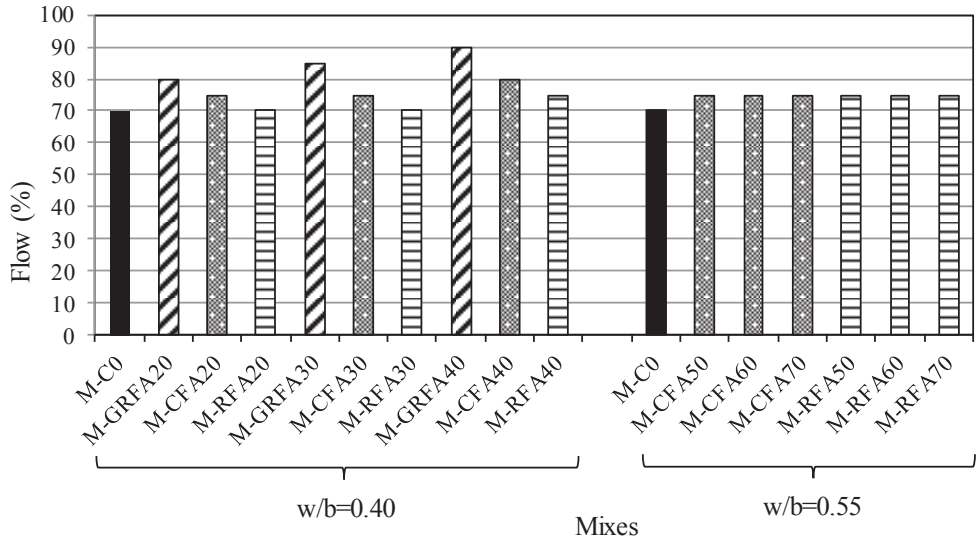


**Figure 6-1: Flow of mortar mixes with fly ash replacement**

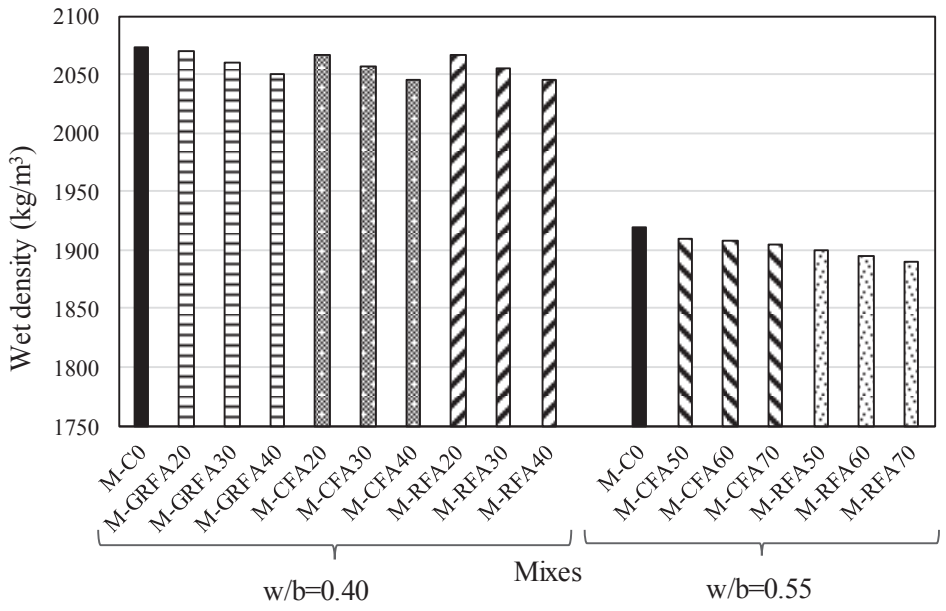


**Figure 6-2: Wet density of mortar mixes with fly ash replacement**

### 6.2.2 Compressive strength

The influence of partially replacing cement with various levels of fly ash with different fineness on compressive strength of two categories of mortar mixes is given in Tables 6-1 and 6-2. The plots of relative strength versus curing time of mortar mixes with different fly ash content is shown in Figures 6-3 and 6-4. Relative strength is the ratio of the strength of the mortar mix containing fly ash to the strength of the mortar mix devoid of fly ash addition at each particular curing time in percentages. From Table 6-1, it is noted that the compressive strength at 28 days was at a range of between 28 MPa to 47 MPa. The lowest and the highest compressive strength at 28 days were associated with M-RFA40 and M-GRFA20 mixes respectively. From Table 6-2, M-RFA70 mix with the lowest compressive strength was about 6.6 MPa and M-C0 mix with the highest one of about 17 MPa found for mixes with a fixed w/b=0.55 and s/b=5.0 at 56 days. As shown in

Figures 6-3 and 6-4, partially replacing cement with GRFA made a significant reduction in early age strength (1 and 7 days) with greater reduction in CFA following with RFA mixes compared to PC mix. In addition, this reduction increased with higher replacement levels. The lowest and the highest relative strength in mixes containing fly ashes to PC mix at 1 day were 32.2% and 74.7% for M-RFA40 and M-GRFA20 respectively and increased to 56.8% and 96% at 7 days. This could be due to the dilution of the total quantity of cement, which is able to hydrate and provide early-age strength with partially replacing cement with fly ash, which has the potential to inhibit the strength development of the mortar mixes. The effect is more evident in mortar mixes with higher w/b ratio with larger replacement levels due to the slow pozzolanic reaction between the fly ash and calcium hydroxide (CH) generated from cement hydration [55].

The finding is in agreement with the XRD results on the blended cement paste containing fly ash with different fineness as shown in Figure 5-11 in chapter 5. It was concluded that there was no substantial reduction in CH intensity in the mixes with fly ash content at early ages (up to 7 days). However, there was a significant increase in CH consumption with curing time (28 days) due to pozzolanic reactivity, especially in the mixes containing GRFA. After 28 days, the relative strength increased by up to 110% for M-GRFA20 mix, while M-RFA40 only increased by 66%. This is due to the formation of the secondary C-S-H gel as a result of pozzolanic reaction at a later age which fills the capillary pores and increases the compressive strength by enhancing the microstructural density and reducing the mortar porosity [10]. It is in agreement with SEM images taken from blended cement paste with fly ash content as shown in Figure 5-15. It showed that

most of the finer fly ash particles were covered by C-S-H gel and encapsulated with hydration products compared to the coarser ones. ACI [57] reported the siliceous glass is the primary contributor from the fly ash to the pozzolanic reaction in concrete since it is the amorphous silica that combines with free lime and water to form calcium silicate hydrate (C-S-H), the binder in concrete.

From Figures 6-3 and 6-4, it can be seen that the rate of compressive strength development of mortar mixes was improved by decreasing the fly ash particle size and increasing the fineness, possibly because of packing effect, the filling of the small pores and increasing density. This indicated that finer fly ash (GRFA) is more reactive compared to coarser types (CFA and RFA) due to the higher specific surface area and availability of particles to be attacked by hydroxide and thus produce more secondary C-S-H gel. It is in agreement with the XRD and SEM results of blended pastes containing fly ash with different fineness at 28 days as shown in Figure 5-12 and Figure 5-15. It demonstrated a significant number of finer fly ash particles have reacted and converted to C-S-H with more fibrous sheets evident at 28 days compared to the coarser fly ash particles, and also the findings of other researchers [160, 161].

**Table 6-1: Compressive strength of mortar mixes (MPa) with w/b=0.4 and S/b=2.5**

| Age | Mixes | | | | | | | | | |
|---|---|---|---|---|---|---|---|---|---|---|
| | w/b=0.4, S/b=2.5 | | | | | | | | | |
| | M-C0 | M-CFA20 | M-CFA30 | M-CFA40 | M-RFA20 | M-RFA30 | M-RFA40 | M-GRFA20 | M-GRFA30 | M-GRFA40 |
| **1-Day** | 19.8 | 13.2 | 10.0 | 6.5 | 13.0 | 9.7 | 6.4 | 14.8 | 11.7 | 7.6 |
| **7-Day** | 35.2 | 28.9 | 24.7 | 20.0 | 28.8 | 23.7 | 20.0 | 33.8 | 29.0 | 25.0 |
| **28-Day** | 42.4 | 37.9 | 35.9 | 31.2 | 36.0 | 33.9 | 28.0 | 47.0 | 42.6 | 40.6 |

**Table 6-2: Compressive strength of mortar mixes (MPa) with w/b=0.55 and S/b=5.0**

| Age | Mixes | | | | | | |
|---|---|---|---|---|---|---|---|
| | w/b=0.55, S/b=5.0 | | | | | | |
| | M-C0 | M-CFA50 | M-CFA60 | M-CFA70 | M-RFA50 | M-RFA60 | M-RFA70 |
| **7-Day** | 11.7 | 5.2 | 3.4 | 2.3 | 4.4 | 3.4 | 2.2 |
| **28-Day** | 14.5 | 9.2 | 6.4 | 4.7 | 8.7 | 5.3 | 4.2 |
| **56-Day** | 17.0 | 12.3 | 9.6 | 8.2 | 10.5 | 8.3 | 6.6 |

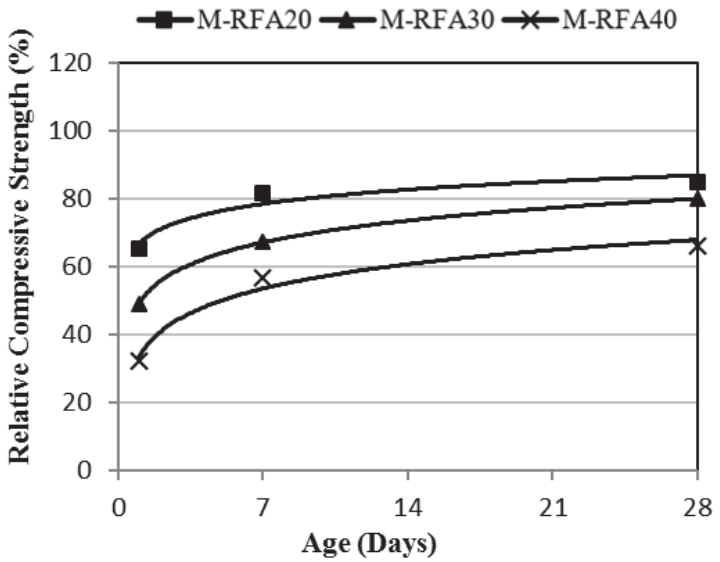
M-RFA20
M-RFA30
M-RFA40
Relative Compressive Strength (%)
120
100
80
60
40
20
0
0
7
14
21
28
Age (Days)

(a)

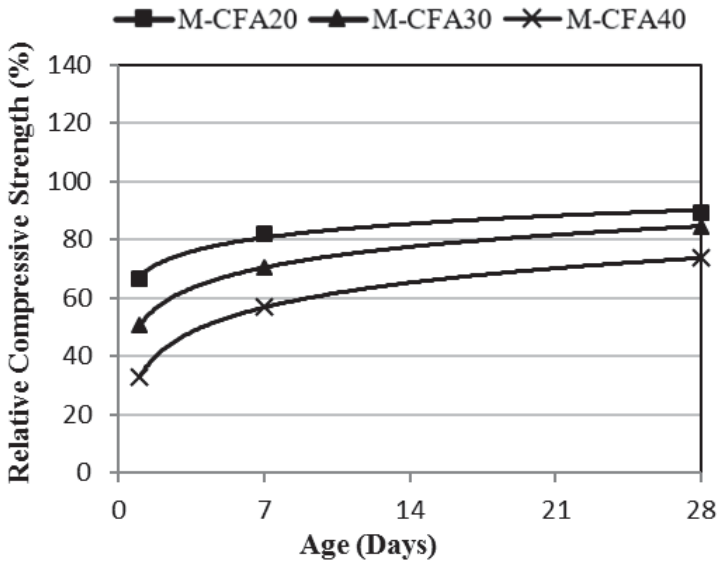
M-CFA20
M-CFA30
M-CFA40
Relative Compressive Strength (%)
140
120
100
80
60
40
20
0
0
7
14
21
28
Age (Days)

(b)

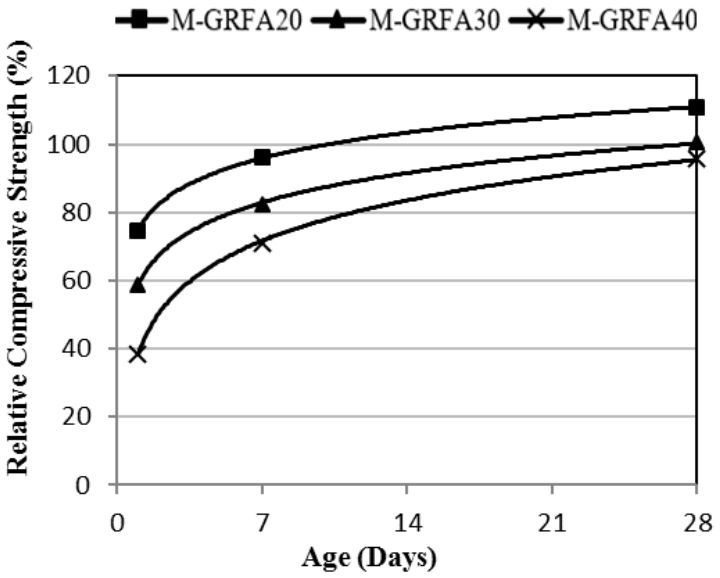


(c)

**Figure 6-3: Relative strength of high strength mortar with different cement replacement levels of fly ash at w/b=0.40 and s/b=2.5 (a=RFA, b=CFA and c=GRFA)**

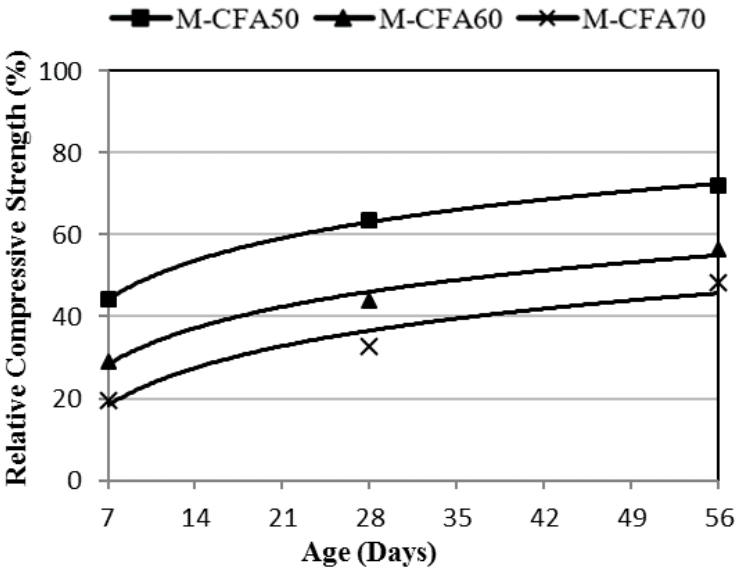


(a)

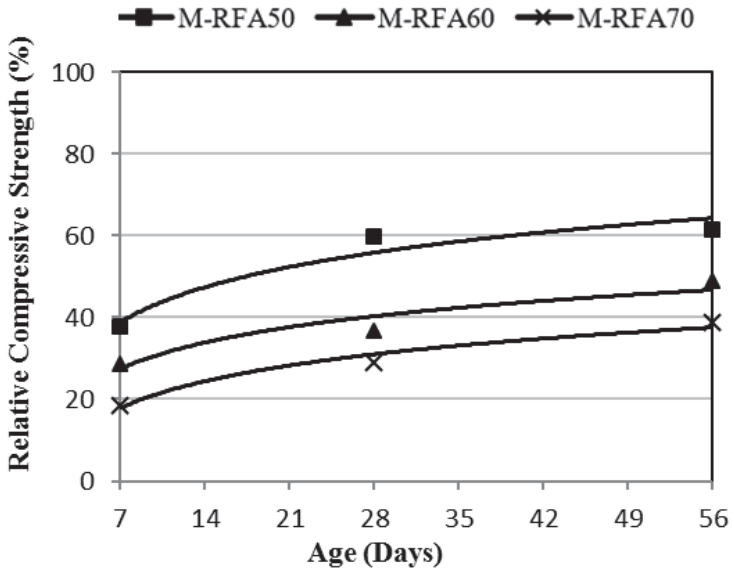


(b)

**Figure 6-4: Relative strength of low strength mortar with different cement replacement levels with CFA and RFA at w/b=0.55 and s/b=5.0**

### 6.2.3 Strength activity index

The results of the strength activity index (SAI) for mortar mixes containing fly ash of different fineness are shown in Figure 6-5. It can be seen that the SAI increased as the fineness of the fly ash increased. At the age of 28 days, SAI of GRFA mix increased to 107% compared to 76% for RFA mix. SAI data showed GRFA works better in gaining strength at both 7 and 28 days followed by CFA compared to RFA. This is possibly due to the finer particle size and higher specific surface area of GRFA as shown in Tables 4-1 and 4-2 and also due to the presence of less crystallinity according to the XRD results shown in Figure 4-5. As discussed by Barry [140], coarser fly ash may act as inert (i.e. non-pozzolanic) and merely dilute the Portland cement possibly due to the highly crystalline phase and lower specific surface area.

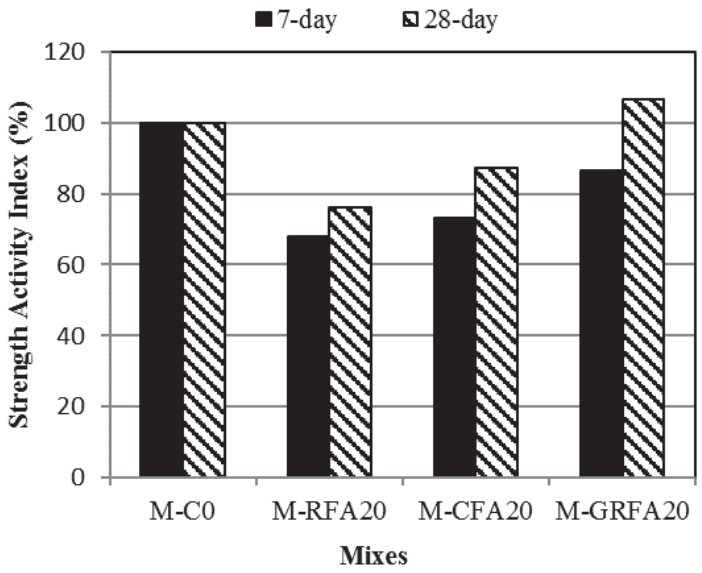


**Figure 6-5: Strength activity index of mortar mixes with fly ash replacement**

### 6.2.4 Drying shrinkage

The results of the drying shrinkage test after 56 days for mortar mixes are given in Tables 6-3 and 6-4. Deformation of the mortar specimens due to the drying shrinkage can be explained by the evaporation of free water within the hardened state. There are many factors affecting the drying shrinkage of mortar and concrete such as type and aggregate content, water to binder ratio, water content, the amount of hardened cement paste, specimen size, the curing system and test methods [164]. In this research, only a variation in binder type was investigated. The results demonstrated the influence of fly ash in decreasing the drying shrinkage of mortar mixes at almost all ages. All three kinds of fly ashes showed a considerable reduction in drying shrinkage compared to the PC mix and this reduction was increased by decreasing the particle size and increasing the fly ash content in the mixes. From Table 6-3, the 56 day drying shrinkage of mortar

mixes containing 20%, 30% and 40% GRFA decreased by about 45%, 46% and 48% compared to PC mix (M-C0) respectively, while it was about 37%, 38% and 41% for CFA mix and 36%, 37% and 38% for RFA mix with the same cement replacement level respectively. This reduction trend was almost the same in the mixes with higher replacement levels with CFA and RFA as shown in Table 6-4. The shrinkage value is related to the cement paste as cement paste volume is a dominant feature in this phenomenon. As the cement content increases for a unit volume of the mix, shrinkage will increase [64, 164]. Therefore, the reduction in the drying shrinkage of fly ash mixes can be possibly related to the reduction in the cement content. Brooks and Johari [165] reported that the pozzolans are effective in reducing the drying shrinkage due to less water evaporation as the pozzolanic reaction consumes a significant amount of free water. Moreover, the effect of SCMs in the pore refinement due to increasing the mesopores and reducing the macropores improve the quality of the microstructure. It is another reason for the prevention of the evaporation of water from the hardened concrete [49, 166].

**Table 6-3: Drying shrinkage of high strength mortar mixes at different ages with different cement replacement levels of fly ash (w/b=0.40, s/b=2.5)**

| Mixes | Drying Shrinkage (Microstrain) | | | | |
|---|---|---|---|---|---|
| | 7 days | 14 days | 21 days | 28 days | 56 days |
| **M-PC** | 513 | 815 | 877 | 923 | 936 |
| **M-CFA20** | 318 | 479 | 533 | 587 | 590 |
| **M-CFA30** | 287 | 485 | 531 | 577 | 585 |
| **M-CFA40** | 285 | 467 | 505 | 551 | 556 |
| **M-RFA20** | 349 | 523 | 551 | 574 | 597 |
| **M-RFA30** | 300 | 459 | 500 | 533 | 590 |
| **M-RFA40** | 385 | 508 | 533 | 546 | 579 |
| **M-GRFA20** | 297 | 415 | 460 | 498 | 515 |
| **M-GRFA30** | 290 | 407 | 440 | 490 | 502 |
| **M-GRFA40** | 291 | 404 | 435 | 472 | 486 |

**Table 6-4: Drying shrinkage of low strength mortar mixes at different ages with different cement replacement levels of fly ash (w/b=0.55, s/b=5.0)**

| Mixes | Drying Shrinkage (Microstrain) | | | | |
|---|---|---|---|---|---|
| | 7 days | 14 days | 21 days | 28 days | 56 days |
| **M-PC** | 438 | 538 | 577 | 585 | 692 |
| **M-CFA50** | 269 | 319 | 358 | 362 | 438 |
| **M-CFA60** | 292 | 331 | 355 | 360 | 435 |
| **M-CFA70** | 304 | 331 | 353 | 358 | 431 |
| **M-RFA50** | 346 | 381 | 400 | 400 | 446 |
| **M-RFA60** | 323 | 338 | 346 | 362 | 438 |
| **M-RFA70** | 315 | 331 | 335 | 338 | 415 |

## 6.3 Effects of different types and levels of SCMs on fresh and hardened properties of mortar

### 6.3.1 Flow and wet density

The results of the effect of different SCMs on the flow of mortar mixes with various cement replacement levels are shown in Figure 6-6. It is noted that CFA improved the flow of the mix at all replacement levels compared to the PC mix. This is due to the smooth texture and spherical shape of CFA particles as shown in SEM image shown in Figure 4-8 compared to PC particles contributing to improving the rheology of the mortars. In addition, the lower specific gravity of CFA compared to cement makes more paste content available for fixed binder content in the mix and thus increases the flow [159].

Mortar mixes containing SL showed better flow compared to the PC mix at all replacement levels due to the superior cementitious particle dispersion and the physical appearances of the SL particles, which are smooth and compact, reducing the absorption of water through mixing [29, 167].

It was seen that the flow in mixes containing MK were reduced with the increase in MK content. This may be due to the high specific surface area and small particle size of MK compared to PC which consumes more water, and thus decreases the flow of the mix [49, 168]. From Figure 6-7, it is noted that the wet density decreased for the mixes with SCMs. Moreover, it reduced further with the increase of SCMs content. This is due to the specific gravity differences between the mentioned SCMs and PC, which are 2.08, 2.90 and 2.49 for CFA, SL and MK respectively while specific gravity for PC is 3.09.

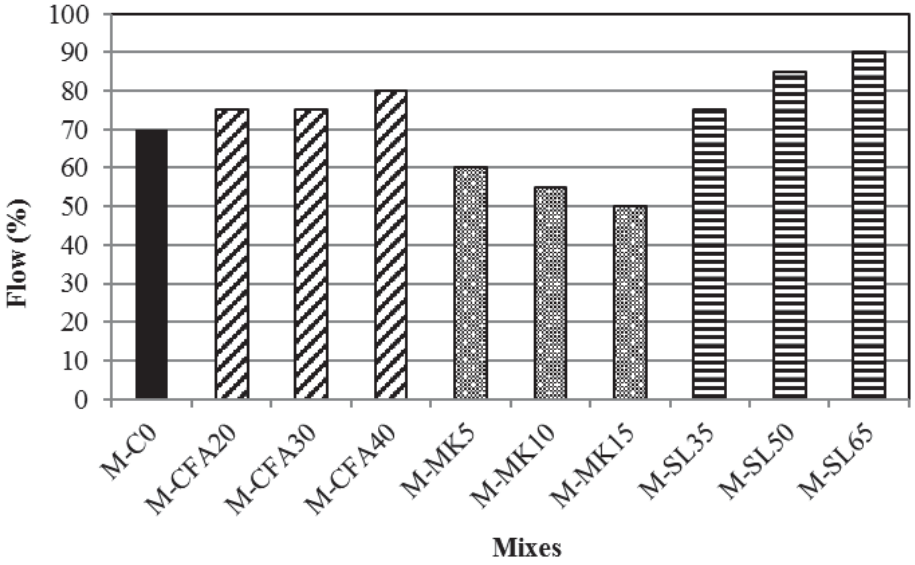


**Figure 6-6: Flow of mortar mixes with different cement replacement levels of SCMs**

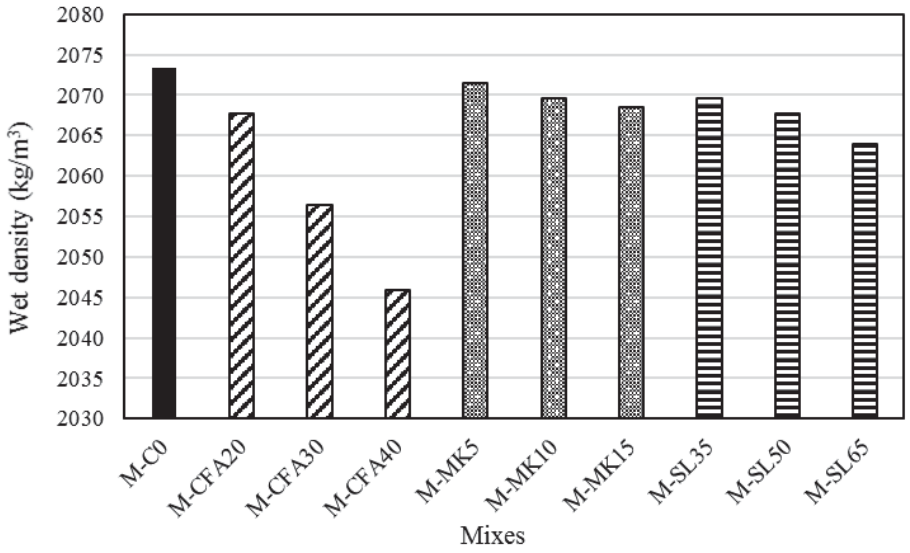


**Figure 6-7: Wet density of mortar mixes with different cement replacement levels of SCMs**

### 6.3.2 Compressive strength

The influence of partial replacement of cement with different SCMs on compressive strength of mortar mixes is given in Table 6-5. The plots of the relative strength versus curing time of mortar mixes with different SCM content are shown in Figure 6-8. Relative strength is the ratio of the strength of the mortar mix containing SCM to the strength of the mortar mix devoid of SCM addition at each particular curing time in percentage. From Table 6-5, it can be seen that the compressive strength at 28 days was in a range between 31.2 MPa to 52.6 MPa. The lowest and the highest compressive strength at 28 days were associated with M-CFA40, and M-MK15 mortar mixes respectively. The results showed that reduction in PC content and replacing PC with SCMs in most of the mortar mixes ended up with comparable and even higher 28-day compressive strength than PC mix. This reduction in PC consumption has significant economic, environmental and technical benefits such as cost saving, reducing $CO_2$ emission and enhancement in fresh and hardened properties of mortar mixes. The effect of each SCM on strength development relative to PC mix will be discussed in the following paragraphs.

#### 6.3.2.1 Effect of fly ash

As shown in Figure 6-8, partially replacing cement with CFA made a significant reduction in early age strength (1 and 7 days) compared to the PC mix. This reduction increased with higher replacement levels. The lowest and the highest relative strength in mixes containing CFA to PC mix at 1 day were 32.9% and 66.8% for M-CFA40 and M-CFA20 respectively and increased to 56.8% and 82.1% at 7 days. This could be due to dilution of the total quantity of cement,

which is able to hydrate and provide early-age strength with partial cement replacement with CFA, which has the potential of inhibiting the strength development of the mortar mixes. It is in line with the XRD and SEM results at 7 days for the blended cement paste with fly ash content shown in Figures 5-11 and 5-14 respectively. The effect is more evident at a higher replacement level due to the slow pozzolanic reaction between the fly ash and calcium hydroxide (CH) generated by cement hydration [55]. However, there was an increase in compressive strength with curing time. After 28 days, the relative strength increased up to 89.3% for M-CFA20 mix, while M-CFA40 only increased up to 73.6%. It is due to the formation of the secondary C-S-H gel as a result of pozzolanic reaction at a later age which fills the capillary pores and increases the compressive strength by enhancing the microstructural density and reducing mortar porosity [10]. It was confirmed by the SEM micrographs of blended cement pastes containing fly ash at 28 days that finer grade fly ash was more involved in the pozzolanic reactivity compared to the coarser grade fly ash as shown in Figure 5-15.

#### 6.3.2.2 **Effect of slag**

The effects of SL in mortar mixes are demonstrated in Table 6-5 and Figure 6-8b. It can be seen that the inclusion of SL decreased the 1-day compressive strength significantly and this reduction increased at higher replacement levels up to 72 percent in M-SL65 mix relative to M-PC mix. It is likely due to the slow-developing reactivity of SL in accordance to SAI results shown in Figure 6-9 in early ages as well as the dilution effect, as part of cement was substituted by slow reactive material [60, 61]. In contrast, the 28-day relative strength of mixes

containing SL was higher at all replacement levels. The relative strength of M-SL35, M-SL50 and M-SL65 mixes at 28 days were 109%, 102% and 101% respectively. It could be due to a sufficient quantity of glassy particles, finer particle size and higher specific surface area of SL compared to PC as shown in Table 4-1 which fills the capillary pores, thus increasing the strength. It is in agreement with the previous findings of other researchers [169].

#### 6.3.2.3 **Effect of metakaolin**

The effect of partial replacement of cement with MK is presented in Table 6-5 and Figure 6-8c. At 1 day, there was a strength reduction in comparison with the control mix in very early age due to the dilution effect by replacing part of the cement with MK especially at 15 percent replacement. However, the compressive strength only after 3 days curing significantly increased, even more than the PC mix at all replacement levels. The relative strength of M-MK5, M-MK10 and M-MK15 at 7 days was 111%, 117% and 122% respectively. The compressive strength increased by increasing the moist curing time up to 28 days, even though the effectiveness of MK in improving the strength is reduced with the increase in age as shown in Figure 6-8c. The relative strength of the M-MK5, M-MK10 and M-MK15 at 28 days were 113%, 119% and 124% respectively. The effectiveness of MK in increasing the relative strength only after 3 days is due to finer particle size and the higher specific surface area of MK, which accelerates the pozzolanic reaction and packs into cement particles gaps. The loose structure of MK after heat activation at high temperature is another reason for its high reactivity [63]. These are in agreement with the previous findings of other researchers [53, 54].

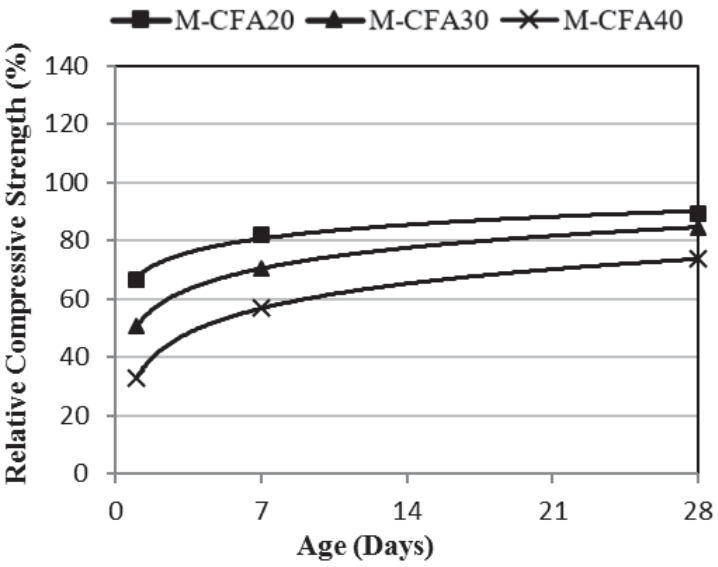
M-CFA20
M-CFA30
M-CFA40
Relative Compressive Strength (%)
140
120
100
80
60
40
20
0
0
7
14
21
28
Age (Days)

(a)

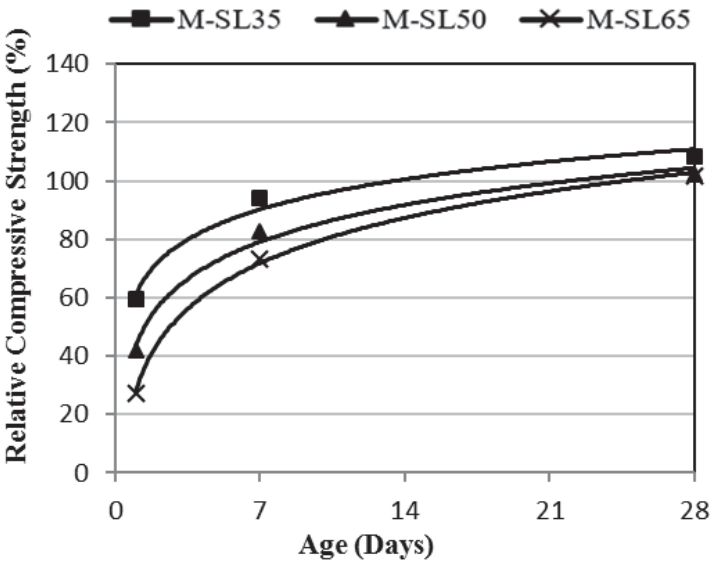
M-SL35
M-SL50
M-SL65
Relative Compressive Strength (%)
140
120
100
80
60
40
20
0
0
7
14
21
28
Age (Days)

(b)

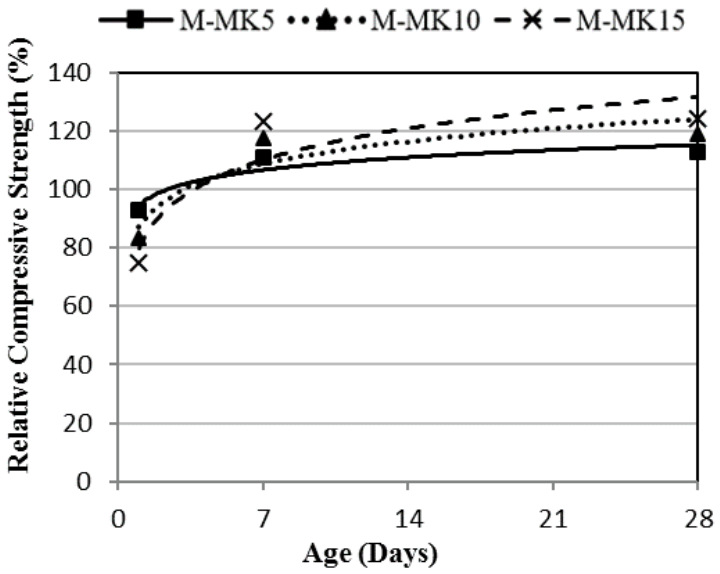


(c)

**Figure 6-8: Relative strength of mortar mixes with different cement replacement levels of SCMs (a=CFA, b=SL and c=MK)**

**Table 6-5: Compressive strength of mortar mixes with different cement replacement levels of SCMs at different ages (MPa)**

| Age | Mixes w/b=0.4, S/b=2.5 | | | | | | | | | |
|---|---|---|---|---|---|---|---|---|---|---|
| | M-PC | M-CFA20 | M-CFA30 | M-CFA40 | M-SL35 | M-SL50 | M-SL65 | M-MK5 | M-MK10 | M-MK15 |
| **1-Day** | 19.8 | 13.2 | 10.0 | 6.5 | 11.8 | 8.3 | 5.4 | 18.4 | 16.5 | 14.8 |
| **7-Day** | 35.2 | 28.9 | 24.7 | 20.0 | 33.2 | 29.2 | 25.9 | 39.1 | 41.4 | 43.6 |
| **28-Day** | 42.4 | 37.9 | 35.9 | 31.2 | 46.0 | 43.3 | 43.2 | 47.7 | 50.4 | 52.6 |

### 6.3.3 Strength activity index

The results of the strength activity index (SAI) test of mortar mixes containing SCMs are shown in Figure 6-9. SAI data showed that MK works better in gaining strength at both 7 and 28 days followed by SL compared to CFA mix. This is due to the finer particle size and higher specific surface area shown in Tables 4-1 and 4-2, as well as less crystallinity according to XRD results shown in Figure 4-7. This is generally in line with previous findings [161, 162]. The results for MK mixes showed similar SAI after 7 days curing to PC mix and 15 percent improvement at 28 days which is likely due to the high specific surface area of MK which accelerates the hydration reaction and packs into cement particle gaps [62]. SAI of SL was lower than PC at 7 days due to the slow reactivity of SL in early ages whereas it is higher after 28 days as a result of the sufficient quantity of glassy particles according to XRD results as well as small particle size and high specific surface area.

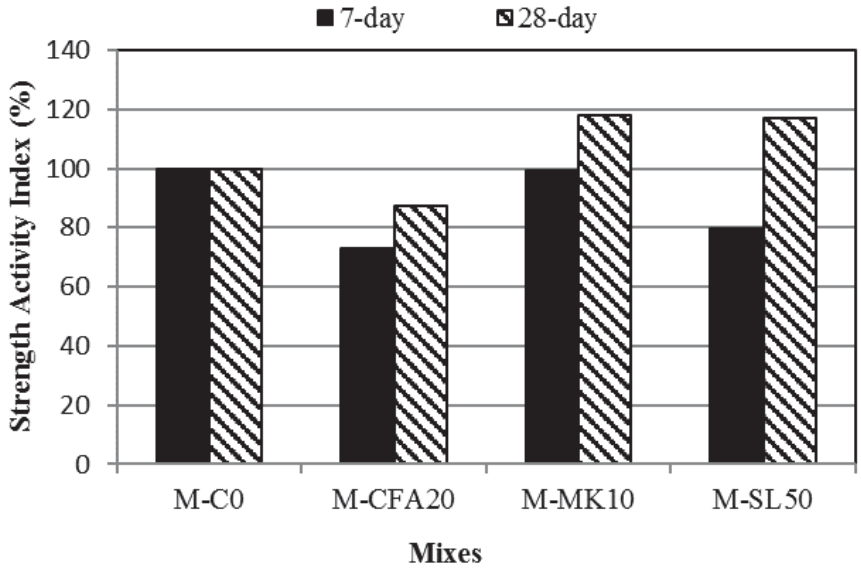


**Figure 6-9: Strength activity index of mortar mixes with different cement replacement levels of SCMs**

### 6.3.4 **Drying shrinkage**

The results of the drying shrinkage test after 56 days for mortar mixes are given in Table 6-6. The results demonstrated the influence of SCMs in decreasing the drying shrinkage of mortar mixes up to 56 days. CFA showed a considerable reduction in drying shrinkage compared to the PC mix and this reduction increased by increasing the CFA content in the mixes. From Table 6-6, the 56-day drying shrinkage of mortar containing 20%, 30% and 40% CFA decreased by about 37%, 38% and 41% compared to PC mix respectively, while replacing cement with 35%, 50% and 65% SL reduced 56-day drying shrinkage values by about 23%, 24% and 24% respectively. The effect of partially replacing cement with 5%, 10% and 15% MK was to reduce the 56-day drying shrinkage by about 21%, 22% and 23% respectively in mortar mixes. The shrinkage value is related to the cement paste, as cement paste volume is a dominant feature in this phenomenon. As the cement content increases for a unit volume of the mix, shrinkage will increase [64, 164]. Therefore, the reduction in the drying shrinkage of SCM mixes can be possibly related to the reduction in the cement content.

Brooks and Johari [165] reported the pozzolans consume a considerable amount of free water during the pozzolanic reaction and thus cause a reduction in drying shrinkage because of reduced water evaporation. In addition, the effect of SCMs in pore refinement due to increasing the mesopores and reducing the macropores improve the quality of microstructure which is another reason that prevents water evaporation [49, 166].

**Table 6-6: Drying shrinkage of mortar mixes at different ages with different cement replacement levels of SCMs**

| Mixes | Drying Shrinkage (Microstrain) | | | | |
|---|---|---|---|---|---|
| | 7 days | 14 days | 21 days | 28 days | 56 days |
| **M-PC** | 513 | 815 | 877 | 923 | 936 |
| **M-CFA20** | 318 | 479 | 533 | 587 | 590 |
| **M-CFA30** | 287 | 485 | 531 | 577 | 585 |
| **M-CFA40** | 285 | 467 | 505 | 551 | 556 |
| **M-SL35** | 487 | 521 | 620 | 660 | 720 |
| **M-SL50** | 431 | 504 | 605 | 640 | 710 |
| **M-SL65** | 372 | 433 | 600 | 640 | 708 |
| **M-MK5** | 428 | 569 | 654 | 682 | 736 |
| **M-MK10** | 408 | 546 | 631 | 677 | 731 |
| **M-MK15** | 385 | 513 | 610 | 651 | 723 |

## 6.4 Summary

Based on the results of this study, the following conclusions can be drawn.

1. The results showed that increasing the fineness of fly ash improved the flow of the mortar mix. A greater influence was observed at higher cement replacement levels.
2. The use of all three kinds of fly ashes in mortar decreased the early age strength up to 7 days compared to control mortar devoid of fly ash addition. There was a correlation in the results with the observations from SAI data and from XRD data suggesting pozzolanic reactivity to be the cause of the decrease in early age strength.
3. Mortar mixes containing 20% ground run-of-station fly ash enhanced compressive strength to a similar and even higher level than the

control mix at 28 days. The degree of pozzolanic reaction increased due to smaller particle size, higher specific surface area and more amorphicity of ground run-of-station fly ash. However, there was a reduction in the compressive strength of the mixes containing classified fly ash or run-of-station fly ash compared to the control at 28 days. This is due to the lower reactivity of coarser fly ash which results in reduced consumption of calcium hydroxide and thus less secondary CSH gel as confirmed by XRD results performed on the blended cement pastes.

4. Replacing cement with fly ash reduced 56-day drying shrinkage compared to the control mix devoid of fly ash addition. The reduction increased by increasing the cement replacement level and fineness of fly ash. It is possibly due to the reduction in the cement paste content by partially replacing cement with fly ash as well as consumption of more water by the pozzolanic reaction, especially by finer fly ash with higher specific surface area.
5. The results showed the effect of fly ash and slag in improving the flow of the mix while the inclusion of the metakaolin decreased the flow of the mortar mix.
6. The inclusion of slag in mortar mixes reduced early age strength (1 and 7 days) compared to the control mix devoid of slag addition. These results are also confirmed by the strength activity index test. An increase in compressive strength was noted at 28 days in mortar mix

containing 35% slag compared to the control mix devoid of slag addition.

7. Partially replacing cement with metakaolin in mortar mixes decreased 1-day strength compared to control mix devoid of metakaolin addition. However, the compressive strength of mortar mixes containing metakaolin preceded the control mix only after 3 days due to higher reactivity and specific surface area of metakaolin particles.
8. The effect of partially replacing cement with slag or metakaolin in mortar mixes was to reduce drying shrinkage after 56 days, and the reduction increased at higher levels.

# Chapter 7

## EFFECT OF RUN-OF-STATION FLY ASH AND OTHER SCMS ON VARIOUS PROPERTIES OF LEAN AND HIGH-PERFORMANCE CONCRETE

# 7 EFFECT OF RUN-OF-STATION FLY ASH AND OTHER SCMS ON VARIOUS PROPERTIES OF LEAN AND HIGH-PERFORMANCE CONCRETE

## 7.1 Preface

This chapter records the results of a laboratory investigation, which was carried out to examine the possible use of RFA and other SCMs in concrete applications. Firstly, the possible use of RFA in 12 MPa subbase paving concrete mix was examined and compared to CFA concrete according to the properties specified in Roads and Maritime Services (RMS) specification R82 [110]. Then, the effect of RFA and other SCMs such as SL and MK in High-Performance Concrete (HPC) was investigated and compared to CFA concrete. HPC refers to 40 MPa base pavement mix in accordance RMS R83 specification [111] for concrete pavement base, and 50 MPa bridge mix in accordance RMS B80 specification [112] for concrete work for bridges.

## 7.2 Effect of RFA and CFA on plastic and hardened properties in lean concrete mixes

Lean concrete mixes with 60% CFA and RFA in the binder and a control mix without any SCM were designed to achieve a similar 28-day target mean strength of 16 MPa. The target mean strength was derived from the specified characteristic strength of 12 MPa with varying total binder content and varying w/b ratio as shown in Table 7-1. The designed mixes should comply with the requirements of the RMS R82 specification shown in Table 7-2. In addition, the target slump of 30±10 mm and air content of 5±2% by introducing entrained air using air-entrained admixture (AEA) were considered in designing the concrete mixes

according to R82 specification [110]. Introducing entrained air reduces compressive strength by about 5.5% for each 1% by volume of AEA in the mix. Therefore, the modified target mean strength of 22 MPa was used for all lean mixes. Lean mixes were designed using a variable dosage of WR and AEA in order to comply with the requirements of R82 specification [110]. The combined aggregate grading for all lean mixes according to Road Note No.4 are shown in Figure 7-1. The whole process of designing the lean mixes is presented in Appendix A. The results are discussed in following paragraphs.

**Table 7-1: Mix design composition for lean concrete mixes**

| Material/Property | Concrete Mixes | | |
|---|---|---|---|
| | C12-C0 | C12-CFA60 | C12-RFA60 |
| GP Cement (kg/m$^3$) | 200 | 110 | 110 |
| SCM (kg/m3) | 0 | 165 | 165 |
| 20 mm Aggregate (kg/m$^3$) | 730 | 660 | 655 |
| 10 mm Aggregate (kg/m$^3$) | 470 | 425 | 425 |
| Coarse Sand (kg/m$^3$) | 505 | 455 | 450 |
| Fine Sand (kg/m$^3$) | 250 | 225 | 225 |
| Water (kg/m$^3$) | 165 | 165 | 165 |
| WR, ml | 600 | 830 | 875 |
| AEA, ml | 160 | 150 | 150 |
| w/b | 0.82 | 0.6 | 0.6 |
| 28-Day Compressive Strength (MPa) | 14.0 | 12.0 | 11.0 |
| Slump (mm) | 35 | 40 | 40 |
| Air content (%) | 6.0 | 5.1 | 5.2 |

**Table 7-2: Plastic and hardened concrete property requirements for lean mix according to RMS R82 specification [110]**

| Description | Trial mix concrete |
|---|---|
| Characteristic compressive strength | 6.0 MPa min @ 28 days<br>15 MPa max @ 28 days |
| Consistency<br>(by measuring the slump) | 20-40 mm for slipformed concrete |
| Air content (with AEA) | 5 ± 2 % |
| Drying shrinkage<br>(maximum aggregate size ≤ 20 mm) | 550 microstrain maximum<br>@ 21 days in air |

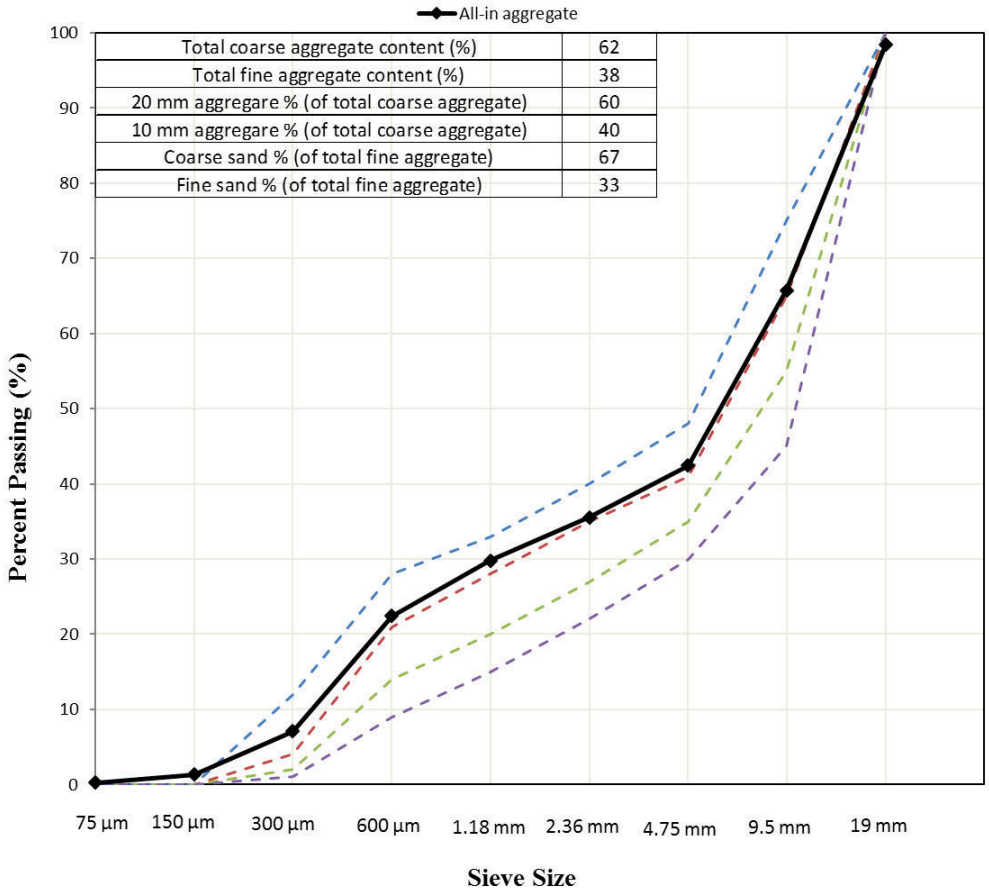


**Figure 7-1: Combined aggregate grading for C12-0, C12-CFA60 and C12-RFA60 mixes according to Road Note No.4**

### 7.2.1 Plastic concrete properties

From Table 7-3, required workability using slump test and air content percentage was achieved according to the R82 specification [110] as shown in Table 7-2, where slump should be between 20- 40 mm and air content 5 ± 2 %. Both CFA and RFA mixes (C12-CFA60 and C12-RFA60) were designed with a w/b ratio of 0.60 while the control mix (C12-C0) had a w/b ratio of 0.82. This difference in w/b ratios between the mixes is due to the fact that all mixes were designed for similar 28-day compressive strength with variable w/b ratio, variable binder content and similar targeted slump. Therefore, the higher binder content of

275 kg/m$^3$ in fly ash mixes instead of 200 kg/m$^3$ for control mix decreased the w/b ratio in fly ash mixes.

The wet density of the control mix was more than CFA and RFA mixes, which is most likely due to the specific gravity differences between fly ash and cement, which are about 2.08 and 3.09 respectively.

**Table 7-3: Plastic property results for lean mixes**

| Mixes | Slump (mm) | Air content (%) | Density (kg/m$^3$) |
|---|---|---|---|
| C12-C0 | 35 | 6.0 | 2320 |
| C12-CFA60 | 40 | 5.1 | 2205 |
| C12-RFA60 | 40 | 5.2 | 2200 |

### 7.2.2 Hardened concrete properties

According to the RMS R82 specification [110], compressive strength and drying shrinkage are the main hardened concrete properties that should be controlled and achieved as shown in Table 7-2. In this research, all lean concrete mixes were designed to achieve similar 28-day compressive strength with varying total binder content and varying w/b ratio. The results will be discussed in following paragraphs.

#### 7.2.2.1 Compressive strength

Compressive strength developments and relative strength of the concrete mixes are shown in Figures 7-2 and 7-3, respectively. Relative strength is the ratio of the strength of concrete mix at each particular curing time to the 28-day

strength of the same mix in percentage. It can be seen that the effect of RFA in gaining strength at all ages in lean concrete mix was lower compared to concrete mix with CFA, despite having similar mix design. It is due to the increased reactivity of finer fly ash by consumption of more portlandite compared to the coarser grade fly ash and thus the production of more secondary C-S-H gel in the system resulting in a denser microstructure as confirmed by XRD and SEM results reported in chapter 5 on blended cement pastes. The higher reactivity of the finer fly ash could be due to the smaller particle size and higher specific surface area of CFA according to PSA and the Blaine fineness test compared to RFA as shown in Figure 4-1 and Table 4-1. The higher reactivity of CFA compared to RFA was also confirmed by 28-day strength activity index test results shown in Figure 6-5.

From Figure 7-3, it can be noted that the incorporation of RFA or CFA in concrete reduced relative strength at earlier ages as compared to control concrete due to the slower pozzolanic reaction of fly ash, as confirmed by XRD results reported in Chapter 5. The reduction in early age strength of the concrete mixes with 60% CFA and RFA is in agreement with the findings of the work done on mortars with 50%, 60% and 70% CFA and RFA as shown in Table 6-2.

These results are in agreement with the findings of Lee et al. [170] who reported the higher degree of pozzolanic reactivity of finer fly ash compared to the coarser one. In addition, Sumer [26] and Uysal & Akyuncu [20] reported that the silica and alumina content of fly ash allows the material to consume calcium hydroxide (a by-product of cement hydration) and forms a secondary C-S-H gel which is responsible for increasing the compressive strength. The detailed

comparison of compressive strength of lean mixes at various ages can be found in Appendix B.

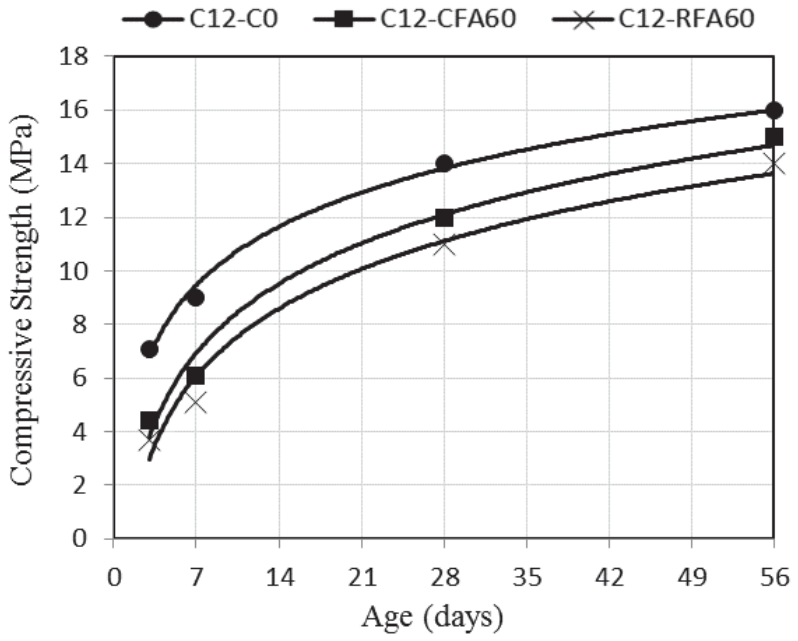


**Figure 7-2: Compressive strength development in lean concrete mixes**

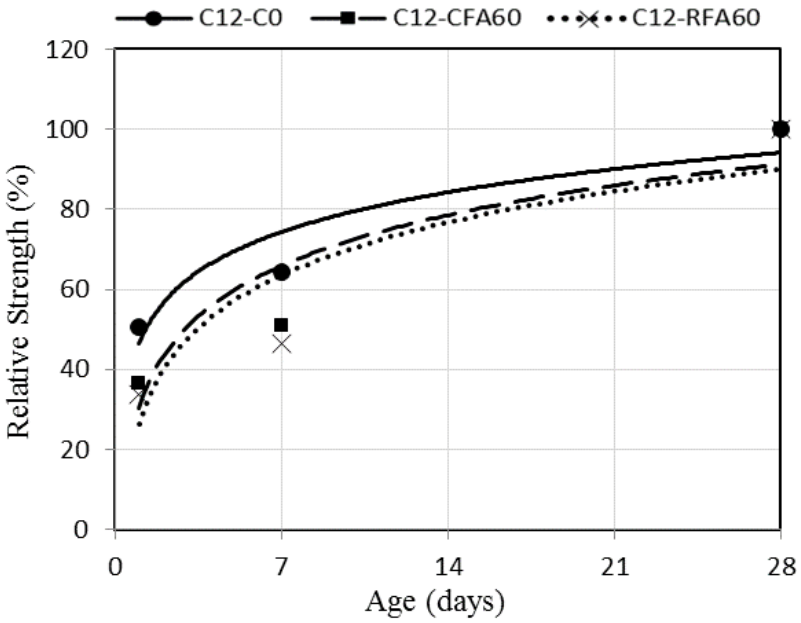


**Figure 7-3: Relative strength in lean concrete mixes**

#### 7.2.2.2 **Drying shrinkage**

From Figure 7-4, it is noted that mixes with fly ash content showed less drying shrinkage than control concrete, especially at later ages. As shown in Table 7-1, all lean mixes were designed for similar 28-day compressive strength with variable w/b ratio and variable binder content and a similar target for the slump. Therefore, concrete mixes containing CFA and RFA have a w/b ratio of 0.60 while control concrete mix has a w/b ratio of 0.82. The main reason for reduced drying shrinkage of about 10% at 56 days for concrete mixes with fly ash content is due to having less w/b ratio compared to the control mix. In addition, the lower drying shrinkage of high volume fly ash concrete compared to control concrete is a function not only of low unit water used but also use of high volume fly ash that reduced the amount of cement paste in unit volume of the concrete mix as reported by Atis [171]. It should be mentioned that all mixes comply with RMS R82 requirement for drying shrinkage as shown in Table 7-2 which should be less than 550 microstrain after 21 days. The detailed comparison of results of drying shrinkage of lean mixes at various ages can be found in Appendix B.

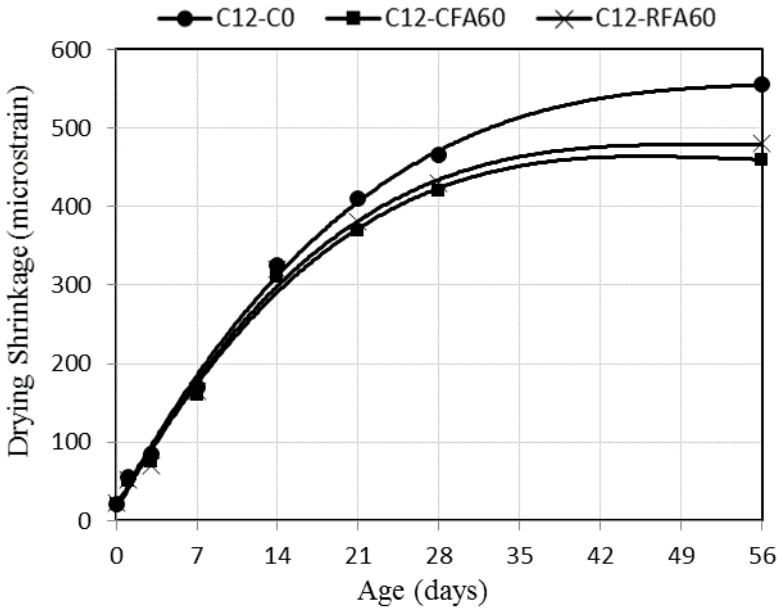


**Figure 7-4: Drying shrinkage in lean concrete mixes**

### 7.2.3 Possible use of RFA replacing CFA in the lean concrete mix

The possible use of RFA in 12 MPa subbase paving concrete mix was evaluated and compared to the similar concrete mix containing CFA according to the properties specified in RMS R82 specification [110]. Compressive strength and drying shrinkage are the main hardened concrete properties that should be controlled and achieved according to the RMS R82 specification [110] as shown in Table 7-2. The results revealed that partially replacing cement with RFA in the lean concrete mix was able to comply the specified RMS R82 requirements which are the 28-day compressive strength between 6-15 MPa and 21-day drying shrinkage less than 550 microstrain. It indicates that RFA is a possible alternative to CFA in producing low strength concrete such as lean concrete mix. Therefore, apart from economical and environmental advantages of using RFA, it helps to save finer grade fly ash for use in high-performance concrete due to growing

concern about the shortage of fine grade fly ash in recent years. However, the 28-day compressive strength of the concrete mix containing RFA was about 9% lower than the CFA concrete mix while the 21-day drying shrinkage was almost the same. These findings are in agreement with the compressive strength and drying shrinkage results of the mortar mixes containing 60% CFA or RFA reported in Chapter 6. Mortar results showed a similar reduction in 28-day compressive strength by replacing cement with 60% RFA compared to CFA. Therefore, there is a need to modify the mix design for the lean concrete mix containing 60% RFA according to the analytical and experimental outcomes to get similar strength property to the lean concrete mix with 60% CFA. Decreasing the w/b ratio to 0.56 for the mix containing 60% RFA instead of using w/b ratio of 0.60 similar to the CFA concrete mix is recommended. This reduction in w/b ratio possibly compensates for the strength difference between RFA and CFA lean concrete mixes investigated in this study which is due to the reduced reactivity of RFA particles compared to CFA ones. It means the cement and RFA content in the mix should increase by about 7%, compared to the CFA concrete mix and with an adjustment of the proportion of fine and coarse aggregate accordingly.

## 7.3 Effect of RFA and other SCMs on plastic and hardened properties of pavement concrete mixes

Pavement concrete mixes containing 20% CFA and RFA and 50% SL in the binder as well as the control mix (GP cement) were designed to achieve a similar 28-day target mean strength of 47 MPa. The target mean strength derived from the specified characteristic strength of 40 MPa with varying total binder content and varying w/b ratio as shown in Table 7-4. The designed mixes should satisfy the requirements of the RMS R83 specification shown in Table 7-5 [111]. Furthermore, the target slump of 30±10 mm and air content of 4.5±1.5% were considered in designing the concrete mixes according to R83 specification [111]. However, the modified target mean strength of 60 MPa was used for all pavement mixes to accommodate the strength reduction due to 4% entrained air content in the mix. All pavement mixes were designed using a variable dosage of WR and AEA to comply with the requirements of R83 specifications. The combined aggregate grading for all pavement mixes according to Road Note No.4 are shown in Figure 7-5. The whole process of designing the pavement mixes are presented in Appendix A. The results are discussed in following paragraphs.

**Table 7-4: Mix design composition for pavement concrete mixes**

| Material/Property | Concrete Mixes | | | |
|---|---|---|---|---|
| | C40-C0 | C40-CFA20 | C40-RFA20 | C40-SL50 |
| GP Cement (kg/m$^3$) | 380 | 330 | 330 | 185 |
| SCM (kg/m$^3$) | 0 | 80 | 80 | 185 |
| 20 mm Aggregate (kg/m$^3$) | 795 | 775 | 770 | 800 |
| 10 mm Aggregate (kg/m$^3$) | 520 | 510 | 505 | 520 |
| Coarse Sand (kg/m$^3$) | 480 | 470 | 465 | 480 |
| Fine Sand (kg/m$^3$) | 85 | 85 | 85 | 85 |
| Water (kg/m$^3$) | 160 | 155 | 160 | 165 |
| WR, ml | 1050 | 1150 | 1460 | 1050 |
| AEA, ml | 100 | 100 | 130 | 150 |
| w/b | 0.43 | 0.38 | 0.38 | 0.43 |
| 28-Day Compressive Strength (MPa) | 45.5 | 43.0 | 38.5 | 40.5 |
| 28-Day Flexural Strength (MPa) | 5.3 | 5.3 | 4.7 | 5.3 |
| Slump (mm) | 50 | 40 | 40 | 50 |

**Table 7-5: plastic and hardened concrete property requirements for pavement concrete mix according to RMS R83 specification [111]**

| Description | Trial mix concrete |
|---|---|
| Characteristic compressive strength (Mixes with SCMs) | 40 MPa @ 28 days |
| Characteristic flexural strength (Mixes with SCMs) | 4.7 MPa @ 28 days |
| Consistency (by measuring the slump) | 15-50 mm for slipformed concrete |
| Air content (using AEA) | 4.5 ± 1.5 % |
| Drying shrinkage (in 21 days drying period) | 580 microstrain maximum for slag mixes<br>450 microstrain maximum for other mixes |

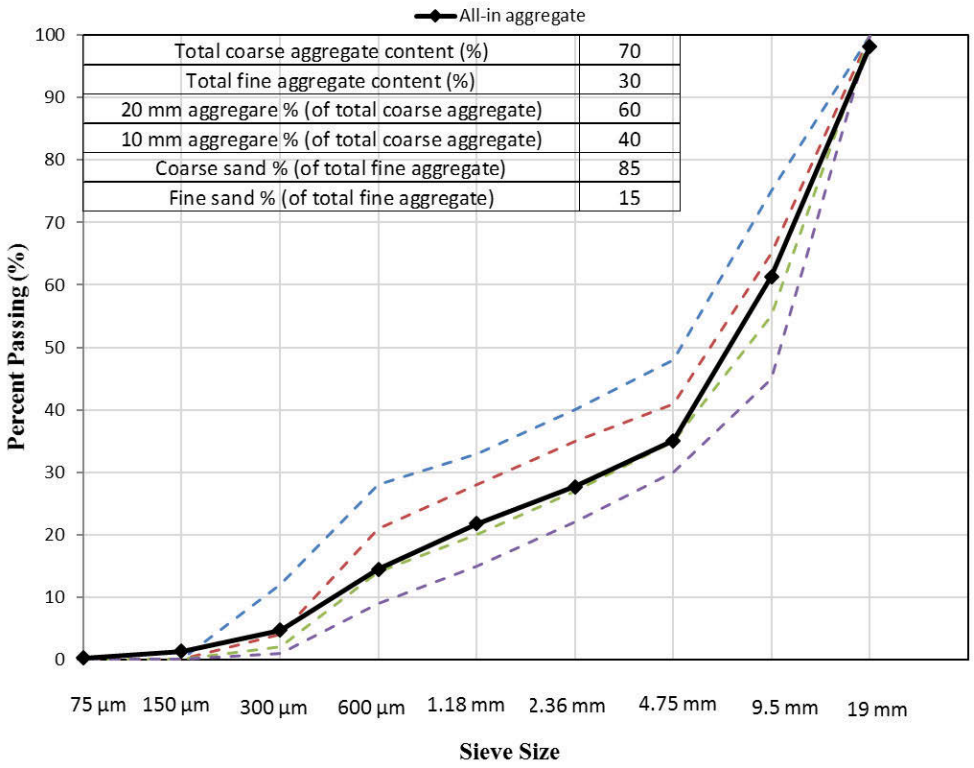


**Figure 7-5: Combined aggregate grading for C40-C0, C40-CFA20, C40-RFA20 and C40-SL50 mixes according to Road Note No.4**

### 7.3.1 Plastic concrete properties

It is noted that the required workability of between 15-50 mm using slump test and air content percentage between 4.5 ± 1.5 % were achieved according to the RMS R83 specification as shown in Table 7-6 [111]. It can be seen that both CFA and RFA mixes have lower w/b ratio compared to the control mix despite designing for similar 28-day compressive strength. The reduction in w/b ratio of fly ash mixes is due to the use of higher binder content in fly ash mixes compared to the control mix to get the similar strength to control. The spherical shape of CFA and RFA particles as shown in SEM images (Figures 4-8 and 4-9) also contributed to improving the rheology of the concrete mixes containing fly ash [159]. It should be mentioned that the wet density of concrete mixes with only

cement as a binder is more than the concrete mixes with partial replacement of cement by SCMs, which is due to differences in specific gravity between SCMs and cement.

**Table 7-6: plastic property results for pavement concrete mixes**

| Mixes | Slump (mm) | Air content (%) | Density ($kg/m^3$) |
|---|---|---|---|
| C40-C0 | 50 | 4.6 | 2420 |
| C40-CFA20 | 40 | 4.4 | 2400 |
| C40-RFA20 | 40 | 4.7 | 2390 |
| C40-SL50 | 50 | 5.1 | 2415 |

### 7.3.2 Hardened concrete properties

According to RMS R83 specification [111], compressive strength, flexural strength and drying shrinkage are the main hardened concrete properties that should be controlled and achieved as shown in Table 7-5. In this research, all pavement mixes were designed to achieve similar 28-day compressive strength with varying total binder content and varying w/b ratio. The results are discussed in the following paragraphs.

#### 7.3.2.1 Compressive strength

The compressive strength developments and relative strength of the pavement concrete mixes are shown in Figures 7-6 and 7-7, respectively. Relative strength is the ratio of the strength of the each concrete mix at each particular curing time to the 28-day strength of the same mix in percentage. The compressive strength results up to 56 days for pavement concrete mixes is also tabulated in Table 7-7. It can be seen that the incorporation of SCMs in concrete decreased the strength at

earlier ages in comparison to the control mix due to the slower pozzolanic reaction, slow-developing reactivity for slag and the reduction of the total quantity of cement which is responsible for early-age strength, especially at higher cement replacement levels [10, 26]. Early-age strength reduction was more evident in the concrete mix containing 50% slag due to the high cement replacement level. However, there was an increase in compressive strength with curing time especially for the pavement mixes with CFA and SL, which reached the strength level close to the control mix at 56 days.

The effect of RFA on the strength property of pavement concrete compared to the same mix containing CFA was the reduction in 28-day compressive strength from 43 MPa to 38.5 MPa, which is about a 10% reduction despite having the similar mix design. This reduction in compressive strength is due to the lesser reactivity of coarser fly ash compared to the finer fly ash. It was confirmed by XRD and SEM results on blended pastes containing CFA or RFA which showed a significant number of finer fly ash particles have reacted and converted to C-S-H with more fibrous sheets evident at 28 days compared to the coarser fly ash particles as shown in Figures 5-12 and 5-15. This finding is in line with findings of the work done was confirmed by the lower strength activity index of RFA mix compared to the mix with CFA shown in Figure 6-5. These observed trends are in agreement with mortar results reported in Chapter 6 and Lee et al. [170] who reported the larger degree of pozzolanic reactivity of fine fly ash in comparison with the coarser one.

The reduction in compressive strength in early age for SL mix is likely due to the slow-developing reactivity of SL in accordance with SAI results as confirmed

by Barnett et al. [61]. However, the reason for the reduction in compressive strength at later ages for SL mix compared to the cement mix despite similar w/b ratio of 0.43 is possibly due to the late reaction of SL especially in higher replacement levels. Nevertheless, the results confirmed the concrete mix with SL at 56 days reached the strength level almost similar to control mix. The detailed results of compressive strength of pavement mixes in various ages can be found in Appendix B.

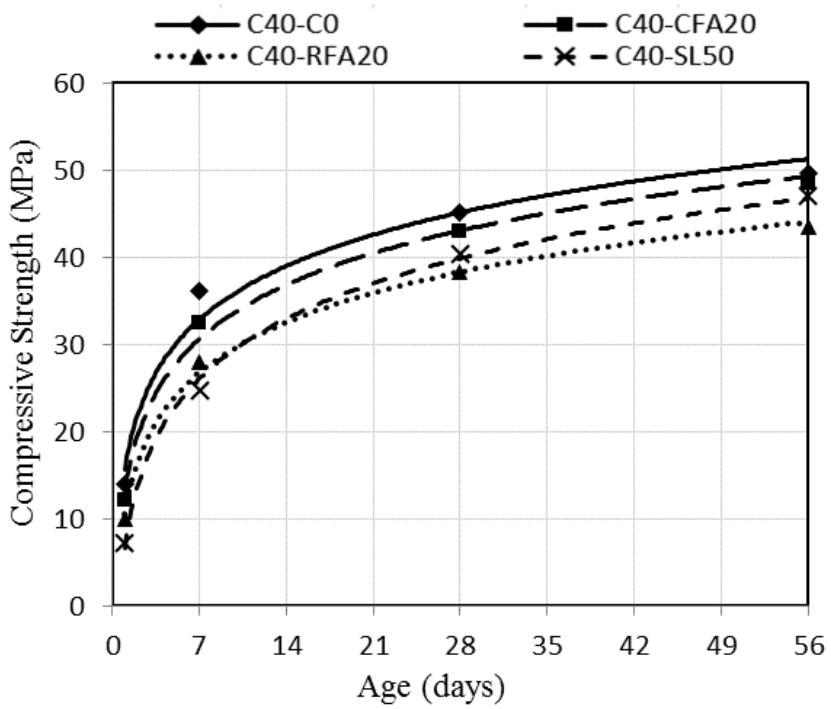


**Figure 7-6: Compressive strength development in pavement concrete mixes containing SCMs**

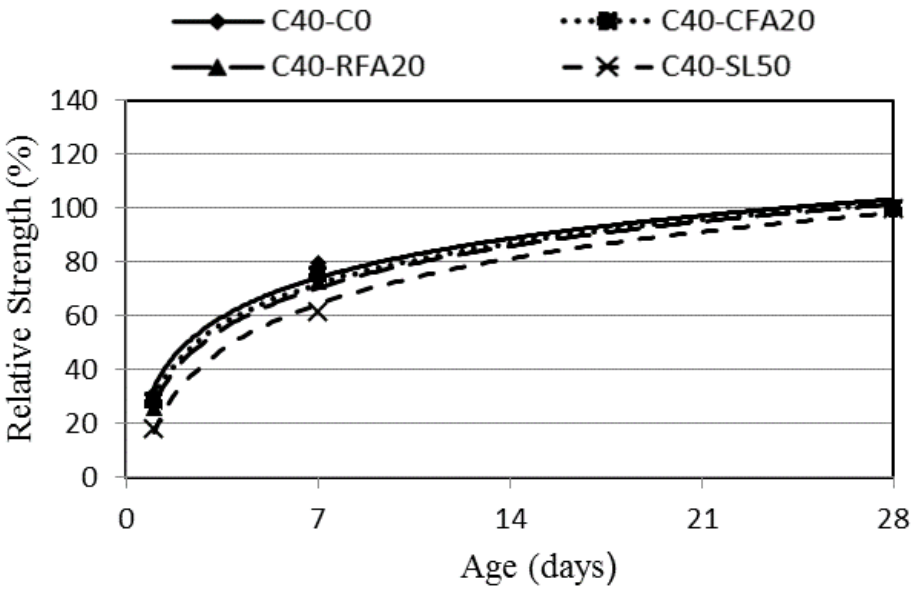


**Figure 7-7: Relative strength in pavement concrete mixes**

**Table 7-7: Compressive strength results of pavement concrete mixes up to 56 days**

| Category | Mix | w/b | Mean Compressive Strength (MPa) | | | |
|---|---|---|---|---|---|---|
| | | | 1-day | 7-day | 28-day | 56-day |
| Pavement Mix | C40-C0 | 0.42 | 14.0 | 36.1 | 45.2 | 49.7 |
| | C40-CF20 | 0.38 | 12.2 | 32.5 | 43.1 | 48.4 |
| | C40-RFA20 | 0.38 | 10.0 | 28.0 | 38.3 | 43.5 |
| | C40-SL50 | 0.43 | 7.3 | 24.8 | 40.4 | 47.0 |

#### 7.3.2.2 **Flexural strength**

Flexural strength development results for pavement concrete mixes are shown in Figure 7-8. It is noted that CFA and SL concrete mixes achieved flexural strength similar to control mix after 28 days while it was not the case for the mix with RFA content. The effect of RFA in gaining strength at 28 days was lower compared to the CFA mix despite having similar mix design due to larger particle size and the reduced reactivity of RFA. The detailed comparison of flexural strength of pavement mixes in various ages can be found in Appendix B.

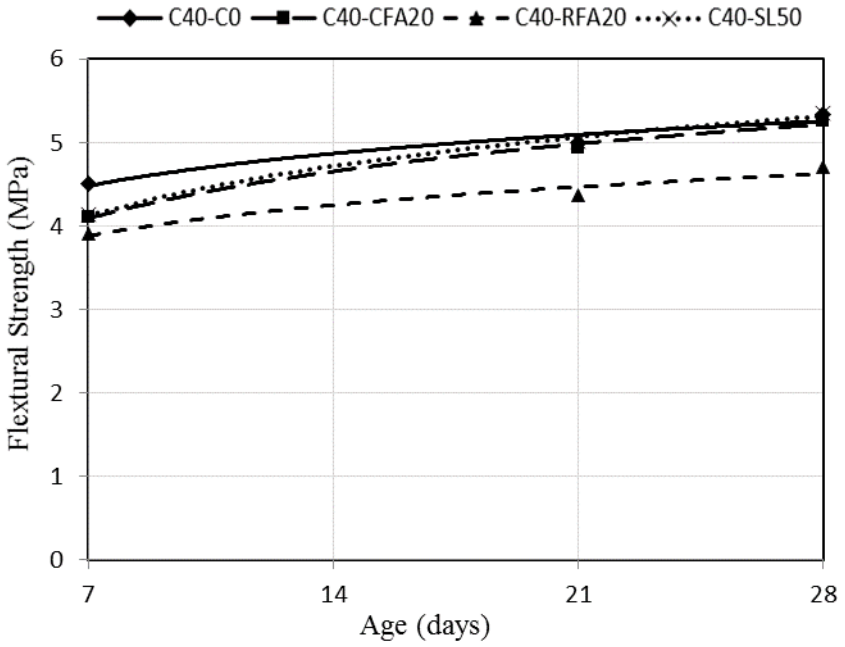


**Figure 7-8: Flexural strength development in pavement concrete mixes**

#### 7.3.2.3 **Drying shrinkage**

Drying shrinkage results for pavement concrete mixes are shown in Figure 7-9. It can be noted that drying shrinkage of pavement concrete mix containing 20% CFA was lower than the control mix in all ages, which might be due to the lower w/b ratio. The reduction in w/b ratio of concrete mixes containing fly ash is due to the higher binder content of fly ash concrete and thus a lower w/b ratio used in a concrete mix containing fly ash. In addition, the lower drying shrinkage of fly ash concrete in comparison to control concrete is a function not only of low unit water used but also use of fly ash that reduces the amount of cement paste in unit volume of concrete mix as reported by Atis [171]. However, despite having similar w/b ratio of the concrete mix containing RFA to the mix with CFA, there was an increase by about 16% in the 21-day drying shrinkage of RFA mix compared to CFA mix. This is possibly due to using a higher dosage of WR to get similar slump with CFA mix. It reduces the surface tension of water and causes larger shrinkage strains in cement paste [172]. However, pavement concrete mix with RFA still complies with the R83 specification requirement for drying shrinkage, which should be less than 450 microstrain at 21 days as shown in Table 7-5. Drying shrinkage of SL concrete also complies with R83 specification requirements [111] despite having a higher drying shrinkage compared to control mix.

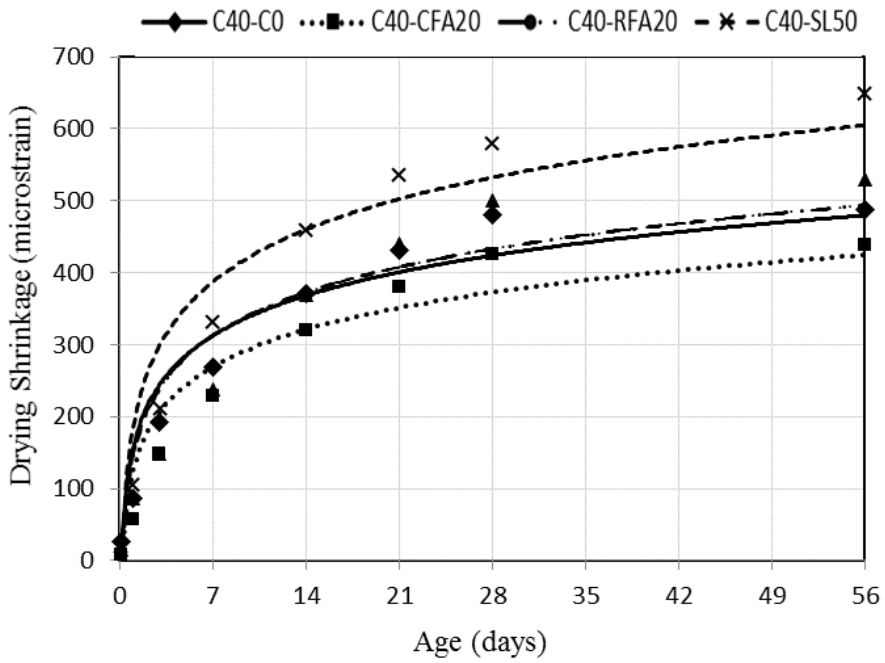


**Figure 7-9: Drying shrinkage in pavement concrete mixes up to 56 days**

### 7.3.3 Possible use of RFA or SL replacing CFA in the pavement concrete mix

The possible use of RFA or SL was evaluated as an alternative to CFA in pavement concrete mix according to the specified requirements of the RMS R83 specification [111]. Compressive strength, flexural strength and drying shrinkage are the main hardened concrete properties that should be controlled and achieved according to the RMS R83 specification [111]. The results revealed the mixes with SCM content did not comply the specified strength requirements according to RMS R83 specification [111] while the acceptable level of the 21-day drying shrinkage was achieved. However, the specified strength requirements will be possibly achievable by only adjusting the mix design such as considering lower w/b ratio for the mixes with SCM content according to the strength development

results of the mortars as well as the results of the fineness, crystaline phase and oxide composition of SCM particles reported in Chapter 4.

Regarding the effect of RFA compared to CFA in pavement concrete mix, the reduction of about 10% at 28-day compressive and flexural strength was noted in the mix containing RFA compared to the same mix with CFA content. These results are in agreement with work done on mortars in Chapter 6, which showed a similar reduction trend when cement was replaced with 20% RFA compared to the same mortar mix with CFA. The reduction in the strength of the RFA mix is due to the reduced reactivity of RFA particles compared to CFA. It was confirmed by XRD results reported in Chapter 4 which showed higher crystallinity of RFA particles compared to CFA particles. Apart from designing the concrete mix with CFA or RFA to comply the strength requirement, achieving the similar strength property for the pavement mix with RFA to the CFA mix is vital. For instance, for the mixes investigated in this study, reducing the w/b ratio of the RFA concrete mix to 0.35 instead of using w/b ratio of 0.38 similar to the CFA concrete mix to compensate for the strength difference is recommended. However, it causes an increase in the cement and RFA content by about 8% for the concrete mix with 20% RFA compared to the mix with 20% CFA.

It can be concluded that SL or RFA could be used as an alternative SCM to CFA in pavement concrete mixes. Utilization of SL or RFA as an SCM addition for partial replacement of cement in concrete introduces several economical, technical and environmental benefits such as the conservation of natural resources and the reduction of greenhouse gas emissions [173]. It is more evident by

partially replacing cement with SL in concrete mixes as replacement happens in higher levels.

## 7.4 Effect of RFA and other SCMs on plastic, hardened and durability properties of bridge concrete

Bridge concrete mixes containing 25% CFA, 25% RFA, 50% SL and 15% MK in the binder as well as the control mix (only PC) were designed to achieve a similar 28-day target mean strength of 57 MPa. The target mean strength derived from the specified characteristic strength of 50 MPa with varying total binder content and varying w/b ratios are shown in Table 7-8. The designed mixes should comply with the requirements of RMS B80 specification [112] shown in Table 7-9. The target slump of maximum 180 mm and exposure classification of C were considered in designing the concrete mixes according to B80 specification [112].

All mixes were designed using a variable dosage of HWR to comply with slump requirement of the B80 specification [112]. The combined aggregate grading for all bridge mixes according to Road Note No.4 are shown in Figure 7-10. The whole process of designing the bridge mixes is presented in Appendix A. The results are discussed in the following paragraphs.

**Table 7-8: Mix design composition for bridge concrete mixes**

| Material/Property | Concrete Mixes | | | | |
|---|---|---|---|---|---|
| | C50-C0 | C50-CFA25 | C50-RFA25 | C50-SL50 | C50-MK15 |
| GP Cement (kg/m$^3$) | 410 | 335 | 335 | 200 | 335 |
| SCM (kg/m$^3$) | 0 | 110 | 110 | 200 | 60 |
| 20 mm Aggregate (kg/m$^3$) | 785 | 760 | 760 | 785 | 785 |
| 10 mm Aggregate (kg/m$^3$) | 420 | 395 | 395 | 405 | 410 |
| Coarse Sand (kg/m$^3$) | 580 | 555 | 550 | 570 | 560 |
| Fine Sand (kg/m$^3$) | 145 | 140 | 140 | 145 | 140 |
| Water (kg/m$^3$) | 155 | 155 | 155 | 155 | 160 |
| HWR, ml | 3680 | 3350 | 4000 | 3590 | 3570 |
| w/b | 0.37 | 0.35 | 0.35 | 0.39 | 0.40 |
| 28-Day Compressive Strength (MPa) | 59.0 | 52.5 | 47.0 | 51.0 | 48.0 |
| Slump (mm) | 175 | 180 | 175 | 180 | 170 |

**Table 7-9: Plastic and hardened concrete property requirements for bridge concrete mix according to RMS B80 specification [112]**

| Description | Trial mix concrete |
|---|---|
| Consistency (by measuring the slump) | Less than 180 mm |
| Characteristic compressive strength (exposure classification C) | 50 MPa min @ 28 days |
| Drying shrinkage (in 21 days drying period) (exposure classification C) | 550 microstrain maximum for slag mixes<br>430 microstrain maximum for other mixes |
| Maximum acid-soluble chloride ion content (Unreinforced concrete at C exposure classification) ($kg/m^3$) | 0.8 |
| Percentage by mass of acid-soluble $SO_3$ to cement | Must not exceed 5.0% |

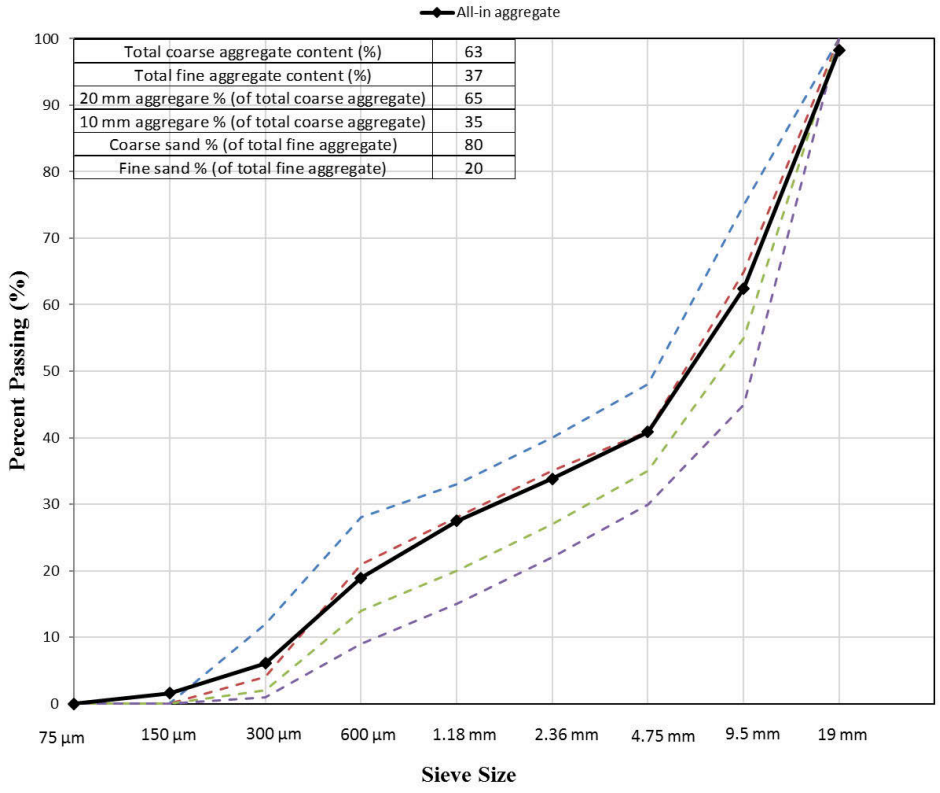


**Figure 7-10: Combined aggregate grading for C50-C0, C50-CFA25, C50-RFA25, C50-SL50 and C50-MK15 mixes according to Road Note No.4**

### 7.4.1 Plastic concrete properties

Plastic properties of concrete for bridge mixes are presented in Table 7-10. It can be seen that the required slump and air content were achieved according to the B80 specification [112]. Both CFA and RFA mixes have lower w/b ratio compared to the control mix despite designing for similar 28-day compressive strength. The reason for the reduction in w/b ratio is using higher binder content in fly ash mixes compared to the control mix to get similar strength to the control mix. The spherical shape of CFA and RFA particles also contributed to improving the rheology of the concrete [159]. It should be mentioned that the wet density of concrete mixes with only cement as a binder is more than the concrete mixes

containing SCMs, which is due to differences in specific gravity between SCMs and cement.

**Table 7-10: Plastic property results for bridge concrete mixes**

| Mixes | Slump (mm) | Air content (%) | Density (kg/m$^3$) |
|---|---|---|---|
| C50-C0 | 175 | 1.7 | 2495 |
| C50-CFA25 | 180 | 1.2 | 2455 |
| C50-RFA25 | 175 | 1.3 | 2445 |
| C50-SL50 | 180 | 1.5 | 2460 |
| C50-MK15 | 170 | 1.6 | 2450 |

### 7.4.2 Hardened concrete properties

According to RMS B80 specification [112], compressive strength and drying shrinkage are the main hardened concrete properties that should be controlled and achieved as shown in Table 7-9. In this research, all bridge mixes were designed to achieve a similar 28-day compressive strength with varying total binder content and varying w/b. The results are discussed in the following paragraphs.

#### 7.4.2.1 Compressive Strength

The relative strength and compressive strength developments of the concrete mixes are shown in Figures 7-11 and 7-12. Relative strength is the ratio of the strength of each concrete mix at each particular curing time to the 28-day strength of the same mix in percentage. It is noted that there is a reduction in early age strength for the concrete mixes containing CFA or RFA compared to control mix shown in Figure 7-11. This reduction in early age strength is due to reduced

reactivity of both fly ashes in early age because of pozzolanic properties compared to cement as confirmed by strength activity index results shown in Figure 6-5. It is also in agreement with the findings from SEM and XRD tests on the blended paste containing CFA or RFA reported in Chapter 5, which showed slow pozzolanic reactivity of CFA and RFA in early age. In later age at 56 days, the bridge concrete mix with 25% CFA achieved an almost similar compressive strength to the control mix while it did not happen for the RFA concrete mix despite using similar mix design.

The reduction in compressive strength of concrete mix with RFA compared to the similar concrete mix containing CFA shown in Figure 7-12 may be due to two main reasons: (i) larger particle size and lower specific surface area of RFA according to PSA and Blaine fineness test results, compared to CFA shown in Figure 4-1 and Table 4-1 respectively; (ii) less reactivity of RFA according to XRD and SAI test results shown in Figures 4-5 and 6-5, respectively. These findings are in line with SEM results on the blended pastes, which exhibited fewer hydration products on the RFA particle surfaces, especially at 28 days compared to CFA particle surfaces due to less reactivity. Lee et al. [170] reported higher glass content and more pozzolanic reactivity of the finer fly ash compared to the coarser one from the same batch.

From Figure 7-11, the considerable reduction in relative strength in early age for the mix containing 50% SL is noted likely due to high replacement level as well as the slow-developing reactivity of SL according to SAI results as confirmed by Barnett et al. [61]. The effect of replacing cement with 15% MK at early age strength of concrete mix was not significant due to the high specific

surface area of MK as well as lower replacement level. The reason for the reduction in 56-day compressive strength of the concrete mixes with SL or MK content compared to control mix as shown in Figure 7-12 could be due to the higher w/b ratio of SL and MK mixes, which were 0.39 and 0.40 respectively in comparison to the control mix of 0.37. The detail results of compressive strength of bridge mixes in various ages can be found in Appendix B.

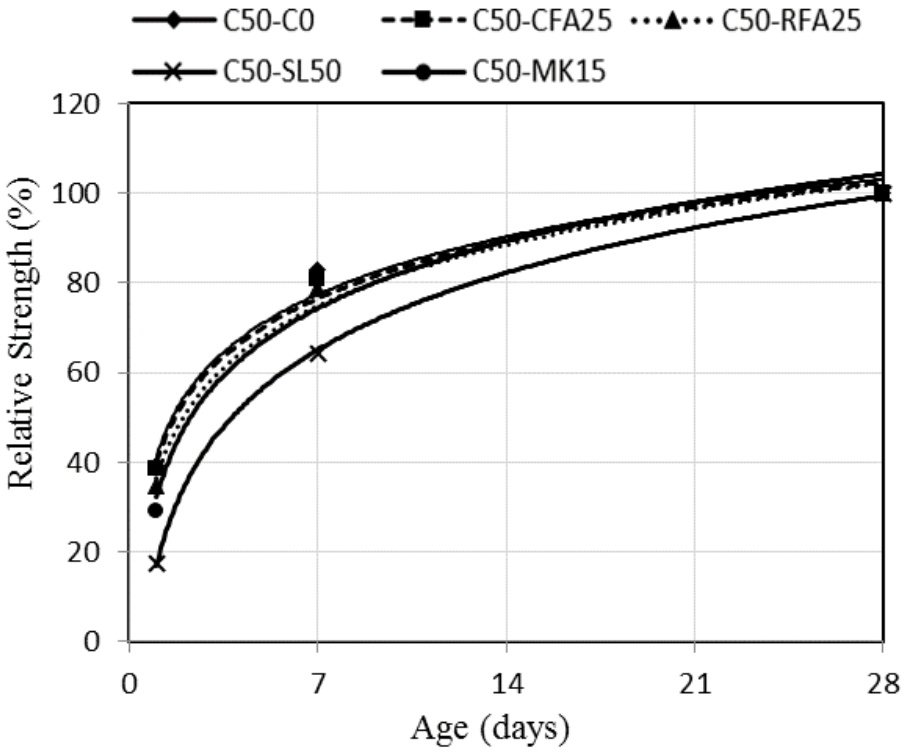


**Figure 7-11: Relative strength in bridge concrete mixes**

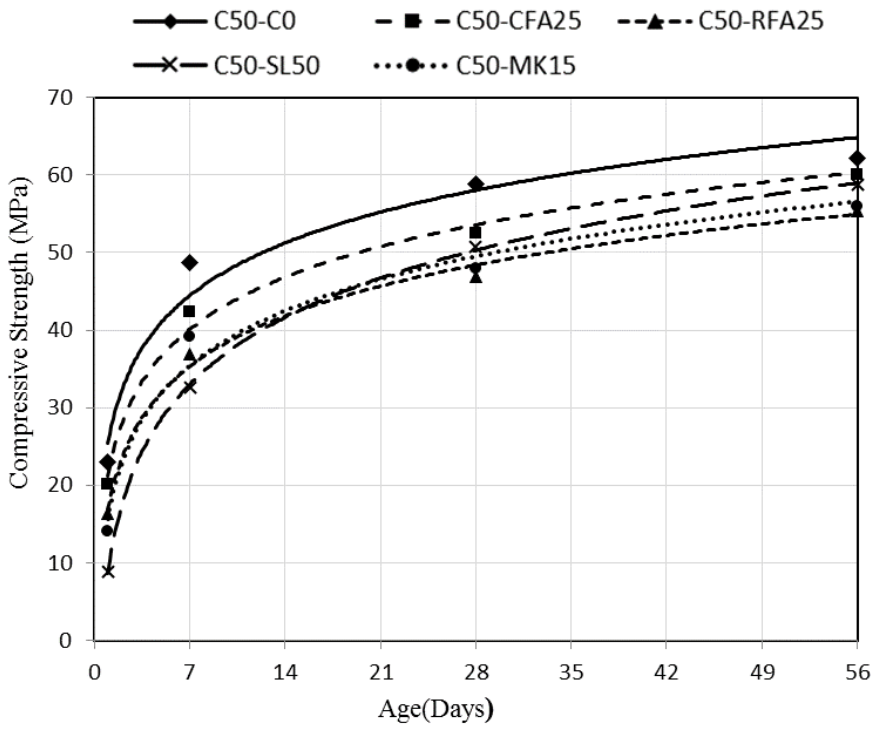


**Figure 7-12: Compressive strength development in bridge concrete mixes**

### 7.4.2.2 **Drying shrinkage**

Drying shrinkage results up to 56 days for bridge concrete mixes are shown in Figure 7-13. Drying shrinkage of bridge concrete mix containing 25% CFA was found to be slightly lower than the control mix due to the lower w/b ratio. The reason for the reduction in w/b ratio of the mix containing fly ash compared to the control mix is due to the higher binder content used in a mix with fly ash content to get the same 28-day strength to control mix. In addition, the reduction of the amount of cement paste in unit volume of the concrete mix by partially replacing cement with fly ash could be another reason to reduce the drying shrinkage of fly ash concrete compared to control concrete as reported by Atis [171].

On the contrary, 21-day drying shrinkage of concrete mix with 25% RFA was slightly higher than the mix containing 25% CFA, possibly due to using a higher

dosage of HWR to get similar slump with CFA mix. It reduces the surface tension of water and causes larger shrinkage strains in cement paste as reported by Brooks et al. [172].

Drying shrinkage of concrete mixes containing SL or MK was higher than in the control mix, which is possibly due to higher w/b ratios of 0.39 and 0.40 respectively, compared to the w/b of 0.37 for the control mix. Therefore, increasing drying shrinkage could be attributed to the increased rate of water loss from hardened paste in concrete mixes with SL or MK.

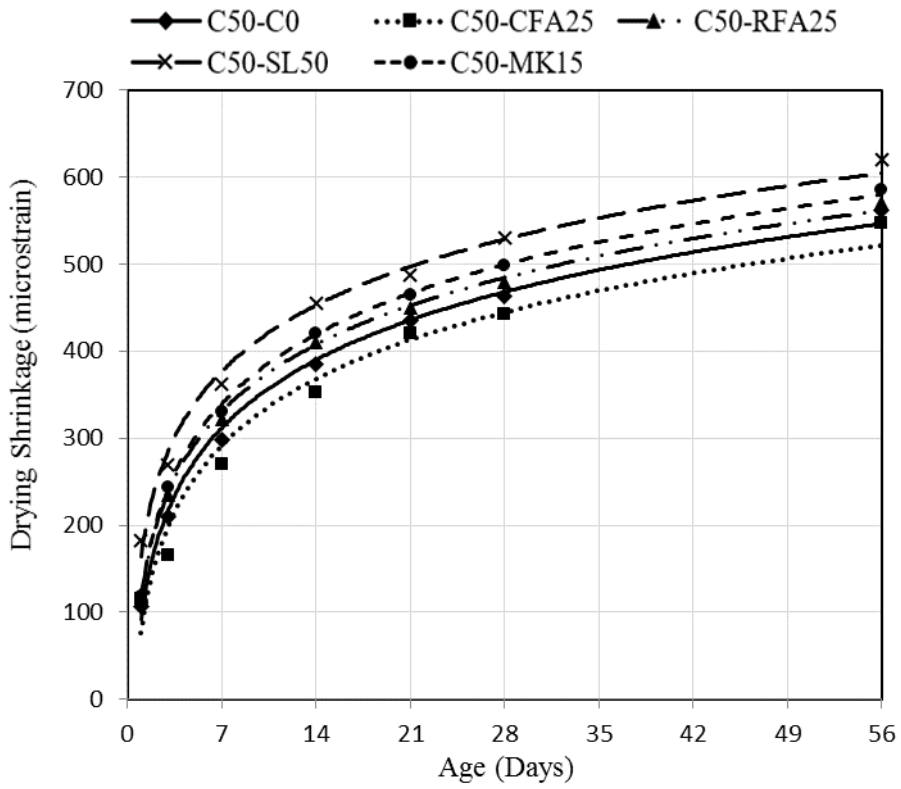


**Figure 7-13: Drying shrinkage in bridge concrete mixes**

### 7.4.3 **Durability properties**

The long-term durability of reinforced and prestressed concrete structures is threatened by the ingress of various aggressive liquid or gaseous agents. It is widely accepted that the availability and transport of water through the permeable voids (interconnected voids) of the pore structure of concrete is one of the main reasons which influence or promote all deterioration mechanisms in concrete. Water provides the medium by which many aggressive agents (i.e., chlorides, sulfates etc.) are transported into concrete. Therefore, restricting the movement of moisture in concrete can possibly control deterioration processes such as corrosion of the steel reinforcement, chloride ingress, alkali-aggregate reactions and sulfate and chemical attack [74].

According to RMS B80 specification [112], ASR and chloride resistance are the main durability properties that should be controlled and achieved. However, the ASR was not an issue for the bridge concrete mixes in this research because of the use of non-reactive aggregate. Regarding the chloride and sulfate resistance of the concrete mixes, only relative performance determined rather than properties specified in the RMS B80 specification due to time constraints and a shortage of the required equipment. The effect of varying levels of SCMs (CFA, RFA, SL and MK) on the expansion of mortar bars using a reactive Dacite aggregate was investigated due to the ASR according to AS1141.60.1 [109]. The results of the mentioned study have been discussed in the following paragraphs.

#### 7.4.3.1 **Chloride resistance**

The main effect of chloride ingress through the pore structure of the concrete is the corrosion of steel reinforcement, and thus damage to the surrounding concrete as a result of this corrosion. The AVPV test method in accordance with AS 1012.21 [73] was used to measure the interconnected void space within the concrete that can absorb water following normal immersion and subsequent boiling as a result of capillary suction. From Figure 7-14, it is noted that the water absorption percentage and apparent volume permeability voids in bridge concrete mixes with SCM content are higher than control concrete due to two main reasons. Firstly, the higher w/b ratio of the concrete mixes containing SL or MK compared to the control mix increases the capillary pores in hardened concrete and thus leads to the higher water absorption and volume of permeable voids in concrete specimens. Secondly, this can also be due to the fact that the pozzolanic effect has not had enough time to proceed because the mentioned tests were initiated after only 28 days of hydration. It is more obvious especially in the case of fly ash and metakaolin with more pozzolanic activity compared to slag which has both hydraulic and pozzolanic activities. It is in agreement with the findings of Courard et al. [174].

However, the effect of partially replacing cement with SCMs is to significantly reduce the volume of macropores and increase the volume of mesopores as reported by Johari et al. [175]. This could be due to the pozzolanic reaction (secondary C-S-H gel), which refines the pore structure by changing the coarser pores into finer ones. This change in pore sizes has a significant influence on the chloride and sulfate resistance of the hardened concrete.

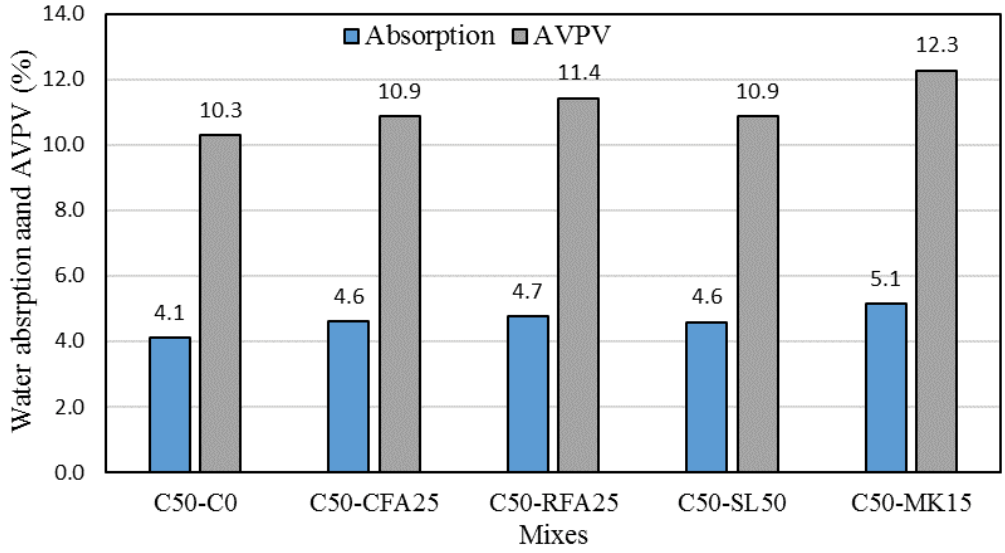


**Figure 7-14: Water absorption and AVPV percentage at 28 days according to AS 1012.21**

Figure 7-15 and Table 7-11 show the results of the electrical charge passing from bridge concrete mixes at 28 days using the Rapid Chloride Permeability Test RCPT in accordance with ASTM C1202 [75]. Qualitative indications of the chloride ion penetrability based on the measured values from this test method are provided in Table 7-12.

**Table 7-11: Charge passed for individual specimens measured at 28 days in various concrete mixes using RCPT test**

| Rapid Chloride Permeability Results (28 days) | | | | |
|---|---|---|---|---|
| Mixes | Charge Passed (Coulomb) | | | |
| | Sample 1 | Sample 2 | Sample 3 | Average |
| C50-C0 | 2230 | 2168 | 2082 | 2160 |
| C50-CFA25 | 1501 | 1676 | 1612 | 1596 |
| C50-RFA25 | 1764 | 1845 | 1798 | 1802 |
| C50-SL50 | 822 | 784 | 754 | 787 |
| C50-MK15 | 603 | 640 | 632 | 625 |

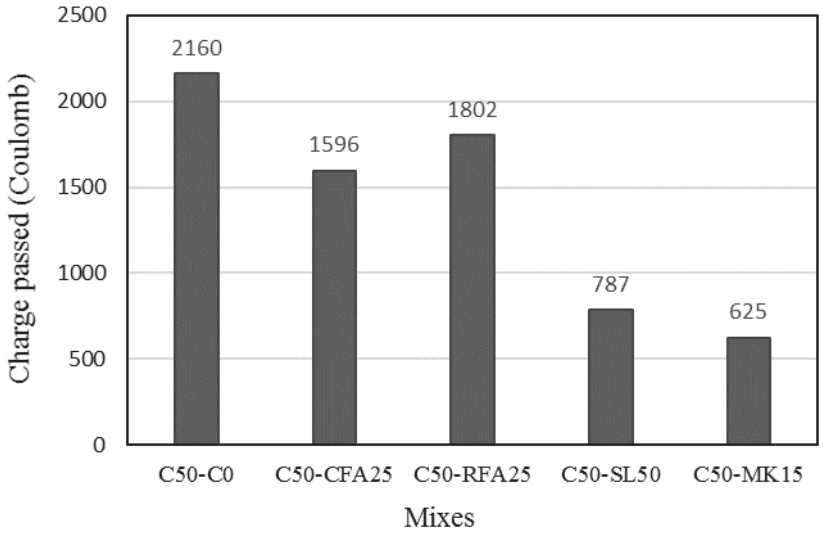


**Figure 7-15: Charge passed measured at 28 days in various concrete mixes using RCPT test**

According to Table 7-12, a charge passing from control concrete (C50-C) showed moderate chloride ion penetrability from concrete at 28 days while by replacing cement with 25% CFA or RFA, the penetrability by chloride ions

decreased to a low level, which was a charge passing between 1000-2000 coulombs. This could be due to the pozzolanic reaction of fly ash, which is able to decrease the penetrability of chloride ions by developing a discontinuous pore system since chloride ions usually penetrate into concrete by diffusion along the water paths or open pores as reported by Dinakar et al. [72]. It is evident that CFA decreased the penetrability of chloride ions into the concrete specimens by about 13% more compared to RFA due to its finer particle size and hence more reactivity which produces a denser microstructure. This is in agreement with the XRD and SEM results on blended pastes containing CFA or RFA reported in Chapter 5. It indicated that a significant number of finer fly ash particles have reacted and converted to C-S-H with more fibrous sheets evident at 28 days compared to the coarser fly ash particles as shown in Figures 5-12 and 5-15.

**Table 7-12: Chloride ion penetrability based on charge passes according to ASTM C1202**

| Charge Passed (Coulombs) | Chloride Ion Penetrability |
|---|---|
| >4000 | High |
| 2000-4000 | Moderate |
| 1000-2000 | Low |
| 100-1000 | Very Low |
| <100 | Negligible |

From Figure 7-15, the level of penetrability of chloride ions in charge passing the concrete mixes decreases to a very low level by replacing cement by SL and MK in C50-SL50 and C50-MK15 mixes. This could be possibly due to the hydraulic and pozzolanic nature of SL, generating reaction products (CSH) in early ages that refine the capillary pores as reported by Arya et al. [71] and was confirmed by Aponte et al. [176].

In concrete mixes containing MK, as Dhir & Jones [177] reported, MK with the high specific surface area is able to produce a dense microstructure and consequently enhanced resistance to chloride ingress. Kim et al. [24] also claimed that the resistance of the concrete consisting of MK to chloride attack increases due to continued hydration, accompanied by a decrease in porosity and pore size because of large Blaine values and more reactivity of MK.

#### 7.4.3.2 **Sulfate resistance**

The resistance of concrete to sulfate attack in aggressive environments is of vital importance to the performance of important infrastructure. This study was carried out to investigate the importance of permeability in governing the sulfate resistance of concretes. The resistance of concrete to sulfate ion penetration into the bridge concrete mixes was measured using the rapid sulfate permeability test developed by Sirivivatnanon and Lucas [90] as mentioned in the literature review Chapter. This test method only gauged the physical resistance of the concrete to sulfate attack while chemical resistance to sulfate attack should be measured by the expansion test of the binder. They proposed that using blended cement and rapid sulfate permeability $\leq 2000$ coulombs produce sulfate resisting concrete. Hooton [178] also reported that the chemical resistance of the concrete to sulfate

attack increases by partially replacing cement with SCMs. It is mainly due to the reduction of tricalcium aluminate hydrate and calcium hydroxide content in the mix, which limits the formation of ettringite and gypsum and thus increases the chemical resistance of concrete to sulfate attack.

In this study, it assumes that concrete mixes containing SCMs are chemically resistant to sulfate attack because of the use of the blended cement. Therefore, only the physical resistance to sulfate attack was evaluated using rapid sulfate permeability test. Table 7-13 and Figure 7-16 show the results of the electrical charge passing from bridge concrete mixes at 28 days using the rapid sulfate permeability test. It is noted that current passing in all concrete mixes is less than 2000 coulombs, which confirms all mixes are resistant to sulfate ion penetration according to the findings of Sirivivatnanon and Lucas [90].

It indicated that replacing cement with 25% CFA and RFA in bridge concrete mixes increased resistance of the concrete to penetration by sulfate ions at 28 days at about 9 and 1 percent respectively, compared to the control concrete. While replacing cement with 50% SL or 15% MK in bridge concrete mixes had a significant influence on decreasing the sulfate ion penetration into the concrete at about 58 and 62 percent respectively, compared to control concrete. Increasing the physical resistance of concrete to sulfate attack by proportional replacement of Portland cement with SCMs is possibly due to pore structure refinement as secondary C-S-H gel refines the capillary pores and decreases the permeability of concrete as reported by Khatib and Wild [179]. In addition, the finer particle size of SL and MK compared to the particle size of CFA and RFA should be another

reason which decreases the permeability of concrete significantly in these mixes as reported by Al-Akhras [95].

**Table 7-13: Charge passed for individual specimens measured at 28 days using rapid sulfate permeability test**

| Rapid Sulphate Permeability Results (28 days) | | | | |
|---|---|---|---|---|
| Mixes | Charge Passed (Coulomb) | | | |
| | Sample 1 | Sample 2 | Sample 3 | Average |
| C50-C0 | 1516 | 1394 | 1368 | 1426 |
| C50-CFA25 | 1315 | 1335 | 1283 | 1311 |
| C50-RFA25 | 1442 | 1368 | 1401 | 1404 |
| C50-SL50 | 584 | 616 | 603 | 601 |
| C50-MK15 | 531 | 566 | 557 | 551 |

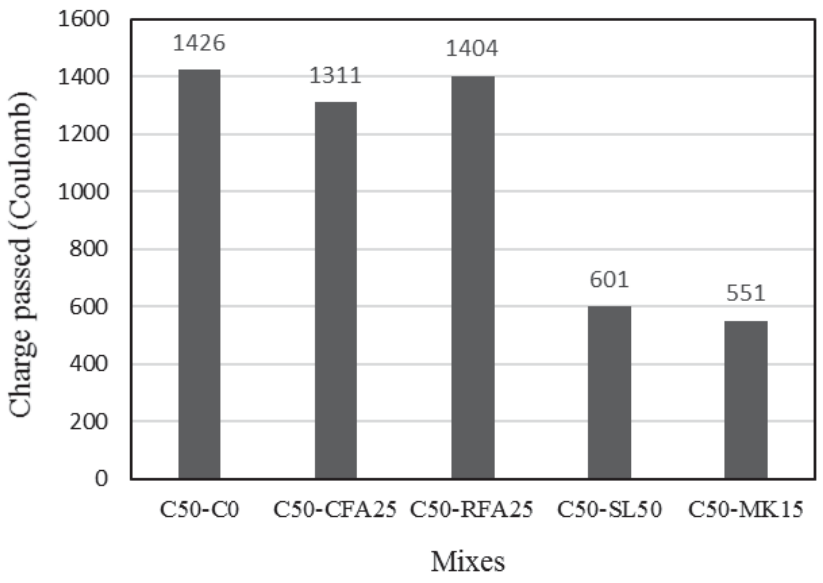


**Figure 7-16: Rapid sulfate permeability of various concrete mixes at 28 days**

#### 7.4.3.3 **Alkali-silica reactivity**

Mortar mixes using a reactive Dacite aggregate with 10%, 15% and 25% cement replacement with CFA and RFA, 30%, 40% and 50% SL and 7%, 10%, 15% MK were cast with w/b ratio of 0.47 for the AMBT test according to Australian standard AS 1141.60.1 [109]. The effect of varying levels of CFA and RFA on the expansion of mortar bars due to the ASR according to AS1141.60.1 [109] are shown in Figures 7-17 and 7-18 respectively.

The detailed calculation of the amount of alkali, available alkali and Ca/Si ratio of SCMs by use of Tables 4-4 and 4-5 are presented in Table 7-14. It is noted that the critical expansion limits proposed within AS1141.60.1 are less than 0.1 at 21 days to classify as a non-reactive aggregate or less than 0.1 at 10 days and less than 0.3 at 21 days to classify as a slowly reactive aggregate. It indicates that as the level of CFA and RFA used to partially replace Portland cement increases, the expansion of mortar bars due to ASR decreases.

Replacing cement with 10% and 15% of CFA and RFA was not effective in reducing the expansion to less than 0.1 after 21 days. However, 15% CFA replacement level kept the expansion at less than 0.3 after 21 days. On the contrary, replacing cement with 25% CFA or RFA was effective in decreasing the expansion percentage to less than 0.1 after 21 days. CFA used (25%) achieved a reduction in the expansion of 97.4% at the age of 10 days and 96.5% at the age of 21 days relative to the control mix. While the reduction in the expansion by replacing cement with 25% RFA was by about 95.9% after 10 days and 95.1% after 21 days. The reason for mitigating the expansion by replacing cement with CFA and RFA is due to the reduction in alkalinity of pore solution by the

pozzolanic reaction and thus minimising the reaction of alkalis with reactive silica in the aggregate, which facilitates ASR as reported by Barger et al. [88]. It should be mentioned that CFA was slightly more effective than RFA in reducing the expansion of mortar bars. It can be explained by the less available alkali in CFA compared to RFA as shown in Table 7-14. It is in agreement with the findings of Thomas [99]. In addition, greater fineness and the smaller particle size of CFA compared to RFA as shown in Table 4-1 and Figure 4-1 respectively, cause CFA particles to consume more hydroxide ions and reduce the alkalinity of the pore solution. Bhatty and Greening [180] found the reduction in the pore solution alkalinity with replacement cement with fly ash is linked to the effect of fly ash on the composition and alkali-binding capacity of the hydrates (especially C–S–H).

Therefore, C–S–H with a low Ca/Si ratio was able to retain more alkali (Na + K) compared to hydrates of higher Ca/Si ratios. Similar results were observed by other researchers [99, 102]. This is possibly another reason for reduced expansion of mixes containing CFA compared to the RFA mixes.

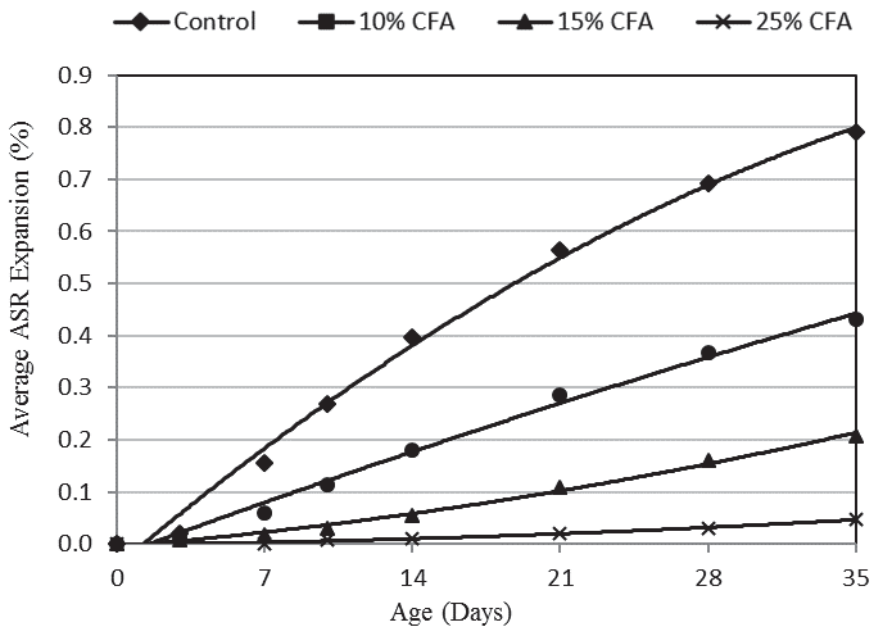


**Figure 7-17: Effect of CFA levels on average ASR expansion of mortar bars**

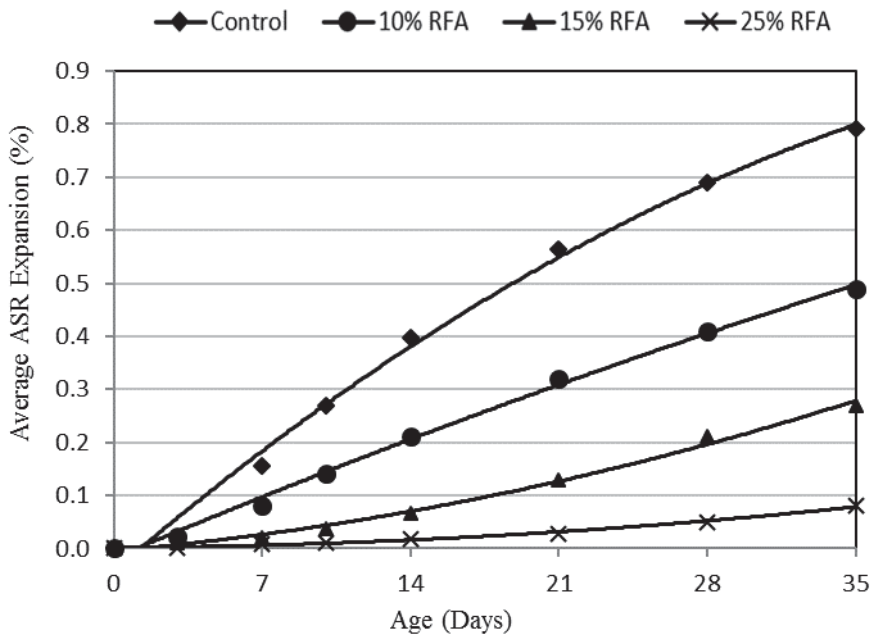


**Figure 7-18: Effect of RFA levels on average ASR expansion of mortar bars**

The effects of 30%, 40% and 50% cement replacement with SL on mitigating ASR in mortar bars are shown in Figure 7-19. It demonstrates that increasing the SL content was effective in decreasing the expansion at different ages. However, only mortar containing 50% SL rendered the aggregate as non-reactive at the critical age of 21 days by having an expansion of less than 0.1%, in line with AS1141.60.1[109]. The reason for this reduction is possibly due to the effect of SL in reducing the alkalinity of concrete, the mobility of alkalis and the free lime in concrete and improving the permeability resistance of concretes. However, its influence depends on the nature of the SL, the aggregate reactivity and the Portland cement alkali content [100]. From Table 7-14, it can be seen that Ca/Si ratio of SL is higher than the other SCMs which possibly is the reason for the need for higher replacement levels to control the expansion due to ASR as confirmed by other researchers [180, 181]

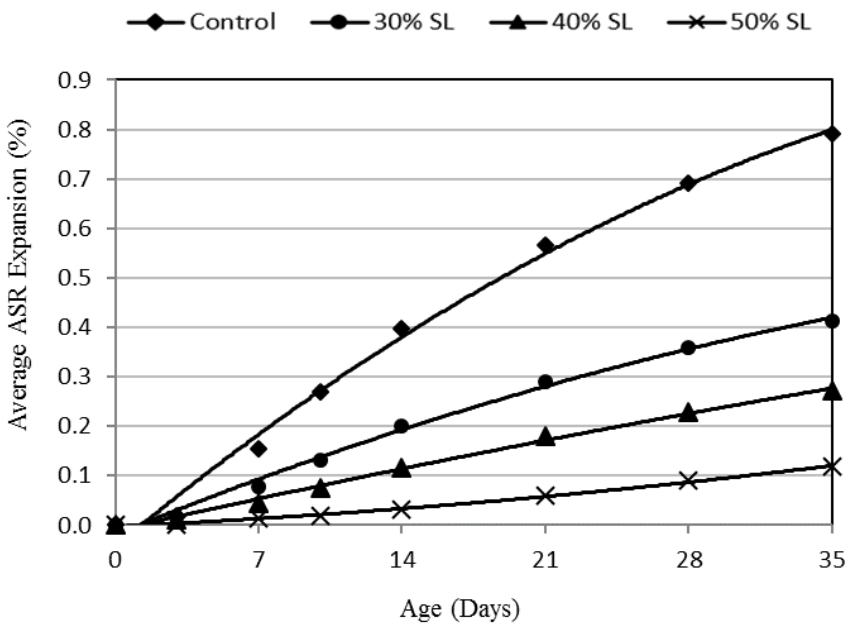


**Figure 7-19: Effect of slag levels on average ASR expansion of mortar bars**

From Figure 7-20, it can be seen that as the level of MK used to partially replace Portland cement increased, the expansion of mortar bars due to ASR decreased. However, only 15% MK proportion was effective in mitigating ASR expansion at the critical age of 21 days to less than 0.1% according to AS 1141.60.1 [109]. This is possibly due to the consumption of portlandite contained within the pore solution of the paste by the secondary C-S-H gel. In doing so, MK directly consumes alkalis, removing them from the pore solution of the cement paste, thus minimizing the quantity of available alkali which is able to react with reactive silica in the aggregates [99, 108]. From Table 7-14, it can be noted that MK has the least amount of available alkali as well as Ca/ Si ratio, which make it very effective in reducing the alkalinity of pore solution and thus decreasing the expansion due to ASR especially in higher levels as confirmed by other researchers [180, 181]. The detailed expansion results of all mortar mixes can be found in Appendix B.

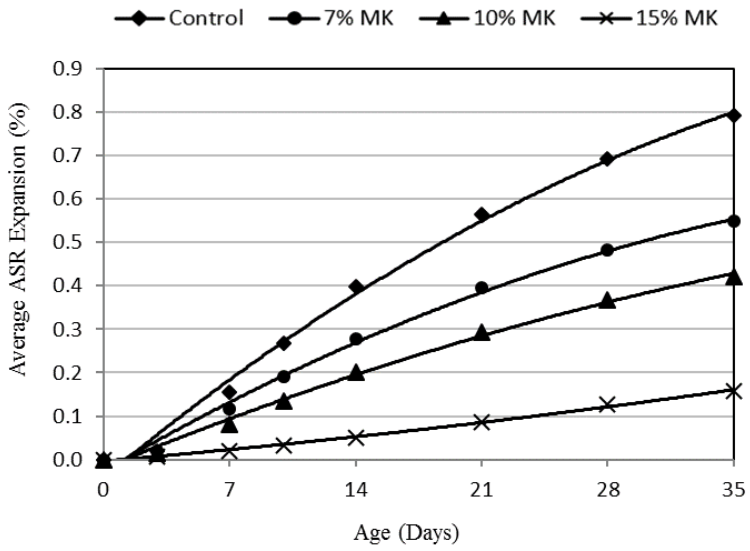


**Figure 7-20: Effect of metakaolin levels on average ASR expansion of mortar bars**

**Table 7-14: Alkali, available alkali and Ca/Si ratio of SCMs**

| Oxide | SCMs | | | |
|---|---|---|---|---|
| | CFA | RFA | SL | MK |
| $Na_2O$ (%) | 0.63 | 0.62 | 0.35 | 0.22 |
| $K_2O$ (%) | 1.18 | 1.24 | 0.26 | 0.28 |
| $Na_2Oe$ (%) | 1.41 | 1.44 | 0.52 | 0.40 |
| Available $Na_2O$ (%) | 0.11 | 0.12 | 0.06 | 0.04 |
| Available $K_2O$ (%) | 0.19 | 0.23 | 0.05 | 0.03 |
| Available $Na_2Oe$ (%) | 0.24 | 0.27 | 0.09 | 0.06 |
| Cao (%) | 2.48 | 3.00 | 41.59 | 0.07 |
| $Sio_2$ (%) | 59.21 | 60.06 | 34.12 | 62.50 |
| Ca/Si | 0.042 | 0.050 | 1.219 | 0.001 |

### 7.4.4 Possible use of RFA or SL or MK replacing CFA in bridge concrete mix

The possible use of 25% RFA, 50% SL and 15% MK as an alternative to CFA on 50 MPa bridge concrete mixes was evaluated according to the specified requirements of RMS B80 specification [112]. The main hardened and durability properties for the bridge concrete mixes that should be controlled and achieved according to the RMS B80 specification [112] are compressive strength, drying shrinkage, chloride resistance and alkali-silica reactivity. The results indicated that none of the mixes with SCM content reached the desired target strength of 57 MPa at 28 days. However, according to the characterisation of the raw materials reported in Chapter 4, the effect of partially replacing cement with SCMs in mortars with fixed w/b ratio reported in Chapter 6 and the strength

development results up to 56 days for the bridge concrete mixes, it can be concluded that by only adjusting the mix design, is the required strength for all mixes with SCM content for this category of concrete achievable.

The reduction of about 10% at the 28-day compressive strength of the RFA concrete mix was noted and compared to the similar concrete mix with CFA. The reduction in 28-day compressive strength is in line with the findings of the mortar work presented in Chapter 6, which indicated a similar strength reduction trend by replacing cement with 20% or 30% RFA compared to the same mortar mix containing 20% or 30% CFA. The mortar results showed that the 28-day compressive strength of the mix with 20% RFA was almost the same as that of the mix containing 30% CFA. The reduction in the strength of RFA mix is due to the reduced reactivity of RFA particles compared to CFA particles. It was confirmed by XRD results reported in Chapter 4 which showed higher crystallinity of RFA particles compared to CFA ones.

The 21-day drying shrinkage of the bridge concrete mix with 25% RFA was slightly higher than the same mix with CFA content. The mortar results presented in Chapter 6 indicated that increasing the cement replacement level with RFA in the mix was effective in the reduction of the drying shrinkage. However, the increase in the RFA content in the mortar mixes decreased the compressive strength as well.

Therefore, in order for the concrete mix with RFA to be able to achieve the same strength property as the same mix containing CFA, it is necessary to modify the mix design based on the analytical and experimental outcomes. For instance, for the concrete mixes with 25% CFA and RFA, reducing the w/b ratio of the

RFA concrete mix to 0.33 instead of using w/b ratio of 0.35 similar to the CFA concrete mix to compensate for the strength difference is recommended. However, it causes an increase in the cement and RFA content by about 8% for the concrete mix with 25% RFA compared to the mix with 25% CFA. In addition, decreasing the w/b ratio of the RFA concrete mix from 0.35 to 0.33 will probably decrease the 21-day drying shrinkage close to the CFA mix as well. The acceptability of the mixes for chloride and sulfate resistance was not investigated according to the test methods specified in RMS B80 specification [112]. However, according to the qualitative tests performed on the concrete mixes containing RFA or CFA, the reduction in the chloride and sulfate ions' penetration into the concrete was noted compared to the control concrete as mentioned in section 7.4.3.

It was noted that partially replacing cement with 50% SL or 15% MK in bridge concrete mixes was not able to reach the designed target strength at 28 days, which is mainly due to high w/b ratio used compared to the control mix. The findings from mortar mixes with a fixed w/b ratio reported in Chapter 6 revealed that the 28-day compressive strength of mortar mixes with 5%, 10% and 15% MK or 35%, 50% and 65% SL were higher than in the control mix. It was also confirmed by strength activity index results showing more reactivity of mortar mix with 10% MK and 50% SL compared to the control mix at 28 days. In addition, the drying shrinkage results up to 56 days for the mentioned mortar mixes containing SL or MK, indicated a significant reduction in drying shrinkage in all ages compared to the control mix with the fixed w/b ratio. Considering the aforementioned information and also the significant performance of concrete with

SL or MK in reducing the penetration of chloride and sulfate ions into the concrete, it is concluded that only by considering a w/b ratio of SL or MK mix similar to the control mix, will the required strength and drying shrinkage be achieved.

Finally, it is concluded that RFA could possibly be used as an alternative SCM to CFA in bridge concrete mixes investigated in this study by considering w/b ratio of 0.33 for RFA concrete instaed of 0.35 similar to CFA concrete and then modifying the mix design accordingly. Partially replacing cement with MK or SL could also be another alternative to CFA, especially because of their significant influence in improving the durability properties of the bridge concrete mixes. However, durability properties of the bridge concrete mixes were not investigated according to the test methods specified in RMS B80 specification [112], and only the relative performance of the mixes was controlled.

## 7.5 Summary

Based on the results of this study, the following conclusions can be drawn.

1. It was found that RFA is almost as effective as CFA in the lean concrete mixes according to the specified requirements of the R82 specification.
2. The results revealed that partially replacing cement with 60% RFA in the lean concrete mix complied with the specified requirements of RMS R82 specification. However, the 28-day compressive strength of the RFA mix was 9% lower compared to a similar mix with CFA.
3. The results demonstrated that the 28-day compressive strength of lean, pavement and bridge concrete mixes containing RFA were about 9%, 11% and 11% lower respectively, compared to similar concrete mixes with CFA. This reduction in strength is due to the larger particle size and reduced reactivity of RFA particles compared to CFA ones.
4. Incorporation of RFA in pavement concrete mix decreased the 28-day flexural strength by about 11% compared to similar concrete mix with CFA.
5. RFA could be used in pavement applications by modifying the concrete mix design and considering lower w/b ratio for mixes with RFA than the similar mix with CFA.
6. The results of replacing cement with 50% SL in pavement mixes showed that SL could be a suitable alternative to CFA for the use of the pavement application.

7. The hardened and durability results of the bridge concrete mixes containing RFA, SL and MK revealed that these SCMs can be used as an alternative to CFA. However, more testing needs to be done regarding durability properties of the bridge mixes especially for the mixes containing RFA as only the relative performance of the mixes was assessed.
8. Binder containing 25% CFA or RFA decreased the level of penetrability of chloride ions into the concrete by 27% and 17% respectively, compared to the control mix at 28 days. In addition, incorporating CFA and RFA in bridge concrete mixes reduced sulfate ion penetration into the concrete by about 9% and 1% respectively compared to the control mix. The penetration of chloride and sulfate ions into the concrete decreased significantly at 28 days by incorporating 50% SL and 15% MK in the mixes.
9. The substitution of cement by fly ash, slag and metakaolin at any replacement level decreased the expansion of mortar bars due to ASR. The results revealed increasing the levels of CFA and RFA from 10% to 25%, SL from 30% to 50% and MK from 7% to 15% used to partially replace Portland cement decreased the expansion of mortar bars significantly due to ASR. For the Dacite aggregate, 25% CFA and RFA or 50% SL or 15% MK are required to mitigate the ASR based on AS1141.60.1 [109].

# Chapter 8

## Conclusions and Recommendations

# 8 CONCLUSIONS AND RECOMMENDATIONS

## 8.1 Conclusions

The characterisation of SCMs, microstructural analysis and experimental studies conducted on the blended cement pastes, mortars and a range of concrete mixes containing various SCMs with different fineness and levels have led to the following conclusions:

1. The increased fineness of fly ash improved the flow of the blended paste and mortar mixes compared to the control mixes possibly due to the spherical shape of the particles and also due to the presence of a higher number of fly ash particles per mass unit, which increases the lubricant effect in the mix. However, the effect of the fineness of fly ash on the workability of concrete mixes was not directly investigated as each category of concrete mixes was designed to achieve the same slump.
2. Replacing cement with 60%, 20% and 25% RFA in the lean, pavement and bridge concrete mixes, respectively resulted in a 9%, 11% and 11% reduction in 28-day compressive strength compared to the same mixes containing CFA. It was noted that the effect of RFA in gaining strength in all ages (up to 56 days) in a range of concrete mixes was lower compared to concrete mixes with CFA, despite having similar mix design. Gaining higher compressive strength for the concrete mixes containing CFA in all categories investigated than the same mixes with RFA could be due to the following reasons:
    - The finer particle size, higher specific surface area and more amorphicity of finer fly ash (CFA) are the dominant factors, which

increases the reactivity of CFA particles and thus creates more pozzolanic reactivity compared to coarser fly ash (RFA).

- Increasing the hydration products on the surface of fly ash particles with a smaller particle size (CFA) especially at 28 days indicated higher reactivity of CFA particles compared to the RFA particles.
- Increasing the fineness of fly ash caused a higher consumption of portlandite, a by-product of cement hydration at all ages especially at 28 days due to the higher surface area as well as more amorphous content of finer fly ash compared to the coarser fly ash. More consumption of portlandite by finer fly ash led to more hydration products in the system and thus a denser microstructure compared to the mix with coarser fly ash.
- Partially replacing cement with fly ash, of different fineness, decreased the cumulative heat evolution compared to the control mix. However, the finer fly ash generated more heat of hydration compared to coarser fly ash suggesting its higher reactivity.

3. Partially replacing cement with RFA in all categories of concrete investigated was not as effective as CFA in reducing 21-day drying shrinkage. This finding is in line with the results of the mortar work conducted in this study with various dosages of CFA and RFA at the fixed w/b ratio, which showed better performance of CFA in decreasing the drying shrinkage at all ages (up to 56 days) compared to RFA. The greater reactivity, in addition to the higher specific surface area of finer fly ash causes greater consumption of free water in the pore solution and thus less

drying shrinkage compared to the coarser fly ash. The 21-day drying shrinkage for the concrete mixes containing SL and MK was higher than the control mix mainly due to the higher w/b ratio used compared to the control mix. Conversely, mortar mixes containing SL and MK with the fixed w/b ratio resulted in reduced drying shrinkage compared to the control mix. The effectiveness of SCMs in reducing the drying shrinkage could be due to two main factors. Firstly, the reduction in the cement paste by partially replacing cement with SCMs, as cement paste volume is a dominant feature in this phenomenon. Secondly, reduced water evaporation due to the consumption of a considerable amount of free water by pozzolanic reaction might be another reason for the reduction of drying shrinkage.

4. Mortar mixes containing 35%, 50% and 65% of SL and 5%, 10% and 15% of MK with the fixed w/b ratio showed higher 28-day compressive strength compared to control mix at all replacement levels. These findings were confirmed by the 28-day strength activity index results which showed better performance of SL and MK in gaining strength compared to PC at 28 days. However, the reduction in strength of bridge concrete mixes containing SL or MK was noted due to higher w/b ratio compared to the control mix. The effectiveness of partially replacing cement with SL or MK in improving the 28-day strength in mortar and concrete mixes could be due to the finer particle size, higher specific surface area and sufficient quantity of amorphicity of SL or MK compared to cement.

5. Level of penetration of chloride and sulfate ions into the bridge concrete mixes was decreased by partially replacing cement with 25% CFA or RFA compared to the control mix. However, the CFA was more effective in decreasing the penetration of aggressive ions into the concrete compared to RFA. The effectiveness of CFA could be due to the finer particle size and hence more reactivity compared to RFA particles which produce a denser microstructure as confirmed by SEM results on blended pastes. The effect of substituting cement with 50% SL and 15% MK in bridge concrete was significant in reducing the chloride and sulfate ions' penetration. This is mainly due to sufficient quantity of amorphicity, finer particle size and higher specific surface area of SL and MK compared to PC particles, which possibly refines the capillary pores and thus prevents penetration of aggressive ions.
6. Partially replacing cement with SCMs decreased the expansion of mortar bars due to ASR; the reduction in expansion increased with an increase in SCM content. For the reactive aggregate investigated in this study, 25% CFA and RFA or 50% SL or 15% MK were required to mitigate the ASR based on AS1141.60.1 [109]. The effectiveness of SCMs in reducing the expansion due to ASR could be due to two main reasons. Firstly, less available alkali, as well as a lower Ca/Si ratio in SCMs compared to cement, reduces the alkalinity of the pore solution and thus decreases the expansion. Secondly, consumption of portlandite by SCMs due to the formation of the secondary C-S-H gel reduces the alkalinity of pore

solution and minimises the quantity of the available alkali, which can react with reactive silica in the aggregate and thus mitigates the ASR.

This experimental investigation has demonstrated the value and benefits of using RFA as an alternative SCM in concrete. RFA has proven abilities to achieve the same level of performance as CFA when used in various concrete applications such as lean, pavement and bridge concrete mix designs. SL and MK could also be used as other alternatives to CFA in concrete.

## 8.2 **Recommendations**

Microstructural analysis and experimental results on the influence of RFA on plastic, mechanical and durability properties of a range of concrete applications demonstrated that RFA is not as effective as CFA especially in strength development in all concrete mixes used in this study. Based on the above conclusion, RFA, SL and MK might possibly be an alternative SCM to CFA in range of concrete applications. However, there is a need to modify the mix design for each category of concrete mixes containing RFA to get similar properties of the concrete mixes containing CFA as follows:

1) Based on results on mechanical properties of lean concrete mixes, concrete containing 60% RFA showed satisfactory performance with respect to strength and drying shrinkage. RFA might possibly be an alternative SCM to CFA in low strength concrete such as lean concrete mix despite not getting similar properties to lean concrete mix with CFA. Decreasing the w/b ratio from 0.60 to 0.56 for the lean

mix with RFA investigated in this study is recommended to get similar strength property to the mix containing CFA.

2) Where the compressive strength, flexural strength and drying shrinkage are of prime importance for pavement concrete, partially replacing cement with SL is recommended for pavement applications according to its satisfactory performance based on the mortar and concrete results. Regarding possible use of RFA in pavement concrete mix, the reduction in strength properties was noted compared to the concrete mix with CFA. For the RFA to be a possible alternative SCM to CFA in pavement mix, it is recommended to design the concrete mix containing RFA with a lower w/b ratio compared to the similar mix with CFA to achieve the same strength properties. For instance, for the pavement mix with 20% RFA investigated in this study, decreasing the w/b ratio from 0.38 to 0.35 will possibly compensate the strength difference of RFA mix to CFA mix.

3) According to the above conclusion, it is possible to partially replace cement with RFA in bridge applications by considering lower w/b ratios than the same mix with CFA. Substituting cement with SL or MK might be another alternative to CFA in bridge concrete especially because of their significant influence in improving durability properties of the concrete. However, the effect of mentioned SCMs in improving the durability properties of concrete needs to be investigated more as the only relative performance of the mixes was examined.

## 8.3 **Future work**

A number of future research areas, currently beyond the scope of this study, are suggested as follows:

- Investigation of a wide variety of run-of-station fly ash from various power plants all over Australia to assess the variation in production and its effect on different properties of concrete mixes.
- Evaluation of the long-term performance of concrete containing run-of-station fly ash regarding durability properties.
- Experimental investigation of the influence of fineness of fly ash on durability properties of concrete structures such as alkali-silica reactivity and chloride resistance.
- Case studies specifically investigating the effect of changes in the physical and chemical properties of fly ash from the same source over a long period of time on the various properties of concrete mixes.

# Appendix A

Concrete mix design process

Table A-1 to Table A-62 demonstrate the process of designing all the concrete mixes (lean, pavement and bridge).

The complete process of designing the lean concrete mix without cement replacement with SCMs (C12-C0) are presented in five steps as shown in Table A-1 to Table A-5 and the final mix design is demonstrated in Table A-6.

**Table A-1: Step 1 in designing the lean concrete mix (C12-C0)**

| Step | Item | Reference/Calculation | Value |
|---|---|---|---|
| 1 | Characteristic strength (fc) @ 28 days (MPa) | Specified | 12 |
| | Proportion defective (k) % | Table 3-7 | 1.64 |
| | Standard deviation (S) (MPa) | Figure 3-5 | 2.2 |
| | Percentage by volume of air entrained (a) | Specified | 5 |
| | Target mean strength (MPa) | Equation 3-2 | 22 |
| | Cement strength class | Specified | 42.5 |
| | Type of coarse aggregate | Specified | Crushed |
| | Free water/cement ratio | Table 3-8, Figure 3-6 | 0.84 |

**Table A-2: Step 2 in designing the lean concrete mix (C12-C0)**

| Step | Item | Reference/Calculation | Value |
|---|---|---|---|
| 2 | Slump (mm) | Specified | 40 |
| | Maximum aggregate size (mm) | Specified | 20 |
| | Coarse aggregate type | Specified | Crushed |
| | Fine aggregate type | Specified | Uncrushed |
| | Free water content (kg/m$^3$) | Table 3-9, Eq.3-4 | 170 |
| | SCM replacement (%) | Specified | 0 |
| | Reduction in water content because of SCMs (kg) | | 0 |
| | Type of admixture | Specified | WR |
| | Reduction of water content by admixture (%) | Specified | 7 |
| | Reduction in water content because of admixture (kg) | | 12 |
| | Final free water content (kg) | | 158 |

**Table A-3: Step 3 in designing the lean concrete mix (C12-C0)**

| Step | Item | Reference/Calculation | Value |
|---|---|---|---|
| 3 | Cement content (kg) | Equation 3-5 | 188 |
| | Maximum cement content (kg) | Specified | - |
| | Minimum cement content (kg) | Specified | - |
| | Final Cement content (kg) | | 188 |
| | SCM content | Equation 3-7 | |
| | Modified W/b ratio | | 0.84 |

**Table A-4: Step 4 in designing the lean concrete mix (C12-C0)**

| Step | Item | Reference/Calculation | Value |
|---|---|---|---|
| 4 | Percentage of fine aggregate passing 600 μm sieve | Specified | 50 |
| | Maximum aggregate size (mm) | Specified | 20 |
| | Slump zone (mm) | Specified | 10-30 |
| | Water to cement ratio | | 0.84 |
| | Proportion of fine aggregate (%) | Figure 3-7 | 38 |
| | Proportion of coarse aggregate (%) | | 62 |
| | 20 mm coarse aggregate content (%) | According to grading curve of Road Note No.4 (Figure 7-1) | 60 |
| | 10 mm coarse aggregate content (%) | | 40 |
| | Coarse sand content (%) | | 67 |
| | Fine sand content (%) | | 33 |

**Table A-5: Step 5 in designing the lean concrete mix (C12-C0)**

| Step | Item | Reference/Calculation | Value |
|---|---|---|---|
| 5 | Cement content (kg/m$^3$) | Step 3 | 188 |
| | SCM content (kg/m$^3$) | Step 3 | 0 |
| | Free water content (kg/m$^3$) | Step 2 | 158 |
| | Volume of cement (m$^3$) | | 0.061 |
| | Volume of fly ash (m$^3$) | | 0 |
| | Volume of water (m$^3$) | | 0.158 |
| | Volume of air (m$^3$) | | 0.05 |
| | Volume of total aggregate (m$^3$) | | 0.731 |
| | Total aggregate (kg) | | 1882.7 |
| | 20 mm coarse aggregate content (kg) | | 700.4 |
| | 10 mm coarse aggregate content kg) | | 466.9 |
| | Coarse sand content (kg) | | 479.3 |
| | Fine sand content (kg) | | 236.1 |
| | Admixture content (ml) | 350 ml per 100kg cementitious material | 564.6 |
| | Air-entrained agent (ml) | | 150 |

**Table A-6: Final lean concrete mix (C12-C0)**

| | Paste | | | Coarse Aggregate | | Fine Aggregate | | Admixture (ml) | | Total (kg) |
|---|---|---|---|---|---|---|---|---|---|---|
| | Cement | SCM | Water | 20 mm | 10 mm | Coarse Sand | Fine Sand | Water Reducer | A.E.A | |
| Design Weights (kg/m$^3$) | 188 | 0 | 158 | 700 | 467 | 479 | 236 | 565 | 150 | 2229 |
| Lab batch weight (kg) | 6.02 | 0 | 5.06 | 22.41 | 14.94 | 15.34 | 7.55 | 18.07 | 4.8 | 71.33 |
| W.A (%) | | | | 1.68 | 1.85 | 1.1 | 2.5 | | | |
| M.C (%) | | | | 3.72 | 7.47 | 2.3 | 2.4 | | | |
| Water contained (kg) | | | | 0.457 | 0.84 | 0.184 | -0.008 | | | 1.47 |
| Lab cast weights (kg) | 6.02 | 0 | 3.46 | 22.41 | 14.94 | 15.34 | 7.55 | 18.07 | 4.8 | 69.73 |
| Corrected lab cast weights (kg) | 6.02 | 0 | 4.93 | 21.95 | 14.1 | 15.15 | 7.56 | 18.07 | 4.8 | 69.73 |
| Corrected designed weights (kg/m$^3$) | 200 | 0 | 164 | 731 | 469 | 504 | 252 | 665 | 140 | 2321 |

| | |
|---|---|
| Lab Batch volume (m$^3$) | 0.032 |
| Density (kg/m$^3$) | 2321 |
| Lab Yield (m$^3$) | 0.03 |
| Modified w/b | 0.82 |

The complete process of designing the lean concrete mix with 60% cement replacement with CFA (C12-CFA60) are presented in five steps as shown in Table A-7 to Table A-11 and the final mix design is demonstrated in Table A-12.

**Table A-7: Step 1 in designing the lean concrete mix (C12-CFA60)**

| Step | Item | Reference/Calculation | Value |
|---|---|---|---|
| 1 | Characteristic strength (fc) @ 28 days (MPa) | Specified | 12 |
| | Proportion defective (k) % | Table 3-7 | 1.64 |
| | Standard deviation (S) (MPa) | Figure 3-5 | 2.2 |
| | percentage by volume of air entrained (a) | Specified | 5 |
| | Target mean strength (MPa) | Equation 3-2 | 22 |
| | Cement strength class | Specified | 42.5 |
| | Type of coarse aggregate | Specified | Crushed |
| | Free water/cement ratio | Table 3-8, Figure 3-6 | 0.84 |

**Table A-8: Step 2 in designing the lean concrete mix (C12-CFA60)**

| Step | Item | Reference/Calculation | Value |
|---|---|---|---|
| 2 | Slump (mm) | Specified | 40 |
| | Maximum aggregate size (mm) | Specified | 20 |
| | Coarse aggregate type | Specified | Crushed |
| | Fine aggregate type | Specified | Uncrushed |
| | Free water content (kg/m$^3$) | Table 3-9, Eq.3-4 | 170 |
| | CFA or RFA replacement (%) | Specified | 60 |
| | Reduction in water content because of SCMs (kg) | | 25 |
| | Type of admixture | Specified | WR |
| | Reduction of water content by admixture (%) | Specified | 7 |
| | Reduction in water content because of admixture (kg) | | 10 |
| | Final free water content (kg) | | 135 |

**Table A-9: Step 3 in designing the lean concrete mix (C12-CFA60)**

| Step | Item | Reference/Calculation | Value |
|---|---|---|---|
| 3 | Cement content (kg) | Equation 3-6 | 111 |
| | Maximum cement content (kg) | Specified | - |
| | Minimum cement content (kg) | Specified | - |
| | Final Cement content (kg) | | 111 |
| | CFA or RFA content | Equation 3-7 | 166 |
| | Modified W/b ratio | | 0.49 |

**Table A-10: Step 4 in designing the lean concrete mix (C12-CFA60)**

| Step | Item | Reference/Calculation | Value |
|---|---|---|---|
| 4 | Percentage of fine aggregate passing 600 μm sieve | Specified | 50 |
| | Maximum aggregate size (mm) | Specified | 20 |
| | Slump zone (mm) | Specified | 10-30 |
| | Water to cement ratio | | 0.49 |
| | Proportion of fine aggregate (%) | Figure 3-7 | 38 |
| | Proportion of coarse aggregate (%) | | 62 |
| | 20 mm coarse aggregate content (%) | According to grading curve of Road Note No.4 (Figure 7-1) | 60 |
| | 10 mm coarse aggregate content (%) | | 40 |
| | Coarse sand content (%) | | 67 |
| | Fine sand content (%) | | 33 |

**Table A-11: Step 5 in designing the lean concrete mix (C12-CFA60)**

| Step | Item | Reference/Calculation | Value |
|---|---|---|---|
| 5 | Cement content (kg/m$^3$) | Step 3 | 111 |
| | CFA or RFA content (kg/m$^3$) | Step 3 | 166 |
| | Free water content (kg/m$^3$) | Step 2 | 135 |
| | Volume of cement (m$^3$) | | 0.036 |
| | Volume of fly ash (m$^3$) | | 0.079 |
| | Volume of water (m$^3$) | | 0.135 |
| | Volume of air (m$^3$) | | 0.05 |
| | Volume of total aggregate (m$^3$) | | 0.7 |
| | Total aggregate (kg) | | 1802.5 |
| | 20 mm coarse aggregate content (kg) | | 670.5 |
| | 10 mm coarse aggregate content kg) | | 447 |
| | Coarse sand content (kg) | | 458.9 |
| | Fine sand content (kg) | | 226 |
| | Admixture content (ml) | 300 ml per 100kg cementitious material | 830.4 |
| | Air-entrained agent (ml) | | 150 |

**Table A-12: Final lean concrete mix (C12-CFA60)**

| | Paste | | | Coarse Aggregate | | Fine Aggregate | | Admixture (ml) | | Total (kg) |
|---|---|---|---|---|---|---|---|---|---|---|
| | Cement | SCM | Water | 20 mm | 10 mm | Coarse Sand | Fine Sand | Water Reducer | A.E.A | |
| Design Weights (kg/m3) | 111 | 166 | 135 | 670.5 | 447 | 458.9 | 226 | 830.4 | 150 | 2214.1 |
| Lab batch weight (kg) | 3.54 | 5.31 | 4.32 | 21.46 | 14.3 | 14.69 | 7.23 | 26.57 | 4.8 | 70.85 |
| W.A (%) | | | | 1.68 | 1.85 | 1.1 | 2.5 | | | |
| M.C (%) | | | | 3.5 | 6.86 | 2.3 | 2.4 | | | |
| Water contained (kg) | | | | 0.391 | 0.717 | 0.176 | -0.007 | | | 1.28 |
| Poured lab batch weights (kg) | 3.54 | 5.31 | 4 | 21.46 | 14.3 | 14.69 | 7.23 | 26.57 | 4.8 | 70.54 |
| Corrected poured lab batch weights (kg) | 3.54 | 5.31 | 5.28 | 21.07 | 13.59 | 14.51 | 7.24 | 26.57 | 4.8 | 70.54 |
| Corrected designed weights (kg/m3) | 110.7 | 166 | 164.9 | 658.2 | 424.6 | 453.4 | 226.2 | 830.2 | 150 | 2204 |

| | |
|---|---|
| Lab Batch volume (m3) | 0.032 |
| Density (kg/m3) | 2204 |
| Lab Yield (m3) | 0.032 |
| Modified w/b | 0.6 |

The complete process of designing the lean concrete mix with 60% cement replacement with RFA (C12-RFA60) is presented in five steps as shown in Table A-13 to Table A-17 and final mix design is demonstrated in Table A-18.

**Table A-13: Step 1 in designing the lean concrete mix (C12-RFA60)**

| Step | Item | Reference/Calculation | Value |
|---|---|---|---|
| 1 | Characteristic strength (fc) @ 28 days (MPa) | Specified | 12 |
| | Proportion defective (k) % | Table 3-7 | 1.64 |
| | Standard deviation (S) (MPa) | Figure 3-5 | 2.2 |
| | percentage by volume of air entrained (a) | Specified | 5 |
| | Target mean strength (MPa) | Equation 3-2 | 22 |
| | Cement strength class | Specified | 42.5 |
| | Type of coarse aggregate | Specified | Crushed |
| | Free water/cement ratio | Table 3-8, Figure 3-6 | 0.84 |

**Table A-14: Step 2 in designing the lean concrete mix (C12-RFA60)**

| Step | Item | Reference/Calculation | Value |
|---|---|---|---|
| 2 | Slump (mm) | Specified | 40 |
| | Maximum aggregate size (mm) | Specified | 20 |
| | Coarse aggregate type | Specified | Crushed |
| | Fine aggregate type | Specified | Uncrushed |
| | Free water content ($kg/m^3$) | Table 3-9, Eq.3-4 | 170 |
| | CFA or RFA replacement (%) | Specified | 60 |
| | Reduction in water content because of SCMs (kg) | | 25 |
| | Type of admixture | Specified | WR |
| | Reduction of water content by admixture (%) | Specified | 7 |
| | Reduction in water content because of admixture (kg) | | 10 |
| | Final free water content (kg) | | 135 |

**Table A-15: Step 3 in designing the lean concrete mix (C12-RFA60)**

| Step | Item | Reference/Calculation | Value |
|---|---|---|---|
| 3 | Cement content (kg) | Equation 3-6 | 111 |
| | Maximum cement content (kg) | Specified | - |
| | Minimum cement content (kg) | Specified | - |
| | Final Cement content (kg) | | 111 |
| | CFA or RFA content | Equation 3-7 | 166 |
| | Modified W/b ratio | | 0.49 |

**Table A-16: Step 4 in designing the lean concrete mix (C12-RFA60)**

| Step | Item | Reference/Calculation | Value |
|---|---|---|---|
| 4 | Percentage of fine aggregate passing 600 μm sieve | Specified | 50 |
| | Maximum aggregate size (mm) | Specified | 20 |
| | Slump zone (mm) | Specified | 10-30 |
| | Water to cement ratio | | 0.49 |
| | Proportion of fine aggregate (%) | Figure 3-7 | 38 |
| | Proportion of coarse aggregate (%) | | 62 |
| | 20 mm coarse aggregate content (%) | According to grading curve of Road Note No.4 (Figure 7-1) | 60 |
| | 10 mm coarse aggregate content (%) | | 40 |
| | Coarse sand content (%) | | 67 |
| | Fine sand content (%) | | 33 |

**Table A-17: Step 5 in designing the lean concrete mix (C12-RFA60)**

| Step | Item | Reference/Calculation | Value |
|---|---|---|---|
| 5 | Cement content (kg/m$^3$) | Step 3 | 111 |
| | CFA or RFA content (kg/m$^3$) | Step 3 | 166 |
| | Free water content (kg/m$^3$) | Step 2 | 135 |
| | Volume of cement (m$^3$) | | 0.036 |
| | Volume of fly ash (m$^3$) | | 0.079 |
| | Volume of water (m$^3$) | | 0.135 |
| | Volume of air (m$^3$) | | 0.05 |
| | Volume of total aggregate (m$^3$) | | 0.7 |
| | Total aggregate (kg) | | 1802.5 |
| | 20 mm coarse aggregate content (kg) | | 670.5 |
| | 10 mm coarse aggregate content kg) | | 447 |
| | Coarse sand content (kg) | | 458.9 |
| | Fine sand content (kg) | | 226 |
| | Admixture content (ml) | 300 ml per 100kg cementitious material | 830.4 |
| | Air-entrained agent (ml) | | 150 |

**Table A-18: Final lean concrete mix (C12-RFA60)**

| | Paste | | | Coarse Aggregate | | Fine Aggregate | | Admixture (ml) | | Total |
|---|---|---|---|---|---|---|---|---|---|---|
| | Cement | SCM | Water | 20 mm | 10 mm | Coarse Sand | Fine Sand | Water Reducer | A.E.A | (kg) |
| Design Weights (kg/m3) | 111 | 166 | 135 | 670.5 | 447 | 458.9 | 226 | 830.4 | 150 | 2214.1 |
| Lab batch weight (kg) | 3.54 | 5.31 | 4.32 | 21.46 | 14.3 | 14.69 | 7.23 | 26.57 | 4.8 | 70.85 |
| W.A (%) | | | | 1.68 | 1.85 | 1.1 | 2.5 | | | |
| M.C (%) | | | | 3.5 | 6.86 | 2.3 | 2.4 | | | |
| Water contained (kg) | | | | 0.391 | 0.717 | 0.176 | -0.007 | | | 1.28 |
| Poured lab batch weights (kg) | 3.54 | 5.31 | 4 | 21.46 | 14.3 | 14.69 | 7.23 | 26.57 | 4.8 | 70.54 |
| Corrected poured lab batch weights (kg) | 3.54 | 5.31 | 5.28 | 21.07 | 13.59 | 14.51 | 7.24 | 26.57 | 4.8 | 70.54 |
| Corrected designed weights (kg/m3) | 110.3 | 166 | 164.3 | 656.2 | 423.2 | 451.9 | 225.5 | 975 | 150 | 2197 |

| | |
|---|---|
| Lab Batch volume (m3) | 0.032 |
| Density (kg/m3) | 2197 |
| Lab Yield (m3) | 0.032 |
| Modified w/b | 0.6 |

The complete process of designing the pavement concrete mix without cement replacement with SCMs (C40-C0) is presented in five steps as shown in Table A-19 to Table A-23, and the final mix design is demonstrated in Table A-24.

**Table A-19: Step 1 in designing the pavement concrete mix (C40-C0)**

| Step | Item | Reference/Calculation | Value |
|---|---|---|---|
| 1 | Characteristic strength (fc) @ 28 days (MPa) | Specified | 40 |
| | Proportion defective (k) % | Table 3-7 | 1.64 |
| | Standard deviation (S) (MPa) | Figure 3-5 | 4 |
| | percentage by volume of air entrained (a) | Specified | 4 |
| | Target mean strength (MPa) | Equation 3-2 | 60 |
| | Cement strength class | Specified | 42.5 |
| | Type of coarse aggregate | Specified | Crushed |
| | Free water/cement ratio | Table 3-8, Figure 3-6 | 0.45 |

**Table A-20: Step 2 in designing the pavement concrete mix (C40-C0)**

| Step | Item | Reference/Calculation | Value |
|---|---|---|---|
| 2 | Slump (mm) | Specified | 40 |
| | Maximum aggregate size (mm) | Specified | 20 |
| | Coarse aggregate type | Specified | Crushed |
| | Fine aggregate type | Specified | Uncrushed |
| | Free water content (kg/m$^3$) | Table 3-9, Eq.3-4 | 170 |
| | SCM replacement (%) | Specified | |
| | Reduction in water content because of SCMs (kg) | | |
| | Type of admixture | Specified | WR |
| | Reduction of water content by admixture (%) | Specified | 7 |
| | Reduction in water content because of admixture (kg) | | 12 |
| | Final free water content (kg) | | 158 |

**Table A-21: Step 3 in designing the pavement concrete mix (C40-C0)**

| Step | Item | Reference/Calculation | Value |
|---|---|---|---|
| 3 | Cement content (kg) | Equation 3-5 | 351 |
| | Maximum cement content (kg) | Specified | - |
| | Minimum cement content (kg) | Specified | - |
| | Final Cement content (kg) | | 351 |
| | SCM content | Equation 3-7 | |
| | Modified W/b ratio | | 0.45 |

**Table A-22: Step 4 in designing the pavement concrete mix (C40-C0)**

| Step | Item | Reference/Calculation | Value |
|---|---|---|---|
| 4 | Percentage of fine aggregate passing 600 μm sieve | Specified | 50 |
| | Maximum aggregate size (mm) | Specified | 20 |
| | Slump zone (mm) | Specified | 10-30 |
| | Water to cement ratio | | 0.45 |
| | Proportion of fine aggregate (%) | Figure 3-7 | 30 |
| | Proportion of coarse aggregate (%) | | 70 |
| | 20 mm coarse aggregate content (%) | According to grading curve of Road Note No.4 (Figure 7-5) | 60 |
| | 10 mm coarse aggregate content (%) | | 40 |
| | Coarse sand content (%) | | 85 |
| | Fine sand content (%) | | 15 |

**Table A-23: Step 5 in designing the pavement concrete mix (C40-C0)**

| Step | Item | Reference/Calculation | Value |
|---|---|---|---|
| 5 | Cement content (kg/m$^3$) | Step 3 | 351 |
| | SCM content (kg/m3) | Step 3 | 0 |
| | Free water content (kg/m$^3$) | Step 2 | 158 |
| | Volume of cement (m$^3$) | | 0.114 |
| | Volume of fly ash (m$^3$) | | 0 |
| | Volume of water (m$^3$) | | 0.158 |
| | Volume of air (m$^3$) | | 0.04 |
| | Volume of total aggregate (m$^3$) | | 0.688 |
| | Total aggregate (kg) | | 1769.8 |
| | 20 mm coarse aggregate content (kg) | | 743.3 |
| | 10 mm coarse aggregate content kg) | | 495.5 |
| | Coarse sand content (kg) | | 451.3 |
| | Fine sand content (kg) | | 79.6 |
| | Admixture content (ml) | 300 ml per 100 kg cementitious material | 1229.7 |
| | Air-entrained agent (ml) | | 100 |

**Table A-24: Final pavement concrete mix design (C40-C0)**

| | Paste | | | Coarse Aggregate | | Fine Aggregate | | Admixture (ml) | | Total (kg) |
|---|---|---|---|---|---|---|---|---|---|---|
| | Cement | SCM | Water | 20 mm | 10 mm | Coarse Sand | Fine Sand | Water Reducer | A.E.A | |
| Design Weights (kg/m3) | 351.3 | 0 | 158.1 | 743.3 | 495.5 | 451.3 | 79.6 | 1229.7 | 100 | 2279.2 |
| Lab batch weight (kg) | 17.6 | 0 | 7.9 | 37.2 | 24.8 | 22.6 | 4 | 61.5 | 5 | 114 |
| W.A (%) | | | | 1.7 | 1.9 | 1.1 | 2.5 | | | |
| M.C (%) | | | | 2.2 | 4 | 2.3 | 2.4 | | | |
| Water contained (kg) | | | | 0.2 | 0.5 | 0.3 | 0 | | | 1 |
| Real lab batch weights (kg) | 17.6 | 0 | 6.6 | 37.2 | 24.8 | 22.6 | 4 | 61.5 | 5 | 112.6 |
| Corrected Real lab batch weights (kg) | 17.6 | 0 | 7.6 | 37 | 24.2 | 22.3 | 4 | 61.5 | 5 | 112.6 |
| Corrected designed weights (kg/m3) | 377.5 | 0 | 162.3 | 794.5 | 520.9 | 479.1 | 85.7 | 1321.3 | 107.5 | 2420 |

| | |
|---|---|
| Lab Batch volume (m3) | 0.05 |
| Density (kg/m3) | 2420 |
| Lab Yield (m3) | 0.047 |

The complete process of designing the pavement concrete mix with 20% cement replacement with CFA and RFA replacement (C40-CFA20 & C40-RFA20) is presented in five steps as shown in Table A-25 to Table A-29 and the final mix design for each one is demonstrated in Table A-30 and Table A-31.

**Table A-25: Step 1 in designing the pavement concrete mix (C40-CFA20 and C40-RFA20)**

| Step | Item | Reference/Calculation | Value |
|---|---|---|---|
| 1 | Characteristic strength (fc) @ 28 days (MPa) | Specified | 40 |
| | Proportion defective (k) % | Table 3-7 | 1.64 |
| | Standard deviation (S) (MPa) | Figure 3-5 | 4 |
| | percentage by volume of air entrained (a) | Specified | 4 |
| | Target mean strength (MPa) | Equation 3-2 | 60 |
| | Cement strength class | Specified | 42.5 |
| | Type of coarse aggregate | Specified | Crushed |
| | Free water/cement ratio | Table 3-8, Figure 3-6 | 0.45 |

**Table A-26: Step 2 in designing the pavement concrete mix (C40-CFA20 and C40-RFA20)**

| Item | Reference/Calculation | Value |
|---|---|---|
| Slump (mm) | Specified | 40 |
| Maximum aggregate size (mm) | Specified | 20 |
| Coarse aggregate type | Specified | Crushed |
| Fine aggregate type | Specified | Uncrushed |
| Free water content (kg/m$^3$) | Table 3-9, Eq.3-4 | 170 |
| CFA or RFA replacement (%) | Specified | 20 |
| Reduction in water content because of SCMs (kg) | | 10 |
| Type of admixture | Specified | WR |
| Reduction of water content by admixture (%) | Specified | 7 |
| Reduction in water content because of admixture (kg) | | 11 |
| Final free water content (kg) | | 149 |

**Table A-27: Step 3 in designing the pavement concrete mix (C40-CFA20 and C40-RFA20)**

| Step | Item | Reference/Calculation | Value |
|---|---|---|---|
| 3 | Cement content (kg) | Equation 3-6 | 308 |
| | Maximum cement content (kg) | Specified | - |
| | Minimum cement content (kg) | Specified | - |
| | Final Cement content (kg) | | 308 |
| | CFA or RFA content | Equation 3-7 | 77 |
| | Modified W/b ratio | | 0.39 |

**Table A-28: Step 4 in designing the pavement concrete mix (C40-CFA20 and C40-RFA20)**

| Step | Item | Reference/Calculation | Value |
|---|---|---|---|
| 4 | Percentage of fine aggregate passing 600 μm sieve | Specified | 50 |
| | Maximum aggregate size (mm) | Specified | 20 |
| | Slump zone (mm) | Specified | 10-30 |
| | Water to cement ratio | | 0.39 |
| | Proportion of fine aggregate (%) | Figure 3-7 | 30 |
| | Proportion of coarse aggregate (%) | | 70 |
| | 20 mm coarse aggregate content (%) | According to grading curve of Road Note No.4 (Figure 7-5) | 60 |
| | 10 mm coarse aggregate content (%) | | 40 |
| | Coarse sand content (%) | | 85 |
| | Fine sand content (%) | | 15 |

**Table A-29: Step 5 in designing the pavement concrete mix (C40-CFA20 and C40-RFA20)**

| Step | Item | Reference/Calculation | Value |
|---|---|---|---|
| 5 | Cement content (kg/m$^3$) | Step 3 | 308 |
| | CFA or RFA content (kg/m$^3$) | Step 3 | 77 |
| | Free water content (kg/m$^3$) | Step 2 | 149 |
| | Volume of cement (m$^3$) | | 0.1 |
| | Volume of fly ash (m$^3$) | | 0.037 |
| | Volume of water (m$^3$) | | 0.149 |
| | Volume of air (m$^3$) | | 0.04 |
| | Volume of total aggregate (m$^3$) | | 0.675 |
| | Total aggregate (kg) | | 1735.5 |
| | 20 mm coarse aggregate content (kg) | | 728.9 |
| | 10 mm coarse aggregate content kg) | | 485.9 |
| | Coarse sand content (kg) | | 442.6 |
| | Fine sand content (kg) | | 78.1 |
| | Admixture content (ml) | 300 ml per 100kg cementitious material | 1153.5 |
| | Air-entrained agent (ml) | | 150 |

**Table A-30: Final pavement concrete mix design (C40-CFA20)**

| | Paste | | | Coarse Aggregate | | Fine Aggregate | | Admixture (ml) | | Total (kg) |
|---|---|---|---|---|---|---|---|---|---|---|
| | Cement | SCM | Water | 20 mm | 10 mm | Coarse Sand | Fine Sand | Water Reducer | A.E.A | |
| Design Weights (kg/m3) | 308 | 77 | 149 | 729 | 486 | 443 | 78 | 1153 | 150 | 2268.8 |
| Lab batch weight (kg) | 15.4 | 3.8 | 7.4 | 36.4 | 24.3 | 22.1 | 3.9 | 57.7 | 7.5 | 113.4 |
| Water absorption (%) | | | | 1.7 | 1.9 | 1.1 | 2.5 | | | |
| Moisture content (%) | | | | 2.2 | 4 | 2.3 | 2.4 | | | |
| Water contained (kg) | | | | 0.193 | 0.53 | 0.266 | -0.004 | | | 1 |
| Real lab batch weights (kg) | 15.4 | 3.8 | 6.3 | 36.4 | 24.3 | 22.1 | 3.9 | 57.7 | 7.5 | 112.3 |
| Corrected Real lab batch weights (kg) | 15.4 | 3.8 | 7.3 | 36.3 | 23.8 | 21.9 | 3.9 | 57.7 | 7.5 | 112.3 |
| Corrected designed weights (kg/m3) | 329 | 82 | 156 | 775 | 508 | 468 | 84 | 1234 | 160 | 2402 |

| | |
|---|---|
| Lab Batch volume (m3) | 0.05 |
| Density (kg/m3) | 2402 |
| Lab Yield (m3) | 0.047 |
| Modified w/b | 0.38 |

**Table A-31: Final pavement concrete mix design (C40-RFA20)**

| | Paste | | | Coarse Aggregate | | Fine Aggregate | | Admixture (ml) | | Total (kg) |
|---|---|---|---|---|---|---|---|---|---|---|
| | Cement | SCM | Water | 20 mm | 10 mm | Coarse Sand | Fine Sand | Water Reducer | A.E.A | |
| Design Weights (kg/m3) | 308 | 77 | 149 | 729 | 486 | 443 | 78 | 1153 | 150 | 2268.8 |
| Lab batch weight (kg) | 15.4 | 3.8 | 7.4 | 36.4 | 24.3 | 22.1 | 3.9 | 57.7 | 7.5 | 113.4 |
| Water absorption (%) | | | | 1.7 | 1.9 | 1.1 | 2.5 | | | |
| Moisture content (%) | | | | 2.4 | 4 | 2.3 | 2.4 | | | |
| Water contained (kg) | | | | 0.262 | 0.53 | 0.266 | -0.004 | | | 1.1 |
| Real lab batch weights (kg) | 15.4 | 3.8 | 6.3 | 36.4 | 24.3 | 22.1 | 3.9 | 57.7 | 7.5 | 112.3 |
| Corrected Real lab batch weights (kg) | 15.4 | 3.8 | 7.4 | 36.2 | 23.8 | 21.9 | 3.9 | 57.7 | 7.5 | 112.3 |
| Corrected designed weights (kg/m3) | 328 | 82 | 157 | 771 | 506 | 466 | 83 | 1228 | 160 | 2392 |

| | |
|---|---|
| Lab Batch volume (m3) | 0.05 |
| Density (kg/m3) | 2392 |
| Lab Yield (m3) | 0.047 |
| Modified w/b | 0.38 |

The complete process of designing the pavement concrete mix with 50% cement replacement with SL (C40-SL50) is presented in five steps as shown in Table A-32 to Table A-36 and the final mix design is demonstrated in Table A-37.

**Table A-32: Step 1 in designing the pavement concrete mix (C40-SL50)**

| Step | Item | Reference/Calculation | Value |
|---|---|---|---|
| 1 | Characteristic strength (fc) @ 28 days (MPa) | Specified | 40 |
| | Proportion defective (k) % | Table 3-7 | 1.64 |
| | Standard deviation (S) (MPa) | Figure 3-5 | 4 |
| | percentage by volume of air entrained (a) | Specified | 4 |
| | Target mean strength (MPa) | Equation 3-2 | 60 |
| | Cement strength class | Specified | 42.5 |
| | Type of coarse aggregate | Specified | Crushed |
| | Free water/cement ratio | Table 3-8, Figure 3-6 | 0.45 |

**Table A-33: Step 2 in designing the pavement concrete mix (C40-SL50)**

| Step | Item | Reference/Calculation | Value |
|---|---|---|---|
| 2 | Slump (mm) | Specified | 40 |
| | Maximum aggregate size (mm) | Specified | 20 |
| | Coarse aggregate type | Specified | Crushed |
| | Fine aggregate type | Specified | Uncrushed |
| | Free water content (kg/m3) | Table 3-9, Eq.3-4 | 165 |
| | SL replacement (%) | Specified | 50 |
| | Reduction in water content because of SCMs (kg) | | |
| | Type of admixture | Specified | WR |
| | Reduction of water content by admixture (%) | Specified | 7 |
| | Reduction in water content because of admixture (kg) | | 12 |
| | Final free water content (kg) | | 153 |

**Table A-34: Step 3 in designing the pavement concrete mix (C40-SL50)**

| Step | Item | Reference/Calculation | Value |
|---|---|---|---|
| 3 | Cement content (kg) | Equation 3-6 | 171 |
| | Maximum cement content (kg) | Specified | - |
| | Minimum cement content (kg) | Specified | - |
| | Final Cement content (kg) | | 171 |
| | SL content | Equation 3-7 | 171 |
| | Modified W/b ratio | | 0.45 |

**Table A-35: Step 4 in designing the pavement concrete mix (C40-SL50)**

| Step | Item | Reference/Calculation | Value |
|---|---|---|---|
| 4 | Percentage of fine aggregate passing 600 μm sieve | Specified | 50 |
| | Maximum aggregate size (mm) | Specified | 20 |
| | Slump zone (mm) | Specified | 10-30 |
| | Water to cement ratio | | 0.45 |
| | Proportion of fine aggregate (%) | Figure 3-7 | 30 |
| | Proportion of coarse aggregate (%) | | 70 |
| | 20 mm coarse aggregate content (%) | According to grading curve of Road Note No.4 (Figure 7-5) | 60 |
| | 10 mm coarse aggregate content (%) | | 40 |
| | Coarse sand content (%) | | 85 |
| | Fine sand content (%) | | 15 |

**Table A-36: Step 5 in designing the pavement concrete mix (C40-SL50)**

| Step | Item | Reference/Calculation | Value |
|---|---|---|---|
| 5 | Cement content (kg/m$^3$) | Step 3 | 171 |
| | SL content (kg/m$^3$) | Step 3 | 171 |
| | Free water content (kg/m$^3$) | Step 2 | 153 |
| | Volume of cement (m$^3$) | | 0.055 |
| | Volume of fly ash (m$^3$) | | 0.059 |
| | Volume of water (m$^3$) | | 0.153 |
| | Volume of air (m$^3$) | | 0.040 |
| | Volume of total aggregate (m$^3$) | | 0.693 |
| | Total aggregate (kg) | | 1781.1 |
| | 20 mm coarse aggregate content (kg) | | 748 |
| | 10 mm coarse aggregate content kg) | | 498.7 |
| | Coarse sand content (kg) | | 454.2 |
| | Fine sand content (kg) | | 80.1 |
| | Admixture content (ml) | 300 ml per 100kg cementitious material | 1023 |
| | Air-entrained agent (ml) | | 150 |

**Table A-37: Final pavement concrete mix design (C40-SL50)**

| | Paste | | | Coarse Aggregate | | Fine Aggregate | | Admixture (ml) | | Total (kg) |
|---|---|---|---|---|---|---|---|---|---|---|
| | Cement | SCM | Water | 20 mm | 10 mm | Coarse Sand | Fine Sand | Water Reducer | A.E.A | |
| Design Weights (kg/m3) | 171 | 171 | 153 | 748 | 499 | 454 | 80 | 1023 | 100 | 2275.5 |
| Lab batch weight (kg) | 8.5 | 8.5 | 7.7 | 37.4 | 24.9 | 22.7 | 4 | 51.2 | 5 | 113.8 |
| Water absorption (%) | | | | 1.7 | 1.9 | 1.1 | 2.5 | | | |
| Moisture content (%) | | | | 2.4 | 4.9 | 2.3 | 2.4 | | | |
| Water contained (kg) | | | | 0.269 | 0.761 | 0.273 | -0.004 | | | 1.3 |
| Real lab batch weights (kg) | 8.5 | 8.5 | 6.3 | 37.4 | 24.9 | 22.7 | 4 | 51.2 | 5 | 112.4 |
| Corrected Real lab batch weights (kg) | 8.5 | 8.5 | 7.6 | 37.1 | 24.2 | 22.4 | 4 | 51.2 | 5 | 112.4 |
| Corrected designed weights (kg/m3) | 183 | 183 | 163 | 798 | 520 | 482 | 86 | 1099 | 107 | 2416 |

| | |
|---|---|
| Lab Batch volume (m3) | 0.05 |
| Density (kg/m3) | 2416 |
| Lab Yield (m3) | 0.047 |
| Modified w/b | 0.45 |

The complete process of designing the bridge concrete mix without cement replacement with SCMs (C50-C0) is presented in five steps as shown in Table A-38 to Table A-42 and the final mix design is demonstrated in Table A-43.

**Table A-38: Step 1 in designing the bridge concrete mix (C50-C0)**

| Step | Item | Reference/Calculation | Value |
|---|---|---|---|
| 1 | Characteristic strength (fc) @ 28 days (MPa) | Specified | 50 |
| | Proportion defective (k) % | Table 3-7 | 1.64 |
| | Standard deviation (S) (MPa) | Figure 3-5 | 4 |
| | percentage by volume of air entrained (a) | Specified | |
| | Target mean strength (MPa) | Equation 3-2 | 57 |
| | Cement strength class | Specified | 42.5 |
| | Type of coarse aggregate | Specified | Crushed |
| | Free water/cement ratio | Table 3-8, Figure 3-6 | 0.42 |

**Table A-39: Step 2 in designing the bridge concrete mix (C50-C0)**

| Step | Item | Reference/Calculation | Value |
|---|---|---|---|
| 2 | Slump (mm) | Specified | 40 |
| | Maximum aggregate size (mm) | Specified | 20 |
| | Coarse aggregate type | Specified | Crushed |
| | Fine aggregate type | Specified | Uncrushed |
| | Free water content (kg/m3) | Table 3-9, Eq.3-4 | 205 |
| | SCM replacement (%) | Specified | |
| | Reduction in water content because of SCMs (kg) | | |
| | Type of admixture | Specified | HWR |
| | Reduction of water content by admixture (%) | Specified | 22 |
| | Reduction in water content because of admixture (kg) | | 45 |
| | Final free water content (kg) | | 160 |

**Table A-40: Step 3 in designing the bridge concrete mix (C50-C0)**

| Step | Item | Reference/Calculation | Value |
|---|---|---|---|
| 3 | Cement content (kg) | Equation 3-5 | 381 |
| | Maximum cement content (kg) | Specified | - |
| | Minimum cement content (kg) | Specified | - |
| | Final Cement content (kg) | | 381 |
| | SCM content | Equation 3-7 | |
| | Modified W/b ratio | | 0.42 |

**Table A-41: Step 4 in designing the bridge concrete mix (C50-C0)**

| Step | Item | Reference/Calculation | Value |
|---|---|---|---|
| 4 | Percentage of fine aggregate passing 600 μm sieve | Specified | 50 |
| | Maximum aggregate size (mm) | Specified | 20 |
| | Slump zone (mm) | Specified | 60-180 |
| | Water to cement ratio | | 0.42 |
| | Proportion of fine aggregate (%) | Figure 3-7 | 37 |
| | Proportion of coarse aggregate (%) | | 63 |
| | 20 mm coarse aggregate content (%) | According to grading curve of Road Note No.4 (Figure 7-5) | 65 |
| | 10 mm coarse aggregate content (%) | | 35 |
| | Coarse sand content (%) | | 80 |
| | Fine sand content (%) | | 20 |

**Table A-42: Step 5 in designing the bridge concrete mix (C50-C0)**

| Step | Item | Reference/Calculation | Value |
|---|---|---|---|
| 5 | Cement content (kg/m$^3$) | Step 3 | 381 |
| | SCM content (kg/m$^3$) | Step 3 | 0 |
| | Free water content (kg/m$^3$) | Step 2 | 160 |
| | Volume of cement (m$^3$) | | 0.123 |
| | Volume of fly ash (m$^3$) | | 0.000 |
| | Volume of water (m$^3$) | | 0.160 |
| | Volume of air (m$^3$) | | 0.000 |
| | Volume of total aggregate (m$^3$) | | 0.717 |
| | Total aggregate (kg) | | 1841.1 |
| | 20 mm coarse aggregate content (kg) | | 753.9 |
| | 10 mm coarse aggregate content kg) | | 406.0 |
| | Coarse sand content (kg) | | 545.0 |
| | Fine sand content (kg) | | 136.2 |
| | Admixture content (ml) | 900 ml per 100kg cementitious material | 3426.4 |
| | Air-entrained agent (ml) | | 0.000 |

**Table A-43: Final bridge concrete mix design (C50-C0)**

| | Paste | | | Coarse Aggregate | | Fine Aggregate | | Admixture (ml) | | Total (kg) |
|---|---|---|---|---|---|---|---|---|---|---|
| | Cement | SCM | Water | 20 mm | 10 mm | Coarse Sand | Fine Sand | Water Reducer | A.E.A | |
| Design Weights (kg/m3) | 381 | 0 | 160 | 754 | 406 | 545 | 136 | 3426 | 0 | 2382 |
| Lab batch weight (kg) | 16.4 | 0 | 6.9 | 32.4 | 17.5 | 23.4 | 5.9 | 147.3 | 0 | 102.4 |
| W.A (%) | | | | 1.7 | 1.9 | 1.1 | 2.5 | | | |
| M.C (%) | | | | 4.7 | 5.7 | 2.3 | 2.4 | | | |
| Water contained (kg) | | | | 0.986 | 0.669 | 0.281 | -0.006 | | | 1.9 |
| Real lab batch weights (kg) | 16.4 | 0 | 4.2 | 32.4 | 17.5 | 23.4 | 5.9 | 147.3 | 0 | 99.7 |
| Corrected Real lab batch weights (kg) | 16.4 | 0 | 6.1 | 31.4 | 16.8 | 23.2 | 5.9 | 147.3 | 0 | 99.7 |
| Corrected designed weights (kg/m3) | 409 | 0 | 153 | 786 | 420 | 579 | 147 | 3684 | 0 | 2494 |

| | |
|---|---|
| Lab Batch volume (m3) | 0.043 |
| Density (kg/m3) | 2494 |
| Lab Yield (m3) | 0.040 |
| Modified w/b | 0.38 |

The complete process of designing the bridge concrete mix with 25% cement replacement with CFA and RFA (C50-CFA25 & C50-RFA25) is presented in five steps as shown in Table A-44 to Table A-48 and the final mix design for each one is demonstrated in Table A-49 and Table A-50.

**Table A-44: Step 1 in designing the bridge concrete mix (C50-CFA25 & C50-RFA25)**

| Step | Item | Reference/Calculation | Value |
|---|---|---|---|
| 1 | Characteristic strength (fc) @ 28 days (MPa) | Specified | 50 |
| | Proportion defective (k) % | Table 3-7 | 1.64 |
| | Standard deviation (S) (MPa) | Figure 3-5 | 4 |
| | percentage by volume of air entrained (a) | Specified | |
| | Target mean strength (MPa) | Equation 3-2 | 57 |
| | Cement strength class | Specified | 42.5 |
| | Type of coarse aggregate | Specified | Crushed |
| | Free water/cement ratio | Table 3-8, Figure 3-6 | 0.42 |

**Table A-45: Step 2 in designing the bridge concrete mix (C50-CFA25 & C50-RFA25)**

| Step | Item | Reference/Calculation | Value |
|---|---|---|---|
| 2 | Slump (mm) | Specified | 40 |
| | Maximum aggregate size (mm) | Specified | 20 |
| | Coarse aggregate type | Specified | Crushed |
| | Fine aggregate type | Specified | Uncrushed |
| | Free water content ($kg/m^3$) | Table 3-9, Eq.3-4 | 205 |
| | CFA or RFA replacement (%) | Specified | 25 |
| | Reduction in water content because of SCMs (kg) | | 15 |
| | Type of admixture | Specified | HWR |
| | Reduction of water content by admixture (%) | Specified | 22 |
| | Reduction in water content because of admixture (kg) | | 42 |
| | Final free water content (kg) | | 148 |

**Table A-46: Step 3 in designing the bridge concrete mix (C50-CFA25 & C50-RFA25)**

| Step | Item | Reference/Calculation | Value |
|---|---|---|---|
| 3 | Cement content (kg) | Equation 3-6 | 321 |
| | Maximum cement content (kg) | Specified | - |
| | Minimum cement content (kg) | Specified | - |
| | Final Cement content (kg) | | 321 |
| | CFA or RFA content | Equation 3-7 | 107 |
| | Modified W/b ratio | | 0.35 |

**Table A-47: Step 4 in designing the bridge concrete mix (C50-CFA25 & C50-RFA25)**

| Step | Item | Reference/Calculation | Value |
|---|---|---|---|
| 4 | Percentage of fine aggregate passing 600 μm sieve | Specified | 50 |
| | Maximum aggregate size (mm) | Specified | 20 |
| | Slump zone (mm) | Specified | 60-180 |
| | Water to cement ratio | | 0.35 |
| | Proportion of fine aggregate (%) | Figure 3-7 | 37 |
| | Proportion of coarse aggregate (%) | | 63 |
| | 20 mm coarse aggregate content (%) | According to grading curve of Road Note No.4 (Figure 7-10) | 65 |
| | 10 mm coarse aggregate content (%) | | 35 |
| | Coarse sand content (%) | | 80 |
| | Fine sand content (%) | | 20 |

**Table A-48: Step 5 in designing the bridge concrete mix (C50-CFA25 & C50-RFA25)**

| Step | Item | Reference/Calculation | Value |
|---|---|---|---|
| 5 | Cement content (kg/m$^3$) | Step 3 | 321 |
| | CFA or RFA content (kg/m$^3$) | Step 3 | 107 |
| | Free water content (kg/m$^3$) | Step 2 | 148 |
| | Volume of cement (m$^3$) | | 0.104 |
| | Volume of fly ash (m$^3$) | | 0.045 |
| | Volume of water (m$^3$) | | 0.148 |
| | Volume of air (m$^3$) | | 0.000 |
| | Volume of total aggregate (m$^3$) | | 0.703 |
| | Total aggregate (kg) | | 1806.5 |
| | 20 mm coarse aggregate content (kg) | | 739.8 |
| | 10 mm coarse aggregate content kg) | | 398.3 |
| | Coarse sand content (kg) | | 534.7 |
| | Fine sand content (kg) | | 133.7 |
| | Admixture content (ml) | 900 ml per 100kg cementitious material | 3849.4 |
| | Air-entrained agent (ml) | | 0.000 |

**Table A-49: Final bridge concrete mix design (C50-CFA25)**

| | Paste | | | Coarse Aggregate | | Fine Aggregate | | Admixture (ml) | | Total (kg) |
|---|---|---|---|---|---|---|---|---|---|---|
| | Cement | SCM | Water | 20 mm | 10 mm | Coarse Sand | Fine Sand | Water Reducer | A.E.A | |
| Design Weights (kg/m3) | 321 | 107 | 148 | 740 | 398 | 535 | 134 | 3220 | 0 | 2382 |
| Lab batch weight (kg) | 13.8 | 4.6 | 6.4 | 31.8 | 17.1 | 23 | 5.7 | 138.4 | 0 | 102.4 |
| W.A (%) | | | | 1.7 | 1.9 | 1.1 | 2.5 | | | |
| M.C (%) | | | | 3.7 | 6.9 | 2.3 | 2.4 | | | |
| Water contained (kg) | | | | 0.643 | 0.865 | 0.276 | -0.006 | | | 1.8 |
| Real lab batch weights (kg) | 13.8 | 4.6 | 4.7 | 31.8 | 17.1 | 23 | 5.7 | 138.4 | 0 | 100.8 |
| Corrected Real lab batch weights (kg) | 13.8 | 4.6 | 6.5 | 31.2 | 16.3 | 22.7 | 5.8 | 138.4 | 0 | 100.8 |
| Corrected designed weights (kg/m3) | 336 | 112 | 156 | 759 | 396 | 553 | 140 | 3348 | 0 | 2454 |

| | |
|---|---|
| Lab Batch volume (m3) | 0.043 |
| Density (kg/m3) | 2454 |
| Lab Yield (m3) | 0.041 |
| Modified w/b | 0.35 |

**Table A-50: Final bridge concrete mix design (C50-RFA25)**

| | Paste | | | Coarse Aggregate | | Fine Aggregate | | Admixture (ml) | | Total (kg) |
|---|---|---|---|---|---|---|---|---|---|---|
| | Cement | SCM | Water | 20 mm | 10 mm | Coarse Sand | Fine Sand | Water Reducer | A.E.A | |
| Design Weights (kg/m3) | 321 | 107 | 148 | 740 | 398 | 535 | 134 | 3849 | 0 | 2382 |
| Lab batch weight (kg) | 13.8 | 4.6 | 6.4 | 31.8 | 17.1 | 23 | 5.7 | 165.5 | 0 | 102.4 |
| W.A (%) | | | | 1.7 | 1.9 | 1.1 | 2.5 | | | |
| M.C (%) | | | | 2.7 | 6.9 | 2.3 | 2.4 | | | |
| Water contained (kg) | | | | 0.324 | 0.865 | 0.276 | -0.006 | | | 1.5 |
| Real lab batch weights (kg) | 13.8 | 4.6 | 5 | 31.8 | 17.1 | 23 | 5.7 | 165.5 | 0 | 101.1 |
| Corrected Real lab batch weights (kg) | 13.8 | 4.6 | 6.5 | 31.5 | 16.3 | 22.7 | 5.8 | 165.5 | 0 | 101.1 |
| Corrected designed weights (kg/m3) | 334 | 111 | 156 | 761 | 393 | 549 | 139 | 4002 | 0 | 2444 |

| | |
|---|---|
| Lab Batch volume (m3) | 0.043 |
| Density (kg/m3) | 2444 |
| Lab Yield (m3) | 0.041 |
| Modified w/b | 0.35 |

The complete process of designing the bridge concrete mix with 15% cement replacement with metakaolin (C50-MK15) is presented in five steps as shown in Table A-51 to Table A-55 and the final mix design is demonstrated in Table A-56.

**Table A-51: Step 1 in designing the pavement concrete mix (C50-MK15)**

| Step | Item | Reference/Calculation | Value |
|---|---|---|---|
| 1 | Characteristic strength (fc) @ 28 days (MPa) | Specified | 50 |
| | Proportion defective (k) % | Table 3-7 | 1.64 |
| | Standard deviation (S) (MPa) | Figure 3-5 | 4 |
| | percentage by volume of air entrained (a) | Specified | |
| | Target mean strength (MPa) | Equation 3-2 | 57 |
| | Cement strength class | Specified | 42.5 |
| | Type of coarse aggregate | Specified | Crushed |
| | Free water/cement ratio | Table 3-8, Figure 3-6 | 0.42 |

**Table A-52: Step 2 in designing the pavement concrete mix (C50-MK15)**

| Step | Item | Reference/Calculation | Value |
|---|---|---|---|
| 2 | Slump (mm) | Specified | 40 |
| | Maximum aggregate size (mm) | Specified | 20 |
| | Coarse aggregate type | Specified | Crushed |
| | Fine aggregate type | Specified | Uncrushed |
| | Free water content (kg/m$^3$) | Table 3-9, Eq.3-4 | 205 |
| | MK replacement (%) | Specified | 15 |
| | Reduction in water content because of SCMs (kg) | | |
| | Type of admixture | Specified | HWR |
| | Reduction of water content by admixture (%) | Specified | 20 |
| | Reduction in water content because of admixture (kg) | | 41 |
| | Final free water content (kg) | | 164 |

**Table A-53: Step 3 in designing the pavement concrete mix (C50-MK15)**

| Step | Item | Reference/Calculation | Value |
|---|---|---|---|
| 3 | Cement content (kg) | Equation 3-6 | 320 |
| | Maximum cement content (kg) | Specified | - |
| | Minimum cement content (kg) | Specified | - |
| | Final Cement content (kg) | | 320 |
| | MK content | Equation 3-7 | 56 |
| | Modified W/b ratio | | 0.44 |

**Table A-54: Step 4 in designing the pavement concrete mix (C50-MK15)**

| Step | Item | Reference/Calculation | Value |
|---|---|---|---|
| 4 | Percentage of fine aggregate passing 600 μm sieve | Specified | 50 |
| | Maximum aggregate size (mm) | Specified | 20 |
| | Slump zone (mm) | Specified | 60-180 |
| | Water to cement ratio | | 0.44 |
| | Proportion of fine aggregate (%) | Figure 3-7 | 37 |
| | Proportion of coarse aggregate (%) | | 63 |
| | 20 mm coarse aggregate content (%) | According to grading curve of Road Note No.4 (Figure 7-10) | 65 |
| | 10 mm coarse aggregate content (%) | | 35 |
| | Coarse sand content (%) | | 80 |
| | Fine sand content (%) | | 20 |

**Table A-55: Step 5 in designing the pavement concrete mix (C50-MK15)**

| Step | Item | Reference/Calculation | Value |
|---|---|---|---|
| 5 | Cement content (kg/m$^3$) | | 320 |
| | MK content (kg/m3) | | 56 |
| | Free water content (kg/m$^3$) | | 164 |
| | Volume of cement (m$^3$) | | 0.104 |
| | Volume of metakaolin (m$^3$) | | 0.024 |
| | Volume of water (m$^3$) | | 0.164 |
| | Volume of air (m$^3$) | | 0.000 |
| | Volume of total aggregate (m$^3$) | | 0.709 |
| | Total aggregate (kg) | | 1820.7 |
| | 20 mm coarse aggregate content (kg) | | 745.6 |
| | 10 mm coarse aggregate content kg) | | 401.5 |
| | Coarse sand content (kg) | | 538.9 |
| | Fine sand content (kg) | | 134.7 |
| | Admixture content (ml) | 900 ml per 100kg cementitious material | 3387.3 |
| | Air-entrained agent (ml) | | 0.000 |

**Table A-56: Final bridge concrete mix design (C50-MK15)**

| | Paste | | | Coarse Aggregate | | Fine Aggregate | | Admixture (ml) | | Total (kg) |
|---|---|---|---|---|---|---|---|---|---|---|
| | Cement | SCM | Water | 20 mm | 10 mm | Coarse Sand | Fine Sand | Water Reducer | A.E.A | |
| Design Weights (kg/m3) | 320 | 56 | 164 | 746 | 401 | 539 | 135 | 3387 | 0 | 2361 |
| Lab batch weight (kg) | 13.8 | 2.4 | 7.1 | 32.1 | 17.3 | 23.2 | 5.8 | 145.7 | 0 | 101.5 |
| W.A (%) | | | | 1.7 | 1.9 | 1.1 | 2.5 | | | |
| M.C (%) | | | | 2.1 | 5.3 | 2.3 | 2.4 | | | |
| Water contained (kg) | | | | 0.141 | 0.589 | 0.278 | -0.006 | | | 1 |
| Real lab batch weights (kg) | 13.8 | 2.4 | 5.5 | 32.1 | 17.3 | 23.2 | 5.8 | 145.7 | 0 | 100 |
| Corrected Real lab batch weights (kg) | 13.8 | 2.4 | 6.5 | 31.9 | 16.7 | 22.9 | 5.8 | 145.7 | 0 | 100 |
| Corrected designed weights (kg/m3) | 337 | 60 | 159 | 783 | 409 | 562 | 142 | 3572 | 0 | 2452 |

| | |
|---|---|
| Lab Batch volume (m3) | 0.043 |
| Density (kg/m3) | 2452 |
| Lab Yield (m3) | 0.041 |
| Modified w/b | 0.40 |

The complete process of designing the bridge concrete mix with 50% cement replacement with slag (C50-SL50) is presented in five steps as shown in Table A-57 to Table A-61 and the final mix design is demonstrated in Table A-62.

**Table A-57: Step 1 in designing the bridge concrete mix (C50-SL50)**

| Step | Item | Reference/Calculation | Value |
|---|---|---|---|
| 1 | Characteristic strength (fc) @ 28 days (MPa) | Specified | 50 |
| | Proportion defective (k) % | Table 3-7 | 1.64 |
| | Standard deviation (S) (MPa) | Figure 3-5 | 4 |
| | percentage by volume of air entrained (a) | Specified | |
| | Target mean strength (MPa) | Equation 3-2 | 57 |
| | Cement strength class | Specified | 42.5 |
| | Type of coarse aggregate | Specified | Crushed |
| | Free water/cement ratio | Table 3-8, Figure 3-6 | 0.42 |

**Table A-58: Step 2 in designing the bridge concrete mix (C50-SL50)**

| Step | Item | Reference/Calculation | Value |
|---|---|---|---|
| 2 | Slump (mm) | Specified | 40 |
| | Maximum aggregate size (mm) | Specified | 20 |
| | Coarse aggregate type | Specified | Crushed |
| | Fine aggregate type | Specified | Uncrushed |
| | Free water content (kg/m3) | Table 3-9, Eq.3-4 | 200 |
| | SL replacement (%) | Specified | 50 |
| | Reduction in water content because of SCMs (kg) | | |
| | Type of admixture | Specified | HWR |
| | Reduction of water content by admixture (%) | Specified | 22 |
| | Reduction in water content because of admixture (kg) | | 44 |
| | Final free water content (kg) | | 156 |

**Table A-59: Step 3 in designing the bridge concrete mix (C50-SL50)**

| Step | Item | Reference/Calculation | Value |
|---|---|---|---|
| 3 | Cement content (kg) | Equation 3-6 | 186 |
| | Maximum cement content (kg) | Specified | - |
| | Minimum cement content (kg) | Specified | - |
| | Final Cement content (kg) | | 186 |
| | SL content | Equation 3-7 | 186 |
| | Modified W/b ratio | | 0.42 |

**Table A-60: Step 4 in designing the bridge concrete mix (C50-SL50)**

| Step | Item | Reference/Calculation | Value |
|---|---|---|---|
| 4 | Percentage of fine aggregate passing 600 μm sieve | Specified | 50 |
| | Maximum aggregate size (mm) | Specified | 20 |
| | Slump zone (mm) | Specified | 60-180 |
| | Water to cement ratio | | 0.42 |
| | Proportion of fine aggregate (%) | Figure 3-7 | 37 |
| | Proportion of coarse aggregate (%) | | 63 |
| | 20 mm coarse aggregate content (%) | According to grading curve of Road Note No.4 (Figure 7-10) | 65 |
| | 10 mm coarse aggregate content (%) | | 35 |
| | Coarse sand content (%) | | 80 |
| | Fine sand content (%) | | 20 |

**Table A-61: Step 5 in designing the bridge concrete mix (C50-SL50)**

| Step | Item | Reference/Calculation | Value |
|---|---|---|---|
| 5 | Cement content (kg/m$^3$) | | 186 |
| | SL content (kg/m$^3$) | | 186 |
| | Free water content (kg/m$^3$) | | 156 |
| | Volume of cement (m$^3$) | | 0.06 |
| | Volume of slag (m$^3$) | | 0.077 |
| | Volume of water (m$^3$) | | 0.156 |
| | Volume of air (m$^3$) | | 0.000 |
| | Volume of total aggregate (m$^3$) | | 0.707 |
| | Total aggregate (kg) | | 1814.5 |
| | 20 mm coarse aggregate content (kg) | | 743 |
| | 10 mm coarse aggregate content kg) | | 400.1 |
| | Coarse sand content (kg) | | 537.1 |
| | Fine sand content (kg) | | 134.3 |
| | Admixture content (ml) | 900 ml per 100kg cementitious material | 3342.9 |
| | Air-entrained agent (ml) | | 0.000 |

**Table A-62: Final bridge concrete mix design (C50-SL50)**

| | Paste | | | Coarse Aggregate | | Fine Aggregate | | Admixture (ml) | | Total (kg) |
|---|---|---|---|---|---|---|---|---|---|---|
| | Cement | SCM | Water | 20 mm | 10 mm | Coarse Sand | Fine Sand | Water Reducer | A.E.A | |
| Design Weights (kg/m3) | 186 | 186 | 156 | 743 | 400 | 537 | 134 | 3343 | 0 | 2342 |
| Lab batch weight (kg) | 8 | 8 | 6.7 | 31.9 | 17.2 | 23.1 | 5.8 | 143.7 | 0 | 100.7 |
| W.A (%) | | | | 1.7 | 1.9 | 1.1 | 2.5 | | | |
| M.C (%) | | | | 3.7 | 7.5 | 2.3 | 2.4 | | | |
| Water contained (kg) | | | | 0.645 | 0.967 | 0.277 | -0.006 | | | 1.9 |
| Real lab batch weights (kg) | 8 | 8 | 4.3 | 31.9 | 17.2 | 23.1 | 5.8 | 143.7 | 0 | 98.3 |
| Corrected Real lab batch weights (kg) | 8 | 8 | 6.2 | 31.3 | 16.2 | 22.8 | 5.8 | 143.7 | 0 | 98.3 |
| Corrected designed weights (kg/m3) | 200 | 200 | 155 | 783 | 406 | 571 | 145 | 3596 | 0 | 2459 |

| | |
|---|---|
| Lab Batch volume (m3) | 0.043 |
| Density (kg/m3) | 2459 |
| Lab Yield (m3) | 0.04 |
| Modified w/b | 0.39 |

# Appendix B

Tables B-1 to B-3 demonstrate the compressive strength results up of to 56 days and Tables B-5 to B-7 present the drying shrinkage up to 28 days of all the concrete mixes (lean, pavement and bridge). Flexural strength results for pavement mixes are shown in Table B-4. Expansion results of mortar bars due to the alkali-silica reactivity according to AS1141.60.1 [109] with various levels of cement replacement with SCMs are indicated in Table B-8.

**Table B-1: Compressive strength results of lean concrete mixes (MPa)**

| Mixes | Compressive Strength (MPa) | | | |
|---|---|---|---|---|
| | 1-day | 7-day | 28-day | 56-day |
| C12-C0 | 7.1 | 9 | 14 | 16 |
| C12-CFA60 | 4.4 | 6.1 | 12 | 15 |
| C12-RFA60 | 3.7 | 5.1 | 11 | 14 |

**Table B-2: Compressive strength results of pavement concrete mixes (MPa)**

| Mixes | Compressive Strength (MPa) | | | |
|---|---|---|---|---|
| | 1-day | 7-day | 28-day | 56-day |
| C40-C0 | 14.0 | 36.1 | 45.2 | 49.7 |
| C40-CFA20 | 12.2 | 32.5 | 43.1 | 48.4 |
| C40-RFA20 | 10.0 | 28.0 | 38.3 | 43.5 |
| C40-SL50 | 7.3 | 24.8 | 40.4 | 47.0 |

**Table B-3: Compressive strength results of bridge concrete mixes (MPa)**

| Mixes | Compressive Strength (MPa) | | | |
|---|---|---|---|---|
| | 1-day | 7-day | 28-day | 56-day |
| C50-C0 | 23.1 | 48.7 | 58.8 | 62.1 |
| C50-CFA25 | 20.2 | 42.4 | 52.5 | 60.1 |
| C50-RFA25 | 16.3 | 36.9 | 46.9 | 55.4 |
| C50-SL50 | 8.8 | 32.5 | 50.8 | 58.8 |
| C50-MK15 | 14.0 | 39.2 | 48.0 | 56.1 |

**Table B-4: Flexural strength results of pavement concrete mixes (MPa)**

| Mixes | Flexural Strength (MPa) | |
|---|---|---|
| | 1-day | 7-day |
| C40-C0 | 4.50 | 5.33 |
| C40-CFA20 | 4.10 | 5.26 |
| C40-RFA20 | 3.90 | 4.70 |
| C40-SL50 | 4.13 | 5.35 |

**Table B-5: Drying shrinkage results of lean concrete mixes**

| Mixes | Drying Shrinkage (microstrain) | | | | | |
|---|---|---|---|---|---|---|
| | 1-day | 3-day | 7-day | 14-day | 21-day | 28-day |
| C12-C0 | 55 | 85 | 170 | 326 | 410 | 466 |
| C12-CFA60 | 50 | 75 | 160 | 310 | 370 | 420 |
| C12-RFA60 | 53 | 70 | 165 | 320 | 380 | 430 |

**Table B-6: Drying shrinkage results of pavement concrete mixes**

| Mixes | Drying Shrinkage (microstrain) | | | | | |
|---|---|---|---|---|---|---|
| | 1-day | 3-day | 7-day | 14-day | 21-day | 28-day |
| C40-C0 | 86 | 192 | 270 | 370 | 432 | 480 |
| C40-CFA20 | 58 | 148 | 229 | 319 | 379 | 426 |
| C40-RFA20 | 87 | 149 | 238 | 369 | 440 | 501 |
| C40-SL50 | 106 | 211 | 333 | 459 | 535 | 580 |

**Table B-7: Drying shrinkage results of bridge concrete mixes**

| Mixes | Drying Shrinkage (microstrain) | | | | | | |
|---|---|---|---|---|---|---|---|
| | 1-day | 3-day | 7-day | 14-day | 21-day | 28-day | 56-day |
| C50-C0 | 107 | 210 | 299 | 385 | 435 | 463 | 562 |
| C50-CFA25 | 115 | 165 | 271 | 353 | 420 | 442 | 547 |
| C50-RFA25 | 121 | 235 | 321 | 410 | 450 | 480 | 570 |
| C50-SL50 | 183 | 270 | 362 | 455 | 487 | 530 | 620 |
| C50-MK15 | 119 | 244 | 330 | 420 | 464 | 499 | 585 |

**Table B-8: Expansion of mortar bars due to the alkali-silica reactivity**

| Mixes | AMBTExpansion (%) | | | | | | |
|---|---|---|---|---|---|---|---|
| | 3-day | 7-day | 10-day | 14-day | 21-day | 28-day | 35-day |
| Control | 0.020 | 0.155 | 0.269 | 0.397 | 0.565 | 0.691 | 0.791 |
| 10% CFA | 0.011 | 0.059 | 0.113 | 0.180 | 0.286 | 0.367 | 0.432 |
| 15% CFA | 0.007 | 0.017 | 0.031 | 0.055 | 0.109 | 0.160 | 0.208 |
| 25% CFA | -0.001 | 0.001 | 0.007 | 0.011 | 0.020 | 0.030 | 0.047 |
| 30% SL | 0.017 | 0.079 | 0.132 | 0.200 | 0.290 | 0.359 | 0.414 |
| 40% SL | 0.012 | 0.045 | 0.075 | 0.116 | 0.179 | 0.228 | 0.273 |
| 50% SL | 0.002 | 0.013 | 0.020 | 0.031 | 0.060 | 0.090 | 0.118 |
| 7% MK | 0.020 | 0.117 | 0.191 | 0.277 | 0.395 | 0.482 | 0.548 |
| 10% MK | 0.015 | 0.081 | 0.135 | 0.200 | 0.293 | 0.367 | 0.422 |
| 15% MK | 0.007 | 0.020 | 0.033 | 0.051 | 0.087 | 0.127 | 0.157 |
| 10% RFA | 0.022 | 0.080 | 0.140 | 0.210 | 0.320 | 0.410 | 0.490 |
| 15% RFA | 0.010 | 0.021 | 0.037 | 0.065 | 0.130 | 0.210 | 0.270 |
| 25% RFA | 0.001 | 0.008 | 0.011 | 0.018 | 0.028 | 0.050 | 0.080 |

# *References*

# References

1. Mehta, P.K., Global concrete industry sustainability. Concrete International, 2009. 31(02): p. 45-48.

2. Malhotra, V., Supplementary cementing materials for concrete. 1987: Canada Centre for Mineral and Energy Technology.

3. Sirivivatnanon, V., H. Cao, R. Khatri, and L. Bucea, Guidelines for the use of high volume fly ash concretes. 1995.

4. Ambroise, J., S. Maximilien, and J. Pera, Properties of metakaolin blended cements. Advanced Cement Based Materials, 1994. 1(4): p. 161-168.

5. Zhang, M. and V. Malhotra, Characteristics of a thermally activated alumino-silicate pozzolanic material and its use in concrete. Cement and Concrete Research, 1995. 25(8): p. 1713-1725.

6. Standards Australia, AS 3582.1 Standard test method for supplementary cementitious materials for use with Portland and blended cement. 2016.

7. Moretti, A. and C.S. Jones, Advanced emissions control technologies for coal-fired power plants, in Power-Gen Asia. 2012: Thailand.

8. Chalmers, D., SCM supply chain challenges for Australia. Concrete in Australia, 2016. 42: p. 33-36.

9. Frydenberg, J., Demands grow of an energy market in steady flux, in The Australian. 2016.

10. Siddique, R. and M.I. Khan, Supplementary cementing materials. Vol. 37. 2011: Springer.

11. Roy, W.R., R.G. Thiery, R.M. Schuller, and J. Suloway, Coal fly ash: a review of the literature and proposed classification system with emphasis on environental impacts. 1981, Illinois State Geological Survey, Urbana (USA).

12. Kutchko, B.G. and A.G. Kim, Fly ash characterization by SEM–EDS. Fuel, 2006. 85(17): p. 2537-2544.

13. Ahmaruzzaman, M., A review on the utilization of fly ash. Progress in Energy and Combustion Science, 2010. 36(3): p. 327-363.

14. Manz, O.E., Coal fly ash: a retrospective and future look. Fuel, 1999. 78(2): p. 133-136.

15. Mehta, P.K., Pozzolanic and cementitious by-products as mineral admixtures for concrete-a critical review. ACI Special Publication, 1983. 79.

16. Thomas, M., Supplementary Cementing Materials in Concrete. 2013: CRC Press.

17. Tasong, W.A., S. Wild, and R.J. Tilley, Mechanisms by which ground granulated blastfurnace slag prevents sulphate attack of lime-stabilised kaolinite. Cement and concrete research, 1999. 29(7): p. 975-982.

18. Murat, M., Hydration reaction and hardening of calcined clays and related minerals. I. Preliminary investigation on metakaolinite. Cement and Concrete Research, 1983. 13(2): p. 259-266.

19. Marsh, B.K. and R.L. Day, Pozzolanic and cementitious reactions of fly ash in blended cement pastes. Cement and Concrete Research, 1988. 18(2): p. 301-310.

20. Uysal, M. and V. Akyuncu, Durability performance of concrete incorporating Class F and Class C fly ashes. Construction and Building Materials, 2012. 34: p. 170-178.

21. Bijen, J., Benefits of slag and fly ash. Construction and Building Materials, 1996. 10(5): p. 309-314.

22. Wild, S., J. Khatib, and L. Roose, Chemical shrinkage and autogenous shrinkage of Portland cement—metakaolin pastes. Advances in Cement Research, 1998. 10(3): p. 109-119.

23. Kinuthia, J., S. Wild, B. Sabir, and J. Bai, Self-compensating autogenous shrinkage in Portland cement—metakaolin—fly ash pastes. Advances in Cement Research, 2000. 12(1): p. 35-43.

24. Kim, H.-S., S.-H. Lee, and H.-Y. Moon, Strength properties and durability aspects of high strength concrete using Korean metakaolin. Construction and Building Materials, 2007. 21(6): p. 1229-1237.

25. Poon, C.-S., L. Lam, S. Kou, Y.-L. Wong, and R. Wong, Rate of pozzolanic reaction of metakaolin in high-performance cement pastes. Cement and Concrete Research, 2001. 31(9): p. 1301-1306.

26. Sumer, M., Compressive strength and sulfate resistance properties of concretes containing Class F and Class C fly ashes. Construction and Building Materials, 2012. 34: p. 531-536.

27. Helmuth, R., Fly ash in cement and concrete. 1987.

28. Mora, E.P., J. Paya, and J. Monzó, Influence of different sized fractions of a fly ash on workability of mortars. Cement and Concrete Research, 1993. 23(4): p. 917-924.

29. Shi, C. and J. Qian, High performance cementing materials from industrial slags—a review. Resources, Conservation and Recycling, 2000. 29(3): p. 195-207.

30. Meusel, J. and J. Rose, Production of granulated blast furnace slag at sparrows point, and the workability and strength potential of concrete incorporating the slag. ACI Special Publication, 1983. 79.

31. Bai, j., S. Wild, B.B. Sabir, and J.M. Kinuthia, Workability of concrete incorporating pulverized fuel ash and metakaolin, in Magazine of Concrete Research. 1999. p. 207-216.

32. Mostafa, N. and P. Brown, Heat of hydration of high reactive pozzolans in blended cements: isothermal conduction calorimetry. Thermochimica acta, 2005. 435(2): p. 162-167.

33. Shi, C. and R.L. Day, Some factors affecting early hydration of alkali-slag cements. Cement and Concrete Research, 1996. 26(3): p. 439-447.

34. Taylor, P.C., S.H. Kosmatka, and G.F. Voigt, Integrated materials and construction practices for concrete pavement: A state-of-the-practice manual. 2006.

35. Bullard, J.W., H.M. Jennings, R.A. Livingston, A. Nonat, G.W. Scherer, J.S. Schweitzer, K.L. Scrivener, and J.J. Thomas, Mechanisms of cement hydration. Cement and Concrete Research, 2011. 41(12): p. 1208-1223.

36. Snelson, D.G., S. Wild, and M. O'Farrell, Heat of hydration of Portland Cement–Metakaolin–Fly ash (PC–MK–PFA) blends. Cement and Concrete Research, 2008. 38(6): p. 832-840.

37. Pacewska, B., G. Blonkowski, and I. Wilińska, Investigations of the influence of different fly ashes on cement hydration. Journal of Thermal Analysis and Calorimetry, 2006. 86(1): p. 179-186.

38. Łaskawiec, K., J. Małolepszy, and G. Zapotoczna-Sytek, Wpływ popiołów lotnych powstających przy spalaniu węgla kamiennego i brunatnego w kotłach fluidalnych na skład fazowy AAC. Materiały Ceramiczne/Ceramic Materials, 2011. 63(1): p. 88-92.

39. Ballim, Y. and P.C. Graham, The effects of supplementary cementing materials in modifying the heat of hydration of concrete. Materials and Structures, 2009. 42(6): p. 803-811.

40. Gruyaert, E., N. Robeyst, and N. De Belie, Study of the hydration of Portland cement blended with blast-furnace slag by calorimetry and thermogravimetry. Journal of Thermal Analysis and Calorimetry, 2010. 102(3): p. 941-951.

41. Kadri, E.-H., S. Kenai, K. Ezziane, R. Siddique, and G. De Schutter, Influence of metakaolin and silica fume on the heat of hydration and compressive strength development of mortar. Applied Clay Science, 2011. 53(4): p. 704-708.

42. Frıas, M., M.S. De Rojas, and J. Cabrera, The effect that the pozzolanic reaction of metakaolin has on the heat evolution in metakaolin-cement mortars. Cement and Concrete Research, 2000. 30(2): p. 209-216.

43. De Silva, P. and F. Glasser, Hydration of cements based on metakaolin: thermochemistry. Advances in Cement Research, 1990. 3(12): p. 167-177.

44. Talero, R. and V. Rahhal, Calorimetric comparison of portland cements containing silica fume and metakaolin: Is silica fume, like metakaolin, characterized by pozzolanic activity that is more specific than generic? Journal of Thermal Analysis and Calorimetry, 2009. 96(2): p. 383-393.

45. Chindaprasirt, P., C. Jaturapitakkul, and T. Sinsiri, Effect of fly ash fineness on compressive strength and pore size of blended cement paste. Cement and Concrete Composites, 2005. 27(4): p. 425-428.

46. Chindaprasirt, P., C. Jaturapitakkul, and T. Sinsiri, Effect of fly ash fineness on microstructure of blended cement paste. Construction and Building Materials, 2007. 21(7): p. 1534-1541.

47. Sybertz, F. and U. Wiens. Effect of fly ash fineness on hydration characteristics and strength development. in Blended cements in construction. papers presented at the International Conference, University of Sheffield, UK, 9-12 September 1991. 1991.

48. Harris, H.A., J.L. Thompson, and T.E. Murphy, Factors affecting the reactivity of fly ash from Western coals. Cement, Concrete and Aggregates, 1987. 9(1): p. 34-37.

49. Johari, M., J. Brooks, S. Kabir, and P. Rivard, Influence of supplementary cementitious materials on engineering properties of high strength concrete. Construction and Building Materials, 2011. 25(5): p. 2639-2648.

50. Detwiler, R.J. and P.K. Mehta, Chemical and physical effects of silica fume on the mechanical behavior of concrete. Materials Journal, 1989. 86(6): p. 609-614.

51. Goldman, A. and A. Bentur, The influence of microfillers on enhancement of concrete strength. Cement and Concrete Research, 1993. 23(4): p. 962-972.

52. Khatib, J. and S. Wild, Pore size distribution of metakaolin paste. Cement and Concrete Research, 1996. 26(10): p. 1545-1553.

53. Güneyisi, E., M. Gesoğlu, S. Karaoğlu, and K. Mermerdaş, Strength, permeability and shrinkage cracking of silica fume and metakaolin concretes. Construction and Building Materials, 2012. 34: p. 120-130.

54. Poon, C., S. Kou, and L. Lam, Compressive strength, chloride diffusivity and pore structure of high performance metakaolin and silica fume concrete. Construction and Building Materials, 2006. 20(10): p. 858-865.

55. Joshi, R.C. and R. Lohita, Fly ash in concrete: production, properties and uses. 1997: CRC Press.

56. Siddique, R., Effect of fine aggregate replacement with Class F fly ash on the mechanical properties of concrete. Cement and Concrete Research, 2003. 33(4): p. 539-547.

57. ACI, Evaluation of Properties of High-Volume Fly-Ash Concrete.

58. Cheng, A., R. Huang, J.-K. Wu, and C.-H. Chen, Influence of GGBS on durability and corrosion behavior of reinforced concrete. Materials Chemistry and Physics, 2005. 93(2): p. 404-411.

59. Khatib, J. and J. Hibbert, Selected engineering properties of concrete incorporating slag and metakaolin. Construction and Building Materials, 2005. 19(6): p. 460-472.

60. Teng, S., T.Y.D. Lim, and B. Sabet Divsholi, Durability and mechanical properties of high strength concrete incorporating ultra fine Ground Granulated Blast-furnace Slag. Construction and Building Materials, 2013. 40: p. 875-881.

61. Barnett, S., M. Soutsos, S. Millard, and J. Bungey, Strength development of mortars containing ground granulated blast-furnace slag: Effect of curing temperature and determination of apparent activation energies. Cement and Concrete Research, 2006. 36(3): p. 434-440.

62. Qian, X. and Z. Li, The relationships between stress and strain for high-performance concrete with metakaolin. Cement and Concrete Research, 2001. 31(11): p. 1607-1611.

63. Li, Z. and Z. Ding, Property improvement of Portland cement by incorporating with metakaolin and slag. Cement and Concrete Research, 2003. 33(4): p. 579-584.

64. Atiş, C.D., A. Kilic, and U.K. Sevim, Strength and shrinkage properties of mortar containing a nonstandard high-calcium fly ash. Cement and Concrete Research, 2004. 34(1): p. 99-102.

65. Li, J. and Y. Yao, A study on creep and drying shrinkage of high performance concrete. Cement and Concrete Research, 2001. 31(8): p. 1203-1206.

66. Brooks, J. and M. Johari, Effect of metakaolin on creep and shrinkage of concrete. Cement and Concrete Composites, 2001. 23(6): p. 495-502.

67. Neville, A., Chloride attack of reinforced concrete: an overview. Materials and Structures, 1995. 28(2): p. 63.

68. Justnes, H., A review of chloride binding in cementitious systems. Nordic Concrete Research-Publications -, 1998. 21: p. 48-63.

69. Lambert, P., C. Page, and P. Vassie, Investigations of reinforcement corrosion. 2. Electrochemical monitoring of steel in chloride-contaminated concrete. Materials and Structures, 1991. 24(5): p. 351-358.

70. Luping, T. and L.-O. Nilsson, Chloride binding capacity and binding isotherms of OPC pastes and mortars. Cement and Concrete Research, 1993. 23(2): p. 247-253.

71. Arya, C., N. Buenfeld, and J. Newman, Factors influencing chloride-binding in concrete. Cement and Concrete Research, 1990. 20(2): p. 291-300.

72. Dinakar, P., K. Babu, and M. Santhanam, Durability properties of high volume fly ash self compacting concretes. Cement and Concrete Composites, 2008. 30(10): p. 880-886.

73. Standards Australia, AS 1012.21 Standard test method for testing concrete - Determination of water absorption and apparent volume of permeable voids in hardened concrete. 1999.

74. Roads, V., Test methods for the assessment of durability of concrete. 2007.

75. ASTM International, ASTM C1202 Standard test method for electrical indication of concrete's ability to resist chloride ion penetration. 2012.

76. Sherman, M.R., D.B. McDonald, and D.W. Pfeifer, Durability aspects of precast prestressed concrete Part 2: Chloride permeability study. PCI journal, 1996. 41(4): p. 76-95.

77. Shi, C., J.A. Stegemann, and R.J. Caldwell, Effect of supplementary cementing materials on the specific conductivity of pore solution and its implications on the rapid chloride permeability test (AASHTO T277 and ASTM C1202) results. Materials Journal, 1998. 95(4): p. 389-394.

78. Papadakis, V.G., Effect of supplementary cementing materials on concrete resistance against carbonation and chloride ingress. Cement and Concrete Research, 2000. 30(2): p. 291-299.

79. Hooton, R. and M. Titherington, Chloride resistance of high-performance concretes subjected to accelerated curing. Cement and Concrete Research, 2004. 34(9): p. 1561-1567.

80. Hadj-sadok, A., S. Kenai, L. Courard, and A. Darimont, Microstructure and durability of mortars modified with medium active blast furnace slag. Construction and Building Materials, 2011. 25(2): p. 1018-1025.

81. Khatri, R., V. Sirivivatnanon, and J. Yang, Role of permeability in sulphate attack. Cement and Concrete Research, 1997. 27(8): p. 1179-1189.

82. Khatri, R. and V. Sirivivatnanon, Methods for the determination of water permeability of concrete. ACI Materials Journal, 1997. 94(3): p. 257-261.

83. ASTM Intenational, ASTM C1012 Standar Test Method for Length Change of Hydraulic-Cement Mortars Exposed to a Sulfate Solution. 2015.

84. Cao, H., L. Bucea, A. Ray, and S. Yozghatlian, The effect of cement composition and pH of environment on sulfate resistance of Portland cements and blended cements. Cement and Concrete Composites, 1997. 19(2): p. 161-171.

85. Mehta, P.K., Durability--Critical issues for the future. Concrete International, 1997. 19(7): p. 27-33.

86. Naik, T.R., S.S. Singh, and M.M. Hossain, Permeability of concrete containing large amounts of fly ash. Cement and Concrete Research, 1994. 24(5): p. 913-922.

87. Saricimen, H., M. Maslehuddin, A.J. Al-Tayyib, and A.I. Al-Mana, Permeability and durability of plain and blended cement concretes cured in field and laboratory conditions. Materials Journal, 1995. 92(2): p. 111-116.

88. Barger, G.S., R.L. Hill, B.W. Ramme, A. Bilodeau, R.D. Hooton, D. Ravina, M.A. Bury, H.J. Humphrey, D. Reddy, and R.L. Carrasquillo, Use of Fly Ash in Concrete. 2003, American Concrete Institute: Farmington Hills, MI, USA.

89. Sirivivatnanon, V. and R. Khatri. Performance based specification for sulphate resisting concrete. in Infrastructure regeneration and rehabilitation improving the quality of life through better construction. International conference. 1999.

90. Sirivivatnanon, V. and G. Lucas. Specifying sulfate-resisting concrete. in Austroads Bridge Conference, 8th, 2011, Sydney, New South Wales, Australia. 2011.

91. Tian, B. and M.D. Cohen, Does gypsum formation during sulfate attack on concrete lead to expansion? Cement and Concrete Research, 2000. 30(1): p. 117-123.

92. Santhanam, M., M.D. Cohen, and J. Olek, Modeling the effects of solution temperature and concentration during sulfate attack on cement mortars. Cement and Concrete Research, 2002. 32(4): p. 585-592.

93. Wee, T., A.K. Suryavanshi, S. Wong, and A. Rahman, Sulfate resistance of concrete containing mineral admixtures. ACI Materials Journal, 2000. 97(5): p. 536-549.

94. Higgins, D., Increased sulfate resistance of ggbs concrete in the presence of carbonate. Cement and Concrete Composites, 2003. 25(8): p. 913-919.

95. Al-Akhras, N.M., Durability of metakaolin concrete to sulfate attack. Cement and Concrete Research, 2006. 36(9): p. 1727-1734.

96. Glasser, L.D. and N. Kataoka, The chemistry of 'alkali-aggregate'reaction. Cement and Concrete Research, 1981. 11(1): p. 1-9.

97. Thomas, M. and K. Folliard, Concrete aggregates and the durability of concrete. Durability of concrete and cement composites. Cambridge (UK): Woodhead Publishing Limited, 2007: p. 247-81.

98. Hanson, W. Studies Relating To the Mechanism by Which the Alkali-Aggregate Reaction Produces Expansion in Concrete. Journal Proceedings. 1944.

99. Thomas, M., The effect of supplementary cementing materials on alkali-silica reaction: A review. Cement and Concrete Research, 2011. 41(12): p. 1224-1231.

100. Thomas, M., Review of the effect of fly ash and slag on alkali-aggregate reaction in concrete. 1996: Building Research Establishment.

101. Duchesne, J. and M. Bérubé, The effectiveness of supplementary cementing materials in suppressing expansion due to ASR: another look at the reaction mechanisms part 2: pore solution chemistry. Cement and Concrete Research, 1994. 24(2): p. 221-230.

102. Shehata, M.H., M.D. Thomas, and R.F. Bleszynski, The effects of fly ash composition on the chemistry of pore solution in hydrated cement pastes. Cement and Concrete Research, 1999. 29(12): p. 1915-1920.

103. ASTM International, Concrete Aggregates by Determination of Length Change of Concrete Due to Alkali-Silica Reaction. 1995.

104. Hester, D., C. McNally, and M. Richardson, A study of the influence of slag alkali level on the alkali–silica reactivity of slag concrete. Construction and Building Materials, 2005. 19(9): p. 661-665.

105. Standards, B., Standard Test Method for determination of alkali-silica reactivity - Concrete prism method. 1999.

106. Kandasamy, S. and M.H. Shehata, The capacity of ternary blends containing slag and high-calcium fly ash to mitigate alkali silica reaction. Cement and Concrete Composites, 2014. 49: p. 92-99.

107. Kwon, Y.-j., A study on the alkali-aggregate reaction in high-strength concrete with particular respect to the ground granulated blast-furnace slag effect. Cement and Concrete Research, 2005. 35(7): p. 1305-1313.

108. Ramlochan, T., M. Thomas, and K.A. Gruber, The effect of metakaolin on alkali–silica reaction in concrete. Cement and Concrete Research, 2000. 30(3): p. 339-344.

109. Standards Australia, AS 1141.60.1 Standard test method for Potential alkali-silica reactivity-accelerated mortar bar method 2014: Australia.

110. Roads and Maritime Services, R82 Specification for lean-mix concrete subbase. 2010.

111. Road and Maritime Services, R83 Specification for concrete pavement base. 2013.

112. Road and Maritime Services, B80 Specification for concrete work for bridges. 2013.

113. Standards Australia, AS 2350.9 Standard test method for determination of residue on the 45 micrometre sieve. 2016.

114. Standards Australia, AS 2350.8 Standard test method for determination of fineness index by air permeability method. 2006.

115. Standards Australia, AS 3583.5 Standard test method for determination of relative density. 1991.

116. Standards Australia, AS 3583.12 Standard test method for supplementary cementitious materials for use with Portland cement - Determination of available alkali. 1991.

117. Standards Australia, AS 1141.6.1 Standard test method for sampling and testing aggregates - Particle density and water absorption of coarse aggregate. 2000.

118. Standards Australia, AS 1141.5 Standard test method for sampling and testing aggregates - Particle density and water absorption of fine aggregate. 2000.

119. Standards Australia, AS 1141.11.1 Standard test method for sampling and testing aggregates - Particle size distribution - Sieving nethod. 2009.

120. ASTM International, ASTM C305-13 Standard practice for mechanical mixing of hydraulic cement pastes and mortars of plastic consistency. 2013.

121. ASTM International, ASTM C1679 Standard Practice for Measuring Hydration Kinetics of Hydraulic Cementitious Mixtures Using Isothermal Calorimetry. 2014.

122. De Schutter, G., Hydration and temperature development of concrete made with blast-furnace slag cement. Cement and Concrete Research, 1999. 29(1): p. 143-149.

123. ASTM International, ASTM C1437 Standard Test Method for Flow of Hydraulic Cement Mortar. 2015.

124. ASTM International, ASTM C109 Standard Test Method for Compressive Strength of Hydraulic Cement Mortars. 2016.

125. ASTM International, ASTM C188 Standard Test Method for Density of Hydraulic Cement. 2016.

126. ASTM International, ASTM C311 Standard Test Method for Sampling and Testing Fly ash or Natural Pozzolan for Use in Portland-Cement Concrete. 2016.

127. ASTM International, ASTM C 989 Standard Specification for Slag Cement for Use in Concrete and Mortars. 2016.

128. Standards Australia, AS 2350.13 Standard test methods of testing Portland cement, blended and masonry cements- Determination of drying shrinkage of cement mortars. 2006.

129. Building Research Establishment (BRE), Design of normal concrete mixes. 1998.

130. Smith, I.A. The design of fly-ash concretes. in Inst Civil Engineers Proc London,/UK/. 1967.

131. Standards Australia, AS 1012.2 Standard test method of testing concrete - Preparing concrete mixes in the laboratory. 2014.

132. Standards Australia, AS 1012.3.1 Standard test method for determination of properties related to consistency of concrete-slump test. 2014.

133. Standards Australia, AS 1012.4.2 Standard test method for determination of air content of freshly mixed concrete. 2014.

134. Standards Australia, AS 1012.2 Standard test method of testing concrete - Determination of mass per unit volume of freshly mixed concrete. 2014.

135. Standards Australia, AS 1012.9 Standard test method for compressive strength tests-Concrete, mortar and grout specimens. 2014.

136. Standards Australia, AS 1012.11 Standard test method for determination of the modulus of rupture. 2014.

137. Standards Australia, AS 1012.13 Standard test method for determination of the drying shrinkage of concrete for samples prepared in the field or in the laboratory. 2015.

138. Taylor, H., Cement Chemistry, Thomas Telford Publishing. 1997, London.

139. Lothenbach, B., K. Scrivener, and R. Hooton, Supplementary cementitious materials. Cement and Concrete Research, 2011. 41(12): p. 1244-1256.

140. Barry, E., Beneficiated fly ash: hydration, microstructure, and strength development in Portland cement systems. American Concrete Institute ACI 1989. 114: p. 241-274.

141. Chindaprasirt, P., S. Ruangsiriyakul, H. Cao, and L. Bucea. Influence of Mae Moh fly ash fineness on characteristics, strength and drying shrinkage development of blended cement mortars. in The Eighth East Asia-Pacific Conference on Structural Engineering and Construction, Singapore. 2001.

142. Barry, E.E., Beneficiated Fly Ash: Hydration, Microstructure, and Strength Development in Portland Cement Systems. Special Publication. 114.

143. Diamond, S., On the glass present in low-calcium and in high-calcium fly ashes. Cement and Concrete Research, 1983. 13(4): p. 459-464.

144. Hooton, R., The reactivity and hydration products of blast-furnace slag. Supplementary Cementing Materials for Concrete, Ed. Malhotra VM, Canadá, 1987: p. 291-333.

145. Wilson, M. and S. Kosmatka, Design and control of concrete mixtures. Portland Cement Association: USA, 2011.

146. Standards Australia, AS 2758.1 Standard test method for aggregates and rock for engineering purposes. 2014: Australia.

147. Ge, Z., K. Wang, P.J. Sandberg, and J.M. Ruiz, Characterization and performance prediction of cement-based materials using a simple isothermal calorimeter. Journal of Advanced Concrete Technology, 2009. 7(3): p. 355-366.

148. Neville, A.M., Properties of concrete. 1995.

149. Rahhal, V. and R. Talero, Influence of two different fly ashes on the hydration of portland cements. Journal of Thermal Analysis and Calorimetry, 2004. 78(1): p. 191-205.

150. Siler, P., J. Kratky, and N. De Belie, Isothermal and solution calorimetry to assess the effect of superplasticizers and mineral admixtures on cement hydration. Journal of Thermal Analysis and Calorimetry, 2012. 107(1): p. 313-320.

151. Aïtcin, P.-C., High performance concrete. 2011: CRC press.

152. Pane, I. and W. Hansen, Investigation of blended cement hydration by isothermal calorimetry and thermal analysis. Cement and Concrete Research, 2005. 35(6): p. 1155-1164.

153. Wu, X., D. Roy, and C. Langton, Early stage hydration of slag-cement. Cement and Concrete Research, 1983. 13(2): p. 277-286.

154. Hewlett, P., Lea's chemistry of cement and concrete. 2003: Elsevier.

155. Shiqun, L., R. Della M, and K. Amithaba, Quantitative determination of pozzolans in hydrated systems of cement or Ca(OH)2 with fly ash or silica fume. Cement and Concrete Research, 1985. 13: p. 1079-1086.

156. Xu, A. and S.L. Sarkar, Microstructural development in high-volume fly-ash cement system. Journal of Materials in Civil Engineering, 1994. 6(1): p. 117-136.

157. Jun-Yuan, H., B.E. Scheetz, and D.M. Roy, Hydration of fly ash-portland cements. Cement and Concrete Research, 1984. 14(4): p. 505-512.

158. Berry, E.E., R.T. Hemmings, M.-H. Zhang, B.J. Cornelius, and D.M. Golden, Hydration in high-volume fly ash concrete binders. Materials Journal, 1994. 91(4): p. 382-389.

159. Ferraris, C.F., K.H. Obla, and R. Hill, The influence of mineral admixtures on the rheology of cement paste and concrete. Cement and Concrete Research, 2001. 31(2): p. 245-255.

160. Chindaprasirt, P., C. Chotithanorm, H. Cao, and V. Sirivivatnanon, Influence of fly ash fineness on the chloride penetration of concrete. Construction and Building Materials, 2007. 21(2): p. 356-361.

161. Kiattikomol, K., C. Jaturapitakkul, S. Songpiriyakij, and S. Chutubtim, A study of ground coarse fly ashes with different finenesses from various sources as pozzolanic materials. Cement and Concrete Composites, 2001. 23(4): p. 335-343.

162. Slanička, Š., The influence of fly ash fineness on the strength of concrete. Cement and Concrete Research, 1991. 21(2-3): p. 285-296.

163. Iyer, R. and J. Scott, Power station fly ash—a review of value-added utilization outside of the construction industry. Resources, Conservation and Recycling, 2001. 31(3): p. 217-228.

164. Bissonnette, B.t., P. Pierre, and M. Pigeon, Influence of key parameters on drying shrinkage of cementitious materials. Cement and Concrete Research, 1999. 29(10): p. 1655-1662.

165. Brooks, J. and M.M. Johari, Effect of metakaolin on creep and shrinkage of concrete. Cement and Concrete Composites, 2001. 23(6): p. 495-502.

166. Itim, A., K. Ezziane, and E.-H. Kadri, Compressive strength and shrinkage of mortar containing various amounts of mineral additions. Construction and Building Materials, 2011. 25(8): p. 3603-3609.

167. Virgalitte, S.J., M.D. Luther, J.H. Rose, B. Mather, L.W. Bell, B.A. Ehmke, P. Klieger, D.M. Roy, B.M. Call, and R.D. Hooton, Ground Granulated Blast-Furnace Slag as a Cementitious Constituent in Concrete. American Concrete Institute ACI Report 233R-95, 1995.

168. Wild, S., J. Khatib, and A. Jones, Relative strength, pozzolanic activity and cement hydration in superplasticised metakaolin concrete. Cement and Concrete Research, 1996. 26(10): p. 1537-1544.

169. Güneyisi, E. and M. Gesoğlu, A study on durability properties of high-performance concretes incorporating high replacement levels of slag. Materials and Structures, 2008. 41(3): p. 479-493.

170. Lee, S.H., E. Sakai, M. Daimon, and W.K. Bang, Characterization of fly ash directly collected from electrostatic precipitator. Cement and Concrete Research, 1999. 29(11): p. 1791-1797.

171. Atis, C.D., High-volume fly ash concrete with high strength and low drying shrinkage. Journal of Materials in Civil Engineering, 2003. 15(2): p. 153-156.

172. Brooks, J., M. Johari, and M. Mazloom, Effect of admixtures on the setting times of high-strength concrete. Cement and Concrete Composites, 2000. 22(4): p. 293-301.

173. Erdoğdu, K. and P. Türker, Effects of fly ash particle size on strength of Portland cement fly ash mortars. Cement and Concrete Research, 1998. 28(9): p. 1217-1222.

174. Courard, L., A. Darimont, M. Schouterden, F. Ferauche, X. Willem, and R. Degeimbre, Durability of mortars modified with metakaolin. Cement and Concrete Research, 2003. 33(9): p. 1473-1479.

175. Johari, M.M., J. Brooks, S. Kabir, and P. Rivard, Influence of supplementary cementitious materials on engineering properties of high strength concrete. Construction and Building Materials, 2011. 25(5): p. 2639-2648.

176. Aponte, D.F., M. Barra, and E. Vàzquez, Durability and cementing efficiency of fly ash in concretes. Construction and Building Materials, 2012. 30: p. 537-546.

177. Dhir, R. and M. Jones, Development of chloride-resisting concrete using fly ash. fuel, 1999. 78(2): p. 137-142.

178. Hooton, R., Influence of silica fume replacement of cement on physical properties and resistance to sulfate attack, freezing and thawing, and alkali-silica reactivity. Materials Journal, 1993. 90(2): p. 143-151.

179. Khatib, J. and S. Wild, Sulphate resistance of metakaolin mortar. Cement and Concrete Research, 1998. 28(1): p. 83-92.

180. Bhatty, M. and N. Greening. Interaction of alkalies with hydrating and hydrated calcium silicates. in Proceedings. 1978.

181. Hong, S.-Y. and F. Glasser, Alkali binding in cement pastes: Part I. The CSH phase. Cement and Concrete Research, 1999. 29(12): p. 1893-1903.